Dissertation

submitted to the

Combined Faculty of Mathematics, Engineering and Natural Sciences

of Heidelberg University, Germany

for the degree of

Doctor of Natural Sciences

Put forward by

Davide*, Lettera*

born in: Rome (IT)

Oral examination: 2024, July 15

Non-perturbative aspects of Quantum Field Theory

Referees: Prof. Razvan Gurau

Prof. Manfred Salmhofer

Topic in German

Wir untersuchen einige nichtperturbative Aspekte von Quantenfeldtheorien (QFT), wobei wir das Problem aus zwei Blickwinkeln angehen: durch Verwendung von large-N-Entwicklungen und durch Verwendung von Techniken der konstruktiven QFT. Die large-N-Entwicklung wird auf eine tensorielle QFT mit langreichweitiger Wechselwirkung und $O(N)^3$-Symmetrie, sowie auf eine vektorielle QFT mit langreichweitiger Wechselwirkung und O(N)-Symmetrie angewendet. Für die tensorielle QFT berechnen wir die freie Energie bis zur übernächsten führenden Ordnung in d=3 auf der Sphäre und wir bestätigen, dass diese Größe entlang des Renormierungsgruppenflusses monoton abnimmt. Für die vektorielle QFT untersuchen wir die Auswirkungen der Kompaktifizierung einer räumlichen Dimension auf die kritische Theorie und berechnen einige neue Daten dieser konformen Feldtheorie, und zwar Einpunktfunktionen von bilinearen Operatoren. Darüber hinaus führen wir eine Klasse von anisotropen Modellen ein, die wir fraktionale Lifshitz-Quanten\-feldtheorien nennen, und initiieren ihre Untersuchung. Was den Teil zur konstruktiven QFT betrifft, so untersuchen wir das O(N)-Vektor-Modell in d=0 mittels der Loop-Vertex-Entwicklung (LVE), die in diesem Fall einer small-N-Entwicklung entspricht. Wir zeigen die Borel-Summierbarkeit der Zustandssumme und der freien Energie als Funktionen der Kopplungskonstante in der gesamten komplexen Ebene und berechnen ihre Transreihenentwicklung.

Topic in English

We investigate some non perturbative aspects of Quantum Field Theories (QFT), tackling the problem from two angles: using large-N expansions or using constructive field theory techniques. As for the large-N expansion, it is applied on a long-range tensor QFT with $O(N)^3$ symmetry and on a long-range vector QFT with O(N) symmetry. On the tensor QFT we compute the free energy to the next-to-next-to-leading order in d=3 on the sphere, and we confirm that it is a monotonically decreasing quantity along the renormalization group flow. On the vector QFT we study the effects of the compactification of one dimension on the critical theory and we compute some new Conformal Field Theory data, i.e. one point functions of bilinear operators. Furthermore, we introduce a class of anisotropic models that we call quantum fractional Lifshitz field theories and initiate their study. As for the constructive field theory part, we study the vector O(N) model in d=0 by means of the Loop Vertex Expansion (LVE), that in this case corresponds to a small-N expansion. We prove the Borel summability of the partition function and the free energy in the whole complex plane of the coupling constant, and compute their transseries expansion.

Acknowledgements

In this few lines i am happy to express my gratitude to all people who were part of my four years journey in Heidelberg.

First of all my supervisors Razvan and Dario, thank you for believing in me from the beginning, and for your careful supervision. Razvan, thank you for your support, you always found a moment for me despite your many commitments. And thank you not only for your scientific guidance but also for your personal involvement which made the work environment much more pleasant, please never change that. Dario, I consider myself extremely lucky for having had the chance to visit you so often in Paris and interact with you. Thank you for hosting me in your office, for giving me so much of your time, for your great patience and ability to share with me a part of your great knowledge, and for all your advice even beyond physics.

I am grateful to the members of my commitee: Matthias Bartelmann, Lauriane Chomaz, and in particular Manfred Salmhofer for his careful reading of the present manuscript.

Also, I want to warmly thank all the people I had the opportunity to interact with in Razvan's group: Carlos, Daniel, Donald, Felix, Hannes, Leena, Luca, Matteo, Melda, Miao, Niels, Sabine, Zois. Sabine, both your friendship and your help greatly enhanced my first time in Heidelberg. Matteo and Luca, discussing new directions with you has taught me so much, but in particular I am happy to have found in you two good friends more than colleagues, I will always keep with me the memories of the time spent together. Thanks also to Hannes and Carlos, for all the pleasant times we spent together in the office, interacting and working with you was always inspiring. Thank you Melda, you have also been an important part of my journey, your tireless passion should be an example for all of us. Finally thank you Zois, your arrival in the group made the final period of my PhD much more enjoyable and fun.

I would also like to thank the administrative staff of Heidelberg: Anja, Besma, Melanie, Sonja. Too many times I have needed your help, and you, with much patience, have never denied it to me.

Thanks to all the people who organized the conferences, workshops and schools I attended, you gave me the opportunity to travel the world and meet many brilliant people.

Also I want to thank my close friends Saswato and Adrian. Saswato, you were the most welcoming person I could find and made my move to Heidelberg much easier, I am sincerely grateful for your friendship. Adrian, thank you for all the good times we shared, drinking beer, playing sports and traveling. Without those moments my time in Heidelberg would not have been the same.

A special thank you goes to my partner Monica, living apart for so long has certainly been difficult, yet being with you makes everything easier for me.

Finally, thanks to my parents, Aldo and Marcella, and my brother Marco, who have always believed in me and have always helped and supported me to the best of their ability and beyond, despite the distance.

(Grazie infine ai miei genitori, Aldo e Marcella, e a mio fratello Marco, che hanno sempre creduto in me e mi hanno sempre aiutato e sostenuto al meglio delle loro possibilità e oltre, nonostante la distanza.)

Publications

The content of the manuscript is mainly based on the following publications:

1. D. Benedetti, R. Gurau, S. Harribey, and D. Lettera. "The F-theorem in the melonic limit". In: *JHEP* 02 (2022), p. 147. DOI: 10.1007/JHEP02(2022)147. arXiv: 2111.11792 [hep-th].

2. D. Benedetti, R. Gurau, H. Keppler, and D. Lettera. "The small-N series in the zero-dimensional $O(N)$ model: constructive expansions and transseries". In: *Annales Henri Poincare* (Apr. 2024). DOI: https://doi.org/10.1007/s00023-024-01437-y. arXiv: 2210.14776 [hep-th].

3. D. Benedetti, R. Gurau, S. Harribey, and D. Lettera. "Finite-size versus finite-temperature effects in the critical long-range O(N) model". In: *JHEP* 02 (2024), p. 078. DOI: 10.1007/JHEP02(2024)078. arXiv: 2311.04607 [hep-th].

4. D. Benedetti, R. Gurau, and D. Lettera. "Dynamic critical exponent in quantum long-range models". In: (Apr. 2024). arXiv: 2404.13963 [hep-th].

In particular chapters 3, 4, 5 and 6 are respectively adapted versions of [1], [3], [4] and [2].

Summary

The main focus of this thesis is Quantum Field Theory and our investigation goes in two main directions. In a the first part (chapters 3 and 4) we mainly use the large-N expansion as a tool to investigate some non-perturbative properties of $O(N)$ vector models and $O(N)^3$ tensor models. Also (chapter 5), we study the critical properties of cubic and quartic fractional Lifshitz field theory using standard perturbation theory. In the second part (chapter 6) we study again the $O(N)$ vector model, but this time as a zero dimensional toy model of a QFT, on which we develop constructive techniques and describe non-perturbative contributions coming from instantons.

Chapters 1 and 2 are an introduction to the original research results, where we explain the context in which our work needs to be framed and give an overview of the most important technical tools that we used.

In chapter 3 we study a long-range tensor model with $O(N)^3$ symmetry, which was proven to have four lines of fixed points in the large-N limit. In particular, we test the famous F-theorem on such model, stating that in $d = 3$ the free energy on the sphere is monotonically decreasing going from the ultraviolet to the infrared along the renormalization group flow. We compute explicitly the free energy at two fixed points connected by a renormalization group trajectory and find that the F-theorem holds, which can be thought of as a further hint for the unitarity of the theory. The computation was technically challenging and it required to sum and infinite family of diagrams by means of the Conformal Partial Waves expansion. Also, we review the $O(N)$ vector model at large-N, that we use as a warm-up exercise to test our technology.

In chapter 4 we investigate the effects of compatifying one direction on Conformal Field Theories. The compact direction necessarily introduces an energy scale, i.e. the inverse of its size, that breaks conformal invariance. The main consequence is that one-point functions are no more constrained to be zero, enlarging the set of CFT data needed to fully characterize the theory. We review the long-range $O(N)$ vector model with one compact direction, show the existence of a non-trivial solution of the mass gap equation and of a stable IR fixed point at large-N. We compute the one-point functions of a specific family of bilinear operators at the large-N fixed point. Furthermore, we stress and discuss the difference between a classical statistical field theory and its corresponding quantum version, which becomes manifest when dealing with long-range theories. Indeed, long-range interactions are described by an action with a fractional Laplacian in the space directions, while the usual term with the double derivative with respect to time, coming from the quantum-to-classical mapping, is unchanged. Such kind of theories, which we call quantum fractional Lifshitz field theories, are manifestly anisotropic and the different role of time and space is evident, as opposed to the more common short-range theories in which their difference might be overlooked when working in Euclidean signature.

In chapter 5 we investigate the critical properties of quantum fractional Lifshitz field theories with cubic and quartic interaction. One interesting feature of Lifshitz field theories is that, while they break explicitly Lorentz or rotation invariance, they exhibit anisotropic scale invariance at fixed points of the renormalization group. Such anisotropic scale invariance is fully described by the anisotropy exponent z, which we compute to the first non-trivial order in perturbation theory.

In chapter 6 we study the quartic $O(N)$ vector model in zero dimensions, i.e. as a purely combinatorial toy model of a QFT. Working in zero dimensions fully trivialize the problem of computing Feynman amplitudes, making us able to study more easily the properties of the asymptotic perturbative expansion. We study both the partition function and the free energy as functions of the coupling constant by using constructive techniques such as the BKAR formula and Loop Vertex Expansion. The Loop Vertex Expansion requires to introduce an Hubbard–Stratonovich auxiliary field and it has the remarkable feature of having a finite radius of convergence. Furthermore, in the case of the $O(N)$ model, it formally corresponds to a small-N expansion. We prove Borel summability of both the

partition function, the free energy and the coefficients of their small-N expansion in all the directions of the complex plain. In order to do this, we need to analytically continue such quantities on a multi-sheeted Riemann surface, i.e. past a Stokes line. Finally, we compute their full transseries expansion which, past the Stokes lines, includes instanton-like non-analytic contribution encoding all the non-perturbative information. Despite the fact that some of the results on the topic were already understood by other means, we believe that our work is relevant as it set the ground for repeating the same analysis in QFT.

Zusammenfassung

Das Hauptinteresse dieser Dissertation gilt der Quantenfeldtheorie (QFT), und unsere Untersuchungen gliedern sich in die folgenden zwei Hauptrichtungen. Im ersten Teil (Kapitel 3 und 4) verwenden wir hauptsächlich die *large-N*-Entwicklung als Werkzeug, um nichtperturbative Eigenschaften von $O(N)$-Vektormodellen und $O(N)^3$-Tensormodellen zu studieren. Im zweiten Teil (Kapitel 6) untersuchen wir erneut das $O(N)$-Vektormodell, diesmal jedoch als nulldimensionales Spielzeugmodell einer QFT, auf dem wir Techniken der konstruktiven QFT erproben und nichtperturbative Beiträge von Instantonen berechnen.

Die Kapitel 1 und 2 dienen als Einführung in die ursprünglichen Forschungsergebnisse. Wir erläutern den Kontext, in dem unsere Arbeit eingeordnet werden sollte, und geben einen Überblick über die wichtigsten, von uns genutzten, technischen Werkzeuge.

In Kapitel 3 untersuchen wir ein Tensormodell mit langreichweitiger Wechselwirkung und $O(N)^3$-Symmetrie, das im *large-N*-Limit vier Linien von Fixpunkten aufweist. Insbesondere testen wir das berühmte F-Theorem, das besagt, dass in $d = 3$ die freie Energie auf der Sphäre entlang des Renormierungsgruppenflusses vom Ultraviolett- zum Infrarotbereich monoton abnimmt, an solch einem Modell. Wir berechnen explizit die freie Energie an zwei Fixpunkten, die durch eine Renormierungsgruppentrajektorie verbunden sind, und bestätigen die Gültigkeit des F-Theorems. Dies kann als weiterer Hinweis für die Unitarität der Theorie gesehen werden. Die technisch Anspruchsvolle Berechnung erforderte die Summation einer unendlichen Familie von Diagrammen mittels der Entwicklung in konforme Partialwellen. Außerdem betrachten wir das $O(N)$-Vektormodell im *large-N*-Limit und nutzen es als Aufwärmübung, um unsere Technik zu testen.

In Kapitel 4 untersuchen wir die Auswirkungen der Kompaktifizierung einer räumlichen Dimension auf konforme Feldtheorien (CFT). Die Kompaktifizierung führt zwangsläufig zu einer Energieskala, dem Kehrwert ihrer Größe, und bricht somit die konforme Invarianz. Die wichtigste Konsequenz ist, dass Einpunktfunktionen nicht mehr verschwinden müssen, was die Menge der CFT-Daten vergrößert, die zur vollständigen Charakterisierung der Theorie benötigt werden. Wir betrachten das langreichweitige $O(N)$-Vektormodell mit einer kompaktifizierten räumlichen Dimension, zeigen die Existenz einer nichttrivialen Lösung der Massenlückengleichung und eines stabilen IR-Fixpunkts im *large-N*-Limit. In diesem Grenzfall berechnen wir die Einpunktfunktionen einer spezifischen Familie von bilinearen Operatoren am Fixpunkt. Darüber hinaus betonen und diskutieren wir den Unterschied zwischen einer klassischen statistischen Feldtheorie und ihrer entsprechenden quantenmechanischen Version, der sich bei der Behandlung von langreichweitigen Theorien manifestiert. Langreichweitige Wechselwirkungen werden nämlich durch eine Wirkung mit einem fraktionalem Laplace-Operator in den räumlichen Richtungen beschrieben, während der übliche Term mit der zweifachen Zeitableitung, welcher aus der üblichen Zuordnung einer Quanten- zu einer klassischen statistischen Theorie herrührt, unverändert bleibt. Im Gegensatz zu den häufiger studierten kurzreichweitigen Theorien, bei denen der Unterschied zwischen Zeit und Raum, beim arbeiten in euklidischer Signatur übersehen werden kann, sind solche Theorien, die wir fraktional Lifshitz nennen, offensichtlich anisotrop und die unterschiedlichen Rollen von Zeit und Raum deutlich erkennbar.

In Kapitel 5 untersuchen wir die kritischen Eigenschaften von fraktionalen Lifshitz-Quantenfeldtheorien mit kubischer und quartischer Wechselwirkung. Eine interessante Eigenschaft von Lifshitz-Feldtheorien ist, dass sie zwar explizit Lorentz- oder Rotationsinvarianz brechen, aber anisotrope Skaleninvarianz an Fixpunkten der Renormierungsgruppe aufweisen. Eine solche anisotrope Skaleninvarianz wird vollständig durch den Anisotropieexponenten z beschrieben, den wir bis zur ersten nichttrivialen Ordnung in Störungstheorie berechnen.

In Kapitel 6 untersuchen wir das quartische $O(N)$-Vektormodell in null Dimensionen, d.h. als rein kombinatorisches Spielzeugmodell einer QFT. Die Arbeit in null Dimensionen trivialisiert das Problem der Berechnung von Feynman-Amplituden vollständig, so dass wir die Eigenschaften der

asymptotischen Störungsentwicklung leichter untersuchen können. Wir untersuchen sowohl die Zustandssumme als auch die freie Energie als Funktionen der Kopplungskonstante unter Verwendung von Techniken der konstruktiven QFT, wie der *Loop-Vertex*-Entwicklung und der BKAR-Formel. Die *Loop-Vertex*-Entwicklung erfordert die Einführung eines auxiliären Hubbard–Stratonovich-Feldes und hat bemerkenswerter Weise einen endlichen Konvergenzradius. Außerdem entspricht sie im Fall des $O(N)$-Modells formal einer *small-N*-Entwicklung. Wir beweisen die Borel-Summierbarkeit sowohl der Partitionsfunktion, der freien Energie als auch der Koeffizienten ihrer *small-N*-Entwicklung in allen Richtungen in der komplexen Ebene. Dazu müssen wir diese Größen auf einer mehrblättrigen Riemannschen Fläche, d.h. an einer Stokes-Linie vorbei, analytisch fortsetzen. Schließlich berechnen wir ihre vollständige Transreiheneentwicklung, die hinter den Stokes-Linien einen Instanton-ähnlichen nichtanalytischen Beitrag erhalten, der alle nichtperturbativen Informationen enthält. Trotz der Tatsache, dass einige der Ergebnisse zu diesem Thema bereits auf andere Weise verstanden wurden, glauben wir, dass unsere Arbeit relevant ist, da sie den Grundstein für die Wiederholung der gleichen Analyse in einer QFT legt.

Contents

List of Figures

Chapter 1

Introduction and motivations

On 5 July 1687 **Philosophiæ Naturalis Principia Mathematica** by Sir. Isaac Newton was first published. It is considered one of the most important works in the history of science, as it gives for the first time a comprehensive description of one of the fundamental forces of nature: gravity. Since then, thanks to the collective effort of many generations of scientists, we got to the point of understanding that our universe is governed by four fundamental forces: weak force, strong force, electromagnetism and gravity. By irony of fate, we have a satisfying enough description of all of them but gravity. In fact, incorporating the laws of quantum mechanics with gravity remains the biggest open problem of modern fundamental physics. Weak force, strong force and electromagnetism are described with the language of Quantum Field Theory (QFT) by the Standard Model of particle physics (a QFT with gauge group $SU(3) \times SU(2) \times U(1)$). In the Standard Model each fundamental particle is represented by a quantum field and the interaction between particles, i.e. scattering processes, can be described by computing correlation functions. The Standard Model describes with remarkable accuracy the interaction of sub-atomic particles up to the highest energy scale tested so far by the Large Hadron Collider (LHC) at CERN. Gravity is by far the weakest force and its effects can be neglected at the energy scale that is currently accessible ($\sim 14\ TeV$). On one side, this is what allows us to make very precise predictions on small scale phenomena even without fully understanding gravity. On the other hand, the lack of experimental data that can provide us with insights, is probably one of the reasons why a full understanding of gravity is still an open problem. The only information we can access comes from the universe around us, i.e. from astronomical data, which, however, are limited. By observing our universe we learned that, at very big length scales, gravity is the dominant force and it is described quite accurately by the classical theory of gravity: General Relativity. Recently we witnessed the observation of the the first Gravitational Waves, announced by the LIGO and Virgo collaborations on 11 February 2016. In particular, the signal coming from the merger of a pair of black holes of around 36 and 29 solar masses was detected via an interferometry experiment, confirming the old prediction by Einstein. On the other hand, the observation of the universe still provides us with numerous open problems, such as the problem of dark matter, or the black hole information paradox, and many others. The existence of phenomena that we are not able to describe efficiently, suggests that the theory of gravity needs to be improved, and it is believed that the true theory of gravity should be subject to the laws of quantum mechanics as the other three fundamental forces. For this reasons, reconciling gravity and quantum mechanics is the ultimate goal in the background of the work of the majority of theoretical physicists working in fundamental physics nowadays. This has proven to be an extremely difficult task, which led to the development of many different branches of theoretical physics such as: string theory, loop quantum gravity or causal dynamical triangulations. Furthermore it also boosted research in a number of directions more indirectly related to gravity, but still of great interest. For example the formal study of QFT models and their renormalization properties, Conformal Field Theories (CFT), large-N expansions, resurgence, and many others. All of these topics are extremely vast and incredibly interesting even beyond quantum gravity motivations. For example, the language of QFT can also be used in the context of condensed matter to describe quasiparticles, i.e. collective excitations of many particles that behave as one. Also, the theory of the

renormalization group can be use to efficiently describe phase transitions in such condensed matter systems, i.e. critical phenomena in which the macroscopic properties of a system change abruptly. The common feature of phase transitions is a divergent correlation length, which is the manifestation of a scale invariance developed at the transition. Furthermore, typically scale invariance implies conformal invariance, thus critical points are the object of study of CFTs, which can be considered as a special class of QFTs obtained by tuning to a fixed point of the renormalization group. Therefore, QFTs and CFTs are intimately related by the renormalization group and their investigation has to be carried out in parallel, as it is done by both the high energy and the condensed matter communities.

This is the context for my work, which consists of investigating certain selected aspects of QFT. More precisely, the work presented in this manuscript can be divided in two parts: the study of some QFT and CFT models via large-N expansions, and a constructive (convergent) expansion of a zero dimensional QFT toy model. As for the QFT/CFT part, we will mainly focus on long-range theories, which consist of field theoretical models for systems with non-local Gaussian term. Such kind of models are much less studied than short-range ones and they provide us with the opportunity of carrying out original work and new computations, not yet available in literature. From the merely technical point of view they are extremely interesting as they do not exhibit wave function renormalization, and because at the CFT level they have the peculiar property of not having a local stress-energy tensor in the spectrum. Also, from the experimental point of view, it is remarkable that they have been recently realized in laboratory [5]. Lastly, given the long-range nature of the interaction, the quantum statistical partition function is mapped to an anisotropic classical one, as it will be made more precise in chapters 4 and 5. However, despite the fact that Lorentz or rotation symmetries are broken explicitly, it is interesting how they exhibit a form of anisotropic scale invariance at fixed points of the renormalization group, which can be described in terms of the anisotropy exponent $z \neq 1$.

Large-N QFTs. The main tool used in the first part is the large-N expansion, i.e. a perturbative expansion in the inverse of the number of components of the field. As it will be reviewed in the next chapter, QFTs are typically very difficult and ill defined theories, which are fully solvable only in very exceptional cases like free theories, i.e. describing non interacting particles (or any degrees of freedom). A universal strategy available to address QFT is perturbation theory, which consists in making the approximation of small interaction and study deviations from the free theory. However, such approach is inherently limited not to describe efficiently strong interactions. A possible alternative approach, which is sometimes very useful, is to consider QFTs describing a large number of fields, or one field with a big number of components, and organize the perturbation theory as an expansion in $\frac{1}{\mathcal{N}}$ with $\mathcal{N}$ being the large number of components. In the limit of $\mathcal{N}$ strictly infinite, such modified perturbation theory can be truncated at the leading order and it is sometimes fully solvable, or at least easier. We will denote such theories as large-N theories. Furthermore, one can aim at describing theories with a finite number of degrees of freedom, i.e. fields, by including more and more sub-leading orders of the $\frac{1}{\mathcal{N}}$ expansion and setting $\mathcal{N}$ to the desired value afterwards. However, despite not being directly related to any observed phenomenon, already strictly large-N theories are extremely interesting, as they offer a unique ground for testing our understanding of QFT and CFT in a simple but less trivial case than free theories.

Historically, the large-N expansion was introduced in QFT as a computational tool for studying the $O(N)$ vector model [6, 7], in which the fields are taken to be vectors under the action of an $O(N)$ internal symmetry groups, but the same technique easily generalizes to $SU(N)$, $Sp(N)$ etc. In the strict large-N limit the dominant diagrams are extremely simple (local tadpole diagrams) and the theory becomes fully solvable. Furthermore, the $\frac{1}{N}$ expansion is so manageable that it can even be pushed to subleading orders. Such kind of models are very important as they describes real world systems as: the Ising model for $N = 1$, the XY model for $N = 2$, Heisenberg magnets for $N = 3$.

Soon after, the large-N expansion became very popular in the context of high energy physics thanks to its application to Quantum Chromodynamics (QCD), i.e. the sub-sector of the Standard Model describing the strong force. In that case the gauge group was enhanced from $SU(3)$ to $SU(N_c)$ taking N_c big [8], and unlike the vector model case, gauge fields transform as matrices of the $SU(N_c)$ group. In the strict large-N_c limit the dominant family of diagrams are planar diagrams, i.e. diagrams that can be drawn on a sphere without intersecting edges. However, despite this being an enormous simplification with respect to the finite N_c case, planar diagrams are still too many and cannot be re-summed.

After vector and matrix fields, the next natural step is to consider tensor fields with more than two indices. The main feature of tensor theories is that they allow a large-N expansion that is dominated by a subset of planar diagrams: melonic diagrams [9, 10, 11]. It is surprising that, while matrix fields exhibit a more difficult large-N limit than vectors, tensors are again simpler than matrices. Tensor theories were first introduced in zero dimensions as an attempt to describe quantum geometry and quantum gravity [12, 13]. The idea was to discretize the gravitational path integral, which is a sum over all possible geometries of space-time, and it was carried on by noticing that Feynman graphs generated by the perturbative expansion of tensor theories are dual to discretizations of such geometries. In the case of two dimensions, tensors with two indices need to be used, and this program successfully boosted the understanding of two-dimensional quantum gravity and string theories [14]. As for the higher dimensional case, large-N tensors with more than two indices turned out to describe branched polymer geometries, which have Hausdorff dimension 2 and spectral dimension $4/3$, i.e. smaller than two. More recently, tensor QFT ($d > 0$) gained new interests because they can be considered as generalizations of the SYK model [15] to dimension higher than one and without disorder, as they are both dominated by melonic diagrams at large N. Furthermore, tensor QFTs [16, 17, 18] provide a unique example of a models which are even less trivial than vector models, but still manageable at large N. Also, such large-N theories were found to have several interesting fixed points; we will refer to the Conformal Field Theories (CFT) sitting at those fixed points as melonic CFTs [19]. Thanks to the large-N tool, melonic CFTs are among the few existing $d > 2$ examples in which it is possible to compute analytically some of the CFT data.

Constructive expansion. Considering that perturbation theory is one of the main techniques for studying QFT, the problem of rigorously defining it is clearly of crucial importance in mathematical physics. The perturbative expansion in QFT suffers from three main problems: the divergences of amplitudes coming from loop integrals, the divergence of the perturbative series due to the factorial growth of the number of Feynman diagrams, and the problem of renormalons. One by one, all of these problems are relatively well understood, but, when put together, their interplay make things incredibly complicated. For example the problem of the divergence of Feynman diagrams is brilliantly solved by the theory of renormalization [20]. Indeed, perturbative renormalization tells us how to systematically subtract infinities order by order in perturbation theory, making the QFTs predictive at small coupling. The problem of the factorial growth of the perturbative series, in principle, could be addressed by means of the theories of Borel summability and resurgence [21]. Borel summability tells us that, given an asymptotic (i.e. divergent) series that meet the right set of assumptions, we can re-sum it and reconstruct the unique function which has the asymptotic series as its Taylor expansion. On top of that, and provided again that the right regularity conditions are met, Écalle theory of resurgence surprisingly allows to reconstruct also the full non-perturbative content coming from instantons, which is captured by objects known as transseries. However, in the case of QFT, it is in practice impossible to compute many terms of the perturbative expansion. The reason is twofold: first of all the coefficients of the perturbative expansion are a sum of Feynman integrals, which are complicated multidimensional integrals quite difficult to evaluate. Also, as we already mentioned, such Feynman integrals are in general divergent before renormalization, which is a very involved procedure

that cannot be pushed to more than 7 or 8 loops in the easiest theories. The last problem that we mentioned is that of renormalons: families of Feynman diagrams whose renormalized amplitude is factorially big. Renormalons constitute an additional source of divergence of QFTs, they can be dealt with on the same footing as instantons with the theory of resurgence, but they add an additional layer of difficulty to the problem of properly defining perturbation theory. In order to disentangle the three problems it is sometimes useful to investigate zero dimensional QFTs, as in that case the problem of the divergence of Feynamn diagrams and renormalons are completely trivialized.

A promising method for trying to define a convergent perturbative expansion is the Loop Vertex Expansion (LVE) [22]. The LVE relies on the introduction of an auxiliary field with a logarithmic potential interaction, which is bounded much better than polynomials at infinity, and on the Brydges–Kennedy–Abdessalam–Rivasseau (BKAR) Forest Formula [23, 24]. The LVE has been successfully applied to give a constructive treatment of a quartic scalar theory in two dimensions [25].

Plan of the thesis. Before discussing the research results, in chapter 2 we give an overview of the most important tools needed to understand the manuscript. In chapter 3 we investigate the properties of the melonic CFTs arising at the large-N fixed points of the $O(N)^3$ long-range model. In particular we test the famous F-theorem, stating that in three dimensions the free energy F on the sphere is monotonically decreasing along the renormalization group flow. In chapter 4 we study the effects of the compactification of one dimension on CFTs. We work with the long-range $O(N)$ vector model at large N and we compute some new CFT data, i.e. the coefficients of one-point functions. Furthermore, we stress and discuss the difference between a classical statistical field theory and its corresponding quantum version(quantum fractional Lifshitz field theories), which becomes manifest when dealing with long-range theories. In chapter 5 we study the critical properties of quantum fractional Lifshitz field theories, introduced in chapter 4. We consider scalar theories with cubic or quartic interaction, compute the beta functions to the first non-trivial order in perturbation theory and show that they admit an infrared stable fixed point. Afterwards, we compute the first quantum correction to the anisotropy exponent z at those fixed points. Finally, in chapter 6 we discuss the constructive expansion of the zero dimensional $O(N)$ model. We use the LVE, which in this case corresponds to a small-N expansion, to study the analytic properties of the partition function and the free energy in the complex plain of the coupling constant, prove Borel summability, describe the Stokes phenomenon and include the non-perturbative effects (i.e. computing the full transseries). Although at first this may look like an academic exercise, we are setting the ground for repeating the same analysis with a fully-fledged QFT in non zero dimensions.

Chapter 2

Background knowledge

In this chapter we review the basics of few selected topics that are widely used throughout the rest of the thesis, mostly related to QFT. Our goals are both to make the manuscript more self-consistent and to help the non expert readers to follow more easily what comes next. However, we do not aim at producing a comprehensive review, as it would be way beyond the scope of this thesis. Also, since in the thesis we will always consider Lorentz scalars, we will discuss only scalar fields.

2.1 Quantum Field Theory

In most of this manuscript we will assume that the readers are familiar with the basic concepts of Quantum Field Theory. However, in this section we will spend few words about it, more details can be found in the standard references [26, 27, 28, 29, 30].

The notation that we introduce in this section is self-consistent within the chapter, while in the rest of the thesis we sometimes slightly modify it at convenience.[1] However, all important notations are introduced again in each chapter as necessary.

2.1.1 General idea and perturbation theory

QFT can be thought of as a generalization of quantum mechanics to systems with a continuous number of degrees of freedom, i.e. a field Φ. In the framework of QFT it is possible to successfully describe a great number of physical phenomena, ranging from condensed matter physics to cosmology, not to mention particle physics. There are two main possible formulations: the Hamiltonian formulation and the path integral formulation, in this work we will not mention the former as we use only the latter.

The starting point of any QFT is a partition function in the form:

$$\mathcal{Z}_{QFT} = \int [D\Phi]\ e^{\imath S[\Phi]}\ , \tag{2.1.1}$$

where Φ represents schematically the collection of all the fields in the theory, and such fields are functions of the space-time coordinates $\Phi(t, \mathbf{x})$. $S[\Phi]$ is called the action of the theory and it is typically a polynomial function of the fields. The integral is a functional integral and it has a similar interpretation as the Feynman path integral in quantum mechanics, but in this case paths are parametrized by both space and time. Such a partition functions suffers of a number of problems, most of them rooted in the fact the functional integration is ill defined, with the only important exception of Gaussian theories. Another very important object of interests is a slight variation of (2.1.1), that is:

$$\mathcal{Z} = \int [D\Phi]\ e^{-S[\Phi]}\ , \tag{2.1.2}$$

[1] For example, as we will almost never use non-connected correlation functions, we will use the letter C for the propagator (covariance).

which has the advantage of having a real and negative exponent in the integrand. The interpretation of such object is varied. For example it can be obtained from a QFT by performing a Wick rotation, i.e. mapping the physical time to an imaginary "Euclidean" time $t \to -\imath\tau$, with the practical advantage of avoiding some of the divergences arising in perturbative computations. In this case referring to (2.1.2) as a QFT is a bit imprecise, as the description of a true QFT requires to Wick rotate back to the real time, which can be tricky. A partition function like (2.1.2) also describes a statistical field theory, in which the fields Φ are functions of space coordinates only $\Phi(\mathbf{x})$. Lastly, it can describe a QFT at finite temperatures, with the caveat of imposing periodic boundary conditions in the time direction $\Phi(t, \mathbf{x}) = \Phi(t + 1, \mathbf{x})$, this will be the framework of chapter 4. In the following we will always work with (2.1.2) and we will often refer to it as a QFT, always having in mind that it has to be interpreted as an Euclidean QFT or as a statistical field theory.

The fundamental objects of study of QFT are correlation functions, defined through the path integral with the insertion of a string of fields in the functional integral:

$$C^{(n)}(x_1, x_2, ..., x_n) = \frac{1}{\mathcal{Z}} \int [D\Phi]\ e^{-S[\Phi]} \Phi(x_1)\Phi(x_2)...\Phi(x_n)\ . \tag{2.1.3}$$

Correlation functions can be derived from the generating functional $\mathcal{Z}[J]$, defined as:

$$\begin{aligned} \mathcal{Z}[J] &= \int [D\Phi]\ e^{-S[\Phi] + \int_x J(x)\Phi(x)}\ , \\ C^{(n)}(x_1, ..., x_n) &= \frac{\delta}{\delta J(x_1)} ... \frac{\delta}{\delta J(x_n)} \mathcal{Z}[J]|_{J=0}\ . \end{aligned} \tag{2.1.4}$$

In principles, from such correlation functions one can extract the amplitudes of any physical process involving the degrees of freedom of the model Φ. However, as it is often the case in physics, it is practically impossible to compute exactly the object of interest $C^{(n)}(x_1, ..., x_n)$, unless the action is quadratic, i.e. the theory is Gaussian. In general, the best that we can do is to work in perturbation theory[2]. With this purpose, let us split the action in two parts:

$$S[\Phi] = S_0[\Phi] + S_I[\Phi]\ , \tag{2.1.5}$$

where in $S_0[\Phi]$ we collect all the quadratic terms of $S[\Phi]$, while in $S_I[\Phi]$ we collect all the other terms. We can compute correlation functions perturbatively by Taylor expanding in $S_I[\Phi]$:

$$C^{(n)}(x_1, x_2, ..., x_n) = \frac{1}{\mathcal{Z}} \int [D\Phi]\ e^{-S_0[\Phi]} \Phi(x_1)\Phi(x_2)...\Phi(x_n) \sum_{k=0}^{+\infty} \frac{1}{k!} \left(-S_I[\Phi]\right)^k\ , \tag{2.1.6}$$

by using the renowned Wick theorem:[3]

$$C^{(n)}(x_1, ..., x_{2n}) = \sum_{\text{parings}} \prod_{\text{pairs } (i,j)} C_0^{(2)}(x_i, x_j)\ , \tag{2.1.7}$$

where we introduced the notation $C_0^{(n)}$ for correlations of the Gaussian theory, i.e. computed using the quadratic part of the action $S_0[\Phi]$. Clearly $C_0^{(2)}$ plays a special role and it is often referred to as propagator or covariance. From now on we will conform to the standard notation and drop the superscript (2) in two-point functions.

[2] It is sometimes possible to get results beyond perturbation theory, for example via large-N expansions that we will discuss later, or with simulation on a lattice, or using functional renormalization.

[3] Here we aim at a short practical guide of how QFT computations are done. With this aim we do not mention many crucial (but standard) aspects of the theory.

Combining (2.1.6) and (2.1.7) we can evaluate any correlation function as a sum of amplitudes, and each of them can be attached to a graph called Feynman Diagram:

$$C^{(n)}(x_1, ..., x_n) = \sum_{\mathcal{G}} \mathcal{A}_{\mathcal{G}}(x_1, ..., x_n) \ . \tag{2.1.8}$$

In order to clarify the graph interpretation of the sum and to make clear how amplitudes are computed we briefly discuss the easiest possible example of an interactive theory. Let us consider the following action:[4]

$$\begin{aligned} S_0[\varphi] &= \int_x \frac{1}{2} \left(\delta_{\mu\nu} \partial^\mu \varphi(x) \partial^\nu \varphi(x) + m^2 \varphi^2(x) \right) \ , \\ S_I[\varphi] &= \frac{g}{4!} \int_x \ \varphi^4(x) \ , \end{aligned} \tag{2.1.9}$$

where φ is the only field and it is a Lorentz scalar, and g is the coupling constant of a quartic interaction. In this case (2.1.6) becomes:

$$C^{(n)}(x_1, ..., x_n) = \frac{1}{\mathcal{Z}} \int [D\varphi] \ e^{-S_0[\varphi]} \varphi(x_1) ... \varphi(x_n) \sum_{k=0}^{+\infty} \frac{1}{k!} \left(-\frac{g}{4!} \int_x \ \varphi^4(x) \right)^k \ , \tag{2.1.10}$$

then we can use the Wick theorem and we find schematically:

$$C^{(n)}(x_1, ..., x_n) = \sum_{k=0}^{+\infty} (-g)^k \left(\prod_i^k \int_{x_i'} \right) \sum_{\text{Wick contractions}} \prod C_0(x_a, x_b) \ . \tag{2.1.11}$$

We can now understand better the structure of the $\mathcal{A}_{\mathcal{G}}$ in (2.1.8), that is:

$$\mathcal{A}_{\mathcal{G}}(x_1, ..., x_n) = c \ g^p \left(\prod_{k=1}^{p} \int_{x_k} \right) \prod_{(x_i, x_j) \in E(\mathcal{G})} C_0(x_i, x_j) \ , \tag{2.1.12}$$

where $E(\mathcal{G})$ is the set of edges of a graph $\mathcal{G}$ with p internal vertices, while c is a combinatorial factor that counts multiplicity of terms and it is easy to be computed. For practical computation it is often easier to work in Fourier space, where we have $C_0(p) = \frac{1}{p^2 + m^2}$, and using the conservation of momenta at each interaction vertex the number of integrations can be reduced to the number of loops in the graph:

$$\mathcal{A}_G(p_E) = c \ g^p \left(\prod_L \int_{p_L} \right) \prod_e \frac{1}{p_e^2 + m^2} \ , \tag{2.1.13}$$

where we are labelling the external momenta with p_E, the loop momenta with p_L, and the momenta flowing through the edge $e \in E(\mathcal{G})$ with p_e. It is easy to show that the perturbative expansion is equivalent to a loop-expansion, and that loops corrections correspond to the inclusion of quantum

[4] Here and in the following we sometimes use the notation $\int_x = \int d^d x$ or $\int_x = \int d^{d-1}\mathbf{x} dt$ depending whether we work in Lorentzian or Euclidean signature. For integrals in momentum space we use similarly $\int_p = \int \frac{d\omega}{2\pi} \frac{d^{d-1}\mathbf{p}}{(2\pi)^2}$ or $\int_p = \int \frac{d^d p}{(2\pi)^2}$.

effects. For example, we find that $C^{(4)}(x_1,...,x_4)$ at first order in g is:

$$\begin{aligned} C^{(4)}(x_1,...,x_4) = &(C_0(x_1,x_2)C_0(x_3,x_4) + C_0(x_1,x_3)C_0(x_2,x_4) + C_0(x_1,x_4)C_0(x_2,x_3)) \\ &- \frac{1}{2}\, g \int_x C_0(x,x)\,(C_0(x_1,x_2)C_0(x,x_3)C_0(x,x_4) + (13)(24) + (14)(23)) \\ &- g \int_x C_0(x,x_1)C_0(x,x_2)C_0(x,x_3)C_0(x,x_4)\ . \end{aligned} \tag{2.1.14}$$

2.1.2 Connected and 1PI correlations

In order to reduce the number of diagrams that need to be evaluated it is useful to work with connected correlations $G^{(n)}(x_1,...,x_n)$, which are sums of connected Feynman diagrams only. We point out here that typically (but not always) $G(x_1,x_2) = C(x_1,x_2)$ because one-point functions are vanishing by parity, for example this is obviously true for Gaussian theories, hence $G_0(x_1,x_2) = C_0(x_1,x_2)$. As it is very standard in probability theory, going from correlations (moments) to connected correlations (cumulants) is easily achieved by taking the logarithm of the generating functional:

$$\begin{aligned} &W[J] = \log(\mathcal{Z}[J])\ , \\ &G^{(n)}(x_1,...,x_n) = \frac{\delta}{\delta J(x_1)}...\frac{\delta}{\delta J(x_n)}\mathcal{W}[J]|_{J=0}\ . \end{aligned} \tag{2.1.15}$$

Also, it is common to work with amputated correlations, i.e. connected correlations amputated of the external edges. For example, in momentum space we find that $G^{(4)}_{amp.}(p_1,...,p_4)$ at order g^2 writes:

$$G^{(4)}_{amp.}(p_1,...,p_4) = (2\pi)^d \delta(p_1+p_2+p_3+p_4)\left(-g + \frac{3}{2}\, g^2 \int_k \frac{1}{k^2+m^2}\frac{1}{(p+k)^2+m^2}\right)\ , \tag{2.1.16}$$

with $p = p_1 + p_2$ transferred momenta. As we already highlighted in the introduction, such a perturba-

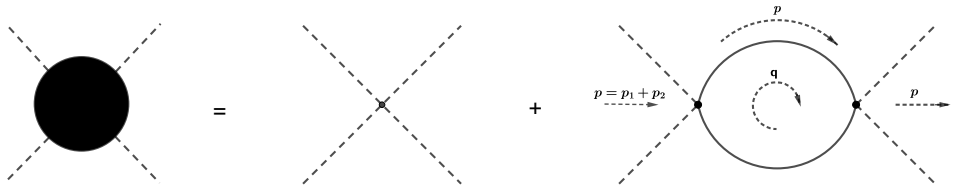

FIGURE 2.1: Amputated connected four-point function to 1-loop.

tive expansion suffers of a number of problems, the most obvious at this point being the fact that loops integrals in the Feynman amplitudes can be divergent. This means that at this stage all our writing is purely formal. In the next section we will address this problem when discussing renormalization.

Other very useful quantities are proper vertices $\Gamma^{(n)}(x_1,...,x_n)$, which are sums of one particle irreducible (1PI) diagrams. A connected and amputated Feynamn diagram is said to be 1PI when it stays connected after cutting one arbitrary internal edge. The generating functional of proper vertices,

known as effective action, is the Legendre transform of $W[J]$:

$$\begin{aligned}\Gamma[\phi] &= \sup_J\{\int_x J(x)\phi(x) - W[J]\} \ , \\ \Gamma[\phi] &= \sum_{n\geq 0}\frac{1}{n!}\left(\prod_{i=1}^{n}\int_{x_i}\right)\Gamma^{(n)}(x_1,...,x_n)\phi(x_1)...\phi(x_n) \ .\end{aligned} \tag{2.1.17}$$

From the definition it follows immediately that $\phi(x) = \frac{\delta W[J]}{\delta J(x)} = G^{(1)}(x)$. An alternative and operationally more useful definition of the effective action is:

$$e^{-\Gamma[\phi]} = \int_{1PI}[d\rho]\ e^{-S_E(\phi+\rho)} \ , \tag{2.1.18}$$

where the subscript of the integral means that, when expanding in diagrams, the sum should be restricted to 1PI terms. The effective action is a very important quantity, as it can be considered as the quantum generalization of the classical action. In fact its equation of motion at vanishing external source resemble the saddle point condition of a classical action, but it fixes the value of the one-point function $\phi(x) = \langle\varphi(x)\rangle$, i.e. the expectation value of the field:

$$\begin{aligned}&\text{Classic:} \quad \frac{\delta S[\varphi]}{\delta\varphi(x)} = 0 \ , \\ &\text{Quantum:} \quad \frac{\delta\Gamma[\phi]}{\delta\phi(x)} = 0 \ .\end{aligned} \tag{2.1.19}$$

Also, it is easy to show that:

$$\Gamma[\phi] = S[\phi] + (\text{quantum corrections}) \ , \tag{2.1.20}$$

where quantum corrections are terms that comes from loop corrections only. In momentum space it is common to redefine the proper vertices to factorize a delta function coming from the global conservation of momenta:

$$\Gamma^{(n)}(p_1,...,p_n) = (2\pi)^d\delta\left(\sum_{i=1}^{n}p_i\right)\bar{\Gamma}^{(n)}(p_1,...,p_n) \ . \tag{2.1.21}$$

The $\bar{\Gamma}^{(n)}(p_1,...,p_n)$ are actually functions of $n-1$ arguments, i.e. the constraint $\sum_{i=1}^{n}p_i = 0$ is always assumed. Lastly, it is also worth to mention the following general property:

$$\int_x \Gamma^{(2)}(x_1,x)G(x,x_2) = \delta(x_1-x_2) \ , \tag{2.1.22}$$

which can be derived easily by taking two derivatives with respect $\phi(x_2)$ and $J(x_1)$ on both sides of (2.1.17).

2.1.3 Schwinger-Dyson and Bethe-Salpeter equations

Schwinger-Dyson equation. A very useful equation for the connected two-point function $G(x_1,x_2)$ can be easily derived graphically. The simple idea is that, starting from the 1PI two-point function $\Gamma^{(2)}(x_1,x_2)$, we can reconstruct the connected one by joining 1PI blocks by propagators (see Fig. 2.2):

$$G^{(2)}(x_1, x_2) = C_0(x_1, x_2) + \int_{x'} \int_{x''} C_0(x_1, x')\Sigma(x', x'')C_0(x'', x_2) + \dots \,, \tag{2.1.23}$$

where $\Sigma(x_1, x_2)$ is the sum of 1PI two-point graphs, which it is called self energy. Then one can resum formally (2.1.23) and find:

$$G^{-1}(x_1, x_2) = C_0^{-1}(x_1, x_2) - \Sigma(x_1, x_2) \,. \tag{2.1.24}$$

Whenever it is possible to express the self energy in terms of $G(x_1, x_2)$, the Schwinger-Dyson equation becomes a self consistent equation for $G(x_1, x_2)$ itself. The diagrammatic derivation that we presented is incredibly simple and intuitive, but it required a formal resummation. In alternative we can take $\Gamma^{(2)}(x_1, x_2) \equiv C_0^{-1}(x_1, x_2) - \Sigma(x_1, x_2)$ as a definition of $\Sigma(x_1, x_2)$, then the Schwinger-Dyson equation follows immediately from (2.1.22).

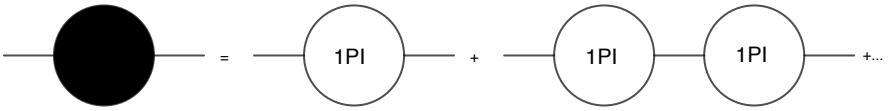

FIGURE 2.2: Diagrammatic representation of the Schwinger-Dyson equation. The line with the full ball on the left hand side represent the two-point function, lines represent propagators and the empty ball represent the self energy.

Bethe-Salpeter equation. A very similar reasoning can be used for the four-point function. Let us define $\mathcal{F}_s(x_1, x_2, x_3, x_4)$ the connected one particle irreducible four-point function in the s-channel $(12 \to 34)$, assuming for simplicity that odd n-point function are vanishing, we have:[5]

$$\mathcal{F}_s(x_1, x_2, x_3, x_4) = C^{(4)}(x_1, x_2, x_3, x_4) - C(x_1, x_2)C(x_3, x_4) \,. \tag{2.1.25}$$

We can now argue that, as $\mathcal{F}_s(x_1, x_2, x_3, x_4)$ is one particle irredicible in the s-channel, it can be written as a sum of ladders whose rungs are two particle irreducible in the s-channel. Defining the Bethe-Salpeter kernel $\mathcal{K}(x_1, x_2, x_3, x_4)$ as the two particle irreducible block that adds such rungs, we can write:

$$\mathcal{F}_s(x_1, x_2, x_3, x_4) = \int_{x'} \int_{x''} \left(\mathbb{I} - \mathcal{K}\right)^{-1} (x_1, x_2, x', x'')G(x', x_3)G(x'', x_4) \,, \tag{2.1.26}$$

where $\mathbb{I}(x_1, x_2, x_3, x_4) = \frac{1}{2}\left(\delta(x_1 - x_3)\delta(x_2 - x_4) + \delta(x_1 - x_4)\delta(x_2 - x_3)\right)$ and $\mathcal{K}(x_1, x_2, x_3, x_4)$ is nothing but the two particle irreducible four-point function in the s-channel amputated from the right (legs 3 and 4). See Fig. 2.3 for a diagrammatic representation.

The Bethe-Salpeter equation is a very powerful tool when the QFT is conformal, as we will discuss section 2.3. A more formal derivation of the Bethe-Salpeter equation, which goes beyond our simple diagrammatic argument, can be found by using the two particle irreducible (2PI) effective action formalism [31].

[5] The last term on the r.h.s of (2.1.25) makes $\mathcal{F}_s(x_1, x_2, x_3, x_4)$ connected in the s-channel. In general we need to subtract also the one particle reducible terms in the s-channel, but such terms are proportional to three-point function and they are zero in the case we are considering.

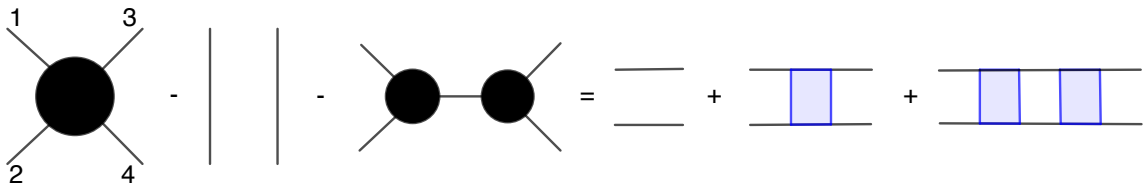

FIGURE 2.3: Diagrammatic representation of the Bethe-Salpeter equation. Left: full balls with n legs represents $n-$point functions, in theories with vanish odd n-point functions we need to subtract only the disconnected contribution in the channel $(12 \to 34)$ in order to define $\mathcal{F}_s$. Right: iterative insertion of the Bethe-Salpeter kernel.

2.1.4 Long-range models

Long-range models can be formally defined as QFTs with the following kinetic term (here we set $m^2 = 0$ for brevity):

$$S_0[\phi] \propto \int_x \phi(x) \left(-\partial^2\right)^\zeta \phi(x) \ , \tag{2.1.27}$$

where $\left(-\partial^2\right)^\zeta$ is the fractional Laplacian. There is more than one possible way to make sense of the fractional Laplacian. The most intuitive and operationally clear being to define it directly in momentum space:

$$S_0[\phi] \propto \int_p \tilde{\phi}(-p) p^{2\zeta} \tilde{\phi}(p) \ , \tag{2.1.28}$$

where $p^{2\zeta} \equiv \left(p^2\right)^\zeta$, which leads to the momentum space propagator $\frac{1}{p^{2\zeta}}$ instead of $\frac{1}{p^2}$. Alternatively one can work in direct space and define it through the action of the bi-local kernel $C_0^{-1}(x,y)$:

$$\begin{aligned} (-\partial^2)^\zeta \phi(x) = \int_y C_0^{-1}(x,y)\phi(y) \propto - \int_y \frac{\phi(y)}{|x-y|^{d+2\zeta}} \\ \Rightarrow \qquad S_0[\phi] \propto - \int_x \int_y \frac{\phi(x)\phi(y)}{|x-y|^{d+2\zeta}} \ . \end{aligned} \tag{2.1.29}$$

When dealing with computations of amplitudes of long-range theories it is often useful to use the Schwinger representation of the propagator:

$$\begin{aligned} C_0(p) &= \frac{1}{p^{2\zeta}} = \frac{1}{\Gamma(\zeta)} \int_0^{+\infty} d\alpha \ \alpha^{\zeta-1} e^{-\alpha p^2} \ , \\ C_0(x-y) &= \frac{1}{(4\pi)^2 \Gamma(\zeta)} \int_0^{+\infty} d\alpha \ \alpha^{\zeta-1-d/2} e^{-\frac{|x-y|^2}{4\alpha}} \ . \end{aligned} \tag{2.1.30}$$

Long-range models are interesting for several reasons, the most technical being that they do not exhibits wave function renormalization (i.e. no anomalous dimension of the fundamental field) due to the non-local kinetic term. Furthermore, their realizations in the context of defect or boundary field theories [32] and the fact that they have been realized experimentally in recent years [5] have also contributed to renewing theoretical interest around them.

2.2 Renormalization

2.2.1 Perturbative renormalization

In the context of QFT, renormalization [33, 20] emerges naturally from the need of taking out infinities and make the theory predictive. In this section we try to sketch how this happens and why it is so powerful.

The idea. In the previous section we defined proper vertices $\Gamma^{(n)}(x_1, ..., x_n)$ and their generating functional $\Gamma[\phi]$. In the following we will always prefer to use proper vertices as they expand in one particle irreducible graphs, which are less than connected graphs. We have:

$$\Gamma^{(n)}(x_1, ..., x_n) = \sum_{1\text{PI } \mathcal{G}} \mathcal{A}_{\mathcal{G}}(x_1, ..., x_n) \ , \tag{2.2.1}$$

and each of the $\mathcal{A}_{\mathcal{G}}$ is an integral of the kind (2.1.12). A priori there is no reason why such integrals should be convergent, and in general they are not. Infrared divergencies are never a big problem, as they can be avoided by keeping a finite mass or by working at non zero external momenta. Ultraviolet divergencies are more problematic and need to be subtracted. The first step for subtracting the divergencies is, of course, to identify them. Given the specific form of the action $S[\Phi]$, it is possible to compute the external degree of divergence of graphs and identify which of the $\Gamma^{(n)}(x_1, ..., x_n)$ suffer from UV divergencies. Starting from (2.1.13) we introduce a sharp UV cutoff at $p_L = \Lambda$, and assuming an interaction of the form:

$$S_I[\varphi] = \frac{g^{(q)}}{q!} \int_x \varphi^q(x) \ , \tag{2.2.2}$$

it is easy to find:

$$\mathcal{A}_{\mathcal{G}}(p_E) \propto \Lambda^{d+V\left(\frac{d(q-2)}{2}-q\right)+n\left(1-\frac{d}{2}\right)} \ , \tag{2.2.3}$$

where n is the number of external points and V is the number of interaction vertices, i.e. the order in perturbation theory. The exponent of (2.2.3) is usually called degree of divergence $\deg(\mathcal{G})$ of the graph $\mathcal{G}$:

$$\deg(\mathcal{G}) = d + V\left(\frac{d(q-2)}{2} - q\right) + n\left(1 - \frac{d}{2}\right) \ . \tag{2.2.4}$$

The example of the previous section corresponds to the case $q = 4$. The $\deg(\mathcal{G})$ tells us if and how a graph is divergent. Whenever $\deg(\mathcal{G}) > 0$ the graph is divergent and the UV cutoff cannot be removed unless divergences are subtracted first. QFTs can be classified as follows

- **Non-renormalizable:** if $\left(\frac{d(q-2)}{2} - q\right) > 0$. In this case a graph in the theory becomes more and more divergent as the order in perturbation theory increase, meaning that we need to renormalize more and more $\Gamma^{(n)}(x_1, ..., x_n)$.
- **Renormalizable:** if $\left(\frac{d(q-2)}{2} - q\right) = 0$. In this case the divergence do not depend at all on the number of vertices. In this case we need to renormalize only the $\Gamma^{(n)}(x_1, ..., x_n)$ for which $d + n\left(1 - \frac{d}{2}\right) > 0$. However, there is still an infinite number of divergent graph, as they can have an arbitrary number of vertices. The statement of renormalizability is that they all contribute to a finite number of proper vertices.
- **Super-renormalizable:** if $\left(\frac{d(q-2)}{2} - q\right) < 0$. In this case going up with order in perturbation theory improves the convergence of graphs, i.e. only a finite number of graphs need to be renormalized.

We define n_{cr} as the solution of $d + n_{cr}\left(1 - \frac{d}{2}\right) = 0$, in the case of renormalizable theories only the $\Gamma^{(n)}(x_1, ..., x_n)$ with $n < n_{cr}$ need to be renormalized. We have that: for $q = 3$ a scalar field theory is renormalizable in $d = 6$ and $n_{cr} = 3$, for $q = 4$ the scalar field theory is renormalizable in $d = 4$ and $n_{cr} = 4$, while for $q = 6$ a scalar field theory is renormalizable in $d = 3$ and $n_{cr} = 6$. From (2.1.20) it follows that:

$$\Gamma^{(q)}(x_1, ..., x_q) = g^{(q)} + \text{quantum corrections} , \tag{2.2.5}$$

where the quantum corrections contain the divergencies. The rough idea of perturbative renormalization is to redefine $g^{(q)} \to g^{(q)} + D_\Lambda$, with D_Λ cutoff dependent and divergent quantities, called counter terms, chosen such that all the $\Gamma^{(n)}(x_1, ..., x_n)$ are finite order by order in perturbation theory. The goal is to make the whole effective action finite.

Systematic procedure. We now make this procedure more systematic for the case $q = 4$. Let us introduce a renormalized action:

$$S_r[\varphi_r] = \int_x \left(\frac{1}{2} Z \delta_{\mu\nu} \partial^\mu \varphi_r(x) \partial^\nu \varphi_r(x) + \frac{1}{2}(m_r^2 + \delta m^2)\varphi_r^2(x) + \frac{1}{4!}\mu^{4-d} g_r \mathcal{Z}_g \varphi_r^4(x) \right) , \tag{2.2.6}$$

in which the space-time dimension d is chosen such that the interaction is exactly marginal, while μ is a renormalization scale that we introduced to make g_r dimensionless. The renormalized action is nothing but the action we started with, usually called bare action, but expressed in terms of renormalized quantities. Notice that, in the case of renormalizable and super-renormalizabile theories it is consistent to set $g_r^{(n)} = 0$, for $n > n_{cr}$. The reason being that the corresponding $\Gamma^{(n)}(x_1, ..., x_n)$ are finite, hence we will never need counterterms for them and they will not be generated by quantum corrections. Therefore, in the action (2.2.6) we included only the quartic interaction.[6]

The statement that the bare and the renormalized action are two reparametrization of the same object, leads to the relation between bare and renormalized quantities:

$$\begin{aligned} &\varphi(x) = Z^{1/2}\varphi_r(x) , \\ &m^2 = (m_r^2 + \delta m^2)/Z , \\ &g = \mu^{4-d} g_r Z_g / Z^2 . \end{aligned} \tag{2.2.7}$$

One find that Z, $\delta m^2/m_r^2$ and Z_g all start from one and expand in powers of g_r:

$$\begin{aligned} Z &= 1 + \sum_{p\geq 1} z^{(p)} g_r^p , \\ \delta m^2/m_r^2 &= 1 + \sum_{p\geq 1} a^{(p)} g_r^p , \\ Z_g &= 1 + \sum_{p\geq 1} z_g^{(p)} g_r^p . \end{aligned} \tag{2.2.8}$$

In more complicated cases, when more than one marginal couplings are present, they expand in a power series of all of them.

Renormalization is always performed in two steps

- **Regularization:** we first need to make the divergent amplitudes finite, i.e. regularize them. This can be achieved with many different techniques, the more intuitive being the introduction a cutoff Λ on the momentum space integrals. Another widely used techniques is that of dimensional

[6] Notice that also $\Gamma^{(3)}(x_1, x_2, x_3) = 0$ by parity.

regularization, which consists in an analytic continuation of the divergent integrals to a space-time dimension for which they are convergent. In the quartic theory that we are using as an example we could compute integrals in $d = 4 - \epsilon$ with $\epsilon > 0$, then infinities manifest themselves as $\frac{1}{\epsilon}$ poles. Dimensional regularization is widely used as it is operationally much simpler than many other regularization techniques.

- **Subtraction:** once the infinities have been isolated we need to subtract them through the right choice of coefficients in (2.2.8), which is called a renormalization scheme. However, such choice is not unique, as not all the renormalization schemes are compatible with all regularization techniques. Also, one is always free to subtract the infinities plus an arbitrary finite quantity. A very common renormalization scheme, consistent with dimensional regularization, is the minimal subtraction, which consist in subtracting only the $\frac{1}{\epsilon}$ poles at some renormalization scale μ. An alternative is to perform the subtraction keeping renormalized proper vertices fixed, for example:

$$\begin{aligned} &\bar{\Gamma}_r^{(2)}(|p| = \mu) = m_r^2 + \mu^2 \ , \\ &\partial^2 \bar{\Gamma}_r^{(2)}(|p| = \mu) = 1 \ , \\ &\bar{\Gamma}_r^{(4)}(\{|p_i| = \mu\}) = g_r \ . \end{aligned} \tag{2.2.9}$$

From now, unless it is stated explicitelly, we will use only dimensional regularization.

Flow equations. By now it should be clear that the procedure of renormalization is not unique, as it involves the choice of a regularization technique and of a renormalization scheme. However, there is at least one feature which is shared by all the possible choices: we always need to introduce a dimensionful parameter that plays the role of the renormalization scale. This seemingly small and technical detail hides a very deep physical consequence, i.e. the renormalized quantities depend on the energy scale. It is always possible to extract all the information about such energy scale dependence by the very natural requirement that bare quantities do no know anything about the artificially introduced energy scale. We now make this more precise in the case of a massless quartic theory with dimensional regularization, which is a particularly interesting case as $m_r^2 = 0$ is a necessary condition in order to have fixed point solutions of the renormalization group flow.

For the proper vertices in momentum space we have:

$$\mu \frac{d}{d\mu}\bigg|_g \bar{\Gamma}^{(n)}(\{p_i\}_n; g) = 0 \ , \tag{2.2.10}$$

Using the relation $\bar{\Gamma}^{(n)}(\{p_i\}_n; g) = Z^{-n/2} \bar{\Gamma}_r^{(n)}(\{p_i\}_n; g_r, \mu)$ and the chain rule of derivatives we find:

$$\left[\mu \partial_\mu + \beta(g_r)\partial_{g_r} - \frac{n}{2}\eta(g_r)\right] \bar{\Gamma}_r^{(n)}(\{p_i\}_n; g_r, \mu) = 0 \ , \tag{2.2.11}$$

where $\beta(g_r)$ and $\eta(g_r)$, are known as beta function and anomalous dimension, and they are given by

$$\beta(g_r) = \mu \frac{d}{d\mu}\bigg|_g g_r \ , \qquad \eta(g_r) = \mu \frac{d}{d\mu}\bigg|_g \log Z \ . \tag{2.2.12}$$

These kind of differential equations are known as Renormalization Group Equations and they describe how correlations (connected or proper vertices) change with the energy scale introduced during

renormalization. By homogeneity[7], such energy scale can be traded for a scaling factor on momenta:

$$\left[-s\partial_s + \beta(g_r)\partial_{g_r} - \frac{n}{2}\eta(g_r) + [\bar{\Gamma}^{(n)}]\right]\bar{\Gamma}_r^{(n)}(\{sp_i\}_n; g_r, \mu) = 0 \ , \tag{2.2.13}$$

where $[\bar{\Gamma}^{(n)}]$ is the mass dimension of $\bar{\Gamma}^{(n)}$. The solution can be found easily with the characteristic curve method:

$$\bar{\Gamma}_r^{(n)}(\{sp_i\}_n, g_r(s), \mu) = s^{[\bar{\Gamma}^{(n)}]}\exp\left\{-\frac{n}{2}\int_1^s \frac{ds'}{s'}\eta(g_r(s'))\right\}\bar{\Gamma}_r^{(n)}(\{p_i\}_n, g_r(s), \mu) \ , \tag{2.2.14}$$

with $g_r(s)$ being the solution of

$$s\partial_s g_r(s) = \beta(g_r(s)) \ , \qquad\qquad g_r(1) = g_r \ . \tag{2.2.15}$$

Equation (2.2.14) describes how correlations depend on the energy at which they are observed. A class of particularly important solutions are fixed point solutions, i.e. the solutions corresponding to a characteristic curve which is sitting at a fixed point $\beta(g^\star) = 0$. In this case, the solution (2.2.14) becomes a simple scaling invariant:

$$\bar{\Gamma}_r^{(n)}(\{sp_i\}_n, g^\star, \mu) = s^{[\bar{\Gamma}^{(n)}]-\frac{n}{2}\eta(g^\star)}\bar{\Gamma}_r^{(n)}(\{p_i\}_n, g^\star, \mu) \ . \tag{2.2.16}$$

If the renormalized coupling at the starting energy scale is not a fixed point, it is needed to study the flow of the coupling. For example for the quartic massless theory with minimal subtraction we have

$$\beta(g_r) = -\epsilon g_r + A g_r^2 + \dots \ , \qquad\qquad A = \frac{3}{16\pi^2} > 0 \tag{2.2.17}$$

which has a fixed point at $g^\star = \frac{\epsilon}{A}$. The characteristic curve of the coupling is:

$$g_r(s) = \frac{\epsilon g_r}{A g_r - (A g_r - \epsilon)s^\epsilon} \ , \tag{2.2.18}$$

which flows at $g^\star$ in the infrared ($s \to 0$) and to zero in the ultraviolet ($s \to +\infty$).

2.3 Basics of Conformal Field Theory

In the previous section we showed how, at fixed points of the renormalization group flow, scaling symmetry for correlations emerges. Therefore, when tuned to a fixed point, any QFT fulfill a bigger symmetry algebra than the Lorentz one. Certainly such symmetry algebra needs to include dilatations on top of Lorentz transformation, but surprisingly it turns out that most of the times there is even more symmetry hiding, i.e. special conformal transformations [34]. The interested reader can find more details in [35, 36]

2.3.1 The Conformal Algebra

The conformal group can be defined formally as the set of diffeomorphisms that leave the metric unchanged up to an overall coordinate dependent scale factor:

$$g'_{\mu\nu}(x') = \frac{\partial x^\rho}{\partial x'^\mu}\frac{\partial x^\sigma}{\partial x'^\nu}g_{\rho\sigma}(x) = \Lambda(x)g_{\mu\nu}(x) \ . \tag{2.3.1}$$

[7] We used $\left(\mu\partial_\mu + s\partial_s - [\bar{\Gamma}^{(n)}]\right)\bar{\Gamma}^{(n)}(\{sp_i\}_n, g_r, \mu) = 0$, $[\bar{\Gamma}^{(n)}]$ being the mass dimension of the proper vertx.

For an infinitesimal transformation of the form $x'^{\mu}(x) = x^{\mu} + \epsilon^{\mu}(x)$ it becomes:

$$\partial_{\mu}\epsilon_{\nu} + \partial_{\nu}\epsilon_{\mu} = \frac{1}{d}\partial^{\rho}\epsilon_{\rho}g_{\mu\nu} \ , \tag{2.3.2}$$

with d being the space-time dimension. The solution of (2.3.2) is:

$$\epsilon^{\mu} = c^{\mu} + a_{\mu\nu}x^{\nu} + b_{\mu\nu\rho}x^{\nu}x^{\rho} \ , \tag{2.3.3}$$

in which $b_{\mu\nu\rho}$ can actually be expressed in terms of one single vector $b_{\sigma\ \mu}^{\ \sigma}$ via $b_{\mu\nu\rho} = \frac{1}{d}\left(b_{\nu}g_{\mu\rho} + b_{\rho}g_{\mu\nu} - b_{\mu}g_{\nu\rho}\right)$. Such infinitesimal parameters correspond to the following infinitesimal transformations:

$$\begin{aligned}
&x'^{\mu} = x^{\mu} + c^{\mu} \ , && \text{(translations)} \\
&x'^{\mu} = x^{\mu} + \lambda x^{\mu} \ , && \text{(dilatations)} \\
&x'^{\mu} = x^{\mu} + a^{\mu}_{\nu}x^{\nu} \ , && \text{(Lorentz rotations)} \\
&x'^{\mu} = x^{\mu} + 2(b_{\rho}x^{\rho})x^{\mu} - x^{2}b^{\mu} \ . && \text{(special conf. transf.)}
\end{aligned} \tag{2.3.4}$$

where in the last line we can see the unexpected extra transformations. Once we have the explicit form of conformal transformations, the commutation rules follows easily. The full conformal algebra writes:

$$\begin{aligned}
&[D, P_{\mu}] = \imath P_{\mu} \ , \\
&[D, K_{\mu}] = -\imath K_{\mu} \ , \\
&[K_{\mu}, P_{\nu}] = 2\imath\left(\eta_{\mu\nu}D - M_{\mu\nu}\right) \ , \\
&[M_{\mu\nu}, P_{\rho}] = -\imath\left(\eta_{\mu\rho}P_{\nu} - \eta_{\nu\rho}P_{\mu}\right) \ , \\
&[M_{\mu\nu}, K_{\rho}] = -\imath\left(\eta_{\mu\rho}K_{\nu} - \eta_{\nu\rho}K_{\mu}\right) \ , \\
&[M_{\mu\nu}, M_{\rho\sigma}] = -\imath\left(M_{\mu\rho}\eta_{\nu\sigma} - M_{\mu\sigma}\eta_{\nu\rho} - M_{\nu\rho}\eta_{\mu\sigma} + M_{\nu\sigma}\eta_{\mu\rho}\right) \ .
\end{aligned} \tag{2.3.5}$$

Where P_{μ}, D, $M_{\mu\nu}$ and K_{μ} are respectively the generators of translations, dilatations, Lorentz rotations and special conformal transformations. Representations of the conformal algebra on fields can be constructed by noticing that P_{μ} and K_{μ} act as raising and lowering operators for D and assuming that in each multiplets there exists an operator $\mathcal{O}(x)$ which is annihilated by K_{μ}. Such kind of operators are called primary operators, while all the other operators in the multiplets are called descendants and can be obtained by acting repeatedly with P_{μ} on the primary.

2.3.2 Conformal n-point functions

Conformal symmetry impose very restrictive conditions on n-point functions of primary operators. Such conditions are so constraining that the functional form of two-point functions is completely fixed and the only free parameter left is the mass dimension of the operators. Three-point functions are completely fixed up to mass dimensions of operators and an overall multiplicative factor. Higher n-point functions can be reduced to a sum of two and three-point functions via the Operator Product Expansion (OPE), that we will discuss shortly. For this reason, it is often said that a CFT is fully defined by the list of the operators in the theory together with two set of numbers: their scaling dimensions and their three-point function coefficients. Such set of numbers is often referred to as CFT data. We will often denote scalar primary operators as $\mathcal{O}_i$, while for the case of symmetric traceless spinning operator with spin J we introduce the notation $\mathcal{O}^{\bar{\mu}}_{(h,J)}$, with h scaling dimension and $\bar{\mu} \equiv (\mu_1, ..., \mu_J)$

2-pt function of scalars. The form of two-point functions of two scalar operators is:

$$\langle \mathcal{O}_i(x_1)\mathcal{O}_j(x_2)\rangle = \frac{\delta_{ij}}{|x_1-x_2|^{2\Delta_i}} \ , \tag{2.3.6}$$

with Δ_i being the scaling dimension of operators $\mathcal{O}_i(\lambda x) = \lambda^{-\Delta_i}\mathcal{O}_i(x)$.

3-pt function of scalars. For the three-point function of scalar operators we have:

$$\langle \mathcal{O}_i(x_1)\mathcal{O}_j(x_2)\mathcal{O}_k(x_3)\rangle = \frac{C_{\Delta_i\Delta_j\Delta_k}}{|x_{12}|^{\Delta_i+\Delta_j-\Delta_k}|x_{13}|^{\Delta_i+\Delta_k-\Delta_j}|x_{23}|^{\Delta_j+\Delta_k-\Delta_i}} \tag{2.3.7}$$

2-pt function of spinning operators. In the case of spinning operators we have:

$$\langle \mathcal{O}^{\bar{\mu}}_{(\Delta,J)}(x_1)\mathcal{O}_{\bar{\mu},(\Delta,J)}(x_2)\rangle = \frac{I^{\mu_1}_{(\nu_1}(x_{12})...I^{\mu_J}_{\nu_J)}(x_{12}) - \text{traces}}{|x_1-x_2|^{2\Delta}} \ , \tag{2.3.8}$$

where $x_{12} \equiv |x_1 - x_2|$ and $I^{\mu}_{\nu}(x) = \delta^{\mu}_{\ \nu} - 2\frac{x^\mu x_\nu}{x^2}$.

3pt functions of a spinning operator with 2 scalars. Lastly, we have that the three-point function of two scalars and one spinning operator is:

$$\langle \mathcal{O}_i(x_1)\mathcal{O}_j(x_2)\mathcal{O}^{\bar{\mu}}_{(h,J)}(x_3)\rangle = C_{\Delta_i\Delta_j(h,J)}\frac{Z_{\mu_1}...Z_{\mu_j} - \text{traces}}{|x_{12}|^{\Delta_i+\Delta_j-h+J}|x_{13}|^{\Delta_i+h-J-\Delta_j}|x_{23}|^{\Delta_j+h-J-\Delta_i}} \ , \tag{2.3.9}$$

with $Z_\mu = \frac{(x_{13})_\mu}{|x_{13}|^2} - \frac{(x_{23})_\mu}{|x_{23}|^2}$.

2.3.3 Operator Product Expansion

The Operator Product Expansion states that the product of two operators can be expanded in an infinite product of local operators. We have:

$$\mathcal{O}_i(x_1)\mathcal{O}_j(x_2) = \sum_{h,J} F^{\bar{\mu}}_{ij(h,J)}(x_{12},\partial_2)\mathcal{O}_{\bar{\mu}(h,J)}(x_2) \ , \tag{2.3.10}$$

but such equality holds only inside correlations, i.e. it is a statement about states and not about operators. In QFT the OPE is only asymptotic, but in CFT it is convergent at finite point separation [37]. The reason of this remarkable property lies in the state-operator correspondence, that we will not discuss here, which allows us to interpret the OPE as expansion in a complete Hilbert space. It can easily be proved that the function $F^{\bar{\mu}}_{ij(h,J)}(x_{12},\partial_2)$ in (2.3.10) is proportional to the coefficient of the three-point functions. In particular we have:

$$\mathcal{O}_i(x_1)\mathcal{O}_j(x_2) = \sum_{h,J} c_{\Delta_i\Delta_j(h,J)} f^{\bar{\mu}}_{ij(h,J)}(x_{12},\partial_2)\mathcal{O}_{\bar{\mu}(h,J)}(x_2) \ , \tag{2.3.11}$$

where $f^{\bar{\mu}}_{ij(h,J)}(x_{12},\partial_2)$ can be computed exactly and is not model dependent.

If we apply the OPE on the s-channel of a four-point function of scalars we find:

$$\langle \mathcal{O}_i(x_1)\mathcal{O}_j(x_2)\mathcal{O}_k(x_3)\mathcal{O}_l(x_4)\rangle = \sum_{h,J} c_{\Delta_i\Delta_j(h,J)}c_{\Delta_k\Delta_l(h,J)}G^{\Delta_i\Delta_j\Delta_k\Delta_l}_{h,J}(x_i) \ , \tag{2.3.12}$$

where $G_{h,J}^{\Delta_i\Delta_j\Delta_k\Delta_l}(x_i)$ are called Conformal Blocks and in many cases they are know explicitly. In equation (2.3.12) we choose arbitrarily to perform the OPE in the s-channel, but we could have done the same in the t or u-channels. Performing the OPE on different channels and equating the results provides self-consistent equations called crossing equations, which are the starting point of the Conformal Bootstrap program [38, 39].

2.3.4 Conformal Partial Waves expansion

A very useful technique used to extract some CFT data is the Conformal Partial Wave (CPW) expansion [40, 41, 42]. Here we give a very short introduction to the topic, but more details can be found in the Appendix 3.E of chapter 3. Conformal Partial Waves can be defined as a convolution of three-point functions:

$$\Psi_{h,J}^{\Delta,\Delta,\widetilde{\Delta},\widetilde{\Delta}}(x_1,x_2,x_3,x_4)=\int \mathrm{d}^d z\,\langle\phi_\Delta(x_1)\phi_\Delta(x_2)\mathcal{O}^{\bar{\mu}}_{(h,J)}(z)\rangle_{\mathrm{cs}}\langle\phi_{\widetilde{\Delta}}(x_3)\phi_{\widetilde{\Delta}}(x_4)\mathcal{O}_{\bar{\mu},(\tilde{h},J)}(z)\rangle_{\mathrm{cs}}\,, \tag{2.3.13}$$

where we introduced the notation $\widetilde{\Delta}=d-\Delta$ for the shadow dimensions, the cs underscript indicates a conformal structure with OPE coefficients set to one, and we are using the notation $\phi_\Delta(x)$ for a scalar operator with dimension Δ to conform with the notation that we will use in the manuscript when studying explicit field theoretical models (in which the fundamental field can be identified with the smallest primary in the theory).

It is possible to think of four-point functions as endomorphism $\mathcal{E}:\mathcal{V}_\Delta\to\mathcal{V}_\Delta$ with $\mathcal{V}_\Delta$ being the appropriate space of bi-local functions[8] and it turns out that conformal three-point functions form a complete and orthonormal basis for $\mathcal{V}_D$, labelled by the spin $J\in\mathbb{N}_0$, the position $x_0\in\mathbb{R}^d$, and the scaling dimension $h\in\mathcal{P}_+$. Where $\mathcal{P}_+$ is known as principal series:

$$\mathcal{P}_+=\left\{h\;\middle|\;h=\frac{d}{2}+\imath r,\,r\in\mathbb{R}_+\right\}. \tag{2.3.15}$$

The completeness relation reads:

$$\begin{aligned}\mathbb{I}(x_1,x_2,x_3,x_4)&\equiv\delta(x_1-x_3)\delta(x_2-x_4)\\&=\sum_{J\in\mathbb{N}_0}\int_{\frac{d}{2}}^{\frac{d}{2}+\imath\infty}\frac{\mathrm{d}h}{2\pi\imath}\rho(h,J)\,\mathcal{N}^{\Delta}_{h,J}\mathcal{N}^{\widetilde{\Delta}}_{\tilde{h},J}\,\Psi_{h,J}^{\Delta,\Delta,\widetilde{\Delta},\widetilde{\Delta}}(x_1,x_2,x_3,x_4)\,,\end{aligned} \tag{2.3.16}$$

where $\mathcal{N}^{\Delta}_{h,J}$ are explicit normalization factors and $\rho(h,J)$ is called Plancherel weight:

$$\rho(h,J)=\frac{\Gamma(\frac{d}{2}+J)}{2(2\pi)^{d/2}J!}\frac{\Gamma(\tilde{h}-1)\Gamma(h-1)}{\Gamma(\frac{d}{2}-h)\Gamma(\frac{d}{2}-\tilde{h})}(h+J-1)(\tilde{h}+J-1)\,. \tag{2.3.17}$$

Using the completeness relation we can always express an endomorphism $\mathcal{E}:\mathcal{V}_\Delta\to\mathcal{V}_\Delta$ in terms of CPWs. If we insert the identity (2.3.16) in the Bethe-Salpeter equation (2.1.26) and use the fact that

[8] More precisely, the space of bilocal functions $\mathcal{V}_\Delta$ can be defined as the space of smooth functions $f(x_1,x_2)$ that are square integrable with respect to the scalar product:

$$(f_1,f_2)=\int_{x_1\ldots x_4}\overline{f_1(x_1,x_2)}C^{-1}(x_1,x_3)C^{-1}(x_2,x_4)f_2(x_3,x_4)\,, \tag{2.3.14}$$

i.e. $(f,f)<\infty$, and satisfy the asymptotic boundary condition $f(x_1,x_2)\sim|x_1|^{-2\Delta}$ for $|x_1|\to\infty$ and similar for $|x_2|\to\infty$.

the three-point functions are eigenfunctions of the Bethe-Salpeter kernel we find:

$$\begin{aligned}\mathcal{F}_s(x_1,x_2,x_3,x_4) = &\sum_{J\in\mathbb{N}_0}\int_{\frac{d}{2}}^{\frac{d}{2}+\imath\infty}\frac{\mathrm{d}h}{2\pi\imath}\frac{\rho(h,J)}{1-k(h,J)}\mathcal{N}^{\Delta}_{h,J}\mathcal{N}^{\Delta}_{\tilde{h},J}\,\Psi^{\Delta,\Delta,\Delta,\Delta}_{h,J}(x_1,x_2,x_3,x_4)\\ &-\sum_{i,J}\mathrm{Res}\left[\frac{\rho(h,J)}{1-k(h,J)}\mathcal{N}^{\Delta}_{h,J}\mathcal{N}^{\Delta}_{\tilde{h},J}\,\Psi^{\Delta,\Delta,\Delta,\Delta}_{h,J}(x_1,x_2,x_3,x_4)\right]_{h=h_i(J)<d/2}.\end{aligned} \tag{2.3.18}$$

In the second line we are adding by hands the contribution from operators with dimension smaller than $\frac{d}{2}$ as such terms are not in $\mathcal{V}_\Delta$, and $k(h,J)$ are the eigenvalues of the Bethe-Salpeter kernel:

$$\int_{x_3,x_4}K(x_1,x_2,x_3,x_4)\,\langle\phi_\Delta(x_3)\phi_\Delta(x_4)\mathcal{O}^{\bar{\mu}}_{(h,J)}(x_0)\rangle_{\mathrm{cs}} = k(h,J)\,\langle\phi_\Delta(x_1)\phi_\Delta(x_2)\mathcal{O}^{\bar{\mu}}_{(h,J)}(x_0)\rangle_{\mathrm{cs}}\,. \tag{2.3.19}$$

A slight improvement of (2.3.18) can be achieved by using the fact that CPWs can be expressed as linear combination of Conformal Blocks:

$$\mathcal{F}_s(x_1,x_2,x_3,x_4) = \sum_{J\in\mathbb{N}_0}\int_{\frac{d}{2}-\imath\infty}^{\frac{d}{2}+\imath\infty}\frac{\mathrm{d}h}{2\pi\imath}\frac{1}{1-k(h,J)}\,\mu^d_\Delta(h,J)\,G^{\Delta\Delta\Delta\Delta}_{h,J}(x_1,x_2,x_3,x_4), \tag{2.3.20}$$

where $\mu^d_{h,J}(h,J)$ is an explicit known number, sometimes called conformal measure (here we are assuming for simplicity that there are no contributions from operators with $\Delta<\frac{d}{2}$). Equation (2.3.20) is the most useful form of the CPW expansion of the four-point function as, in principle, it is very easy to extract some CFT data from it. If we close the contour of integration on the right we pick contributions from poles located at $k(h,J)=1$, hence such condition allow us to find out which operators appear in the OPE of two $\phi_\Delta(x)$. Furthermore, by comparison with (2.3.12), we can read their OPE coefficients, which are nothing but the residues at the poles:

$$c^2_{\Delta\Delta(h,J)} = \left.\frac{\mu^d_\Delta(h,J)}{k'(h,J)}\right|_{k(h,J)=1}. \tag{2.3.21}$$

Of course in general it is difficult to compute $k(h,J)$, but it is sometimes possible for large-N fixed points.

2.4 Large-N limit and non-perturbative renormalization

A very useful means of studying QFT and CFT beyond perturbation theory, is the large number of components expansion, often called large-N expansion. Let us consider a QFT with the fundamental fields being scalars $\phi_i(x)$, with i transforming in an irreducible representation of a global symmetry group $\mathcal{G}$. Such group can be for example $O(N)$, $U(N)$, $Sp(N)$, $O(N)^2$, $O(N)^3$, in all the cases the number of components grows with N. The idea of large-N expansions is to apply the perturbation theory machinery using $\frac{1}{N}$ as the expansion parameter. In this section we summarize some aspects of $O(N)$ (vector) models and $O(N)^3$ (rank-3 tensor) models, while we do not mention the important case of matrix models as it is never studied in the rest of the manuscript.

2.4.1 $O(N)$ model

Let us consider the theory (see [43] for an extensive review):

$$S[\phi_a] = \int_x \frac{1}{2}\phi_a(x)(-\partial^2)\phi_a(x) + \frac{1}{2}m_b^2\phi^2(x) + \frac{\lambda}{4N}(\phi^2(x))^2\,, \tag{2.4.1}$$

where $(-\partial^2)$ stands for $\partial_\mu \partial_\nu \delta^{\mu\nu}$, $\phi_a(x)$ transforms in the fundamental representation of $O(N)$, and $\phi^2(x) = \phi_a(x)\phi_a(x)$. In the graphs arising in perturbation theory there are both explicit factors of $\frac{1}{N}$ coming from the quartic vertex and factors of N coming from contractions of $O(N)$ indices. It is useful to represent vertices as in Fig. 2.4, such that one can keep track of the contraction of $O(N)$ indices. With such graphical representation it is easy to understand how amplitudes of graphs get a factor $\frac{1}{N}$ per dashed line and a factor of N per loop of continuous lines. The graphs contributing to the leading large-N limit are the graphs that maximize the number of loops at given number of dashed lines (powers of λ).

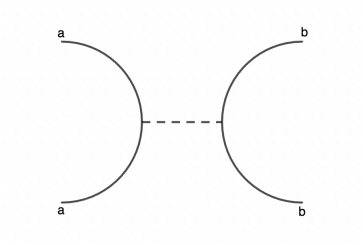

FIGURE 2.4: Graphical representation of the quartic vertex, the dashed line represents the $\frac{\lambda}{4N}$ vertex itself while the continuous lines on the left and on the right keep track of the $O(N)$ indices.

The $\frac{1}{N}$ expansion. Let us now study the N dependence of a generic vacuum graph (see in Fig. 2.5), its amplitute $\mathcal{A}$ is proportional to:

$$\mathcal{A} \propto \left(\frac{\lambda}{N}\right)^V N^{L_N} \,, \tag{2.4.2}$$

where V is the number of vertices, i.e. number of dashed lines, while L_N is the number of loops of the $O(N)$ indices, i.e. loops of solid lines.

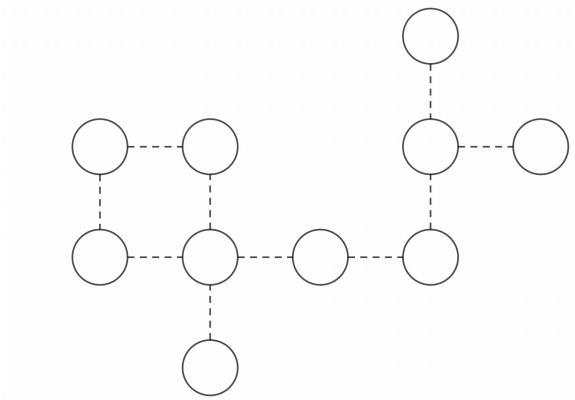

FIGURE 2.5: Example of a vacuum graph.

Now we need to use the Euler formula, stating that for a graph $\mathcal{G}$ embedded on a Riemann surface the following identity holds:

$$v - e + f = 2 - 2g \,, \tag{2.4.3}$$

where v, e and f are respectively the number of vertices, edges and faces of the graph $\mathcal{G}$, while g is the genus of the Riemann surface. Let us consider the graph obtained using the loops of solid lines as

vertices and dashed lines as edges, we have $v = L_N$ and $e = V$. Applying Euler formula we find:

$$\mathcal{A} \propto \left(\frac{\lambda}{N}\right)^V N^{2-2g+V-f} = \lambda^V N^{2-2g-f} = \lambda^V N^{1-l} \,, \tag{2.4.4}$$

where we have used $e-v+1 = l$, with l being the number of dashed lines loops. Therefore, the large-N limit is dominated by trees. Furthermore, the whole $\frac{1}{N}$ expansion corresponds to a loop expansion (an example of a subleading graph with $l = 1$ is in Fig. 2.5).

Large-N Schwinger-Dyson equation. The Schwinger-Dyson equation (2.1.24) of such model simplifies significantly in the large-N limit, in particular we have:

$$G^{-1}(p) = C_0^{-1}(p) + \lambda \int_q G(q) \,, \tag{2.4.5}$$

which is clearly divergent and needs to be renormalized. The fact that $\int_q G(q)$ is local suggests that the momentum dependence of the full two-point function $G(p)$ does not get modified by the interaction. Therefore we can look for solutions in the form $G^{-1}(p) = p^2 + m_r^2$:

$$m_r^2 = m_b^2 + \lambda \int_q \frac{1}{q^2 + m_r^2} \,, \tag{2.4.6}$$

which provides a self-consistent equation for the renormalized mass m_r^2, known as mass gap equation. A very simple solution can be found by tuning the theory to criticality $m_r^2 = 0$ and choosing $m_b^2 = -\frac{\lambda}{2}\int_q \frac{1}{q^2}$.

Large-N Bethe-Salpeter equation. In the large-N limit, the connected four-point function is given by a sum of chains of bubbles diagrams[9], with full leading-order propagator on each edge ($m_r^2 = 0$), see Fig. 2.6. Therefore, the proper vertex in momentum space reads:

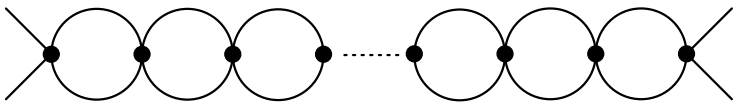

FIGURE 2.6: Chain of bubbles with $n \geq 1$ vertices. The connected four-point function is given by the sum of all such chains.

$$\Gamma^{(4)}(p) = \frac{2\lambda}{1 + \lambda B(p)} \,, \tag{2.4.7}$$

where p is the total transferred momentum and $B(p)$ is the bubble integral:

$$B(p) = \int \frac{d^d q}{(2\pi)^d} \frac{1}{q^2 (p-q)^2} = b(d)|p|^{d-4} \,. \tag{2.4.8}$$

[9]This comes from the Bethe-Salpeter equation (2.1.26) after subtracting the disconnected terms in the t and u channels.

where $b(d) = \frac{\Gamma\left(2-\frac{d}{2}\right)\Gamma\left(\frac{d}{2}-1\right)^2}{(4\pi)^{\frac{d}{2}}\Gamma(d-2)} > 0$. We define the renormalized dimensionless coupling g at some renormalization group scale $|p| = \mu$ as:

$$g = \mu^{d-4}\Gamma^{(4)}(\mu)/2 \,. \tag{2.4.9}$$

It follows that the beta function is:

$$\beta(g) = \mu\frac{dg}{d\mu} = -(4-d)g + b(\Delta_\phi)(4-d)g^2 \,. \tag{2.4.10}$$

Therefore, for $d < 4$ the beta function has a zero (i.e. a fixed point) at $g^\star = \frac{1}{b(d)}$. We can trivially invert the relation between bare and renormalized coupling to get:

$$\mu^{d-4}\lambda = \frac{g}{1 - b(\Delta_\phi)g} \,, \tag{2.4.11}$$

hence the fixed point corresponds to the limit $\lambda \to \infty$[10].

The intermediate field formalism. Another very useful approach is to introduce a auxiliary field $\sigma(x)$ by the Hubbard–Stratonovich trick:

$$\begin{aligned} Z &= \int [D\phi_i][D\sigma] e^{-S[\phi_i,\sigma]} \,, \\ S[\phi_i,\sigma] &= \int_x \left(\frac{1}{2}\phi_a(x)(-\partial^2)\phi_a(x) + \frac{1}{2}m_b^2\phi^2(x) - \frac{N}{4\lambda}\sigma^2(x) + \frac{1}{2}\sigma(x)\phi^2(x) \right) \,. \end{aligned} \tag{2.4.12}$$

Using this representation of the theory there is only one cubic interaction vertex. If we represent $\phi(x)$ propagators with full lines and $\sigma(x)$ propagators with dashed lines, the quartic interaction vertex in Fig. 2.4 can be interpreted as two cubic interaction vertices joined by a $\sigma(x)$ propagator. The $\Phi_a(x)$ integrals can be computed explicitly and we find:

$$\begin{aligned} Z &= \int [D\sigma] e^{-S[\sigma]} \,, \\ S[\sigma] &= \int_x \left(\frac{N}{2}\log\left(-\partial^2 + m_b^2 + \sigma(x)\right) - \frac{N}{4\lambda}\sigma(x)^2 \right) \,. \end{aligned} \tag{2.4.13}$$

All the terms in the action are proportional to N, which now plays the same role as $\frac{1}{\hbar}$ in the semi-classical(loop) expansion. Therefore, in the large-N limit the partition function is dominated by the saddle point of the exponent, located at the solution of the equation of motion for $\sigma(x)$, i.e. $\frac{\delta S[\sigma]}{\delta\sigma(x)} = 0$. Assuming $\sigma(x) = \sigma$ constant, we find:

$$\int_q \frac{1}{q^2 + m_b^2 + \sigma} = \frac{\sigma}{\lambda} \,, \tag{2.4.14}$$

which is clearly divergent for $d > 2$. Let us now define a renormalized mass $m_r^2 = m_b^2 + \sigma$, equation (2.4.13) becomes:

$$m_r^2 = m_b^2 + \lambda \int_q \frac{1}{q^2 + m_r^2} \,, \tag{2.4.15}$$

which is again the mass gap equation that we already derived from the Schwinger-Dyson equation.

[10] Note that it is actually the combination $\mu^{d-4}\lambda$ which goes to infinity, i.e. the bare dimensionless coupling

2.4.2 The $O(N)^3$ model

Tensor field theories are QFTs with tensors $\Phi_{i_1 i_2 i_3 \dots}$ as fundamental degrees of freedom, and they gained a big interests as they can exhibit a $\frac{1}{N}$ expansion similar to the one of the SYK model. There exist a wide variety of such models, which can be divided in two categories:

- **Colored tensor model:** contain more than one tensor field, i.e. we can assemble these tensors into a single one with an additional index labelling colors.
- **Uncolored tensor models** contain one single tensor field, i.e. they are colored tensor model with just one color.

Historically, colored tensor models were studied first and they were shown to have a $\frac{1}{N}$ expansion dominated by melonic diagrams [9, 10], which are a particular subset of planar graphs. Later on, it was discovered that it is not necessary to introduce the complication layer of having multiple colors to lead to a $\frac{1}{N}$ expansion. In particular in [11] it was shown that an uncolored model in $d = 0$[11] with the tensor field transforming in the tri-fundamental representation of $O(N)^3$: $\phi_{abc} \to O_{aa'} O_{bb'} O_{cc'} \phi_{a'b'c'}$ and with quartic interaction:

$$V_I \propto \phi_{a_1 b_1 c_1} \phi_{a_1 b_2 c_2} \phi_{a_2 b_1 c_2} \phi_{a_2 b_2 c_1} \ , \tag{2.4.16}$$

has a $\frac{1}{N}$ expansion with melonic large-N limit. In [16] a similar model with bosonic fields in $d > 0$ was studied for the first time and it was found to have an interesting fixed point in $d = 4 - \epsilon$ dimensions. Another very interesting example is the long-range version of such model [17], which has a number of different features. First of all, by tuning the long-range parameter ζ, it is possible to find fixed points in any dimension $2 < d < 4$ (including the interesting case of $d = 3$), and not only in $d = 4 - \epsilon$. Furthermore, one of the couplings of the theory stays exactly marginal and can be further tuned at wish, leading to 1-parameter families of fixed points (lines of fixed points). In particular four lines of fixed points were found, one of them being IR stable and, with good evidence, unitary. Here we review such long-range model, as it is the starting point of chapter 3.

$O(N)^3$ long-range model. The fundamental field is a real rank-3 tensor field, $\phi_{a_1 a_2 a_3}(x)$, transforming under $O(N)^3$ with indices distinguished by the position (typically labelled by a color). Denoting $\mathbf{a} = (a_1, a_2, a_3)$, the action of the model reads:

$$\begin{aligned} S[\phi] = \frac{1}{2} \int \mathrm{d}^d x \, \phi_{\mathbf{a}} (-\partial^2)^\zeta \phi_{\mathbf{a}} + \frac{m^{2\zeta}}{2} \int \mathrm{d}^d x \, \phi_{\mathbf{a}} \phi_{\mathbf{a}} \\ + \frac{1}{4} \int \mathrm{d}^d x \, \left[\mathrm{i} \, \lambda \hat{\delta}^t_{\mathbf{abcd}} + \lambda_1 \hat{P}^{(1)}_{\mathbf{ab;cd}} + \lambda_2 \hat{P}^{(2)}_{\mathbf{ab;cd}} \right] \phi_{\mathbf{a}} \phi_{\mathbf{b}} \phi_{\mathbf{c}} \phi_{\mathbf{d}} \, , \end{aligned} \tag{2.4.17}$$

where repeated tensor indices are summed over $a^i = 1, \cdots, N$ and we introduced the projectors:

$$\hat{P}^{(1)}_{\mathbf{ab;cd}} = 3(\hat{\delta}^p_{\mathbf{ab;cd}} - \hat{\delta}^d_{\mathbf{ab;cd}}) \, , \qquad \hat{P}^{(2)}_{\mathbf{ab;cd}} = \hat{\delta}^d_{\mathbf{ab;cd}} \, . \tag{2.4.18}$$

and the rescaled operators:

$$\hat{\delta}^t_{\mathbf{abcd}} = \frac{1}{N^{3/2}} \delta^t_{\mathbf{abcd}} \, , \quad \hat{\delta}^p_{\mathbf{ab;cd}} = \frac{1}{N^2} \delta^p_{\mathbf{ab;cd}} \, , \quad \hat{\delta}^d_{\mathbf{ab;cd}} = \frac{1}{N^3} \delta^d_{\mathbf{ab;cd}} \, , \tag{2.4.19}$$

[11] In the paper the authors deal with a combinatorial model in which fields are simple real variable, i.e. there are not Feynman integrals. In the case of QFT the combinatorics and the $\frac{1}{N}$ expansion obviously do not change.

with:

$$\delta^t_{\mathbf{abcd}} = \delta_{a^1b^1}\delta_{c^1d^1}\delta_{a^2c^2}\delta_{b^2d^2}\delta_{a^3d^3}\delta_{b^3c^3}\,,$$
$$\delta^p_{\mathbf{ab;cd}} = \frac{1}{3}\sum_{i=1}^{3}\delta_{a^ic^i}\delta_{b^id^i}\prod_{j\neq i}\delta_{a^jb^j}\delta_{c^jd^j}\,, \qquad \delta^d_{\mathbf{ab;cd}} = \delta_{\mathbf{ab}}\delta_{\mathbf{cd}}\,. \tag{2.4.20}$$

Here t stands for *tetrahedron*, p for *pillow*, and d for *double-trace*. Such names refer to the graphical representation of the respective pattern of contraction of indices (see Fig. 2.7).

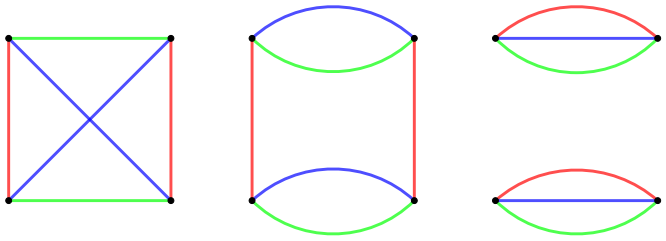

FIGURE 2.7: Graphical representation of the interaction vertices. Each field is represented with a black dot and each $O(N)$ index is represented with a colored half edge, therefore full edges represents contraction of indices. Left: *tetrahedron* vertex. Center: *pillow* vertex. Right: *double-trace* vertex.

The faithfully acting symmetry group of the model is $S_3 \times O(N)^3/\mathbb{Z}_2^2$, where the quotient by $\mathbb{Z}_2^2$ is to eliminate the redundancy of having a $\mathbb{Z}_2$ as subgroup in each $O(N)$, and S_3 is the permutation group acting on the indices. Symmetry under the latter is often called "color symmetry", due to using color as a label distinguishing the indices. For the sake of simplicity we just refer to the model as the $O(N)^3$ model.

The power of the Laplacian is taken to be $\zeta = d/4$, so that the dimension of the field is $\Delta = d/4$ and the quartic couplings are marginal by power counting. Moreover, one assumes $d < 4$ so that the kinetic term is non-local, the propagator is unitary, and local derivative interactions are irrelevant. It should be noted that the usual dimensional regularization setting $d = 4 - \epsilon$ is not suitable for this model, as at $d = 4$ the model becomes short-range and its renormalization properties differ drastically. The appropriate ϵ regularization for the long-range model is to set $\zeta = (d + \epsilon)/4$, corresponding to $\Delta = (d - \epsilon)/4$, at fixed $d < 4$.

The main feature of the $O(N)^3$ model is that in the large-N limit its perturbative expansion is dominated by melonic diagrams built on λ vertices, mixed with cactus diagrams built on λ_1 and λ_2 vertices, as we will prove in the following. Melonic graphs can be constructed recursively by iteratively inserting a prime melonic graphs (Fig. 2.8) on the edges of a melonic graph.

Lastly, the imaginary unit multiplying the tetrahedron interaction is introduced so that in the present notation the large-N OPE spectrum is real for real λ [17, 44]. This is to be contrasted to the short-range $O(N)^3$ model of [45, 16], for which the tetrahedral term is necessarily real due to the fixed point condition, and as a consequence the model contains operators of complex dimension.

4-colored graphs. It is very useful to represent Feynman diagrams as 4-colored graphs, and this is done as follows. Interaction vertices are represented as 3-colored graphs as in Fig. 2.7 which we call bubbles, where each edge represents the contraction of two $O(N)$ indices, and the $O(N)$ indices of the three copies of $O(N)$ are distinguished by the three colors ($i = 1, 2, 3$). Propagators are represented

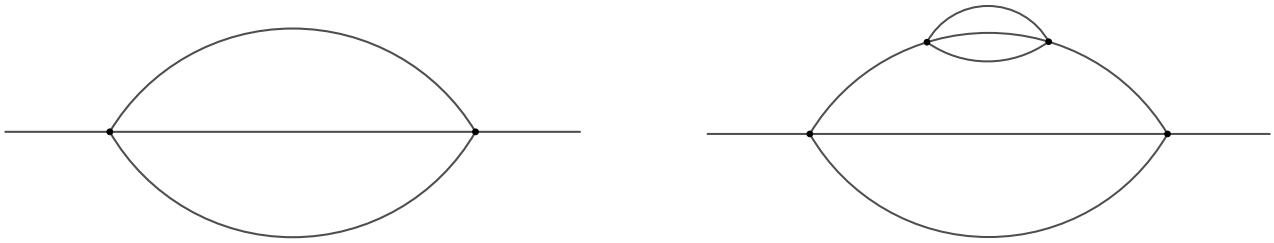

FIGURE 2.8: Left: prime melonic graph. Right: first iterative insertion of the prime melonic graph in one of its edges.

as lines of a fourth color (labelled as 0) joining two vertices (fields) of two different 3-colored bubbles. Propagators (black lines) transmit all of the three indices at the same time, i.e. they can be thought of as lines of any color $1 \leq i \leq 3$ at the same time. The advantage of such representation is that it allow us to keep track of the contraction of $O(N)$ indices. In particular, a graph $\mathcal{G}$ gets a power of N for every loop made with lines of two colors 0 and i, we call faces such two-colored loops. The usual Feynman diagrams can be easily recovered by shrinking the bubbles to points, and they contain enough information to reconstruct the corresponding Feynman integral only, but not the N dependence. See Fig. 2.9 for an example.

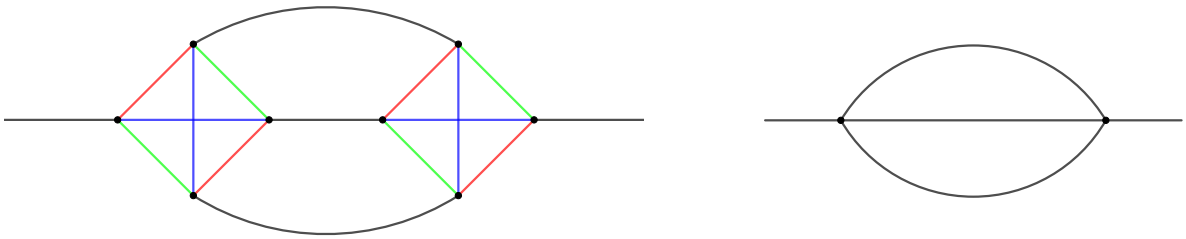

FIGURE 2.9: Left: example of a 4-colored graph contributing to the two-point function. Since there are 3 faces the amplitude of the graph gets a power N^3 from the contraction of $O(N)$ indices. Right: shrinking the two tetrahedral bubbles to a point we go back to the standard Feynman diagram.

Melonic large-N limit. Now we show that the model has a $\frac{1}{N}$ expansion [11, 45]. Let us define $n_t(\mathcal{G})$, $n_p(\mathcal{G})$ and $n_d(\mathcal{G})$ as the number of respectively tetrahedral, pillow and double-trace bubbles. We have that the scaling in N of a generic graph is:

$$\mathcal{A}_{\mathcal{G}} \propto N^{F(\mathcal{G})-\frac{3}{2}n_t(\mathcal{G})-2n_p(\mathcal{G})-3n_d(\mathcal{G})} , \tag{2.4.21}$$

where $F(\mathcal{G})$ is the total number of faces. We notice that it is possible to generate the pillow and the double-trace interaction as radiative correction of tetrahedrons (see Fig. 2.10), then we can also define a new graph $\hat{\mathcal{G}}$ obtained by substituting the pillow and double-trace bubbles with their minimal resolutions in terms of tetrahedrons. Such new graph has only tetrahedron bubbles but the same scaling in N, which now writes:

$$\mathcal{A}_{\hat{\mathcal{G}}} \propto N^{F(\hat{\mathcal{G}})-\frac{3}{2}n_t(\hat{\mathcal{G}})} . \tag{2.4.22}$$

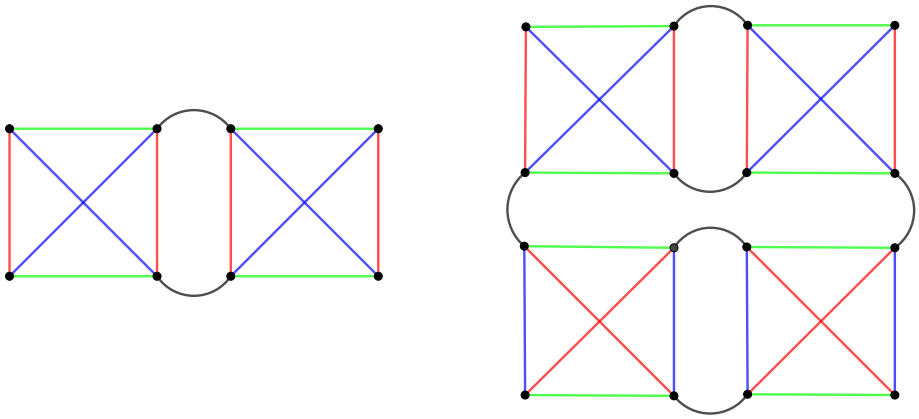

FIGURE 2.10: Left: Feynman graph with external tensor contraction equivalent to the pillow. Right: Feynman graph with external tensor contraction equivalent to the double-trace.

Starting from our 4−colored graph $\hat{\mathcal{G}}$ it is possible to define 3 Ribbon graphs by ignoring the faces of color $0i$, we call them jackets $\mathcal{J}^i$. The number of faces of such jackets can be expressed in terms of their genus $F(\mathcal{J}^i) = n_t(\hat{\mathcal{G}}) - 2 - k(\mathcal{J}^i)$. Since each face of $\hat{\mathcal{G}}$ belongs to two jackets we have that the total number of faces of $\hat{\mathcal{G}}$ is:

$$F(\hat{\mathcal{G}}) = \frac{3}{2} n_t(\hat{\mathcal{G}}) + 3 - \frac{1}{2} \sum_{i=1}^{3} k(\mathcal{J}^i) \ , \tag{2.4.23}$$

which combined with (2.4.22) and fact that $\mathcal{G}$ and $\hat{\mathcal{G}}$ have the same scaling in N leads to:

$$\mathcal{A}_{\mathcal{G}} \propto N^{3-\omega(\mathcal{G})} \ , \tag{2.4.24}$$

where $\omega(\mathcal{G}) = \frac{1}{2}\sum_i^3 k(\mathcal{J}^i)$ is called degree. Considering that $k(\mathcal{J}^i) \geq 0$, equation (2.4.24) is a bound on the polynomial growth of a generic graph in N, which is enough to prove the existence a $\frac{1}{N}$ expansion. Furthermore, the leading order graphs are such that $\omega(\mathcal{G}) = 0$. By the standard arguments [46] $\mathcal{G}$ has degree zero if and only if $\hat{\mathcal{G}}$ is melonic, i.e. the leading order graphs are melonic after substituting all the pillows and double-trace vertices by their minimal realizations in terms of the tetrahedral vertex. In terms of the original interactions, the graph $\mathcal{G}$ is a melon-tadpole graph, which is obtained by iterated insertions of melon and tadpole diagrams in the prime melonic graph (See Fig. 2.11).

Summary of results. The main features of the model are [47, 44, 17]:

- The tetrahedral coupling λ is exactly marginal.
- All the insertions of melonic two-point functions in the diagrams can be eliminated by rescaling each coupling by the square of an appropriate function $\mathcal{Z}(\lambda)$, which is a finite constant. In particular, we define $g = \lambda \mathcal{Z}(\lambda)^2$. This can be achieved by solving the large-N Schwinger-Dyson equation:

$$G^{-1}(x,y) = C_0^{-1}(x,y) + \left(m^{2\zeta} + \lambda_2 G(x,x)\right)\delta(x-y) + \lambda^2 G(x,y)^3 \, , \tag{2.4.25}$$

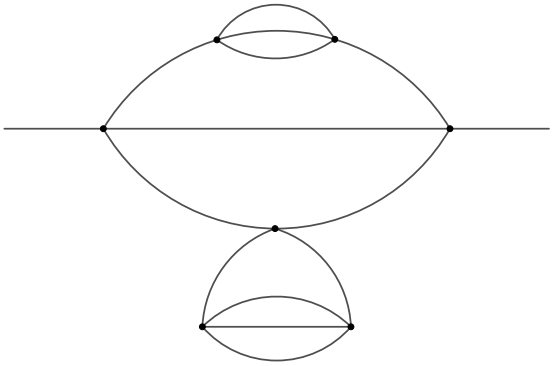

FIGURE 2.11: Example of a melon-tadpole graph.

with the ansatz $G^{-1}(p) = \mathcal{Z}(\lambda)p^{2\zeta}$. The constant $\mathcal{Z}(\lambda)$ is found to be the generating function of 4-Catalan numbers when $\zeta = \frac{d}{4}$.

- In the space of the other two couplings (whose renormalized and rescaled version we denote g_1 and g_2) we have four interacting fixed points parametrized by g:

$$g_{1\pm} = \pm\sqrt{g^2} + \mathcal{O}(g^2)\,, \qquad g_{2\pm} = \pm\sqrt{3g^2} + \mathcal{O}(g^2)\,, \tag{2.4.26}$$

out of which one is IR stable, one is UV stable, and two are saddles (see Fig. 2.12). All four collapse to the trivial fixed point for $g \to 0$.

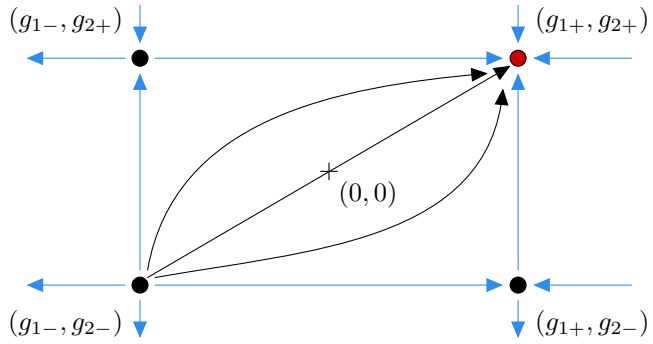

FIGURE 2.12: Trajectory between the fixed points in the space (g_1, g_2). The red dot is the IR stable fixed point.

- n-point functions of the fundamental fields are proved to be conformal.
- The OPE spectrum in the singlet sector $\phi_{\mathbf{a}} \times \phi_{\mathbf{a}}$ has been computed analytically for small λ, and numerically at a non-perturbative level: it consists of bilinear operators with real OPE coefficients and with real dimension of the form:

$$h_{n,J} = 2\Delta + 2n + J + \eta_{n,J}(g^2)\,, \tag{2.4.27}$$

with $n, J/2 \in \mathbb{N}_0$ and $\eta_{n,J}(0) = 0$. These are operators that in the free limit schematically take the form $\phi_{\mathbf{a}}\partial^{\mu_1}\cdots\partial^{\mu_J}(\partial^2)^n\phi_{\mathbf{a}}$, and for $n = 0$ are also known as "double twist" operators.

It is important to notice that while for $(n, J) \neq (0, 0)$ the anomalous dimensions $\eta_{n,J}(g^2)$ are analytic at $g^2 = 0$ and identical at all four fixed points, the anomalous dimension of $\phi_{\mathbf{a}}\phi_{\mathbf{a}}$ has a branch cut:

$$\eta_{0,0}(g^2) = \pm \frac{2\sqrt{3g^2}}{\Gamma(d/2)(4\pi)^{d/2}} \left(1 + O(g^2)\right) , \tag{2.4.28}$$

with the plus sign (resp. the minus sign) corresponding to the value at the IR (resp. UV) fixed point of g_2. This is the reason why the coefficient of the tetrahedron interaction in (2.4.17) needs to be purely imaginary in order to avoid complex scaling dimensions.

2.5 Selected Constructive Techniques

In this section we briefly introduce the notion of Borel summability, the Brydges-Kennedy-Abdesselam-Rivasseau Forest formula and the Loop Vertex Expansion.

2.5.1 Borel summability

When dealing with asymptotic series, a crucial notion is that of Borel summability. Less known, there exists a notion of Borel summability of *functions*, intimately related to the Borel summability of series. In this section we present a brief review of these notions, which will play a central role in chapter 6, as well as a slight generalization of the (optimal) Nevanlinna-Sokal theorem on Borel summability [48].

Notation. We use K as a dustbin notation for irrelevant (real positive) multiplicative constants, and R and ρ for the important (real positive) constants.

Borel summable series. A formal power series $A(z) = \sum_{k=0}^{\infty} a_k z^k$ is called a *Borel summable series along the positive real axis* if the series:

$$B(t) = \sum_{k=0}^{\infty} \frac{a_k}{k!} t^k , \tag{2.5.1}$$

is absolutely convergent in some disk $|t| < \rho$ and $B(t)$ admits an analytic continuation in a strip of width ρ along the positive real axis such that for t in this strip $|B(t)| < Ke^{|t|/R}$ for some real positive R. The function $B(t)$ is called the *Borel transform* of $A(z)$ and the *Borel sum* of $A(z)$ is the Laplace transform of its Borel transform:

$$f(z) = \frac{1}{z} \int_0^{\infty} dt\, e^{-t/z}\, B(t) . \tag{2.5.2}$$

It is easy to check that the function f is analytic in a disk of diameter R tangent to the imaginary axis at the origin, $\text{Disk}_R = \{z \in \mathbb{C} \mid \text{Re}(1/z) > 1/R\}$.

Clearly, if it exists, the Borel sum of a series is unique. This raises the following question: given a function $h(z)$ whose asymptotic series at zero is the Borel summable series $A(z)$, does the Borel resummation of $A(z)$ reconstruct $h(z)$? That is, is $f(z) = h(z)$? The answer to this question is *no* in general: for instance the function $e^{-1/z}$ is asymptotic (along the positive real axis) at 0 to the Borel summable series $a_k = 0$. It turns out that one can formulate necessary and sufficient conditions for $h(z)$ which ensure that it is indeed the Borel sum of its asymptotic series, as we now recall.

Borel summable functions. A function $f : \mathbb{C} \to \mathbb{C}$ is called a *Borel summable function along the positive real axis* if it is analytic in a disk Disk_R and has an asymptotic series at 0 (which can have

zero radius of convergence):

$$f(z) = \sum_{k=0}^{q-1} a_k \, z^k + R_q(z) \, , \tag{2.5.3}$$

such that the rest term of order q obeys the bound:

$$|R_q(z)| \leq K \, q! \, q^\beta \, \rho^{-q} \, |z|^q \, , \qquad z \in \mathrm{Disk}_R \, , \tag{2.5.4}$$

for some fixed $\beta \in \mathbb{R}_+$. Note that the bound in (2.5.4) is slightly weaker that the one in [48]. The positive real axis is selected by the position of the center of Disk_R. We call $\mathrm{Disk}_R = \{z \in \mathbb{C} \mid \mathrm{Re}(1/z) > 1/R\}$ a *Sokal disk*.

These two notions are intimately related: the Borel sums of Borel summable series are Borel summable functions (this is straightforward to prove). Moreover, the asymptotic series of Borel summable functions are Borel summable series.

Theorem 1 (Nevanlinna-Sokal [48], extended)**.** *Let $f : \mathbb{C} \to \mathbb{C}$ be a Borel summable function, hence analytic and obeying the bound (2.5.4) with some fixed β. Then:*

- *the Borel transform of the asymptotic series of f:*

$$B(t) = \sum_{k=0}^{\infty} \frac{1}{k!} \, a_k \, t^k \, , \tag{2.5.5}$$

  is convergent in a disk of radius ρ in t and it defines an analytic function in this domain.

- *$B(t)$ can be analytically continued to the strip $\{t \in \mathbb{C} \mid \mathrm{dist}(t, \mathbb{R}_+) < \rho\}$ and in this strip it obeys an exponential bound $|B(t)| < K e^{|t|/R}$.*

- *for all $z \in \mathrm{Disk}_R$ we can reconstruct the function $f(z)$ by the absolutely convergent Laplace transform:*

$$f(z) = \frac{1}{z} \int_0^\infty dt \, e^{-t/z} \, B(t) \, . \tag{2.5.6}$$

See Appendix 2.A.

We emphasize that both for series and for functions, Borel summability is directional:

- for series, Borel summability along a direction requires the unimpeded analytic continuation of $B(t)$ in a thin strip centered on that direction.

- for functions, Borel summability along a direction requires analyticity and bound on the Taylor rest terms in a Sokal disk (with 0 on its boundary) centered on that direction.

Clearly, the singularities of the Borel transform $B(t)$ are associated to directions along which the function $f(z)$ ceases to be Borel summable.

2.5.2 The Forest formula

The Brydges-Kennedy-Abdesselam-Rivasseau (BKAR) [23, 24] forest formula is a Taylor formula for functions of several variables. Due to its symmetry and positivity properties it is very well adapted for non-perturbative QFT.

Let us consider a set of n-points labeled $i = 1 \dots n$, which we identify with the set of vertices of the complete graph $\mathcal{K}_n$. The set of unordered pairs of such points has $n(n-1)/2$ elements $e = (i, j)$ for $1 \leq i, j \leq n$, $i \neq j$ and can be identified with the set of edges of $\mathcal{K}_n$. Let us consider a smooth (and arbitrarily derivable) function $f : [0,1]^{n(n-1)/2} \to \mathbb{R}$ depending on the edge variables $x_e \equiv x_{ij}$, $e = (i, j)$.

Theorem 2. *[The Forest Formula, [24, 23]] We have (with the convention that empty products are 1):*

$$f(1,\dots 1)=\sum_{\mathcal{F}}\underbrace{\int_0^1\cdots\int_0^1}_{|\mathcal{F}|\text{ times}}\left(\prod_{e\in\mathcal{F}}du_e\right)\left[\left(\prod_{e\in\mathcal{F}}\frac{\partial}{\partial x_e}\right)f\right]\left(w^{\mathcal{F}}_{kl}(u_{\mathcal{F}})\right), \tag{2.5.7}$$

where:

- *the sum runs over the forests*[12] $\mathcal{F}$ *drawn over the* n *labeled vertices* i*, including the empty forest (having no edge). To each edge* $e\in\mathcal{F}$ *we attribute a variable* u_e *that is integrated from* 0 *to* 1 *and we denote* $u_{\mathcal{F}}=\{u_e\,|\,e\in\mathcal{F}\}$*.*
- *the derivative* $\left(\prod_{e\in\mathcal{F}}\frac{\partial}{\partial x_e}\right)f$ *is evaluated at the point:*

$$w^{\mathcal{F}}_{kl}(u_{\mathcal{F}})=\inf_{e'\in P^{\mathcal{F}}_{k-l}}\{u_{e'}\}\,, \tag{2.5.8}$$

where $P^{\mathcal{F}}_{k-l}$ *denotes the unique path in the forest* $\mathcal{F}$ *joining the vertices* k *and* l*, and the infimum is set to zero if such a path does not exist.*

Setting by convention $w^{\mathcal{F}}_{kk}(u_{\mathcal{F}})\equiv 1$*, for any assignment of tree edge variables* $0\le u_{\mathcal{F}}\le 1$ *the symmetric* $n\times n$ *matrix* $W^{\mathcal{F}}(u^{\mathcal{F}})=\left(w^{\mathcal{F}}_{kl}(u_{\mathcal{F}})\right)_{1\le k,l\le n}$ *is* positive.

The most subtle point in this formula is that $W^{\mathcal{F}}(u^{\mathcal{F}})$ is a positive matrix. To see this we proceeded as follows. A forest $\mathcal{F}$ divides the complete graph $\mathcal{K}_n$ into several connected components (or blocks) corresponding to the trees in the forest. For instance, if $\mathcal{F}$ is the empty forest the blocks are all singletons consisting in a unique vertex per block. For any forest $\mathcal{F}$, the matrix:

$$B^{\mathcal{F}}_{kl}=\begin{cases}1\,, & \text{if } k,l \text{ belong to the same block of } \mathcal{F}\\ 0\,, & \text{otherwise}\end{cases}, \tag{2.5.9}$$

is positive. Indeed, denoting $b\subset\mathcal{F}$ the blocks of $\mathcal{F}$ and $k\in b$ the vertices in the block b:

$$\sum_{k,l}B^{\mathcal{F}}_{kl}a_ka_l=\sum_{b\subset\mathcal{F}}\Big(\sum_{k\in b}a_k\Big)^2. \tag{2.5.10}$$

Let us denote the number of edges in $\mathcal{F}$ by $q\equiv|\mathcal{F}|$. We order the edges of $\mathcal{F}$ in decreasing order of their parameters u:

$$1\ge u_{e_1}\ge u_{e_2}\ge\dots u_{e_q}\ge 0\,. \tag{2.5.11}$$

Adding edges one by one starting from the highest edge we obtain a family of subforests of $\mathcal{F}$:

$$\mathcal{F}^0=\emptyset\,,\ \ \mathcal{F}^1=\{e_1\}\,,\ \ \mathcal{F}^2=\{e_1,e_2\}\,,\dots\,,\ \ \mathcal{F}^q=\{e_1,\dots e_q\}=\mathcal{F}\,, \tag{2.5.12}$$

and the matrix $W^{\mathcal{F}}(u_{\mathcal{F}})$ writes as:

$$W^{\mathcal{F}}(u_{\mathcal{F}})=(1-u_{e_1})B^{\mathcal{F}^0}+(u_{e_1}-u_{e_2})B^{\mathcal{F}^1}+\dots+u_{e_q}B^{\mathcal{F}^q}\,. \tag{2.5.13}$$

Indeed, if i and j do not belong to the same block of $\mathcal{F}^q=\mathcal{F}$, then they do not belong to the same block in any of the $\mathcal{F}^s$, $s\le q$ and none of the terms above contribute, hence $w^{\mathcal{F}}_{ij}(u_{\mathcal{F}})=0$. If, on the

[12] Acyclic edge-subgraphs of the complete graph $\mathcal{K}_n$.

other hand, i and j belong to the same block of $\mathcal{F}$, then:

$$\left[(1-u_{e_1})B^{\mathcal{F}^0}+(u_{e_1}-u_{e_2})B^{\mathcal{F}^1}+\cdots+u_{e_q}B^{\mathcal{F}^q}\right]_{ij}=u_{e_s}\ , \tag{2.5.14}$$

where s is such that i and j belong to the same block of $\mathcal{F}^s$, but belong to two different blocks of $\mathcal{F}^{s-1}$. As $u_{e_s}\leq u_{e_{s-1}}\leq u_{e_{s-2}}\leq\dots$ it follows that u_{e_s} is the infimum of the us in the unique path in $\mathcal{F}^s$ joining i and j, hence it is also the infimum of the us in the unique path in $\mathcal{F}$ joining i and j. The matrix $W^{\mathcal{F}}(u_{\mathcal{F}})$ is a convex combination of positive matrices, hence it is itself positive.

2.5.3 The Loop Vertex Expansion

A very useful application of the $BKAR$ formula, that we will widely use in chapter 6, is the Loop Vertex Expansion. Let us consider the toy model of a scalar quartic theory:

$$\begin{aligned} S(\phi,g)&=\frac{1}{2}\phi^2+\frac{g}{8}\phi^4\ ,\\ Z(g)&=\int d\phi e^{-S(\phi,g)}\ . \end{aligned} \tag{2.5.15}$$

Such very simple example does not require to use of the LVE, as the analytic properties of $Z(g)$ can be easily investigated with simpler techniques. Nevertheless, it allows us to introduce and discuss in a very simple setting the LVE, which has been successfully used in more complicated settings [49], i.e. in QFT.

First we need to introduce an intermediate field σ, which allows us to rewrite the partition function in the form:

$$Z(g)=\int d\sigma e^{-\frac{1}{2}\sigma^2-\frac{1}{2}\log\left(1-\imath\sqrt{g}\sigma\right)}=e^{\frac{1}{2}\partial_\sigma\partial_\sigma}e^{-\frac{1}{2}\log\left(1-\imath\sqrt{g}\sigma\right)}\Big|_{\sigma=0}\ , \tag{2.5.16}$$

where the second equality is true in the sense of asymptotic series, i.e. the asymptotic expansion on the two sides is the same one.[13] Let us now introduce a fictitious parameter y in front of the logarithm, the original theory is recovered when setting $y=1$. The Taylor expansion of $Z(g)$ in powers series of y writes:

$$Z(g)=\sum_{n\geq 0}\frac{1}{n!}Z_n(g)\left(\frac{y}{2}\right)^n\ ,\qquad Z_n(g)=e^{\frac{1}{2}\partial_\sigma\partial_\sigma}\left(\log(1-\imath\sqrt{g}\sigma)\right)^n\Big|_{\sigma=0}\ , \tag{2.5.17}$$

where $Z_n(g)$ are the moments of the random variable $\left(\log(1-\imath\sqrt{g}\sigma)\right)$. The logarithm of $Z(g)$, i.e. the free energy $W(g)=\log\left(W(g)\right)$, expands in cumulants of the same random variable:

$$W(g)=\sum_{n\geq 0}\frac{1}{n!}W_n(g)\left(\frac{y}{2}\right)^n\ . \tag{2.5.18}$$

Let us start by studying the coefficients $Z_n(g)$, we rewrite them by introducing n degenerate copies of the field σ_i:

$$Z_n(g)=e^{\sum_{ij}\frac{1}{2}\partial_{\sigma_i}\partial_{\sigma_j}}\left(\prod_{k=1}^{n}\log(1-\imath\sqrt{g}\sigma_k)\right)\Big|_{\sigma_k=0}\ . \tag{2.5.19}$$

[13] Such rewriting of the Gaussian integral can be understood intuitively in terms of Feynman diagrams: the action of each $\frac{1}{2}\partial_\sigma\partial_\sigma$ connects to σ fields through a propagator, i.e. generating the same parings of the Wick theorem.

We now introduce also fictitious link variables $x_{ij} = 1$ in the exponent. The idea is to use the off diagonal elements x_{ij} with $i > j$ (we take $x_{ij} = x_{ji}$) as the variables of the BKAR Forest formula, we find:

$$Z_n(g) = \sum_{\mathcal{F}\in F_n} \int_0^1 \prod_{(i,j)\in\mathcal{F}} du_{ij} \left[e^{\frac{1}{2}\sum_{k,l} w^{\mathcal{F}}_{kl} \frac{\delta^2}{\delta\sigma_k \delta\sigma_l}} \left(\prod_{(i,j)\in\mathcal{F}} \frac{\delta^2}{\delta\sigma_i \delta\sigma_j} \right) \left(\prod_{k=1}^{n} \log(1-\imath\sqrt{g}\sigma_k) \right) \right]_{\sigma_i=0} , \quad (2.5.20)$$

where F_n is the set of all the forests over n labelled vertices. Observing that the contribution of a forest factors over the trees (connected components) in the forest, taking the logarithm is trivial: it comes to restricting the sum above to trees over n vertices (hence with $n-1$ edges):

$$W_n(g) = \sum_{\mathcal{T}\in T_n} \int_0^1 \prod_{(i,j)\in\mathcal{T}} du_{ij} \left[e^{\frac{1}{2}\sum_{k,l} w^{\mathcal{F}}_{kl} \frac{\delta^2}{\delta\sigma_k \delta\sigma_l}} \left(\prod_{(i,j)\in\mathcal{T}} \frac{\delta^2}{\delta\sigma_i \delta\sigma_j} \right) \left(\prod_{k=1}^{n} \log(1-\imath\sqrt{g}\sigma_k) \right) \right]_{\sigma_i=0} , \quad (2.5.21)$$

The sigma derivatives can be taken explicitly:

$$\frac{\delta^d}{\delta\sigma^d} \ln\left(1-\imath\sqrt{g}\sigma\right) = -\frac{(d-1)!\left(\imath\sqrt{g}\right)^d}{\left(1-\imath\sqrt{g}\sigma\right)^d} . \quad (2.5.22)$$

Denoting d_i the degree of the vertex i in $\mathcal{F}$ and recalling that $\sum_i d_i = 2(n-1)$:

$$W_n(g) = -(g)^{n-1} \sum_{\mathcal{T}\in T_n} \int_0^1 \prod_{(i,j)\in\mathcal{T}} du_{ij} \left[e^{\frac{1}{2}\sum_{i,j} w^{\mathcal{T}}_{ij} \frac{\delta}{\delta\sigma_i} \frac{\delta}{\delta\sigma_j}} \prod_i \frac{(d_i-1)!}{\left(1-\imath\sqrt{g}\sigma_i\right)^{d_i}} \right]_{\sigma_i=0} , \quad (2.5.23)$$

for $n \geq 1$, while the $n = 0$ is special, but obviously trivial. It is sufficient to use $|1-\imath\sqrt{g}\sigma| \geq 1$ to get the following bound:

$$|W_n(g)| \leq |g|^{n-1} (n-2)! \sum_{d_i\geq 1}^{\sum_{i=1}^n (d_i-1)=n-2} 1 , \quad (2.5.24)$$

where we used that the u integrals are bounded by one and the fact that there are $(n-2)!/\prod_i (d_i-1)!$ trees over n labeled vertices with degree d_i at the vertex i. The last step is to sum over the possible d_i, that can be done by noticing that the sum over d_i is the coefficient of x^{n-2} in the expansion of $(1-x)^{-n} = \sum_{q\geq 0} \binom{n-1+q}{n-1} x^q$, hence:

$$|W_n(g)| \leq \frac{(2n-3)!}{(n-1)!} |g|^{n-1} . \quad (2.5.25)$$

Using Stirling's formula for the asymptotics of the factorials we find that $W(g)$ is convergent for $|2gy| < 1$, setting $y = 1$ for $g < \frac{1}{2}$. The fact that such expansion is actually convergent for g small enough is surprising, as usually perturbative expansions are only asymptotic. The reason why this happens is that the LVE is only a partial expansion in g, in which an infinite family of terms is repackaged in $\left(\log(1-\imath\sqrt{g}\sigma) \right)$, which is very well bounded. Using similar techniques it is possible to show that $Z_n(g)$, $W_n(g)$, $Z(g)$ and $W(g)$ are Borel summable along $g \in \mathbb{R}_+$, and actually much more than that as we will discuss in Chapter 6.

2.A A simple generalization of the Nevanlinna-Sokal theorem

Proof of Theorem 1. The proof is an infinitesimal variation of the proof of [48] which deals with the case $\beta = 0$. We parallel the notation of [48].

We first observe that:

$$|a_q| = \lim_{z\to 0, z\in \mathrm{Disk}_R} \left| \frac{a_q z^q + R_{q+1}(z)}{z^q} \right| = \lim_{z\to 0, z\in \mathrm{Disk}_R} \frac{|R_q(z)|}{|z|^q} \leq K\, q!\, q^\beta\, \rho^{-q}\,, \tag{2.A.1}$$

hence $B(t)$ is an integer power series which converges in the disk $|t| < \rho$ and defines an analytic function in this domain.

Let us recall Hankel's contour integral representation of the inverse of the Gamma function:

$$\frac{1}{2\pi\imath} \oint_{\mathrm{Re}(z^{-1})=r^{-1}} dz\; e^{x/z} z^{k-1} = \frac{1}{2\pi\imath} \int_{r^{-1}-\imath\infty}^{r^{-1}+\imath\infty} dw\; e^{xw}\; w^{-k-1} = \frac{x^k}{\Gamma(k+1)}\,, \tag{2.A.2}$$

which holds for any $r, x \in \mathbb{R}_+$ and $k \in \mathbb{C}$. We define for $x \in \mathbb{R}_+$ the function:

$$b_0(x) = \frac{1}{2\pi\imath} \oint_{\mathrm{Re}(z^{-1})=r^{-1}} dz\; e^{x/z}\; z^{-1}\; f(z)\,, \tag{2.A.3}$$

which is an r independent function for $r < R$ as long as the integral converges because the integration contour is fully contain in Disk_R. Substituting the asymptotic expansion of $f(z)$ up to order q we obtain:

$$b_0(x) = \sum_{k=0}^{q-1} \frac{a_k}{k!} x^k + \frac{1}{2\pi\imath} \oint_{\mathrm{Re}(z^{-1})=r^{-1}} dz\; e^{x/z}\; z^{-1} R_q(z)\,. \tag{2.A.4}$$

Changing variables to $w = 1/z$ and using the bound on R_q, the remainder term above is bounded by:

$$K\, q!\, q^\beta\, \rho^{-q}\, e^{x/r} \int_{-\infty}^{\infty} dv\; \frac{1}{|r^{-1} + \imath v|^{q+1}} \leq K\, q!\, q^\beta\, \rho^{-q}\, e^{x/r}\, r^q \int_{-\infty}^{\infty} dv \frac{1}{(1+v^2)^{\frac{q+1}{2}}}\,, \tag{2.A.5}$$

and the integral in the last line is always bounded by the case $q = 1$ in which case it is π and can be absorbed in K. Choosing $r = x/q$ (which is possible for q large enough $q > x/R$) and using the Stirling upper bound on the Gamma function, the reminder is finally bounded by $K\, q^{\beta+1/2} (x/\rho)^q$ hence goes to zero in the $q \to \infty$ limit as long as $x < \rho$. It follows that for $0 < x < \rho$, $b_0(x) = B(t)|_{t=x}$.

We now define $b_m(x) = \frac{d^m}{dx^m} b_0(x)$, and using (2.A.4) with $q = m + 1$ we get:

$$b_m(x) = a_m + \frac{1}{2\pi\imath} \oint_{\mathrm{Re}(z^{-1})=r^{-1}} dz\; e^{x/z} z^{-m-1} R_{m+1}(z)\,, \tag{2.A.6}$$

and we have the bound $|b_m(x)| \leq K\; (m+1)!\; (m+1)^\beta\; \rho^{-m-1} e^{x/r}$ (note that this bound covers also the term $|a_m| < K\; m!\; m^\beta\; \rho^{-m}$).

The sum $B_x(t) = \sum_{m\geq 0} \frac{(t-x)^m}{m!} b_m(x)$ defines an analytic function in t as long as it converges. As:

$$|B_x(t)| \leq K e^{x/r} \sum_{m\geq 0} (m+1)^{\beta+1} (|t-x|/\rho)^m\,, \tag{2.A.7}$$

we conclude that $B_x(t)$ is analytic in a disk or radius ρ centered at x. It is immediate to check that $B_x(t) = B_{x'}(t)$ as long as they both converge, hence $B_x(t)$ is the analytic continuation of $B(t)$ to the

strip $\{t \in \mathbb{C} \mid \mathrm{dist}(t, \mathbb{R}_+) < \rho\}$ and it obeys the appropriate exponential bound. The last point follows by noting that for $z' \in \mathrm{Disk}_r$:

$$\frac{1}{z'} \int_0^\infty dx\, e^{-x/z'} \frac{1}{2\pi\imath} \oint_{\mathrm{Disk}_r} dz\, e^{x/z}\, z^{-1}\, f(z) = \frac{1}{2\pi\imath} \oint_{\mathrm{Disk}_r} dz\, \frac{1}{z - z'}\, f(z) = f(z')\,, \tag{2.A.8}$$

by Cauchy's theorem. □

Chapter 3

F theorem

3.1 Introduction

Among the most intriguing features of quantum field theory in various dimensions are the so called c-, a- and F-theorems [50, 51, 52, 53]. These lettered theorems state that under the RG flow between various fixed points some quantities (aptly denoted c, a or F) always decrease. Intuitively, these quantities must in some way count the degrees of freedom in the theory, as the RG flow decimates the degrees of freedom when going from one fixed point to another.

The most well known of the lettered theorems, the c-theorem in dimension 2 was first proven by Zamolodchikov [50]. The quantity c in this case was defined using the two-point functions of the stress-energy tensor. Interestingly, the obtained c-function coincides at the RG fixed point with the Weyl anomaly coefficient c, that is the central charge.

In $d = 4$ dimensions, the a-theorem was first conjectured by Cardy [54]. In this case, there are two universal Weyl anomaly coefficients, usually denoted a and c. Cardy conjectured that the quantity that should decrease along the RG flow is the a-coefficient, multiplying the Euler density. In practice, this coefficient can be computed from the expectation value of the trace of the stress-energy tensor in the Euclidean theory on S^4. After a long time, the a-theorem was finally proven in [51, 55].

The latest addition to this list of monotonicity theorems is the F-theorem, concerning field theories in $d = 3$. In this case, F has a relatively straightforward definition as the free energy of the CFT on the sphere. The compactness of the sphere regulates the infrared divergences, however ultraviolet divergences persist and need to be regularized properly: F is defined as the finite part of the free energy. This choice was first proposed in [56, 52], where various checks were performed on supersymmetric theories, then extended to non-supersymmetric ones in [53] (see also [57] for a review). Shortly after, the F-theorem was proven in [58], using the relation between the free energy and the entanglement entropy across a circle [59]; so far, this is the only method that works for all three theorems [60, 61].

One common feature of the proofs of these theorems is that unitarity plays a crucial role: it is underlying the use of positivity of two-point functions in [50], of the optical theorem in [51], and of the strong subadditive inequality in [58, 60, 61]. At present, it remains unclear to what extent unitarity is a necessary ingredient and if the assumptions of these theorems could be relaxed to include at least some class of non-unitary models. A non-physical counterexample to the necessity of unitarity is provided by the generalized F-theorem tests in non-integer dimensions [62, 63, 64], where it was shown to hold, despite the fact that CFTs in non-integer dimensions have been shown to be non-unitary [65], at least in the case of the Wilson-Fisher fixed point. On the other hand, as we will see below, a trivial counterexample to a generic F-theorem without unitarity is provided by a non-unitary generalized free field theory flow.[1]

[1] It should be remarked that generalized free fields, as the long-range model we will consider here, evade also another hypothesis of the standard proofs, that is, locality. Long-range models in particular do not have a local energy-momentum tensor, which plays a crucial role in the standard proofs of the c- and a-theorems. However, the embedding of such models in a larger space [66] could perhaps provide a workaround for such proofs. In fact, for the special case of an

In most applications, one knows from the start whether the theory of interest is unitary or not, or at least one has a good degree of confidence in that, and therefore testing the F-theorem in a theory satisfying the hypotheses of [59] is at most an interesting exercise. However, in some cases ascertaining the unitarity, or lack thereof, of a theory can be challenging; for instance, in the Wilson-Fisher fixed point at non-integer dimensions [65], or in the $O(N)$ model at non-integer N [69, 70], non-unitarity is a non-trivial result, manifesting itself only in operators of large dimension. The main subject of this chapter will be another non-trivial example, going in the opposite direction: a manifestly non-unitary model, which however in the large-N limit has so far passed all the unitarity tests.

3.2 Flow between Gaussian CFTs

As a warm-up, and for later reference, let us consider the following quadratic action:

$$S_{\text{Gauss}}[\phi] = \frac{1}{2}\int \mathrm{d}^d x\, \phi(x)(-\partial^2)^{\zeta}\phi(x) + \frac{\lambda}{2}\int \mathrm{d}^d x\, \phi(x)(-\partial^2)\phi(x)\,, \tag{3.2.1}$$

with $0 < \zeta < 1$. The non-integer power of the Laplacian is defined in momentum space simply as $p^{2\zeta}$, or in position space by a convolution with a non-local kernel, see (3.B.12)-(3.B.13). The second term in (3.2.1) is the standard short-range free action of scalar fields, while the first is a generalized free field theory (GFFT), constituting the free part of interacting long-range scalar models. The models we will consider in the next two sections are short-range and long-range, respectively, hence this simple example will also allow us to introduce some useful results for later on.

The coupling λ has mass dimension $2\zeta - 2 < 0$, hence it is an irrelevant coupling for the GFFT. Since the theory is Gaussian, the Renormalization Group (RG) flow is rather trivial: the two-point function in momentum space is $(p^{2\zeta} + \lambda p^2)^{-1}$ and goes to the GFFT propagator $1/p^{2\zeta}$ for $p \to 0$, while for $p \to \infty$ it goes to the canonical free theory propagator $1/p^2$ (up to normalization). Therefore, we have a flow between two Gaussian CFTs.

The flow is rather standard from the GFFT side, as the operator $\phi\partial^2\phi$ is a primary in the OPE spectrum of $\phi \times \phi$ in the GFFT (e.g. [44]), and it has scaling dimension greater than d. On the other hand, the flow is somewhat unusual from the canonical free CFT side, as the non-local operator $\phi\partial^{2\zeta}\phi$ is not in the CFT spectrum. One possible way to write the perturbation in the UV in the framework of conformal perturbation theory is to introduce an additional field, following the idea proposed in [71] for the short-range/long-range Ising transition. We thus rewrite the action with a second field χ:

$$S_{\text{Gauss}-2}[\phi,\chi] = \frac{1}{2}\int \mathrm{d}^d x\, \phi(x)(-\partial^2)\phi(x) + \frac{1}{2}\int \mathrm{d}^d x\, \chi(x)(-\partial^2)^{-\zeta}\chi(x) + \frac{\mathrm{i}}{\sqrt{\lambda}}\int \mathrm{d}^d x\, \chi(x)\phi(x)\,. \tag{3.2.2}$$

Integrating out the field χ we recover (3.2.1), up to a rescaling $\phi \to \phi/\sqrt{\lambda}$.[2] This formulation is non-standard in other ways, namely the need of an imaginary coupling (that could however be absorbed into the field χ), and the negative power of the Laplacian, the latter leading to unusual features about the thermodynamic limit, such as inequivalence of statistical ensembles [72]. An important difference between (3.2.1) and (3.2.2) is that, in the second case, the UV theory has an additional, albeit decoupled, degree of freedom, the field χ.

We want to test the F-theorem on this flow between Gaussian CFTs. To that end, we place the fixed-point theories on a spherical background, which is done by the standard procedure recalled in appendix 3.B. In practice, the local Laplacian is replaced by the Weyl covariant version (i.e. the

integer number of extra dimensions, boundary versions of the F-theorem have indeed been proposed [67] (see also [68] for more information on monotonicity theorems in boundary or defect CFTs).

[2] The two formulations of the theory are only equivalent if we restrict to the set of correlators of operators built only with fields ϕ, plus the mixing operator $\chi(x)\phi(x)$. In particular it would make no sense to integrate out ϕ in (3.2.2).

operator in (3.B.4) with the choice (3.B.7)), while the non-local one by the more complicated operator (3.B.22) (with kernel (3.B.18)).

As we are interested in the difference between the free energies at the two limiting theories, the overall normalization of the functional integral over ϕ is not important and will be omitted. However, in the formulation with the action (3.2.2) the auxiliary field χ should better have a unit normalized Gaussian functional measure:

$$\int [\mathrm{d}\chi]\, e^{-S_{\mathrm{Gauss}-2}[0,\chi]} = 1\,, \tag{3.2.3}$$

so that integrating it out leads to to the functional integral for (3.2.1), with the same normalization. Equivalently, this is demanded by imposing that the UV theories obtained from (3.2.2) or from (3.2.1) have the same free energy.

For the weak form of the F-theorem we only need to compare the fixed points theories. These are GFFTs with different values of ζ, hence it is straightforward to compute F. The free energy parametrized by ζ (including the standard $\zeta = 1$ case) is given by:

$$F = \frac{1}{2}\,\mathrm{Tr}[\ln C^{-1}] = \frac{1}{2}\sum_{n\geq 0} D_n\, \ln\left(\omega_n^{(\zeta)}\right), \tag{3.2.4}$$

where D_n is the multiplicity of the eigenvalues, see (3.A.9). The sum is clearly divergent, hence we need a regularization.

The same kind of sum was encountered in [53] as the IR limit of a CFT perturbed by a double-trace operator. Using dimensional regularization as in [73], we find:

$$\frac{dF}{d\zeta} = -\zeta \frac{\sin(\pi\zeta)}{\sin(\pi d/2)} \frac{\Gamma(d/2-\zeta)\Gamma(d/2+\zeta)}{\Gamma(1+d)}\,, \tag{3.2.5}$$

which only has poles for d even. See appendix 3.C for the detailed computation. When $d = 3$, (3.2.5) simplifies to:

$$\frac{dF}{d\zeta} = \frac{1}{24}\pi\zeta\left(1-4\zeta^2\right)\tan(\pi\zeta)\,, \tag{3.2.6}$$

that is positive for $0 \leq \zeta \leq 1$. An immediate consequence is that the free energy F grows with ζ (see Fig. 3.1), showing that an RG trajectory flowing from a short-range free Gaussian model ($\zeta = 1$) to a long-range Gaussian model ($\zeta < 1$) satisfies the F-theorem.

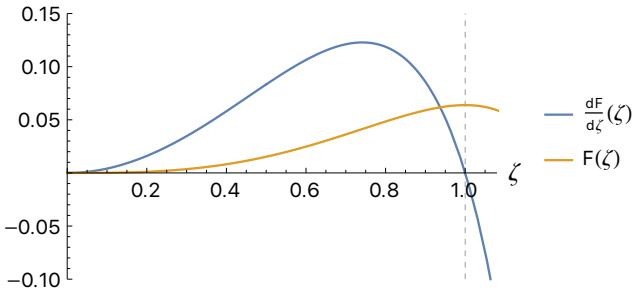

FIGURE 3.1: The free energy is 0 when $\zeta = 0$, grows with ζ, and reaches its maximum at $\zeta = 1$. We plot the $d = 3$ case. The blue curve is the derivative of the free energy with respect to ζ and the orange curve is the free energy itself.

It is interesting to consider the model (3.2.1) with $\zeta > 1$, for which the GFFT is non-unitary.[3] We also restrict to $\zeta < d/2$, to keep $\Delta > 0$ and avoid the logarithmic two-point function at $\Delta = 0$. In this case, the role of UV and IR limiting theory is exchanged, with the $\zeta > 1$ GFFT flowing in the IR to the standard free theory with $\zeta = 1$. And since $\zeta = 1$ is a maximum for F, we find that the free energy increases in the IR. We thus have a trivial counterexample to the F-theorem for non-unitary theories.

3.3 The $O(N)$ model revisited

In this section we look at the three-dimensional $O(N)$ model in the short-range case, i.e. $\zeta = 1$ and $d = 3$:

$$S[\phi] = \frac{1}{2}\int \mathrm{d}^d x\, \phi_a(-\partial^2)\phi_a + \frac{m^2}{2}\int \mathrm{d}^d x\, \phi_a\phi_a + \frac{\lambda}{4N}\int \mathrm{d}^d x\, (\phi_a\phi_a)^2\,, \tag{3.3.1}$$

where repeated indices are summed over the range $a = 1, \cdots, N$. Although this case has been studied before in [53] and we only reproduce here the known result, we will do this by a different method. This helps us prepare the ground for the next chapter. The new elements of our analysis are the following. First, we will frame the discussion within the 2PI effective action formalism (for which we follow [74, 75]). Second, we will show how the result of [53] is reproduced by means of a conformal partial wave expansion.

3.3.1 The sphere free energy at leading order in the large-N expansion

At large N, the leading-order (LO) 2PI effective action is of order N, and reads:

$$\begin{aligned}\mathbf{\Gamma}_{\mathrm{LO}}[G] &= N\left(\frac{1}{2}\int_{x,y} C_1^{-1}(x,y)G(y,x) + \frac{1}{2}\int_{x,y}\ln(G^{-1})(x,y) + \frac{m^2}{2}\int_x G(x,x) + \frac{\lambda}{4}\int_x G(x,x)^2\right)\\ &= \frac{N}{2}\,\mathrm{Tr}\left[C_1^{-1}G + \ln(G^{-1}) + m^2 G + \frac{\lambda}{2}\mathcal{B}\right]\,,\end{aligned} \tag{3.3.2}$$

where $\int_x = \int \mathrm{d}^d x\sqrt{g(x)}$, and $C_1^{-1} = -\partial^2$ is written as the inverse of the free propagator, which is defined in (3.B.8). In the second line we introduced a compact trace notation, as well as the double-propagator operator:

$$\mathcal{B}(x,y) = G(x,y)^2\,. \tag{3.3.3}$$

The logarithmic term $\ln(G^{-1})$ should be understood in terms of its eigenvalues (in particular when G coincides or is proportional to the free propagator C_1), or by a formal expansion around the free propagator.

The first two terms in (3.3.2) are very generic, it is the one-loop part of the effective action. The rest should in general be given by a sum over all the vacuum 2PI diagrams, built from the vertices of the theory, but with the full two-point function $G(x,y)$, to be determined self-consistently at a second stage. The sum of diagrams becomes manageable in the large-N expansion, and at the leading order written in (3.3.2) only two diagrams survive, the mass tadpole, and the interaction double-tadpole, or figure-eight.

[3] As can be seen from the Källén-Lehmann spectral representation of the propagator [19], or from the fact that the unitarity bound $\Delta > d/2 - 1$ is violated.

FIGURE 3.2: The only two vacuum 2PI diagrams occurring in the $O(N)$ model at large N. The tadpole on the left has a two-valent mass vertex, while the figure-eight on the right has a λ vertex.

The true full two-point function of the model is found by solving the Schwinger-Dyson (SD) equations, which are obtained as the field equations of the 2PI effective action:

$$\frac{\delta\Gamma}{\delta G} = 0\,. \tag{3.3.4}$$

From (3.3.2) we find the following form of the SD equations:

$$G^{-1}(x,y) = C_1^{-1}(x,y) + \big(m^2 + \lambda G(x,x)\big)\,\frac{\delta(x-y)}{\sqrt{g(x)}}\,, \tag{3.3.5}$$

where we used:

$$\frac{\delta G(u,w)}{\delta G(x,y)} = \frac{1}{2}\frac{\delta(x-u)\delta(y-w)+\delta(x-w)\delta(y-u)}{\sqrt{g(u)}\sqrt{g(w)}}\,. \tag{3.3.6}$$

Clearly, it is enough to tune the bare mass:

$$m^2 = -\lambda C_1(x,x)\,, \tag{3.3.7}$$

in order to cancel the on-shell tadpole and obtain trivially the solution $G = C_1$.

The free energy F is obtained by evaluating the 2PI effective action on shell, i.e. by substituting the solution of the SD equations into (3.3.2). Evaluating it on the sphere resolves the IR problem arising from the fact that F is proportional to the volume of the d-dimensional background space. However, there are still UV divergences originating from the functional traces, and from the evaluation of the propagator at coincident points. As we will now review, after appropriate regularization, the result is that the tadpole terms will drop out and thus the leading-order free energy is the same as that of the free theory.

When replacing $G = C_1$ in (3.3.2), the first two terms should reproduce (N times) the free energy of the GFFT (3.2.4) at $\zeta = 1$. We have already discussed the regularization and evaluation of $\mathrm{Tr}[\ln C_1^{-1}]$ in the previous section, but what about the first term in (3.3.2)? Clearly, it corresponds to a divergent contribution $\mathrm{Tr}[\mathbf{1}] \sim \delta(0)$. A similar term (with the opposite sign) is however discarded in the typical derivation of the 2PI effective action [74], for which the first term would otherwise read $\mathrm{Tr}[(C_1^{-1} - G^{-1})G]$, and therefore the two cancel out. In any case, when regularized by analytical continuation in the dimension, such terms vanish identically, as shown in (3.C.2).

The bare mass was chosen in (3.3.7) to cancel the tadpole in the SD equation, but the cancellation does not occur in the free energy. However, as we show in appendix 3.D.1, analytic continuation in the dimension gives $C_1(x,x) = 0$, hence the contribution of the tadpole terms to the free energy vanishes. Therefore, at leading order the free energy of the $O(N)$ critical theory is the same as for the free

theory, which in $d = 3$ reads:

$$F_{\rm LO} = \mathbf{\Gamma}_{\rm LO}[C_1] = \frac{1}{2}\,{\rm Tr}[\ln C_1^{-1}] = \frac{N}{16}\left(\ln 4 - \frac{3\,\zeta(3)}{\pi^2}\right) . \tag{3.3.8}$$

In order to find a non-trivial result one thus need to consider the subleading corrections to F.

3.3.2 The next-to-leading order of the large-N expansion

The next-to-leading order (NLO) contribution to the 2PI effective action is of order N^0, and reads [74]:

$$\mathbf{\Gamma}_{\rm NLO}[G] = \frac{1}{2}\,{\rm Tr}[\ln(\mathbf{1} + \lambda\mathcal{B})]\,, \tag{3.3.9}$$

where $\mathcal{B}$ is the two-point kernel (3.3.3), corresponding to a single bubble in the chain of bubbles represented in Fig. 3.3. This is the same contribution found in [53] by introducing an intermediate

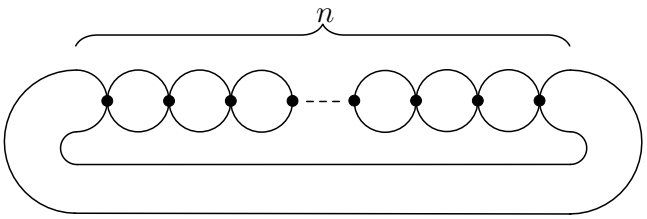

FIGURE 3.3: Chain of bubbles with $n \geq 1$ vertices. The two-point kernel $\mathcal{B}$ corresponds to one of the bubbles in the chain.

field, and their result will thus be reproduced: on shell we replace $G(x,y) \to G_{\rm LO}(x,y) = C_1(x,y)$,[4] and thus the two-point kernel $\mathcal{B}(x,y)$ is a two-point function of an operator of dimension $\Delta = d - 2$, which on the sphere is diagonalized by the spherical harmonics. After going to eigenvalues, and taking the bare coupling to infinity in order to tune to the fixed point,[5] one is left with the same type of computation as in (3.2.4). In $d = 3$, the result is:

$$F_{\rm NLO} = \mathbf{\Gamma}_{\rm NLO}[C_1] = -\frac{\zeta(3)}{8\pi^2}\,, \tag{3.3.10}$$

and thus the free energy of the IR fixed point is smaller than the one of the UV free theory.

However, the fact that the NLO contribution to the 2PI effective action could be expressed in terms of a two-point kernel is a very peculiar feature of the $O(N)$ model at large N. In particular, it does not generalize to other models, such as the melonic ones that we will discuss in the following, for which the NNLO (the NLO is vanishing) contribution is expressed in terms of a four-point kernel. Therefore, as a warm-up to our next computation, we would like to recover the $O(N)$ model result of [53] by expressing the NLO part of the effective action as:

$$\mathbf{\Gamma}_{\rm NLO}[G] = \frac{1}{2}\,{\rm Tr}[\ln(\mathbb{I} - K)]\,, \tag{3.3.11}$$

[4] Notice that the NLO part of the on-shell $G(x,y)$ only contributes at NNLO and beyond. This is obvious by expanding $\mathbf{\Gamma}_{\rm NLO}[G_{\rm LO} + G_{\rm NLO}/N]$, and it is true also for $\mathbf{\Gamma}_{\rm LO}[G_{\rm LO} + G_{\rm NLO}/N]$ because by construction $\frac{\delta\mathbf{\Gamma}_{\rm LO}}{\delta G}[G_{\rm LO}] = 0$.

[5] The bare coupling in (3.3.9) should be expressed as a function of the renormalized coupling, at the leading order of the large-N expansions, as the NLO part would only contribute to NNLO in the effective action. At LO, we have $\lambda = g/(1 - b(d)g/\mu^{4-d})$, where $b(d)$ is a positive constant with a pole at $d = 4$, μ is the renormalization scale, and g is the renormalized coupling. The fixed point of the beta function for the dimensionless coupling $\tilde{g} = g/\mu^{4-d}$ is at $\tilde{g}_\star = 1/b(d)$, hence we have $\lambda \to \infty$.

where we introduced the Bethe-Salpeter four-point kernel:

$$K(x_1,x_2,x_3,x_4) = -\lambda G(x_1,x_3)G(x_2,x_4)\delta(x_3-x_4)\,, \tag{3.3.12}$$

and by a slight abuse of notation we use the same symbol for the trace, which in this case refers to a trace of a bilocal to bilocal operator, that is a four-point kernel that acts by integration on two arguments, e.g. $\mathrm{Tr}[K] = \int_{x_1,x_2} K(x_1,x_2,x_1,x_2)$.

Under quite general assumptions the Bethe-Salpeter kernel of a CFT is diagonalized by the basis of three-point functions (see appendix 3.E), hence once we go on shell ($G(x,y) \to C_1(x,y)$) and tune to the fixed point, we should obtain a representation of the kernel (or functions of it) by applying it on the resolution of the identity (3.E.25). This is not so straightforward for the kernel (3.3.12). As explained in footnote 5, the fixed point is at $\lambda \to \infty$, which requires us to work at finite λ and then take the limit. However, for finite λ, and this being a dimensionful coupling for $d < 4$, the kernel (3.3.12) does not have the right conformal properties to ensure that its convolution with a three-point function (3.E.1) transforms as the three-point function itself. Thus the kernel (3.3.12) applied on a three-point function cannot be proportional to it. Unless of course the proportionality constant is zero or infinite.

On the principal series, we have $\mathrm{Re}(2\Delta - h) < 0$, hence when the delta function in (3.3.12) acts on (3.E.1) the result is zero: the three-point functions with $h \in \mathcal{P}_+$ are indeed eigenfunctions of (3.3.12) with *vanishing eigenvalue*. On the other hand, for the isolated contribution in (3.E.25) we have $2\Delta - h = 0$, hence the delta function gives a finite result, which is not[6] proportional to $\langle\phi(x_1)\phi(x_2)\mathcal{O}_{2\Delta}(x_0)\rangle_{\mathrm{cs}}$. However, the conformal theory is reached at $\lambda \to \infty$, hence the three-point function with $h = 2\Delta$ and $J = 0$ is formally an eigenfunction with *infinite eigenvalue*.

This has the interesting consequence that for the right-amputated four-point function, which is a geometric series in K (see (3.E.20)) and hence the coupling appears in the denominator of the resummed series, we obtain (see appendix 3.E for the notation):

$$\begin{aligned}\mathcal{F}_s(x_1,x_2,x_3,x_4) &= \int \mathrm{d}^d y_1 \mathrm{d}^d y_2 (\mathbb{I}-K)^{-1}(x_1,x_2,y_1,y_2) C_1(y_1,x_3) C_1(y_2,x_4) \\ &= \sum_{J\in\mathbb{N}_0^{\mathrm{even}}} \int_{\frac{d}{2}}^{\frac{d}{2}+\mathrm{i}\,\infty} \frac{\mathrm{d}h}{2\pi\,\mathrm{i}} \rho(h,J)\, \mathcal{N}^{\Delta}_{h,J}\mathcal{N}^{\Delta}_{\tilde{h},J}\, \Psi^{\Delta,\Delta,\Delta,\Delta}_{h,J}(x_1,x_2,x_3,x_4)\,.\end{aligned} \tag{3.3.13}$$

Therefore, the isolated contribution that is present in the free theory (see (3.E.24) with $\Delta = d/2-1$) is suppressed in the critical theory, and the conformal partial wave expansion is the same as in (3.E.23), even tough $\Delta = d/2-1 < d/4$. We thus recover the well-known result that the spectrum of the critical $O(N)$ model (i.e. the poles of the integrand) at large N is the same as in the free theory for $J > 0$, while for $J = 0$ it has the ϕ^2 operator replaced by its shadow.

Applying the above formalism to the free energy on the sphere is however trickier than for the four-point function. Because of the conformal nature of the basis of three-point functions, we expect the eigenbasis of K on the sphere to be obtained by Weyl mapping:[7]

$$\langle\phi_\Delta(x_3)\phi_\Delta(x_4)\mathcal{O}^{\bar{\mu}}_{(h,J)}(x_0)\rangle_{\mathrm{cs}} \to \Omega(x_3)^{-\Delta}\,\Omega(x_4)^{-\Delta}\,\Omega(x_0)^{-h}\,\langle\phi_\Delta(x_3)\phi_\Delta(x_4)\mathcal{O}^{\bar{\mu}}_{(h,J)}(x_0)\rangle_{\mathrm{cs}}\,. \tag{3.3.14}$$

[6] At $h = 2\Delta$ and $J = 0$, the three-point function (3.E.1) is proportional to $C(x_3,x_0)C(x_4,x_0)$, and the action of K on it generates a bubble. The result can be evaluated most easily in Fourier space, and it is found to be proportional to $\lambda b(d) p_1^{-2} p_2^{-2}(p_1+p_2)^{d-4}$, with the same constant $b(d)$ that appeared in footnote 5. Due to the factor $(p_1+p_2)^{d-4}$, the result is not proportional to the Fourier transform of $C(x_3,x_0)C(x_4,x_0)$.

[7] Applying the same mapping in (3.E.10), the $\Omega(z)$ factors cancel, and we obtain an overall factor $\Omega(x_3)^{-d}\Omega(x_4)^{-d}$, which reconstructs the correct factors of $1/\sqrt{g}$ for the delta functions in (3.E.25).

In fact, for a Bethe-Salpeter kernel with the good conformal transformation properties, the Weyl mapping would give:

$$K(x_1,x_2,x_3,x_4) \to \Omega(x_1)^{-\Delta}\,\Omega(x_2)^{-\Delta}\,\Omega(x_3)^{\Delta-d}\,\Omega(x_4)^{\Delta-d}\,K(x_1,x_2,x_3,x_4)\,, \tag{3.3.15}$$

and thus all the $\Omega(x_3)$and $\Omega(x_4)$ factors would drop out in the convolution, leading to a consistent eigenvalue equation. As explained above, the kernel in (3.3.12) does not transform in such a nice way at finite λ, and we have instead:[8]

$$K(x_1,x_2,x_3,x_4) \to \Omega(x_1)^{-\Delta}\,\Omega(x_2)^{-\Delta}\,\Omega(x_3)^{-\Delta-d/2}\,\Omega(x_4)^{-\Delta-d/2}\,K(x_1,x_2,x_3,x_4)\,. \tag{3.3.16}$$

However, the three-point functions with operator in the principal series are still zero modes of K. Therefore, inserting the resolution of the identity inside the trace in (3.3.11), we see that a non-vanishing contribution can only come from the isolated term at $h = 2\Delta$.[9] It turns out that at finite λ this reproduces the same series as (3.3.9), and hence we can from here on follow again the same steps as in [53] and obtain the same result. In fact, it is easy to check that the convolution of K with (3.E.26) equals K. While this is tautological (as we have inserted the identity and the contribution of the principal series is zero, the isolated contribution must reproduce the full identity), one can check directly that indeed the isolated contribution in (3.E.24) acts alone as the identity operator on K, and we are back to having to evaluate the chains of bubbles, for which we can follow the steps of [53]. Although from a practical point of view we have not gained anything by applying the conformal partial wave expansion to this problem, nevertheless this small detour taught us about the importance of the isolated contributions in such formalism, and it serves as a test of the method, in view of the application in the next section.

3.4 The long-range $O(N)^3$ model

In this section we study the F-theorem for the $O(N)^3$ model introduces in section 2.4.2.

3.4.1 Schwinger-Dyson equation for the two-point function

We start here with a brief review of the solution of the Schwinger-Dyson equation, with the slight modification of working on the spherical background.

For large N, the dominant 2PI diagrams are depicted in Fig. 3.4. The resulting leading-order 2PI effective action is of order N^3, and reads:

$$\begin{aligned}\mathbf{\Gamma}[G] &= N^3\left(\frac{1}{2}\int_{x,y} C^{-1}(x,y)G(y,x) + \frac{1}{2}\int_{x,y}\ln(G^{-1})(x,y) + \frac{m^{2\zeta}}{2}\int_x G(x,x)\right.\\ &\qquad \left. +\frac{\lambda_2}{4}\int_x G(x,x)^2 + \frac{\lambda^2}{8}\int_{x,y} G(x,y)^4\right)\\ &= \frac{N^3}{2}\,\mathrm{Tr}\left[C^{-1}G + \ln(G^{-1}) + m^{2\zeta}G + \frac{\lambda_2}{2}\mathcal{B} + \frac{\lambda^2}{4}\mathcal{B}^2\right]\,,\end{aligned} \tag{3.4.1}$$

where we used the notation introduced in (3.3.2), and we used the symmetry of $G(x,y)$ to write the melon integral as a trace of a convolution of two $\mathcal{B}(x,y)$. The latter is of course an arbitrary choice,

[8] The two transformations agree for $\Delta = d/4$, i.e. when λ is dimensionless, but for the short-range $O(N)$ model this only happens at $d = 4$, where there is no interacting fixed point.

[9] One might worry that although the three-point functions with operator in the principal series have a vanishing eigenvalue, the trace of the conformal partial wave is divergent, and thus the product is undefined. However, as we will see in the following section, there is a clean way to regularize the trace of the conformal partial wave, which does not affect the eigenvalues, and hence the product is indeed zero in the present case.

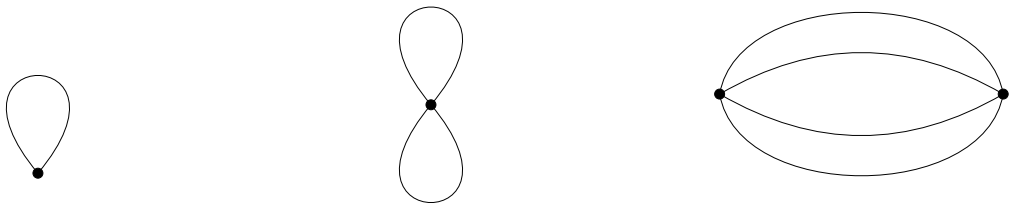

FIGURE 3.4: The only three types of vacuum 2PI diagrams occurring at large N. The tadpole on the left has a two-valent mass vertex. The figure-eight in the middle has a λ_2 vertex, and it is of the same type as in the $O(N)$ model. The melon diagram on the right has two λ vertices, and it is characteristic of tensor models.

and we could as well write it as the trace of the convolution of $G(x,y)$ with $G(y,x)^3$, which will be a useful point of view later on.

The SD equations obtained from (3.4.1):

$$G^{-1}(x,y) = C^{-1}(x,y) + \left(m^{d/2} + \lambda_2 G(x,x)\right)\frac{\delta(x-y)}{\sqrt{g(x)}} + \lambda^2 G(x,y)^3\,, \tag{3.4.2}$$

should be understood in the sense of distributions, that is, denoting by $\mathcal{S}(x,y)$ the right-hand side of (3.4.2), we should demand that in the limit in which any regularization is removed we obtain:

$$\int \mathrm{d}^d y\sqrt{g(y)}\,\mathcal{S}(x,y)\int \mathrm{d}^d z\sqrt{g(z)}\,G(y,z)\phi(z) = \phi(x)\,. \tag{3.4.3}$$

Tuning the bare mass to cancel the tadpole and the divergent part of the melonic integral, and taking the ansatz:

$$G_\star(x,y) = \mathcal{Z}C(x,y) = \mathcal{Z}\frac{c(\Delta)}{s(x,y)^{2\Delta}}\,, \tag{3.4.4}$$

where the coefficient $c(\Delta)$ is defined in (3.B.9), we obtain:

$$\lambda^2\mathcal{Z}^4\int \mathrm{d}^d z\sqrt{g(z)}\,C(x,z)\left(C(z,y)^3 - \frac{\delta(z-y)}{\sqrt{g(z)}}B\right) = (1-\mathcal{Z})\frac{\delta(x-y)}{\sqrt{g(x)}}\,. \tag{3.4.5}$$

The constant B comes from the mass counterterm $m^{d/2} = -\lambda_2 C(x,x) - B$ and should be chosen so as to cancel the divergence of the convolution of C with C^3 and yield a delta function as a result. Since for $\Delta = d/4$ we have $C(x,y)^3 = c(\Delta)^3/s(x,y)^{2(d-\Delta)}$, by comparison to footnote 19 we have:

$$B = c(\Delta)^3\int_{s(u,y)>r}\mathrm{d}^d u\sqrt{g(u)}\,\frac{1}{s(u,y)^{2(d-\Delta)}} - \frac{c(\Delta)^3}{c(d-\Delta)}\frac{\Gamma(d-\Delta)}{\Gamma(\Delta)}\,. \tag{3.4.6}$$

In the spirit of defining (power-) divergent quantities by analytic continuation, we might instead simply set $B=0$. Either way we obtain for $\mathcal{Z}$ the equation:

$$\lambda^2\mathcal{Z}^4\frac{c(\Delta)^3}{c(d-\Delta)} = 1-\mathcal{Z}\,, \tag{3.4.7}$$

or equivalently:

$$\mathcal{Z} = 1 + \lambda^2 \mathcal{Z}^4 \frac{4\Gamma(1-d/4)}{d(4\pi)^d \Gamma(3d/4)}\,, \tag{3.4.8}$$

which is the same equation as in flat space. The solution of this equation is the generating function of 4-Catalan (or Fuss-Catalan) numbers:

$$\mathcal{Z}(\lambda) = \sum_{n=0}^{+\infty} \frac{1}{4n+1} \binom{4n+1}{n} \left(-\lambda^2 \frac{c(\Delta)^3}{c(d-\Delta)}\right)^n\,, \tag{3.4.9}$$

and can also be written in an explicit closed form (see [46]). Here we just point out that it has a square root singularity at:

$$\lambda_c^2 = -\frac{3^3}{2^8} \frac{c(d-\Delta)}{c(\Delta)^3} = \frac{3^3}{2^8} \frac{d(4\pi)^d \Gamma(3d/4)}{4\Gamma(1-d/4)}\,, \tag{3.4.10}$$

at which $\mathcal{Z}(\lambda_c) = 4/3$. The series (3.4.9) resums all the melonic insertions in the two-point function and the critical point corresponds to the radius of convergence of this series, thus determining the maximal value of the coupling for which the model is defined.

In conclusion, at large N the two-point function of the long-range $O(N)^3$ model is proportional to the free propagator, with proportionality constant satisfying (3.4.8). This holds both on flat and spherical background, and the two-point function on S^d is obtained from the two-point function in $\mathbb{R}^d$ by simply replacing the distance in $\mathbb{R}^d$ by the chordal distance in S^d, as expected.

3.4.2 The sphere free energy at leading order in the large-N expansion

We now want to evaluate the on-shell 2PI effective action, i.e. the free energy. We then start from (3.4.1), and replace G by the solution (3.4.4):

$$\begin{aligned}\mathbf{\Gamma}[G] =& N^3 \left(\frac{1}{2}\mathcal{Z}\,\mathrm{Tr}[C^{-1}C] + \frac{1}{2}\,\mathrm{Tr}[\ln(\mathcal{Z}^{-1}C^{-1})] + \frac{m^{2\zeta}}{2}\mathcal{Z}\int_x C(x,x)\right.\\ &\left. + \frac{\lambda_2 \mathcal{Z}^2}{4}\int_x C(x,x)^2 + \frac{\lambda^2\mathcal{Z}^4}{8}\int_{x,y} C(x,y)^4\right)\,.\end{aligned} \tag{3.4.11}$$

We have five terms to evaluate, all of which are UV divergent. The first four are similar to those in the $O(N)$ model, except for some $\mathcal{Z}$ coefficients and for the long-range exponent $\zeta = d/4 < 1$. The latter plays no role in the first term, which is proportional to $\mathrm{Tr}[\mathbf{1}]$, and it is set to zero by analytic continuation in d, as before. Similarly, the $\ln(\mathcal{Z}^{-1})\,\mathrm{Tr}[\mathbf{1}]$ coming from the second term can be dropped. Therefore, the first two terms reproduce (3.2.4).

In order to compute the next two terms, we need first to compute $C(x,x)$ for long-range scaling:

$$C(x,x) = \frac{(d-1)!}{a^d \Gamma(d/2)(4\pi)^{d/2}} \sum_{n=0}^{\infty} \frac{D_n}{\omega_n^{(\zeta)}}\,. \tag{3.4.12}$$

Using dimensional regularization, we find again $C(x,x) = 0$, see appendix 3.D.2.

Finally, we need to evaluate the melon integral, which at leading order is the only qualitative difference with respect to the $O(N)$ model. We call it M:

$$M = \int_{x,y} C(x,y)^4\,. \tag{3.4.13}$$

In order to regulate the UV divergences we set $\Delta = \frac{d-\epsilon}{4}$, and obtain the ϵ regularized melon integral:

$$M_\epsilon = c(\Delta)^4 \int_{x,y} \frac{1}{s(x,y)^{2(d-\epsilon)}} = c(\Delta)^4 (2a)^{2\epsilon} \int \mathrm{d}^d x \int \mathrm{d}^d y \, \frac{1}{(1+x^2)^\epsilon (1+y^2)^\epsilon |x-y|^{2(d-\epsilon)}} \,. \quad (3.4.14)$$

Alternatively, as we already mentioned, M can be thought of as the trace of the convolution $G(x,y)$ with $G(y,x)^3$. On shell and for $\Delta = d/4$ we have $G_\star(y,x)^3 \propto C(x,y)^3 \propto 1/s(x,y)^{3d/2} = 1/s(x,y)^{2(d-\Delta)}$ which is also the two-point function of the shadow field. The regularization can then be viewed as a shift by ϵ of the dimension of the shadow, that is the replacement $\widetilde{\Delta} = d - \Delta \to \widetilde{\Delta} - \epsilon$ at fixed $\Delta = d/4$:

$$M_\epsilon = c(\Delta)^4 \int_{x,y} \langle \phi_\Delta(x) \phi_\Delta(y) \rangle_{\mathrm{cs}} \langle \phi_{\widetilde{\Delta}-\epsilon}(x) \phi_{\widetilde{\Delta}-\epsilon}(y) \rangle_{\mathrm{cs}} \,. \quad (3.4.15)$$

This point of view will be useful in the next subsection.

The regularized melon integral (3.4.14) can be reduced to an integral over a single point by exploiting the homogeneity of the sphere and factoring out a volume of the d-sphere $V_d = \int \mathrm{d}^d z \, \Omega(z)^d$, given in (3.A.7). The remaining integral, which has appeared for example in [54, 53], can be computed for $\epsilon > d/2 > 0$ and then analytically continued to small ϵ, leading to:

$$M_\epsilon = \frac{a^{2\epsilon} \, \Gamma(\frac{d+\epsilon}{4})^4 \, \Gamma(-\frac{d}{2}+\epsilon)}{2^{3d-1} \, \pi^{d-1/2} \, \Gamma(\frac{d-\epsilon}{4})^4 \, \Gamma(\frac{d+1}{2}) \, \Gamma(\epsilon)} \,, \quad (3.4.16)$$

which vanishes in the limit $\epsilon \to 0$, whenever d is not an even number. Given that $C(x,y)^3$ is proportional to $C^{-1}(x,y)$ (see (3.4.5)), we can interpret this result as another instance of $\mathrm{Tr}[\mathbf{1}]$ being set to zero by analytic regularization.

In conclusion, at leading order the sphere free energy of the interacting long-range $O(N)^3$ model reduces to that of the free model, i.e. N^3 times the GFFT free energy (3.2.4). This is an interesting feature, shared with the $O(N)$ model. However, we do not know if there is any deeper reason behind it, or if it is just an accident of these specific large-N limits dominated by tadpole or melonic diagrams.

3.4.3 The next-to-next-to-leading order of the large-N expansion

The free energy of the $O(N)^3$ model has a series expansion in $1/\sqrt{N}$ [11]. At NLO the only 2PI diagram is a figure-eight with one tetrahedron vertex [74], and hence its contribution vanishes like the similar LO contributions from the λ_2 coupling.

At NNLO the combinatorics of the $O(N)^3$ model with only the tetrahedron interaction has been carefully studied in [76]. Restricting to 2PI diagrams, it turns out that there is an infinite family of ladder-like diagrams, closed in a planar way as shown in Fig. 3.5, plus one special diagram, shown in Fig. 3.6. It is straightforward to complement the analysis of [76] by adding the effect of the pillow and double-trace interactions. It turns out that we only need to add to those, diagrams obtained from the ladder diagrams by replacing one or more rungs (each made by two λ vertices) with one or more local λ_1 vertices, as in the chain diagrams of the $O(N)$ model of Fig. 3.3.[10]

As we will show in appendix 3.F, the graph of Fig. 3.6 gives a finite contribution to the sphere free energy. However, since it only depends on the tetrahedron coupling, it takes the same value at all the fixed points, and thus it does not play a role in checking the F-theorem for this model. We will omit it in the rest of this section.

[10] Similar diagrams with λ_2 instead of λ_1, appear only farther in the $1/\sqrt{N}$ expansion. In fact, the λ_2 coupling is associated to a double-trace interaction, which is the same as the $O(N)$ model interaction, with the replacement $N \to N^3$. Therefore, chains of bubbles with λ_2 vertices will only contribute at order N^0, as in the $O(N)$ model.

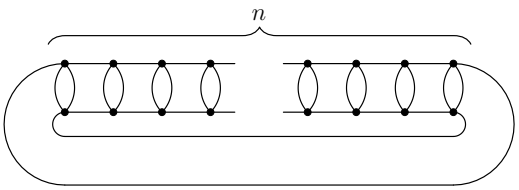

FIGURE 3.5: A generic NNLO vacuum 2PI diagram having the form of a closed ladder with $n \geq 2$ rungs, and vertices corresponding to the tetrahedron interaction. Similar diagrams but with a twist in the rails, thus forming a Möbius strip, appear only at lower order in N.

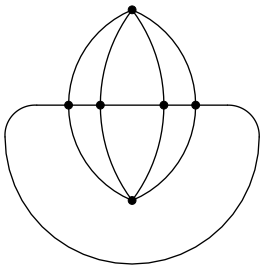

FIGURE 3.6: The unique NNLO vacuum 2PI diagram besides the ladders. All six vertices are tetrahedral.

We thus have an infinite series of diagrams that are a mixture of ladders and chains. Formally, they can be easily resummed in terms of a kernel that is the sum of a ladder kernel and a local kernel:[11]

$$\mathbf{\Gamma}_{\text{NNLO}}[G] = \frac{N^2}{2}\left(\text{Tr}[\ln(\mathbb{I} - K_1)] + \text{Tr}[K_1]\right) , \tag{3.4.17}$$

where K_1 is the familiar Bethe-Salpeter kernel of melonic theories, namely:

$$K_1(x_1, x_2, x_3, x_4) = -G(x_1, x_3)G(x_2, x_4)\Big(\lambda^2\, G(x_3, x_4)^2 + \lambda_1 \delta(x_3, x_4)\Big) , \tag{3.4.18}$$

represented in Fig. 3.7. It should be noted that this kernel displays two differences with respect to the

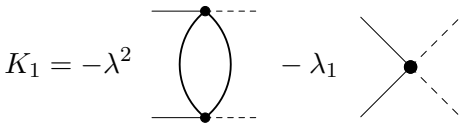

FIGURE 3.7: Graphical representation of the kernel K_1 (3.4.18). Solid lines represent full two-point functions, while dashed lines represent amputated external legs. For obvious reasons we call the first term “ladder kernel" and the second “local kernel".

usual ladder kernel of melonic theories found in the literature (e.g. [45, 16]). First, we have a minus sign in the ladder kernel, due to the imaginary unit multiplying the tetrahedron interaction in (2.4.17). Second, a factor 3 is missing from the ladder kernel. The reason for the latter can be understood from

[11] We have subtracted a $\text{Tr}[K_1]$ from the expansion of the logarithm because its ladder contribution does not correspond to a 2PI diagram. As for its local contribution, it is another figure-eight diagram, which evaluates to zero, and hence we can add or subtract it at will.

the full Bethe-Salpeter kernel obtained from the leading-order 2PI effective action, namely [17]:

$$\begin{aligned}\hat{K}_{\mathbf{ab};\mathbf{cd}}(x_1,x_2,x_3,x_4) &= -G(x_1,x_3)G(x_2,x_4)\Big(\lambda^2\,G(x_3,x_4)^2+\lambda_1\delta(x_3,x_4)\Big)\hat{P}^{(1)}_{\mathbf{ab};\mathbf{cd}}\\ &\quad - G(x_1,x_3)G(x_2,x_4)\Big(3\lambda^2\,G(x_3,x_4)^2+\lambda_2\delta(x_3,x_4)\Big)\hat{P}^{(2)}_{\mathbf{ab};\mathbf{cd}}\\ &\equiv K_1(x_1,x_2,x_3,x_4)\hat{P}^{(1)}_{\mathbf{ab};\mathbf{cd}}+K_2(x_1,x_2,x_3,x_4)\hat{P}^{(2)}_{\mathbf{ab};\mathbf{cd}}\,.\end{aligned} \tag{3.4.19}$$

In most of the previous literature on these models the focus was on the spectrum of singlet operators, which can be obtained by the s-channel OPE of the four-point function $\langle\phi_{\mathbf{a}}(x_1)\phi_{\mathbf{a}}(x_2)\phi_{\mathbf{b}}(x_3)\phi_{\mathbf{b}}(x_4)\rangle$. The latter requires inverting $(\mathbb{I}-\hat{K})_{\mathbf{ab};\mathbf{cd}}$ and taking a trace on the tensor indices by contracting with $\delta_{\mathbf{ab}}\delta_{\mathbf{cd}}$. In such case, the first term is zero because $\hat{P}^{(1)}$ is traceless in this channel, and thus we have a factor $3\lambda^2$ in the ladder part of the surviving kernel contribution. However, the index trace leading to (3.4.17) is taken by contracting with $\delta_{\mathbf{ac}}\delta_{\mathbf{bd}}$. In this case, the $\hat{P}^{(1)}$ term gives the leading contribution of order N^2, while the $\hat{P}^{(2)}$ term only contributes at order N^0, thus explaining the absence of the factor 3 in (3.4.18). Notice that the same part of the kernel is the relevant one for the four-point function $\hat{P}^{(1)}_{\mathbf{ab};\mathbf{a'b'}}\hat{P}^{(1)}_{\mathbf{cd};\mathbf{c'd'}}\langle\phi_{\mathbf{a'}}(x_1)\phi_{\mathbf{b'}}(x_2)\phi_{\mathbf{c'}}(x_3)\phi_{\mathbf{d'}}(x_4)\rangle$, whose s-channel OPE provides the spectrum of bilinear operators that are in a symmetric-traceless matrix representation of one of the $O(N)$'s, and the singlet one of the other two.

As before, in order to evaluate the NNLO free energy we substitute (3.4.4) into (3.4.17), and we use the conformal partial wave formalism reviewed in appendix 3.E. Inserting the resolution of the identity (3.E.8) inside the trace in (3.4.17), we find the following formal expression:

$$F_{\text{NNLO}}=\frac{N^2}{2}\sum_{J\in\mathbb{N}_0}\int_{\frac{d}{2}}^{\frac{d}{2}+\mathrm{i}\,\infty}\frac{\mathrm{d}h}{2\pi\,\mathrm{i}}\rho(h,J)\,\big(\ln(1-k(h,J))+k(h,J)\big)\,\mathcal{N}^{\Delta}_{h,J}\mathcal{N}^{\widetilde{\Delta}}_{\tilde{h},J}\,\mathrm{Tr}[\Psi^{\Delta,\Delta,\widetilde{\Delta},\widetilde{\Delta}}_{h,J}]\,, \tag{3.4.20}$$

with notation defined in appendix 3.E. In addition, we here have $\Delta=d/4$, and the kernel eigenvalue:

$$k(h,J)=-\frac{g^2}{(4\pi)^d}\frac{\Gamma(-\frac{d}{4}+\frac{h+J}{2})\Gamma(\frac{d}{4}-\frac{h-J}{2})}{\Gamma(\frac{3d}{4}-\frac{h-J}{2})\Gamma(\frac{d}{4}+\frac{h+J}{2})}\,, \tag{3.4.21}$$

where g is the effective tetrahedral coupling $g=\lambda\,\mathcal{Z}(\lambda)^2$, which resums all the two-point melonic insertions. The latter are absent by construction in the 2PI effective action, but reappear when going on shell, i.e. when replacing the generic G by the solution of the SD equations $G_\star(x,y)=\mathcal{Z}(\lambda)C(x,y)$. By writing all quantities in terms of g we can keep ignoring the melonic insertions and use the free propagator, but we should restrict its range to $|g|<g_c\equiv\lambda_c\,\mathcal{Z}(\lambda_c)^2$, because of the square root singularity at the critical coupling (3.4.10).

It will actually be convenient to consider the derivative of the free energy in order to get rid of the logarithm:

$$-g\frac{\partial}{\partial g}F_{\text{NNLO}}=N^2\sum_{J\in\mathbb{N}_0}\int_{\frac{d}{2}}^{\frac{d}{2}+\mathrm{i}\,\infty}\frac{\mathrm{d}h}{2\pi\,\mathrm{i}}\rho(h,J)\,\frac{k(h,J)^2}{1-k(h,J)}\,\mathcal{N}^{\Delta}_{h,J}\mathcal{N}^{\widetilde{\Delta}}_{\tilde{h},J}\,\mathrm{Tr}[\Psi^{\Delta,\Delta,\widetilde{\Delta},\widetilde{\Delta}}_{h,J}]\,. \tag{3.4.22}$$

A striking feature of (3.4.20), or (3.4.22), is that the kernel eigenvalue is only sensitive to the ladder part of the kernel, because the local part has vanishing eigenvalue on the principal series.[12] This fact can be puzzling, as the diagrams having λ_1 vertices are necessary at the perturbative level: expressing λ_1 as a series in the renormalized coupling g_1 and in g, they have to cancel the UV divergences of the ladder diagrams [17]. Nevertheless, the result of the resummed series of diagrams, evaluated at the

[12] This is straightforward for $\mathrm{Re}(h)>d/2$, and it is extended by analytic continuation to the principal series and beyond.

fixed point, where g_1 takes a specific g-dependent value, turns out to be expressible in terms of only ladder diagrams. This is a familiar situation in the four-point function of these models [17, 44],[13] and it is due to the fact that in the conformal limit, the local kernel has zero eigenvalues. The resummed series captures the contribution of the chain diagrams in a subtle manner. When evaluating (3.4.22) using conformal partial waves, only the ladder kernel contributes, and thus one needs to integrate over the principal series an analytic function of g^2. However, the result of the integration (for $J = 0$) is a non-analytic function with a $\sqrt{g^2}$ branch cut. In the perturbative expansion such a branch cut can only come from the λ_1 diagrams, due to the branch cut in the $g_{1\pm}$ fixed points (2.4.26). Therefore, the non-perturbative resummation of the ladder diagrams automatically includes the contribution of the chain diagrams as well, which is a very non-trivial fact. We will provide a cross check of this statement below.

The problem with the expression (3.4.22) is that the trace of the conformal partial wave is divergent. From (3.E.10) we have:

$$\mathrm{Tr}[\Psi^{\Delta,\Delta,\widetilde{\Delta},\widetilde{\Delta}}_{h,J}] = \int_{x_1,x_2,z} \langle\phi_\Delta(x_1)\phi_\Delta(x_2)\mathcal{O}^{\bar{\mu}}_{(h,J)}(z)\rangle_{\mathrm{cs}}\langle\phi_{\widetilde{\Delta}}(x_1)\phi_{\widetilde{\Delta}}(x_2)\mathcal{O}^{\bar{\mu}}_{(\tilde{h},J)}(z)\rangle_{\mathrm{cs}}\,. \tag{3.4.23}$$

Formally this integral is conformally invariant, but as a consequence it is also divergent because of the infinite volume of the conformal group. Notice that the same type of integral appears as a natural pairing (or inner product) of n-point functions [79]; however, in that case one divides by the volume of $SO(d+1,1)$ (or in other words, one considers a gauge-fixed version of the integral) in order to define a finite pairing. In our case, we do not have the freedom to divide the free energy by a diverging quantity: the idea of the F-theorem is that instead we should look at the finite part of the free energy. This might be hiding behind some divergence, which we have to regulate and subtract. The melon integral in (3.4.13) is an example of the same kind: for $\Delta = d/4$ it is proportional to a pairing of two-point structures $\int \mathrm{d}^d x_1 \mathrm{d}^d x_2\, \langle\phi_\Delta(x_1)\phi_\Delta(x_2)\rangle_{\mathrm{cs}}\langle\phi_{\widetilde{\Delta}}(x_1)\phi_{\widetilde{\Delta}}(x_2)\rangle_{\mathrm{cs}}$, and it is divergent for the same reason as above. We have regularized the melon integral by analytic continuation in (3.4.15), which is equivalent to subtracting the divergent part, and we have found a vanishing finite part. We are now going to employ a similar analytic continuation in order to extract the finite part of (3.4.23).

In the case of (3.4.23), setting $\Delta = \frac{d-\epsilon}{4}$ everywhere would not help, as the dependence of the integrand on Δ drops out. It is thus useful to take the second point of view we presented on the regularization of the melon integral and shift only the dimensions of the shadow operators. That is, we define:

$$\mathcal{I}_\epsilon(J) = \int_{x_1,x_2,z} \langle\phi_\Delta(x_1)\phi_\Delta(x_2)\mathcal{O}^{\bar{\mu}}_{(h,J)}(z)\rangle_{\mathrm{cs}}\langle\phi_{\widetilde{\Delta}-\epsilon}(x_1)\phi_{\widetilde{\Delta}-\epsilon}(x_2)\mathcal{O}^{\bar{\mu}}_{(\tilde{h}-\epsilon,J)}(z)\rangle_{\mathrm{cs}}\,. \tag{3.4.24}$$

This analytic regularization breaks the conformal invariance of the integral, but not its translation invariance. Therefore, on flat space there is still a space-time volume divergence, which is instead regularized on the sphere. UV divergences (at coincident points) are still there, but will be cured in an appropriate range of ϵ, and then we will use analytic continuation to take the limit $\epsilon \to 0$.

It can be shown (see appendix 3.G) that all the J-dependence in (3.4.24) can be factored out of the integral:

$$\mathcal{I}_\epsilon(J) = \frac{\Gamma(d-2+J)\Gamma(\frac{d-2}{2})}{2^J\Gamma(d-2)\Gamma(\frac{d-2}{2}+J)}\mathcal{I}_\epsilon(0)\,, \tag{3.4.25}$$

with:

$$\mathcal{I}_\epsilon(0) = \int \mathrm{d}^d x_1 \mathrm{d}^d x_2 \mathrm{d}^d z \frac{(\Omega(x_1)\Omega(x_2)\Omega(z))^d}{s(x_1,x_2)^{d-\epsilon}s(x_1,z)^{d-\epsilon}s(x_2,z)^{d-\epsilon}}\,. \tag{3.4.26}$$

[13] As well as in the fishnet model [77, 78].

Because of the homogeneity of the sphere we are free to set $z = 0$, and factor out the volume of the d-sphere $V_d = \int \mathrm{d}^d z\, \Omega(z)^d$, given in (3.A.7). The integral $\frac{\mathcal{I}_\epsilon(0)}{V_d}$ has already been computed in [54] and the results is:[14]

$$\frac{\mathcal{I}_\epsilon(0)}{V_d} = (2a)^{3\epsilon-d} \frac{\pi^d \Gamma\left(\frac{\epsilon}{2}\right)^3 \Gamma\left(\frac{3\epsilon}{2} - \frac{d}{2}\right)}{\Gamma\left(\frac{d}{2}\right) \Gamma\left(\epsilon\right)^3}, \tag{3.4.27}$$

which has a finite limit for $\epsilon \to 0$ as long as d is not an even number:

$$\lim_{\epsilon\to 0} \frac{\mathcal{I}_\epsilon(0)}{V_d} = \frac{8\left(\pi^d \Gamma\left(-\frac{d}{2}\right)\right)}{(2a)^d \Gamma\left(\frac{d}{2}\right)}. \tag{3.4.28}$$

Reinserting the spin and volume factors we have:

$$\mathcal{I}_\epsilon(J) = (2a)^{3\epsilon} \frac{\pi^{3d/2}\Gamma(\frac{\epsilon}{2})^3\Gamma(\frac{3\epsilon}{2} - \frac{d}{2})\Gamma(d-2+J)\Gamma(\frac{d-2}{2})}{2^J\Gamma(\epsilon)^3\Gamma(d-2)\Gamma(\frac{d-2}{2}+J)\Gamma(d)}. \tag{3.4.29}$$

and after removing the regulator ϵ we get:

$$\mathcal{I}_0(J) = \frac{8\pi^{3d/2}\Gamma(-\frac{d}{2})\Gamma(d-2+J)\Gamma(\frac{d-2}{2})}{2^J\Gamma(d-2)\Gamma(\frac{d-2}{2}+J)\Gamma(d)}. \tag{3.4.30}$$

The ϵ regularization thus provides a finite result for the trace of the conformal partial wave. However, it turns out that it is important to consistently shift by ϵ also the normalization factor of the three-point function of shadow operators, as otherwise the resulting series in J would diverge. The product of normalization factors (3.E.11) is then replaced, at large J, by:

$$\mathcal{N}^{\Delta}_{h,J}\mathcal{N}^{\tilde{\Delta}-\epsilon}_{\tilde{h}-\epsilon,J} \sim \frac{2^{3(d+\epsilon)/2+J}}{(2\pi)^d} J^{-3\epsilon}\left(1 + \mathcal{O}(1/J)\right). \tag{3.4.31}$$

This $J^{-3\epsilon}$ factor renders the series over J, whose coefficients otherwise behaves asymptotically as $1/J$, convergent.

We can now perform the integral on h and sum over J in (3.4.22). As explained in appendix 3.H, at large J, the integral behaves as $\frac{f(\epsilon)}{J^{1+3\epsilon}}$ with $f(\epsilon)$ an analytic function at $\epsilon = 0$. We then write:

$$\begin{aligned} -g\frac{\partial}{\partial g}F^{\epsilon}_{\mathrm{NNLO}} = {} & N^2 \int_{\frac{d}{2}}^{\frac{d}{2}+\mathrm{i}\infty} \frac{\mathrm{d}h}{2\pi\,\mathrm{i}} \rho(h,0)\, \frac{k(h,0)^2}{1-k(h,0)}\, \mathcal{N}^{\Delta}_{h,0}\mathcal{N}^{\tilde{\Delta}-\epsilon}_{\tilde{h}-\epsilon,0}\, \mathcal{I}_\epsilon(0) \\ & + N^2 \Bigg[\sum_{J\in\mathbb{N}_+} \left(\int_{\frac{d}{2}}^{\frac{d}{2}+\mathrm{i}\infty} \frac{\mathrm{d}h}{2\pi\,\mathrm{i}} \rho(h,J)\, \frac{k(h,J)^2}{1-k(h,J)}\, \mathcal{N}^{\Delta}_{h,J}\mathcal{N}^{\tilde{\Delta}-\epsilon}_{\tilde{h}-\epsilon,J}\, \mathcal{I}_\epsilon(J) - \frac{f(\epsilon)}{J^{1+3\epsilon}} \right) \\ & + \sum_{J\in\mathbb{N}_+} \frac{f(\epsilon)}{J^{1+3\epsilon}} \Bigg]. \end{aligned} \tag{3.4.32}$$

The first sum is now convergent for $\epsilon = 0$, and thus can be computed numerically, while the second sum gives and explicit pole in ϵ. We thus define the renormalized sphere free energy, or rather its derivative, as:

$$-g\frac{\partial}{\partial g}F_{\mathrm{NNLO}} = \lim_{\epsilon\to 0}\left(-g\frac{\partial}{\partial g}F^{\epsilon}_{\mathrm{NNLO}} - \frac{N^2 f(0)}{3\epsilon}\right), \tag{3.4.33}$$

[14] In appendix 3.G we provide a detailed derivation.

which for example at $d = 3$, $g = 1$ and $a = 1$ gives:

$$-g\frac{\partial}{\partial g}F_{\text{NNLO}} = 7.57 \times 10^{-4}\, N^2\,. \tag{3.4.34}$$

We computed this value at $d = 3$, for $a = 1$ and different values of g up to $g_c \equiv \lambda_c\, \mathcal{Z}(\lambda_c)^2$ (with λ_c given in (3.4.10)). The result is a positive convex function, vanishing at the origin, as shown in Fig. 3.8.

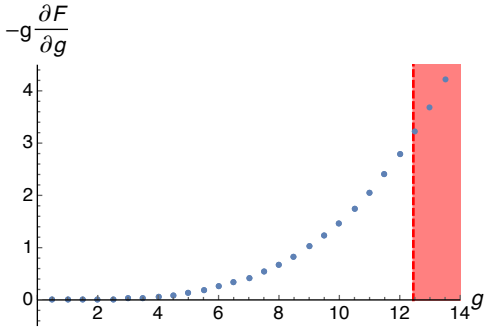

FIGURE 3.8: Derivative of the free energy at $d = 3$ and $a = 1$. The red area corresponds to $g > g_c$, where nothing seems to happen, but in fact there is no λ giving such values of g.

The non-normalizable contribution. In the context of the F-theorem we are interested in the difference between the free energy at the UV fixed point and at the IR fixed point. The value of g being the same at the two fixed points, and the above result being seemingly independent of g_1 or g_2, it would naively seem that the free energy is the same at the two fixed points.

Things are however more subtle than this. As explained in appendix 3.E, the resolution of the identity (3.E.8) is valid in a functional space with appropriate integrability conditions, and the latter are violated by four-point functions whose s-channel OPE contains operators of dimension smaller than $d/2$. It turns out that this is precisely what happens in the ultraviolet CFT, due to a primary operator in the OPE of $\hat{P}^{(1)}_{\mathbf{ab;cd}}(\phi_{\mathbf{c}} \times \phi_{\mathbf{d}})$ whose dimension descends below $d/2$. In fact, at $J = 0$, the equation $k(h, 0)$ has two solutions $h_\pm$ lying respectively on the right and on the left of the integration contour $\mathcal{P}_+$:

$$h_\pm = \frac{d}{2} \pm \frac{2\sqrt{g^2}}{\Gamma(d/2)(4\pi)^{d/2}} + \mathcal{O}(|g|^3)\,, \tag{3.4.35}$$

and in the UV, the physical dimension is actually the one on the left of the contour. Therefore, in evaluating the free energy of the UV theory by the CPW method we need to subtract these contributions from the operator being traced before applying it on the resolution of identity (3.E.8), and then add them back. This amounts to including, besides the principal series integral, an isolated non-normalizable contribution, as in (3.E.21). That is, in the UV version of (3.4.22) we have to add minus the residue of the integrand at $h = h_-$.

With this in mind, it is clear that the difference between the free energy of the UV theory and the one of the IR theory is given precisely by the isolated non-normalizable contribution of the former.

Going again through the same regularization procedure as in the IR case, we thus find:

$$\begin{aligned} g\frac{\partial}{\partial g}\left(F^{UV}_{\text{NNLO}} - F^{IR}_{\text{NNLO}}\right) &= N^2 \,\text{Res}\left[\rho(h,0)\,\frac{k(h,0)^2}{1-k(h,0)}\,\mathcal{N}^{\Delta}_{h,0}\mathcal{N}^{\tilde{\Delta}}_{\tilde{h},0}\,\mathcal{I}_0(0)\right]_{h=h_-} \\ &= 16\frac{\Gamma(-d/2)|g|^3}{2^{3d}\pi^{3d/2}\Gamma(d)}N^2 + \mathcal{O}(|g|^5)\,, \end{aligned} \tag{3.4.36}$$

which is positive for $2 < d < 4$. By numerical evaluation at finite g, it can be checked that the positivity remains valid also at all values of g, within the radius of convergence of the melonic series (see Fig. 3.9).

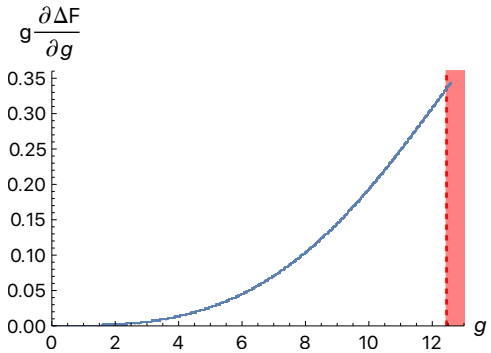

FIGURE 3.9: Difference between the free energy in the UV and the free energy in the IR at $d = 3$. The red area corresponds to $g > g_c$.

This result can also be checked perturbatively. At the fixed points the critical coupling g_1 is [17, 80]:

$$g_{1\pm} = \pm\sqrt{g^2}\big(1+\mathcal{O}(g^2)\big) + g^2\big(\psi(1)+\psi(d/2)-2\psi(d/4)+\mathcal{O}(g^2)\big)\,, \tag{3.4.37}$$

where $\psi(z)$ is the digamma function. When flowing from the UV to the IR, the fixed point value goes from $g_{1-} \simeq -\sqrt{g^2}$ to $g_{1+} \simeq \sqrt{g^2}$ (except for the vertical trajectories in Fig. 2.12, which we will discuss below): therefore, at leading order in g, graphs with an even number of vertices have the same amplitude in the UV as in the IR, while graphs with an odd number of vertices have opposite signs. The difference between the free energy in the UV and the free energy in the IR is thus expanded in odd powers of $|g|$. Up to order $|g|^3$, only the graph of Fig. 3.10 contributes, where the vertices are either two tetrahedron and one g_1 or three g_1.

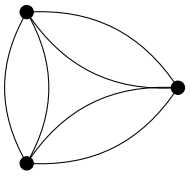

FIGURE 3.10: Feynman graph contributing to the free energy at order 3 in the coupling constant. The vertices are either two tetrahedron and one g_1 or three g_1.

Using the expression of the kernel given in (3.4.19) to fix the combinatorial factors, we have:

$$g\frac{\partial}{\partial g}(F^{UV}_{\text{NNLO}} - F^{IR}_{\text{NNLO}}) = 2|g|^3N^2\mathcal{A} + \mathcal{O}(|g|^5)\,, \tag{3.4.38}$$

where we denoted $\mathcal{A}$ the amplitude of the graph in Fig. 3.10:

$$\mathcal{A} = c(\tfrac{d}{4})^6 \int d^dx d^dy d^dz \frac{(\Omega(x)\Omega(y)\Omega(z))^d}{s(x,y)^{4\Delta}s(x,z)^{4\Delta}s(y,z)^{4\Delta}} \,. \tag{3.4.39}$$

Using again dimensional regularization with $\Delta = \frac{d-\epsilon}{4}$, we notice that this amplitude is proportional to $\mathcal{I}_\epsilon(0)$ in (3.4.26). We then obtain:

$$\mathcal{A} = 8\frac{\Gamma(-d/2)}{2^{3d}\pi^{3d/2}\Gamma(d)} \quad \Rightarrow \quad g\frac{\partial}{\partial g}\left(F^{UV}_{\text{NNLO}} - F^{IR}_{\text{NNLO}}\right) = 16\frac{\Gamma(-d/2)|g|^3}{2^{3d}\pi^{3d/2}\Gamma(d)}N^2 + \mathcal{O}(|g|^5) \,, \tag{3.4.40}$$

in agreement with (3.4.36).

In conclusion, the difference between the sphere free energy at the fixed points (g_{1-}, g_{2-}) or (g_{1-}, g_{2+}) and the one at the fixed points (g_{1+}, g_{2-}) or (g_{1+}, g_{2+}) (see Fig. 2.12)[15] grows with growing $|g|$. Since the difference vanishes at $g = 0$, we conclude that for the fixed points at fixed $g \neq 0$ the sphere free energy satisfies $F^{UV}_{\text{NNLO}} > F^{IR}_{\text{NNLO}}$, in accordance with the F-theorem.

Trajectories at fixed g_1. The reader will note in Fig. 2.12 the presence of two vertical lines: these are two trajectories at fixed g_1 connecting two different pairs of fixed points. As neither the tetrahedral coupling nor g_1 change along these trajectories, the above computation implies that at NNLO the free energy at the two ends of such trajectories is the same. We expect that in order to see a change of the free energy along these trajectories one would need to push the evaluation to lower orders in $1/N$.

The first non-trivial contribution involving the double trace coupling g_2, which does vary along the vertical trajectories, comes from ladder graphs generated by the double trace part $K_2\hat{P}^{(2)}$ of the Bethe-Salpeter kernel (3.4.19). They essentially behave the same as the ladders generated by $K_1\hat{P}^{(1)}$, up to replacing g^2 by $3g^2$, but the isolated contribution to the conformal partial wave expansion in the UV would in this case depend on the fixed-point value of g_2.

However, it should be noted that, as such ladders appear only at order N^0, one should include the effect of the $1/N$ corrections to the on-shell two-point function as well as to the fixed-point values of the couplings. We know from [80] that such corrections have a drastic effect on the fixed-point theory: in order to find a non-trivial precursor of the large-N theory, one needs to keep a finite ϵ, with $\epsilon N \ll 1$; then, the lines of fixed points collapse to isolated points and the scaling dimensions acquire an imaginary part. The whole analysis becomes much more involved, and since in this case the theory is manifestly non-unitary we do not expect the F-theorem to necessarily hold.

3.5 Conclusions

Our main result is the confirmation that the F-theorem holds for the long-range $O(N)^3$ model. We outline here the content of the chapter and the main steps leading to this conclusion.

Flow between Gaussian CFTs. As a warm up, in section 3.2, we consider two Gaussian CFTs with action $\frac{1}{2}\int \mathrm{d}^dx\phi(x)(-\partial^2)^\zeta\phi(x)$, one being the standard short-range action $\zeta = 1$ and the second one having $\zeta \neq 1$ (also known as generalized free field theory). We examine the flow between two such CFTs and find that, on the one hand, the RG always flows in the infrared towards lower ζ, while on the other the sphere free energy is concave with a maximum at $\zeta = 1$. An RG trajectory flowing from a short-range model $\zeta = 1$ to a long-range one $0 < \zeta < 1$ thus satisfies the F-theorem. However

[15] Notice that (g_{1+}, g_{2-}) can be reached only through one trajectory emanating from (g_{1-}, g_{2-}), while (g_{1-}, g_{2+}) has only one trajectory to flow to an IR fixed point, i.e. (g_{1+}, g_{2+}). Between (g_{1-}, g_{2-}) and (g_{1+}, g_{2+}) there is instead an infinite set of trajectories.

a trajectory starting in the "strong short-range" regime $\zeta > 1$ is such that the free energy increases in the IR. This gives a trivial counter-example of the F-theorem for non-unitary (and non-local) theories.

Revisiting the $O(N)$ model: conformal partial wave expansion. Next, in section 3.3, we revisit the vector $O(N)$ model and rederive its sphere free energy, previously obtained in [53]. While the result of this section is not new, we use it as an opportunity to introduce the set of techniques relevant for the rest of the chapter.

First we briefly recall the formalism of the two-particle irreducible (2PI) effective action, which is particularly natural for discussing the free energy of large-N models. At large N, the free energy of the interacting fixed point is the same as in the free theory, hence to test the F-theorem one needs to go beyond the leading order. The diagrams contributing to the free energy at next-to-leading (NLO) order in $1/N$ are resummed to $F_{\text{NLO}} = \frac{1}{2}\operatorname{Tr}\ln(1-K)$, where K is the Bethe-Salpeter kernel, which at the relevant order is a local operator. We note that the component of the four-point function which is one-particle irreducible in the s-channel, $\mathcal{F}_s$, writes in terms of K and the two-point function G as $\mathcal{F}_s = (1-K)^{-1}GG$.

Second, we analyze $\mathcal{F}_s$ and F_{NLO} using the conformal partial waves (CPW) expansion, which we review in appendix 3.E. The use of this technique for the sphere free energy is new, and it has the advantage that it can be generalized to models with different kernels K. In the $O(N)$ model, the CPW expansion of the bilocal to bilocal identity operator includes the principal series and an additional non-normalizable state, as the dimension of the field is smaller than $d/4$. When evaluating the four-point function $\mathcal{F}_s$ in the critical model, one finds that the Bethe-Salpeter kernel is zero on the principal series, and infinite on the non-normalizable state, thus $\mathcal{F}_s$ reduces to the free contribution $\mathcal{F}_s^{\text{free}}$ restricted to the principal series. This implies the well-known result that the spectrum of the critical $O(N)$ model at large N is the same as in the free theory, except that the ϕ^2 operator is replaced by its shadow [81].

Using the same CPW expansion of the identity for F_{NLO}, we obtain a zero contribution from the principal series and a non-trivial one from the isolated non-normalizable state. This isolated contribution gives the only non-trivial part and reproduces by itself the value of F_{NLO} computed in [53].

The long-range $O(N)^3$ model on the sphere. In section 3.4, we study the long-range $O(N)^3$ model on the sphere. The situation is similar to the one in the $O(N)$ model: at the first non-trivial order in $1/N$, i.e. at next-to-next-to-leading (NNLO) order, the diagrams contributing to the free energy (up to an exceptional diagram which is finite and equal at all the fixed points) are resummed to $F_{\text{NNLO}} = \frac{1}{2}\operatorname{Tr}\ln(1-K)$. However, in stark contrast to the $O(N)$ model, K is now a bilocal operator, and the CPW expansion is the only available non-perturbative method of evaluation.

Two different regimes are encountered. In the infrared (IR) CFT, F_{NNLO} has a CPW expansion restricted to the principal series only. Such expansion of the free energy can be evaluated non-perturbatively (numerically) showing in particular how the CPW expansions in CFT can be used to resum infinite classes of vacuum diagrams.

In contrast, for the ultraviolet (UV) CFT one needs to add a non-normalizable state besides the principal series, because the dimension of one of the primary operators in the $\phi\phi \sim \sum c_{\phi\phi O}\, O$ operator product expansion (OPE) descends below $d/2$. Although the inclusion of a non-normalizable state is reminiscent of the $O(N)$ model, the situation is conceptually and practically different, as will be explained.

Due to the inclusion of this non-normalizable state, the free energy decreases between the ultraviolet and the infrared CFT, as in the F-theorem. In perturbation theory, this jump can be seen as the reversal of the sign of an infinite class of diagrams due to the flow of a coupling constant.

Comments on future directions. Independently of the F-theorem, the free energy is a central quantity in statistical field theory, and computing it to higher orders of the $1/N$ expansion can be of interest for many statistical or condensed matter models. The closest example to our setting is certainly the Sachdev-Ye-Kitaev model [82, 83], which is a model of N strongly interacting Majorana fermions in dimension 1 with a melonic large-N limit. The appropriate generalization of the CPW expansion, taking into account the Grassmann nature of the fields and the presence of an extra discrete series in the basis of bilocal functions, has already been considered in [15], where among other things the part of the free energy which is singular in the limit of zero temperature was computed. One could imagine using a similar computation as ours in order to compute also the finite part of the free energy. In fact, as our main calculation concerns a long-range model, it would more naturally be compared to the computation of the free energy of the Gross-Rosenhaus model [84]. Indeed, in this model, the UV part of the action is replaced by a quadratic bilocal term which leads to a line of fixed point in the IR, similarly to what happens for our model. A $O(N)^3$ tensor version of the Gross-Rosenhaus model (i.e. a long-range version of the Klebanov-Tarnopolsky model [45]) would of course also be a natural candidate for such a computation. We expect that the main difference between the Gross-Rosenhaus model and a long-range Klebanov-Tarnopolsky model would be the graph of Fig. 3.6, which arises at next-to-next-to-leading order only for the latter. This generalization is beyond the scope of the present work but would be interesting to study it in the future.

3.A Useful formulas on S^d

We collect here some useful formulas about S^d and the spectrum of the Laplace-Beltrami operator on it.

The d-dimensional round sphere S^d can be defined by the equation:

$$\sum_{\bar{\mu}=1}^{d+1}(\bar{X}^{\bar{\mu}})^2 \equiv \sum_{\mu=1}^{d}(X^\mu)^2 + Z^2 = a^2\,, \tag{3.A.1}$$

where $\bar{X}^{\bar{\mu}} = \{X^\mu, Z\}$ are the Cartesian coordinates in the embedding space $\mathbb{R}^{d+1}$, and a is the radius of the sphere. In the northern and southern hemispheres, the equation can be solved as $Z_\pm(X) = \pm\sqrt{a^2 - X^2}$, respectively, with $X^2 = \sum_{\mu=1}^{d}(X^\mu)^2$.

It is convenient to describe the metric on S^d through the (equatorial) stereographic projection to the d-dimensional flat space $\mathbb{R}^d$. The stereographic projection from the North pole to the equatorial plane is obtained by the change of variables:

$$x^\mu_\pm(X) = \frac{X^\mu}{1 - Z_\pm(X)/a}\,. \tag{3.A.2}$$

Introducing polar coordinates on the equatorial plane, $\{r = \sqrt{x^2}, \theta_1, \ldots, \theta_{d-1}\}$, and denoting θ_d the additional angular coordinate on S^d (i.e. the geodesic distance from the North pole), the stereographic mapping reads simply:

$$r(\theta_d) = a\cot(\theta_d/2)\,. \tag{3.A.3}$$

In stereographic coordinates, the line element takes the following form:

$$ds^2 = \frac{4a^2}{(1+x^2)^2}\sum_{i=1}^{d} {dx_i}^2\,, \qquad x^2 \equiv \sum_{i=1}^{d} {x_i}^2\,. \tag{3.A.4}$$

The metric is conformally flat, i.e.

$$g_{\mu\nu}(x) = \Omega(x)^2\delta_{\mu\nu}\,, \tag{3.A.5}$$

with:

$$\Omega(x) = \frac{2a}{(1+x^2)}\,. \tag{3.A.6}$$

The square root of the determinant of the metric is then given $\sqrt{g} = \Omega(x)^d$, and the Ricci scalar is $R = d(d-1)/a^2$. The volume of the d-sphere is:

$$V_d = \int_{S^d} \mathrm{d}^d x\, \sqrt{g(x)} = \frac{2\pi^{\frac{d+1}{2}}}{\Gamma\left(\frac{d+1}{2}\right)} a^d\,. \tag{3.A.7}$$

The eigenmodes of the scalar Laplacian on the sphere are the spherical harmonics (e.g. [85, 86]):

$$\Psi_{n,j}(\bar{X}) = \rho^{-n}\, T^{(j)}_{\bar{\mu}_1\cdots\bar{\mu}_n} \bar{X}^{\bar{\mu}_1}\cdots\bar{X}^{\bar{\mu}_n}\,, \tag{3.A.8}$$

where $n = 0, 1, 2, ... + \infty$, $\rho = (\bar{X}^{\bar{\mu}}\bar{X}_{\bar{\mu}})^{1/2}$ and $T^{(j)}_{\bar{\mu}_1\cdots\bar{\mu}_n}$ form a basis of constant traceless-symmetric tensors on $\mathbb{R}^{d+1}$, each basis element being labeled by a different value of j. Therefore, we take $j = 1, 2, ...D_n$, with:

$$D_n = \frac{(n+d-2)!\,(2n+d-1)}{n!(d-1)!}\,. \tag{3.A.9}$$

The corresponding eigenvalues are:

$$\omega_n = n(n+d-1)/a^2\,. \tag{3.A.10}$$

They are independent of j, hence they have multiplicity D_n.

The addition theorem of spherical harmonics states that:

$$\sum_{j=1}^{D_n} \Psi_{n,j}(x)\Psi^*_{n,j}(y) = \frac{D_n}{V_d} P_n(\bar{X}\cdot\bar{Y})\,, \tag{3.A.11}$$

where:

$$P_n(z) = \begin{cases} \frac{n!(d-2)!}{(n+d-2)!} C_n^{(d-1)/2}(z)\,, & \text{if } d > 2\,, \\ T_n(z)\,, & \text{if } d = 2\,, \end{cases} \tag{3.A.12}$$

and $C_n^\alpha(z)$ and $T_n(z)$ are the Gegenbauer and Chebyshev polynomials, respectively.

3.B CFTs on S^d

Given a CFT on $\mathbb{R}^d$, and assuming that conformal invariance can be promoted to Weyl invariance[16] (possibly up to an anomaly), we can then define a corresponding CFT on S^d by performing the Weyl transformation (3.A.5), together with the transformation of primary fields:

$$\mathcal{O}(x) \to \Omega(x)^{-\Delta_\mathcal{O}}\mathcal{O}(x)\,, \tag{3.B.1}$$

such that n-point functions are obtained as:

$$\langle \mathcal{O}_1(x_1)\cdots\mathcal{O}_n(x_n)\rangle_{S^d} = \Omega(x)^{-\Delta_1}\cdots\Omega(x)^{-\Delta_n}\langle \mathcal{O}_1(x_1)\cdots\mathcal{O}_n(x_n)\rangle_{\mathbb{R}^d}\,. \tag{3.B.2}$$

[16] See [87] and references therein for the relation between Weyl and conformal invariance.

In practice, the latter amounts to replacing the flat-space distances $|x-y|$ appearing in the conformal correlators with the chordal distance:

$$s(x,y) = 2a\frac{|x-y|}{(1+x^2)^{1/2}(1+y^2)^{1/2}} = |x-y|\Omega(x)^{1/2}\Omega(y)^{1/2}\,. \tag{3.B.3}$$

Notice that this is not the geodesic distance $\sigma(x,y)$ on S^d, but the Euclidean distance in the embedding space $\mathbb{R}^{d+1}$, i.e. $s(x(p),x(p')) = |X(p)-X(p')|$ where $X(p)$ is the embedding map $X : S^d \to \mathbb{R}^{d+1}$ while $x(p)$ is the stereographic map $x : S^d \to \mathbb{R}^d$. Of course, the two are trivially related by a trigonometric relation: $s(x,y) = 2a\sin(\sigma(x,y)/2a)$.

We can check that for a usual free scalar, the propagator on S^d matches the flat one with the flat distance replaced by the chordal distance, if we appropriately tune the non-minimal coupling with the curved background of the sphere. The covariance, or propagator, $C_1(x,y;b)$ is the solution of the equation:

$$(-\nabla_x^2 + b)C_1(x,y;b) = \frac{\delta(x-y)}{\sqrt{g}}\,, \tag{3.B.4}$$

where b is a constant (of squared-mass dimension), $\nabla^2 = \nabla^\mu\nabla_\mu$ is the covariant Laplacian on the d-sphere, and we specified by a subscript the coordinate on which derivatives as in this case there could be an ambiguity. Due to homogeneity of space the propagator depends only on the geodesic distance $\sigma(x,y)$, hence we will also write $C_1(\sigma;b)$ for the propagator. The reason for the subscript 1 in the latter is that this corresponds to the case $\zeta = 1$ of the more general propagator we will consider in the following subsection.

The propagator on S^d has been computed in [88] directly solving (3.B.4), or from an explicit mode sum in [89]. Defining:

$$\gamma_\pm = \frac{d-1}{2} \pm \sqrt{\frac{(d-1)^2}{4} - a^2 b}\,, \tag{3.B.5}$$

the propagator is given by:

$$C_1(\sigma;b) = a^{2-d}\frac{\Gamma(\gamma_+)\Gamma(\gamma_-)}{\Gamma(d/2)\,2^d\,\pi^{d/2}}\,{}_2F_1(\gamma_+,\gamma_-;d/2;\cos(\sigma/2a)^2)\,, \tag{3.B.6}$$

where ${}_2F_1(\alpha,\beta;\gamma;z)$ is the hypergeometric function.

The case of a Weyl invariant free scalar field is obtained with the choice:

$$b = b_W \equiv \frac{d-2}{4(d-1)}R = \frac{d(d-2)}{4a^2}\,, \tag{3.B.7}$$

for which $\gamma_+ = d/2$ and $\gamma_- = (d-2)/2$. In this case, the hypergeometric function reduces to a simple power and we find:

$$C_1(x,y;b_W) = a^{2-d}\frac{\Gamma(d/2-1)}{2^d\,\pi^{d/2}}\left(\sin(\sigma(x,y)/2a)\right)^{2-d} = \frac{\Gamma(d/2-1)}{4\,\pi^{d/2}}\,s(x,y)^{2-d}\,, \tag{3.B.8}$$

which is precisely the massless free scalar propagator of flat space with the replacement $|x-y| \to s(x,y)$.

3.B.1 Generalized free field theory

We now consider the case of a conformal generalized free field theory (GFFT), i.e. a long-range massless Gaussian theory, sometimes called a mean field theory. It is worth discussing it in some detail because it is the simplest case of (non-local) CFT, and because typical long-range models can be defined as perturbations of a GFFT. By definition this is a CFT whose only non-vanishing connected n-point

function is the two-point function, which however has a scaling exponent $\Delta \neq d/2-1$, and which moreover we take to be in the range $\Delta \in (0, d/2)$. On flat space, the two-point function is:

$$C_{\text{flat}}(x,y) = \frac{c(\Delta)}{|x-y|^{2\Delta}}\,, \qquad c(\Delta) = \frac{\Gamma(\Delta)}{2^{d-2\Delta}\pi^{d/2}\Gamma(\frac{d}{2}-\Delta)}\,. \tag{3.B.9}$$

Writing $\Delta = d/2-\zeta$, such GFFT can be obtained from a functional integral with the action:[17]

$$S_{\text{GFFT}}[\phi] = \frac{1}{2}\int \mathrm{d}^d x\, \phi(x)(-\partial^2)^{\zeta}\phi(x)\,, \tag{3.B.10}$$

where the fractional power of the Laplacian can be defined in many equivalent ways [90], among which in particular as the inverse of the "Riesz potential" (3.B.9). The easiest definition is of course in Fourier space, where $(-\partial^2)^{\zeta}$ is defined as the multiplication operator $p^{2\zeta}$, which is the inverse of the Fourier transform of (3.B.9). Going to position space one finds instead a representation as a hypersingular integral operator:[18]

$$(-\partial^2)^{\zeta}\phi(x) = \lim_{r\to 0} c(d-\Delta)\int_{|x-y|>r} \mathrm{d}^d y\, \frac{\phi(y)-\phi(x)}{|x-y|^{2(d-\Delta)}}\,. \tag{3.B.11}$$

In the physics literature such representation is often expressed as:

$$(-\partial^2)^{\zeta}\phi(x) = \int \mathrm{d}^d y\, C^{-1}_{\text{flat}}(x,y)\phi(y)\,, \tag{3.B.12}$$

with convolution kernel:

$$C^{-1}_{\text{flat}}(x,y) = \frac{c(d-\Delta)}{|x-y|^{2(d-\Delta)}}\,, \tag{3.B.13}$$

without any subtraction term. For $\zeta > 0$ the convolution is a formal divergent expression (a "hypersingular" integral), which is to be interpreted through analytic continuation from $\zeta < 0$. For simplicity we will stick to this point of view.

In order to place the GFFT on the d-sphere, we can apply again the Weyl mapping to (3.B.9), and thus write:

$$C(x,y) = \Omega(x)^{-\Delta}\Omega(y)^{-\Delta}C_{\text{flat}}(x,y) = \frac{c(\Delta)}{s(x,y)^{2\Delta}}\,. \tag{3.B.14}$$

Constructing an action associated to such propagator requires as usual identifying the inverse propagator, and from this the type of non-minimal coupling to the background geometry that is needed in order to obtain a conformal theory.

[17] We typically assume $0 < \zeta < 1$. The restriction to $\zeta < 1$ is imposed to preserve reflection positivity (unitarity in Lorentzian signature), but also because $\zeta > 1$ would correspond to a strong short-range rather than long-range action, and moreover the operator with $\zeta = 1$ would in that case be a relevant perturbation. The restriction to $\zeta > 0$ is instead chosen to avoid a strong long-range action, with its associated unusual thermodynamic features [72].

[18] This can be derived by first writing

$$p^{2\zeta} = \frac{1}{\Gamma(-\zeta)}\int_0^{+\infty} \mathrm{d}t \frac{e^{-tp^2}-1}{t^{1+\zeta}}\,,$$

whose validity is trivially checked by rescaling $t \to t/p^2$ and recognizing that the integral reduces to $p^{2\zeta}$ times the Cauchy-Saalschütz representation of $\Gamma(-\zeta)$ for $0 < \zeta < 1$. The singular integral representation is then found by going back to position space and exchanging the order of integration [91].

The covariance $C(x,y)$ in (3.B.14) is also known as the Riesz potential, and it can be written as:

$$C(x,y) = \sum_{n\geq 0}\sum_{j=1}^{D_n} \frac{1}{\omega_n^{(\zeta)}} \Psi_{n,j}(x)\Psi^*_{n,j}(y) = \frac{1}{V_d}\sum_{n\geq 0}\frac{D_n}{\omega_n^{(\zeta)}} P_n(\bar{X}\cdot\bar{Y})\,, \tag{3.B.15}$$

where we used the addition theorem (3.A.11).

The inverse of (3.B.14) is defined by the equation:

$$\int \mathrm{d}^d z\sqrt{g(z)}\, C^{-1}(x,z)\int \mathrm{d}^d y\sqrt{g(y)}\, C(z,y)\phi(y) = \phi(x)\,, \tag{3.B.16}$$

or

$$\int \mathrm{d}^d z\sqrt{g(z)}\, C^{-1}(x,z)C(z,y) = \frac{1}{\sqrt{g}}\delta(x-y)\,. \tag{3.B.17}$$

Given that on flat space (3.B.13) is the inverse of (3.B.9), it is easily seen that the above equations are solved by:

$$C^{-1}(x,y) = \Omega(x)^{\Delta-d}\,\Omega(y)^{\Delta-d}\, C^{-1}_{\text{flat}}(x,y) = \frac{c(d-\Delta)}{s(x,y)^{2(d-\Delta)}}\,, \tag{3.B.18}$$

whose convolution should again be interpreted by analytic continuation. This is of the expected form we would obtain by the Weyl mapping applied to $C^{-1}_{\text{flat}}(x,y)$, formally viewed as the two-point function of the shadow operators [92] of dimension $\widetilde{\Delta} = d-\Delta$. It also means that defining, for $\zeta = d/2-\Delta$, the operator whose kernel is (3.B.18) as:[19]

$$\mathcal{D}_\zeta\phi(x) = \int \mathrm{d}^d y\,\sqrt{g(y)}\, C^{-1}(x,y)\phi(y)\,, \tag{3.B.19}$$

we find that:

$$\mathcal{D}_\zeta\phi(x) = \Omega(x)^{\Delta-d}(-\partial^2)^\zeta\left(\Omega(x)^\Delta\phi(x)\right)\,. \tag{3.B.20}$$

Given the Weyl transformations (3.A.5), (3.B.1) relating the flat space to the sphere, one recognizes in such a relation the definition of conformally covariant operator of order $\zeta = d/2-\Delta$, or conformal biweight $(\Delta, d-\Delta)$ [94, 95].

Therefore, the action replacing (3.B.10) on the sphere is:

$$S_{\text{GFFT}}[\phi] = \frac{1}{2}\int \mathrm{d}^d x\,\sqrt{g(x)},\phi(x)\mathcal{D}_\zeta\phi(x)\,. \tag{3.B.21}$$

However, calling $\mathcal{D}_\zeta$ a conformal "fractional Laplacian" would be deceiving, as it turns out that the operator $\mathcal{D}_\zeta$ is not of the form $(-\nabla^2+b)^\zeta$: the conformal Laplacian of biweight $(\Delta, d-\Delta)$ on the d-sphere can be related to the Laplace-Beltrami operator by the expression [96]:

$$\mathcal{D}_\zeta = a^{-2\zeta}\frac{\Gamma(a\mathcal{D}_{1/2}+\frac{1}{2}+\zeta)}{\Gamma(a\mathcal{D}_{1/2}+\frac{1}{2}-\zeta)}\,,\qquad \mathcal{D}_{1/2} = a\sqrt{-\nabla^2+\left(\frac{d-1}{2a}\right)^2}\,, \tag{3.B.22}$$

[19] As a subtracted hypersingular integral, a rigorous covariant expression is given by (see [93, 86]):

$$\mathcal{D}_\zeta\phi(x) = \lim_{r\to 0} c(d-\Delta)\int_{s(x,y)>r}\mathrm{d}^d y\sqrt{g(y)}\,\frac{\phi(y)-\phi(x)}{s(x,y)^{2(d-\Delta)}} + \frac{\Gamma(d-\Delta)}{\Gamma(\Delta)}\phi(x)\,.$$

which should of course be interpreted in terms of the eigenvalues:

$$\begin{aligned}\omega_n^{(\zeta)} &= a^{-2\zeta}\,\frac{\Gamma(n+\frac{d}{2}+\zeta)}{\Gamma(n+\frac{d}{2}-\zeta)} = a^{-2\zeta}\,\frac{\Gamma(a\,\omega_n^{(1/2)}+\frac{1}{2}+\zeta)}{\Gamma(a\,\omega_n^{(1/2)}+\frac{1}{2}-\zeta)}\,,\\ \omega_n^{(1/2)} &= a^{-1}\left(n+\frac{d-1}{2}\right) = \sqrt{\omega_n+\left(\frac{d-1}{2a}\right)^2} = \sqrt{\omega_n^{(1)}+\frac{1}{4a^2}}\,.\end{aligned} \tag{3.B.23}$$

In the last equality we introduced $\omega_n = n(n+d-1)/a^2$, the eigenvalues of Laplace-Beltrami operator on the sphere. Notice that for $\zeta = 1$ we have $\mathcal{D}_1 = -\nabla^2 + b_W$, as expected, and that for $n \to +\infty$ the eigenvalues of $\mathcal{D}_\zeta$ do asymptotically approach $n^{2\zeta}$, as for a Laplacian to the power ζ. The eigenvalues $\omega_n^{(\zeta)}$ are of course the inverse of the eigenvalues of the Riesz potential (3.B.14), which were known since long to mathematicians (e.g. [97]), and have been later rederived also in the physics literature [81].

Notice that, denoting $c_n \equiv n + \frac{d}{2} - \zeta$, we can write:

$$\frac{1}{a^{2\zeta}\omega_n^{(\zeta)}} = \frac{\Gamma(c_n)}{\Gamma(c_n+2\zeta)} = \frac{1}{\Gamma(2\zeta)}B(c_n,2\zeta)\,, \tag{3.B.24}$$

where $B(x,y)$ is the Euler beta function. Therefore, we have various useful representations, among which in particular the following integral representation:

$$\frac{1}{a^{2\zeta}\omega_n^{(\zeta)}} = \frac{1}{\Gamma(2\zeta)}\int_0^1 dt\, t^{c_n-1}(1-t)^{2\zeta-1} = \frac{1}{\Gamma(2\zeta)}\int_0^{+\infty} ds\, e^{-s\,c_n}(1-e^{-s})^{2\zeta-1}\,. \tag{3.B.25}$$

One way to introduce a UV cutoff in the theory is then to replace the beta function with the incomplete beta function, i.e. truncating the upper end of t-integration at $1-e^{-s_0}$, or the lower end of the s-integration at $s_0 > 0$. From the latter one can see that such cutoff is roughly proportional to an exponential $e^{-s_0 c_n}$. This should be compared to the flat space representation:

$$\frac{1}{p^{2\zeta}} = \frac{1}{\Gamma(2\zeta)}\int_0^{+\infty} ds\, e^{-s\,p} s^{2\zeta-1}\,, \tag{3.B.26}$$

which again can be regularized by replacing the integral representation of the gamma function with that of the incomplete gamma function. This is in the same spirit of what was done in [17], where however the representation of $\Gamma(z)$ was used instead of $\Gamma(2\zeta)$, i.e. the exponential cutoff was with respect to p^2 rather than p. Notice that as expected the two s-integral representations in (3.B.25) and (3.B.26) coincide in the deep UV (small s) but differ in the IR (large s).

3.C Computation of the free energy for GFFT

In this appendix we present a detailed computation of the following sum:

$$F = \frac{1}{2}\sum_{n=0}^{\infty} D_n \ln\left(a^{-2\zeta}\frac{\Gamma(n+d/2+\zeta)}{\Gamma(n+d/2-\zeta)}\right). \tag{3.C.1}$$

This computation was done in [73], but we reproduce it here with more details.

For $d > 0$, this sum is divergent. We will compute it in the regime $2\zeta - 2 < d < 0$ and then perform an analytic continuation to deduce the result for $d > 0$. This computation can also be done for $\zeta > 1$. For $k-1 < \zeta < k$, $k \geq 2$, the sum (3.C.1) would have to be computed in the range $2\zeta - 2k < d < 0$.

However, the computation is very similar than the one for $0 < \zeta < 1$ and leads to the same result so we will detail here only the computation for $0 < \zeta < 1$.

Let us first show that the sum of multiplicity is zero in this regularization:

$$\begin{aligned}\sum_{n=0}^{\infty} D_n &= \sum_{n=0}^{\infty} \frac{(n+d-2)!(2n+d-1)}{n!(d-1)!} = \sum_{n=0}^{\infty} \frac{(n+d-1)!}{n!(d-1)!}\frac{2n+d-1}{n+d-1} \\ &= \sum_{n=0}^{\infty} \frac{(n+d-1)!}{n!(d-1)!}\frac{n}{n+d-1} + \sum_{n=0}^{\infty} \frac{(n+d-1)!}{n!(d-1)!} \\ &= \sum_{n=1}^{\infty} \frac{(n+d-2)!}{(n-1)!(d-1)!} + (1-1)^{-d} = \sum_{n=0}^{\infty} \frac{(n+d-1)!}{(n)!(d-1)!} + 0 = (1-1)^{-d} = 0 \,.\end{aligned} \tag{3.C.2}$$

The term $\ln(a^{-2\zeta})$ can thus be dropped from the expression of F. Taking the derivative with respect to ζ of the remaining expression, we obtain:

$$\frac{dF}{d\zeta} = \frac{1}{2}\sum_{n=0}^{\infty} D_n \left(\psi(n+d/2+\zeta) + \psi(n+d/2-\zeta)\right) \,. \tag{3.C.3}$$

We will now use the following integral representation of the digamma function:

$$\psi(z) = \int_0^{\infty} dt \left(\frac{e^{-t}}{t} - \frac{e^{-tz}}{1-e^{-t}}\right) \,, \tag{3.C.4}$$

which is valid for $z > 0$.

Leaving out the $n = 0$ term [20], we then get:

$$\begin{aligned}\frac{dF}{d\zeta} &= \frac{1}{2}\left(\psi(d/2+\zeta) + \psi(d/2-\zeta)\right) + \frac{1}{2}\sum_{n=1}^{\infty} D_n \int_0^{\infty} dt \left(\frac{2e^{-t}}{t} - \frac{e^{-t(n+d/2)}}{1-e^{-t}}\left(e^{-t\zeta} + e^{t\zeta}\right)\right) \\ &= \frac{1}{2}\left(\psi(d/2+\zeta+1) + \psi(d/2-\zeta+1) - \frac{1}{d/2+\zeta} - \frac{1}{d/2-\zeta}\right) \\ &\quad + \frac{1}{2}\sum_{n=1}^{\infty} D_n \int_0^{\infty} dt \left(\frac{2e^{-t}}{t} - \frac{e^{-t(n+d/2)}}{1-e^{-t}}\left(e^{-t\zeta} + e^{t\zeta}\right)\right) \,,\end{aligned} \tag{3.C.5}$$

where we have used $\psi(z) = \psi(1+z) - \frac{1}{z}$.

We can now use the integral representation of the digamma function for $\psi(n + d/2 \pm \zeta + 1)$. Rearranging the terms and exchanging sum and integral, we obtain:

$$\begin{aligned}\frac{dF}{d\zeta} = &-\frac{1}{2}\left(\frac{1}{d/2+\zeta} + \frac{1}{d/2-\zeta}\right) + \int_0^{\infty} dt \frac{e^{-t}}{t}\sum_{n=0}^{\infty} D_n \\ &- \frac{1}{2}\int_0^{\infty} \frac{e^{-t\zeta} + e^{t\zeta}}{1-e^{-t}} e^{-td/2}\left(e^{-t} + \sum_{n=1}^{\infty} D_n e^{-tn}\right) \,.\end{aligned} \tag{3.C.6}$$

[20] For the case $1 < \zeta < 2$, we would also need to leave out the term $n = 1$.

Again, as the sum of the multiplicities is zero, the second term vanishes. The remaining sum is:

$$\begin{aligned}\sum_{n=1}^{\infty} D_n e^{-tn} &= \sum_{n=1}^{\infty} \frac{(n+d-2)!(2n+d-1)}{n!(d-1)!} e^{-tn} \\ &= 2\sum_{n=1}^{\infty} n\frac{(n+d-2)!}{n!(d-1)!} e^{-tn} + \sum_{n=1}^{\infty} \frac{(n+d-2)!}{n!(d-2)!} e^{-tn} \\ &= 2e^{-t}\sum_{n=0}^{\infty} \frac{(n+d-1)!}{n!(d-1)!} e^{-tn} + (1-e^{-t})^{-(d-1)} - 1 \\ &= 2e^{-t}(1-e^{-t})^{-d} + (1-e^{-t})^{-(d-1)} - 1 = (1-e^{-t})^{-d}(1+e^{-t}) - 1\,.\end{aligned} \tag{3.C.7}$$

Substituting this result into $\frac{dF}{d\zeta}$ and changing variables $u = e^{-t}$, we obtain:

$$\frac{dF}{d\zeta} = -\frac{1}{2}\left(\frac{1}{d/2+\zeta} + \frac{1}{d/2-\zeta}\right) - \frac{1}{2}\int_0^1 du\, u^{d/2-1}(u^{\zeta}+u^{-\zeta})\left((1-u)^{-d-1}(1+u) - 1\right)\,. \tag{3.C.8}$$

We can now compute the last integral using the regular as well as the subtracted integral representations of the beta function: [21]

$$\begin{aligned} B(a,b) &= \int_0^1 dt\, t^{a-1}(1-t)^{b-1}\,,\ a,b>0 \\ B(a,b) - B(a,c) &= \int_0^1 dt\,(1-t)^{a-1}\left(t^{b-1}-t^{c-1}\right)\,,\ a>-1\,,\ b,c>0\,. \end{aligned} \tag{3.C.9}$$

Indeed, we have:

$$\begin{aligned}&\int_0^1 du\, u^{d/2+\zeta-1}\left((1-u)^{-d-1}(1+u)-1\right) \\ &= \int_0^1 du\left(u^{d/2+\zeta}(1-u)^{-d-1} + u^{d/2+\zeta-1}\left((1-u)^{-d-1} - (1-u)^{1-1}\right)\right) \\ &= B(d/2+\zeta+1,-d) + B(d/2+\zeta,-d) - B(d/2+\zeta,1) \\ &= 2\zeta\frac{\Gamma(d/2+\zeta)\Gamma(-d)}{\Gamma(\zeta-d/2+1)} - \frac{1}{\zeta+d/2}\,,\end{aligned} \tag{3.C.10}$$

and similarly:

$$\int_0^1 du\, u^{d/2-\zeta-1}\left((1-u)^{-d-1}(1+u)-1\right) = -2\zeta\frac{\Gamma(d/2-\zeta)\Gamma(-d)}{\Gamma(-\zeta-d/2+1)} - \frac{1}{-\zeta+d/2}\,. \tag{3.C.11}$$

Thus we obtain:

$$\frac{dF}{d\zeta} = \zeta\Gamma(-d)\left(\frac{\Gamma(d/2-\zeta)}{\Gamma(1-\zeta-d/2)} - \frac{\Gamma(d/2+\zeta)}{\Gamma(1+\zeta-d/2)}\right) = -\zeta\frac{\sin(\pi\zeta)}{\sin(\pi d/2)}\frac{\Gamma(d/2-\zeta)\Gamma(d/2+\zeta)}{\Gamma(1+d)}\,, \tag{3.C.12}$$

which can be analytically continued to $d>0$ not even, and is valid for any value of ζ, except at the poles at $\zeta = d/2+k$.

[21] In the case $1<\zeta<2$, we also need the following subtracted integral representation of the beta function:

$$B(a,b) - B(a,1) + (b-1)B(a+1,1) = \int_0^1 dt\, t^{a-1}\left((1-t)^{b-1} + (b-1)t - 1\right)\,,\ a>-2\,,\ b>0\,.$$

3.D Computation of $C(x,x)$ in dimensional regularization

From the expansion of $C(x,y)$ in spherical harmonics in (3.B.15), we find that at coinciding points we have

$$C(x,x) = \frac{1}{V_d}\sum_{n\geq 0}\frac{D_n}{\omega_n^{(\zeta)}}\,, \tag{3.D.1}$$

which of course is divergent and needs regularization. We employ here analytic continuation in the dimension d, treating separately the two cases $\zeta = 1$ and $\zeta < 1$.

3.D.1 $\zeta = 1$ case

With $\zeta = 1$, the expression of the covariance simplifies to:

$$C_1(x,x) = \frac{a^{2-d}}{\Gamma(d/2)(4\pi)^{d/2}}\sum_{n=0}^{\infty}\frac{4\,\Gamma(n+d-1)(2n+d-1)}{n!(2n+d)(2n+d-2)}\,. \tag{3.D.2}$$

The Weyl invariant coupling $b = b_W \equiv \frac{d(d-2)}{4a^2}$ in (3.B.4) provides an IR regularization by removing the zero mode, for $d \neq 2$. However, the sum is divergent for $d > 2$ and needs a regularization. A convenient approach is to compute it for $0 < d < 2$, where it converges, and where we find $C(x,x) = 0$, thanks to a cancellation between the $n = 0$ contribution (negative because $b_W < 0$ in this range of dimensions), and the rest of the series. We then analytically continue the result to $d > 2$.

Let us begin by rewriting the sum as:

$$\begin{aligned}\sum_{n=0}^{\infty}\frac{\Gamma(n+d-1)(2n+d-1)}{n!(n+d/2)(n+d/2-1)} &= \sum_{n=0}^{\infty}\frac{\Gamma(n+d-1)}{n!(n+d/2-1)} + \sum_{n=0}^{\infty}\frac{\Gamma(n+d-1)}{n!(n+d/2)} \\ &= \frac{\Gamma(d-2)}{d/2-1}\sum_{n=0}^{\infty}\frac{1}{n!}\frac{(d-1)_n(d/2-1)_n}{(d/2)_n} + \frac{2\Gamma(d-2)}{d}\sum_{n=0}^{\infty}\frac{1}{n!}\frac{(d-1)_n(d/2)_n}{(d/2+1)_n}\,,\end{aligned} \tag{3.D.3}$$

where $(b)_n = b(b+1)\dots(b+n-1) = \frac{\Gamma(b+n)}{\Gamma(b)}$ and we have used $\frac{(b)_n}{(b+1)_n} = \frac{b}{b+n}$.

We then recognize the hypergeometric function of argument 1:

$${}_2F_1(a,b,c,1) = \sum_{n=0}^{1}\frac{(a)_n(b)_n}{n!(c)_n} = \frac{\Gamma(c)\Gamma(c-b-a)}{\Gamma(c-b)\Gamma(c-a)}\,, \tag{3.D.4}$$

which is valid for $\mathrm{Re}(b), \mathrm{Re}(c) > 0$ and $\mathrm{Re}(c-a-b) > 0$.

In order to apply this formula, we thus need $d > 0$ and $d < 2$: in the first sum of (3.D.3) we have $a = d/2-1, b = d-1, c = d/2$ and in the second sum we have $a = d/2, b = d-1, c = d/2+1$.

We thus get:

$$\begin{aligned}C_1(x,x) &\propto 2\Gamma(d-2)\left(\frac{\Gamma(d/2)\Gamma(2-d)}{(d-2)\Gamma(1-d/2)} + \frac{\Gamma(d/2+1)\Gamma(2-d)}{d\Gamma(2-d/2)}\right) \\ &= \frac{2\Gamma(d-2)\Gamma(d/2)\Gamma(2-d)}{\Gamma(1-d/2)}\left(\frac{1}{d-2} + \frac{d}{2d(1-d/2)}\right) = 0\,.\end{aligned} \tag{3.D.5}$$

3.D.2 $\zeta < 1$ case

We want to compute the following sum:

$$\frac{a^{2\zeta-d}(d-1)!}{\Gamma(d/2)(4\pi)^{d/2}}\sum_{n=0}^{\infty}\frac{D_n}{a^{2\zeta}\omega_n^{(\zeta)}}\,. \tag{3.D.6}$$

We use the integral representation of (3.B.25), which in the range $2\zeta-2<d<0$ is valid for $n>0$. Taking out the $n=0$ term, and exchanging the sum and the integral, we obtain:

$$C(x,x)=\frac{a^{2\zeta-d}(d-1)!}{\Gamma(d/2)(4\pi)^{d/2}}\left[\frac{\Gamma(d/2-\zeta)}{\Gamma(d/2+\zeta)}+\frac{1}{\Gamma(2\zeta)}\int_0^\infty ds(1-e^{-s})^{2\zeta-1}e^{-s(\frac{d}{2}-\zeta)}\sum_{n=1}^{\infty}D_n e^{-sn}\right]. \tag{3.D.7}$$

The remaining sum was already computed in the previous appendix and doing the change of variable $u=e^{-s}$ we obtain:

$$\begin{aligned}C(x,x)=&\frac{a^{2\zeta-d}(d-1)!}{\Gamma(\frac{d}{2})(4\pi)^{d/2}}\left[\frac{\Gamma(d/2-\zeta)}{\Gamma(d/2+\zeta)}\right.\\&\left.+\frac{1}{\Gamma(2\zeta)}\int_0^1 du\,u^{d/2-\zeta-1}(1-u)^{2\zeta-1}\Big((1-u)^{-d}(1+u)-1\Big)\right]\\=&\frac{a^{2\zeta-d}(d-1)!}{\Gamma(d/2)(4\pi)^{d/2}}\left[\frac{\Gamma(d/2-\zeta)}{\Gamma(d/2+\zeta)}\right.\\&\left.+\frac{1}{\Gamma(2\zeta)}\int_0^1 du\,\Big(u^{d/2-\zeta}(1-u)^{2\zeta-d-1}+u^{d/2-\zeta-1}\Big((1-u)^{2\zeta-d-1}-(1-u)^{2\zeta-1}\Big)\Big)\right].\end{aligned} \tag{3.D.8}$$

We perform the integral using the regular and subtracted representations of the Beta function (3.C.9) and obtain:

$$\begin{aligned}C(x,x)=&\frac{a^{2\zeta-d}(d-1)!}{\Gamma(\frac{d}{2})(4\pi)^{d/2}}\left[\frac{\Gamma(\frac{d}{2}-\zeta)}{\Gamma(\frac{d}{2}+\zeta)}+\frac{\Gamma(\frac{d}{2}-\zeta+1)\Gamma(2\zeta-d)}{\Gamma(-\frac{d}{2}+\zeta+1)\Gamma(2\zeta)}\right.\\&\left.+\frac{\Gamma(\frac{d}{2}-\zeta)\Gamma(2\zeta-d)}{\Gamma(\zeta-\frac{d}{2})\Gamma(2\zeta)}-\frac{\Gamma(\frac{d}{2}-\zeta)}{\Gamma(\zeta+\frac{d}{2})}\right]\\=&\frac{a^{2\zeta-d}(d-1)!\Gamma(d/2-\zeta)\Gamma(2\zeta-d)}{\Gamma(d/2)(4\pi)^{d/2}\Gamma(2\zeta)\Gamma(\zeta-d/2)}\left[\frac{d/2-\zeta}{\zeta-d/2}+1\right]=0\,.\end{aligned} \tag{3.D.9}$$

3.E Basics of conformal partial wave expansion

We provide here some important formulas and background on the conformal partial wave expansion used in the main body of the chapter, part of it overlaps with section 2.3.4 in chapter 2 but we prefer to keep this appendix self-consistent. The main results of this appendix have been derived by Dobrev et al. in [41, 40, 42], and largely revived in recent years [98, 99, 100, 79].[22] Here we mostly follow the notation of [110], where a more detailed review can be found.

We work on flat space and comment at the end on the straightforward extension to the sphere. In the conformal limit, the Bethe-Salpeter kernel $K(x_1,x_2,x_3,x_4)$ of scalar fields of dimension Δ is

[22] These methods have been at the heart of a very active field in recent years, see for example their use with Mellin amplitudes [101, 102], their application to the Sachdev-Ye-Kitaev model [15, 103], to the bootstrap crossing equations [104, 105, 106, 107], and to the construction of an AdS/CFT map [108, 109].

diagonalized by functions with the structure of a conformal three-point function of the type:

$$\begin{aligned}\langle\phi_\Delta(x_3)\phi_\Delta(x_4)\mathcal{O}^{\bar{\mu}}_{(h,J)}(x_0)\rangle_{\text{cs}} &= \frac{Z^{\mu_1}\cdots Z^{\mu_J}-\text{“traces"}}{|x_{34}|^{2\Delta-h}|x_{30}|^h|x_{40}|^h}\,,\\ Z^\mu &= \frac{|x_{30}||x_{40}|}{|x_{34}|}\left(\frac{x^\mu_{30}}{|x_{30}|^2}-\frac{x^\mu_{40}}{|x_{40}|^2}\right),\end{aligned} \tag{3.E.1}$$

where $x_{ij}=x_i-x_j$, such that:

$$\int_{x_3x_4} K(x_1,x_2,x_3,x_4)\,\langle\phi_\Delta(x_3)\phi_\Delta(x_4)\mathcal{O}^{\bar{\mu}}_{(h,J)}(x_0)\rangle_{\text{cs}} = k(h,J)\,\langle\phi_\Delta(x_1)\phi_\Delta(x_2)\mathcal{O}^{\bar{\mu}}_{(h,J)}(x_0)\rangle_{\text{cs}}\,. \tag{3.E.2}$$

The subscript “cs" stands for conformal structure, meaning that the three-point function is just a notation for the structure on right-hand side. In particular, there is no structure constant, and the operator $\mathcal{O}^{\bar{\mu}}_{(h,J)}(z)$, of conformal dimension h and in the spin-J symmetric-traceless representation of the rotation group, is in general not part of the spectrum of the CFT. We denote $\phi_\Delta(x)$ a generic scalar primary of dimension Δ, without introducing any flavor/color index structure, which we assume to be already diagonalized, as for example in (3.4.19).

The precise form of the kernel eigenvalue depends on the specific model. In the case of the long-range $O(N)^3$ model studied in section 3.4, we have:

$$k(h,J) = -\frac{g^2}{(4\pi)^d}\frac{\Gamma(-\frac{d}{4}+\frac{h+J}{2})\Gamma(\frac{d}{4}-\frac{h-J}{2})}{\Gamma(\frac{3d}{4}-\frac{h-J}{2})\Gamma(\frac{d}{4}+\frac{h+J}{2})}\,. \tag{3.E.3}$$

Multiplied by the following normalization factor ($\tilde{h}=d-h$ is the dimension of the shadow operator [92]):

$$\mathcal{N}^\Delta_{h,J} = \frac{2^{(2\Delta+h+J)/2}}{(2\pi)^{d/2}}\left(\frac{\Gamma(\frac{\tilde{h}+J+2\Delta-d}{2})\Gamma(\frac{h+J+2\Delta-d}{2})}{\Gamma(\frac{\tilde{h}+J-2\Delta+d}{2})\Gamma(\frac{h+J-2\Delta+d}{2})}\right)^{1/2}\frac{\Gamma(\frac{h+J}{2})}{\Gamma(\frac{\tilde{h}+J}{2})}\,, \tag{3.E.4}$$

the three-point functions (3.E.1) with fixed $\text{Re}(\Delta)\in(d/4,3d/4)$ form a complete and orthonormal basis in an appropriate space of bilocal functions [41, 42], the basis elements being labeled by the spin $J\in\mathbb{N}_0$, the position $x_0\in\mathbb{R}^d$, and the scaling dimension $h\in\mathcal{P}_+$, where:

$$\mathcal{P}_+ = \left\{h\;\middle|\; h=\frac{d}{2}+\mathrm{i}\,r,\, r\in\mathbb{R}_+\right\}, \tag{3.E.5}$$

labels the principal series representations of the conformal group. More precisely, the space of bilocal functions $\mathcal{V}_\Delta$ can be defined as the space of smooth functions $f(x_1,x_2)$ that are square integrable with respect to the scalar product:

$$(f_1,f_2) = \int_{x_1\ldots x_4}\overline{f_1(x_1,x_2)}C^{-1}(x_1,x_3)C^{-1}(x_2,x_4)f_2(x_3,x_4)\,, \tag{3.E.6}$$

i.e. $(f,f)<\infty$, and satisfy the asymptotic boundary condition $f(x_1,x_2)\sim|x_1|^{-2\Delta}$ for $|x_1|\to\infty$ and similar for $|x_2|\to\infty$. Here, we have assumed that the bilocal functions have no symmetry under permutation of their two arguments, and we denoted[23] $C(x_1,x_3)=c(\Delta)/|x_1-x_3|^{2\Delta}$. Similarly, we can introduce the shadow space $\mathcal{V}_{\tilde{\Delta}}$ with its basis of three-point functions defined as above but with

[23] In this appendix we use $C(x,y)$ to denote the full-two-point function $\langle\phi(x)\phi(y)\rangle$ of the CFT, for which we are free to choose the same normalization as the one we used for the GFFT, even if the theory we have in mind is in general interacting.

Δ replaced by its shadow $\widetilde{\Delta} = d - \Delta$. Since the two-point function of ϕ_Δ and that of $\phi_{\widetilde{\Delta}}$ are the inverse of each other (see (3.B.13)), we can write the analogue of the scalar product (3.E.6) for $\mathcal{V}_{\widetilde{\Delta}}$ by replacing C^{-1} with C, the two-point function of ϕ_Δ.

The relation between $\mathcal{V}_\Delta$ and $\mathcal{V}_{\widetilde{\Delta}}$ can better be understood in terms of raising and lowering of indices by the metric associated to the scalar product on them. Let us denote $f^{x_1 x_2}$, with contravariant indices x_1, x_2, the elements of $\mathcal{V}_\Delta$, signaling that f has dimension Δ on each of its arguments. The factor $g_{x_1x_2;x_3x_4} = C^{-1}(x_1, x_3)C^{-1}(x_2, x_4)$ in the scalar product in (3.E.6) is a metric on $\mathcal{V}_\Delta$ with covariant indices, that is with dimension $\tilde{\Delta} = d - \Delta$ on each of its arguments. The inverse metric is $g^{x_1x_2;x_3x_4} = C(x_1, x_3)C(x_2, x_4)$ and the contraction on an index (integral over the position) has dimension $-d$. The metric and its inverse allow one to lower respectively raise indices, i.e. map $\mathcal{V}_\Delta$ to its dual $\mathcal{V}_{\tilde{\Delta}}$. The mapping holds also for the basis elements:[24]

$$\begin{aligned}&\int \mathrm{d}^d x_3 \mathrm{d}^d x_4\, C^{-1}(x_1, x_3)C^{-1}(x_2, x_4)\, \langle \phi_\Delta(x_3)\phi_\Delta(x_4)\mathcal{O}^{\bar{\mu}}_{(h,J)}(x_0)\rangle_{\mathrm{cs}}\, \mathcal{N}^{\Delta}_{h,J} \\ &\quad = \langle \phi_{\widetilde{\Delta}}(x_1)\phi_{\widetilde{\Delta}}(x_2)\mathcal{O}^{\bar{\mu}}_{(h,J)}(x_0)\rangle_{\mathrm{cs}}\, \mathcal{N}^{\widetilde{\Delta}}_{h,J}\,.\end{aligned} \tag{3.E.7}$$

The completeness relation, or resolution of the identity, reads:

$$\begin{aligned}\mathbb{I}(x_1, x_2, x_3, x_4) &\equiv \delta(x_1 - x_3)\delta(x_2 - x_4) \\ &= \sum_{J\in\mathbb{N}_0} \int_{\frac{d}{2}}^{\frac{d}{2}+\mathrm{i}\infty} \frac{\mathrm{d}h}{2\pi\,\mathrm{i}} \rho(h, J)\, \mathcal{N}^{\Delta}_{h,J}\mathcal{N}^{\widetilde{\Delta}}_{h,J}\, \Psi^{\Delta,\Delta,\widetilde{\Delta},\widetilde{\Delta}}_{h,J}(x_1, x_2, x_3, x_4)\,,\end{aligned} \tag{3.E.8}$$

where the equality holds in a distributional sense when acting to the left (integration over x_3 and x_4) on $\mathcal{V}_\Delta$, or to the right (integration over x_1 and x_2) on $\mathcal{V}_{\widetilde{\Delta}}$. We have introduced the Plancherel weight:

$$\rho(h, J) = \frac{\Gamma(\frac{d}{2} + J)}{2(2\pi)^{d/2} J!} \frac{\Gamma(\tilde{h} - 1)\Gamma(h - 1)}{\Gamma(\frac{d}{2} - h)\Gamma(\frac{d}{2} - \tilde{h})}(h + J - 1)(\tilde{h} + J - 1)\,, \tag{3.E.9}$$

and the conformal partial wave, defined as:

$$\Psi^{\Delta,\Delta,\widetilde{\Delta},\widetilde{\Delta}}_{h,J}(x_1, x_2, x_3, x_4) = \int \mathrm{d}^d z\, \langle \phi_\Delta(x_1)\phi_\Delta(x_2)\mathcal{O}^{\bar{\mu}}_{(h,J)}(z)\rangle_{\mathrm{cs}} \langle \phi_{\widetilde{\Delta}}(x_3)\phi_{\widetilde{\Delta}}(x_4)\mathcal{O}^{\bar{\mu}}_{(\tilde{h},J)}(z)\rangle_{\mathrm{cs}}\,. \tag{3.E.10}$$

We notice that the product of normalization factors of the basis simplifies to:

$$\mathcal{N}^{\Delta}_{h,J}\mathcal{N}^{\widetilde{\Delta}}_{h,J} = \frac{2^{3d/2+J}}{(2\pi)^d}\,. \tag{3.E.11}$$

Any endomorphism $\mathcal{E} : \mathcal{V}_\Delta \to \mathcal{V}_\Delta$ associated to a conformal kernel can be diagonalized by convoluting the kernel with the appropriate resolution of the identity, e.g.

$$\begin{aligned}\mathcal{E}(x_1, x_2, x_3, x_4) &= \int \mathrm{d}^d y_1 \mathrm{d}^d y_2\, \mathcal{E}(x_1, x_2, y_1, y_2)\, \mathbb{I}(y_1, y_2, x_3, x_4) \\ &= \sum_{J\in\mathbb{N}_0} \int_{\frac{d}{2}}^{\frac{d}{2}+\mathrm{i}\infty} \frac{\mathrm{d}h}{2\pi\,\mathrm{i}} \rho(h, J)\, \Lambda_{\mathcal{E}}(h, J)\, \mathcal{N}^{\Delta}_{h,J}\mathcal{N}^{\widetilde{\Delta}}_{h,J}\, \Psi^{\Delta,\Delta,\widetilde{\Delta},\widetilde{\Delta}}_{h,J}(x_1, x_2, x_3, x_4)\,,\end{aligned} \tag{3.E.12}$$

[24] The three-point functions are not in $\mathcal{V}$, as they are not integrable, but they form a basis in the continuous sense, just like the Fourier basis does for $\mathrm{L}^2(\mathbb{R}^d)$.

where $\Lambda_{\mathcal{E}}(h,J)$ is the eigenvalue of $\mathcal{E}$, satisfying an equation similar to (3.E.2). Using the following relation between the conformal partial waves and the conformal blocks $\mathcal{G}_{h,J}$ [111, 99]:

$$\begin{aligned}\Psi^{\Delta,\Delta,\widetilde{\Delta},\widetilde{\Delta}}_{h,J}(x_1,x_2,x_3,x_4) = \left(-\tfrac{1}{2}\right)^J \Big(& S_{\tilde{h},J}\, \mathcal{G}^{\Delta,\Delta,\widetilde{\Delta},\widetilde{\Delta}}_{h,J}(x_1,x_2,x_3,x_4) \\ & + S_{h,J}\, \mathcal{G}^{\Delta,\Delta,\widetilde{\Delta},\widetilde{\Delta}}_{\tilde{h},J}(x_1,x_2,x_3,x_4)\Big)\,,\end{aligned} \tag{3.E.13}$$

with:

$$S_{h,J} = \frac{\pi^{d/2}\Gamma(h-\frac{d}{2})\Gamma(h+J-1)\Gamma(\frac{\tilde{h}+J}{2})^2}{\Gamma(h-1)\Gamma(d-h+J)\Gamma(\frac{h+J}{2})^2}\,, \tag{3.E.14}$$

one can then write:

$$\begin{aligned}&\mathcal{E}(x_1,x_2,x_3,x_4)\\ &= \sum_{J\in\mathbb{N}_0}\left(-\tfrac{1}{2}\right)^J \int_{\frac{d}{2}-\mathrm{i}\infty}^{\frac{d}{2}+\mathrm{i}\infty} \frac{\mathrm{d}h}{2\pi\,\mathrm{i}}\rho(h,J)\,\Lambda_{\mathcal{E}}(h,J)\,\mathcal{N}^{\Delta}_{h,J}\mathcal{N}^{\widetilde{\Delta}}_{\tilde{h},J}\,S_{\tilde{h},J}\,\mathcal{G}^{\Delta,\Delta,\widetilde{\Delta},\widetilde{\Delta}}_{h,J}(x_1,x_2,x_3,x_4)\,,\end{aligned} \tag{3.E.15}$$

where we used the symmetry of the measure factor $\rho(h,J)\,\mathcal{N}^{\Delta}_{h,J}\mathcal{N}^{\widetilde{\Delta}}_{\tilde{h},J}$ under shadow reflection $h\to\tilde{h}$ to extend the integration to negative imaginary parts and keep only one conformal block term.

Acting by convolution on the last two arguments of $\mathcal{E}(x_1,x_2,x_3,x_4)$ with the inverse metric, we obtain an operator mapping $\mathcal{V}_{\widetilde{\Delta}}$ to $\mathcal{V}_{\Delta}$, with a similar conformal partial wave expansion, except that the $\widetilde{\Delta}$ arguments are replaced by Δ:

$$\begin{aligned}&\int \mathrm{d}^d y_3 \mathrm{d}^d y_4\, \mathcal{E}(x_1,x_2,y_3,y_4)C(y_3,x_3)C(y_4,x_4)\\ &= \sum_{J\in\mathbb{N}_0}\int_{\frac{d}{2}}^{\frac{d}{2}+\mathrm{i}\infty}\frac{\mathrm{d}h}{2\pi\,\mathrm{i}}\rho(h,J)\,\Lambda_{\mathcal{E}}(h,J)\,\mathcal{N}^{\Delta}_{h,J}\mathcal{N}^{\Delta}_{\tilde{h},J}\,\Psi^{\Delta,\Delta,\Delta,\Delta}_{h,J}(x_1,x_2,x_3,x_4)\\ &= \sum_{J\in\mathbb{N}_0}\left(-\tfrac{1}{2}\right)^J\int_{\frac{d}{2}-\mathrm{i}\infty}^{\frac{d}{2}+\mathrm{i}\infty}\frac{\mathrm{d}h}{2\pi\,\mathrm{i}}\rho(h,J)\,\Lambda_{\mathcal{E}}(h,J)\,\mathcal{N}^{\Delta}_{h,J}\mathcal{N}^{\Delta}_{\tilde{h},J}\,S_{\tilde{h},J}\,\mathcal{G}^{\Delta,\Delta,\Delta,\Delta}_{h,J}(x_1,x_2,x_3,x_4)\,.\end{aligned} \tag{3.E.16}$$

In this case, the product of normalization factors has a ratio of gamma functions, with its own poles:[25]

$$\mathcal{N}^{\Delta}_{h,J}\mathcal{N}^{\Delta}_{\tilde{h},J} = \frac{2^{(2\Delta+d/2+J)}}{(2\pi)^d}\frac{\Gamma(\frac{\tilde{h}+J+2\Delta-d}{2})\Gamma(\frac{h+J+2\Delta-d}{2})}{\Gamma(\frac{\tilde{h}+J-2\Delta+d}{2})\Gamma(\frac{h+J-2\Delta+d}{2})}\,. \tag{3.E.17}$$

For $\mathcal{E}=\mathbb{I}$, (3.E.16), with $\Lambda_{\mathbb{I}}(h,J)=1$, gives a conformal partial wave expansion of the inverse metric. A similar expansion is obtained for the metric itself, replacing C with C^{-1} in the first line, and Δ with $\widetilde{\Delta}$ in the expansion.

[25] These poles do not cross the principal series as long as $\Delta > d/4$. Similarly, the poles of $\mathcal{N}^{\widetilde{\Delta}}_{h,J}\mathcal{N}^{\widetilde{\Delta}}_{\tilde{h},J}$ stay away from $h=d/2$ for $\Delta<3d/4$. Together, these two conditions explain the condition on Δ mentioned below (3.E.4).

In the case of symmetric bilocal functions,[26] the completeness relation is of the same type, but with contribution only from even spin:

$$\begin{aligned}\mathbb{I}_{\text{symm}}(x_1,x_2,x_3,x_4) &\equiv \frac{1}{2}\left(\delta(x_1-x_3)\delta(x_2-x_4)+\delta(x_1-x_4)\delta(x_2-x_3)\right)\\ &= \sum_{J\in\mathbb{N}_0^{\text{even}}}\int_{\frac{d}{2}}^{\frac{d}{2}+\mathrm{i}\infty}\frac{\mathrm{d}h}{2\pi\,\mathrm{i}}\rho(h,J)\,\mathcal{N}^{\Delta}_{h,J}\mathcal{N}^{\widetilde{\Delta}}_{h,J}\,\Psi^{\Delta,\Delta,\widetilde{\Delta},\widetilde{\Delta}}_{h,J}(x_1,x_2,x_3,x_4)\,.\end{aligned} \tag{3.E.18}$$

Non-normalizable contributions. In practical applications, such as those we encounter in the bulk of this chapter, some of the hypotheses behind what we just reviewed can be violated. Typically, we have two possible situations:

1. A four-point kernel $\mathcal{E}(x_1,x_2,x_3,x_4)$ with right conformal transformation might nevertheless not be an endomorphism on $\mathcal{V}_\Delta$ (or a map $\mathcal{V}_{\widetilde{\Delta}}\to\mathcal{V}_\Delta$) because its action on an element $f\in\mathcal{V}_\Delta$ (or $\tilde{f}\in\mathcal{V}_{\widetilde{\Delta}}$) leads to a function not satisfying the integrability condition associated to the scalar product (3.E.6).

2. The scalar field dimension might lie outside the range $(d/4,3d/4)$. This is in particular the case of the standard free theory (or the critical $O(N)$ model at large N) with $\Delta=d/2-1<d/4$, for $d<4$.

In both cases, we can still use the conformal partial wave machinery, as long as we take care of deforming the contour of integration over h, or isolating the non-normalizable contributions from the four-point kernel [99].

The typical example of a four-point kernel which is not an endomorphism is a physical four-point function of one scalar field ϕ whose s-channel OPE contains operators of dimension smaller than $d/2$. The identity operator is one such operator and it is always present, hence we always need to subtract the contribution that is disconnected in the s-channel, $C(x_1,x_2)C(x_3,x_4)$, before applying the expansion (3.E.16).[27] Similarly, if the field ϕ has $\Delta<d/2$ and the three-point function with itself is non-vanishing, then we need to subtract the contribution that is one-particle reducible in the s-channel (the s-channel skeleton tree diagram). It is then useful to define:

$$\begin{aligned}\mathcal{F}_s(x_1,x_2,x_3,x_4) &\equiv \langle\phi(x_1)\phi(x_2)\phi(x_3)\phi(x_4)\rangle - C(x_1,x_2)C(x_3,x_4)\\ &\quad-\int \mathrm{d}^d y_1\mathrm{d}^d y_2\langle\phi(x_1)\phi(x_2)\phi(y_1)\rangle C^{-1}(y_1,y_2)\langle\phi(y_2)\phi(x_3)\phi(x_4)\rangle\,,\end{aligned} \tag{3.E.19}$$

which is obtained in terms of the Bethe-Salpeter kernel K as (e.g. [110]):

$$\mathcal{F}_s(x_1,x_2,x_3,x_4)=\int \mathrm{d}^d y_1\mathrm{d}^d y_2(\mathbb{I}-K)^{-1}(x_1,x_2,y_1,y_2)C(y_1,x_3)C(y_2,x_4)\,. \tag{3.E.20}$$

Applying to $\mathcal{F}_s$ the expansion in the last line of (3.E.16), and pushing the integration contour to the right, the integral is reduced to a sum over the residues at the poles of the integrand (the poles of $\Lambda_{(\mathbb{I}-K)^{-1}}(h,J)$ being now the solutions of $k(h,J)=1$). Together with the sum over J, this reproduces the operator product expansion of the four-point function in the s channel, if no other physical operators have dimension smaller than $d/2$. If instead other primaries have dimension smaller than $d/2$, then on the right of the principal series we pick their shadow pole; this must be corrected by deforming

[26] The corresponding space $\mathcal{V}^{\text{symm}}_\Delta$ is defined as before, except that the metric needs also symmetrization: $g^{\text{symm}}_{x_1x_2;x_3x_4}=\frac{1}{2}(C^{-1}(x_1,x_3)C^{-1}(x_2,x_4)+C^{-1}(x_1,x_4)C^{-1}(x_2,x_3))$.

[27] Convoluting $C(x_1,x_2)C(x_3,x_4)$ with $f(x_3,x_4)\in\mathcal{V}_\Delta$, we obtain a new function proportional to $C(x_1,x_2)$. Regardless of whether the proportionality constant is finite or not, $C(x_1,x_2)$ is not square integrable with respect to the scalar product in (3.E.6), and therefore it is not in $\mathcal{V}_\Delta$.

the contour in the conformal block representation to keep only the physical poles on the right, or equivalently (because of (3.E.13)), by adding to the expansion the appropriate Ψ contributions:

$$\begin{aligned}\mathcal{F}_s(x_1,x_2,x_3,x_4) = &\sum_{J\in\mathbb{N}_0}\int_{\frac{d}{2}}^{\frac{d}{2}+\mathrm{i}\infty}\frac{\mathrm{d}h}{2\pi\,\mathrm{i}}\frac{\rho(h,J)}{1-k(h,J)}\mathcal{N}^{\Delta}_{h,J}\mathcal{N}^{\Delta}_{\tilde{h},J}\,\Psi^{\Delta,\Delta,\Delta,\Delta}_{h,J}(x_1,x_2,x_3,x_4)\\ &-\sum_{i,J}\mathrm{Res}\left[\frac{\rho(h,J)}{1-k(h,J)}\mathcal{N}^{\Delta}_{h,J}\mathcal{N}^{\Delta}_{\tilde{h},J}\,\Psi^{\Delta,\Delta,\Delta,\Delta}_{h,J}(x_1,x_2,x_3,x_4)\right]_{h=h_i(J)<d/2},\end{aligned} \tag{3.E.21}$$

where $h_i(J)$ are the physical solutions of $k(h,J)=1$ on the left of the principal series. These isolated contributions are exactly analogue to the contributions we subtracted from the four-point function to define $\mathcal{F}_s$. If such operators are present, we first subtract them from $\mathcal{F}_s$, then we use the resolution of the identity to decompose the subtracted $\mathcal{F}_s$, and finally we add them back as in (3.E.21) to give the expansion of $\mathcal{F}_s$ itself.

An example of the second situation in which (3.E.16) fails, namely when the dimension of the scalar field is outside the range $(d/4,3d/4)$, can be obtained from a generalized free field theory. Consider $\mathcal{F}_s$ for a GFFT:

$$\mathcal{F}_s^{GFFT}(x_1,x_2,x_3,x_4) = C(x_1,x_3)C(x_2,x_4)+C(x_1,x_4)C(x_2,x_3)\,, \tag{3.E.22}$$

which is also twice the inverse metric of $\mathcal{V}^{\mathrm{symm}}_{\Delta}$. Using (3.E.16) with $\mathcal{E}=\mathbb{I}$, but restricted to even spins to provide the symmetrization, we find:

$$\begin{aligned}&\mathcal{F}_s^{GFFT}(x_1,x_2,x_3,x_4) =\\ &2\sum_{J\in\mathbb{N}_0^{\mathrm{even}}}\left(-\tfrac{1}{2}\right)^J\int_{\frac{d}{2}-\mathrm{i}\infty}^{\frac{d}{2}+\mathrm{i}\infty}\frac{\mathrm{d}h}{2\pi\,\mathrm{i}}\rho(h,J)\,\mathcal{N}^{\Delta}_{h,J}\mathcal{N}^{\Delta}_{\tilde{h},J}\,S_{\tilde{h},J}\,\mathcal{G}^{\Delta,\Delta,\Delta,\Delta}_{h,J}(x_1,x_2,x_3,x_4)\,,\end{aligned} \tag{3.E.23}$$

and from (3.E.17) we know the normalization factors at $J=0$ have a pole at $h=2\Delta$, that is the dimension of ϕ^2. This pole crosses to the left of the principal series when Δ moves below $d/4$. In that case, in order to recover the correct OPE, we must deform the integration contour in such a way that the pole at $h=2\Delta$ stays to its right, and the shadow pole at $h=d-2\Delta$ stays to its left. Exploiting (3.E.13), it can be verified that the same result is obtained by writing, for $\Delta<d/4$:

$$\begin{aligned}\frac{1}{2}\mathcal{F}_s^{GFFT}(x_1,x_2,x_3,x_4) = &\sum_{J\in\mathbb{N}_0^{\mathrm{even}}}\int_{\frac{d}{2}}^{\frac{d}{2}+\mathrm{i}\infty}\frac{\mathrm{d}h}{2\pi\,\mathrm{i}}\rho(h,J)\,\mathcal{N}^{\Delta}_{h,J}\mathcal{N}^{\Delta}_{\tilde{h},J}\,\Psi^{\Delta,\Delta,\Delta,\Delta}_{h,J}(x_1,x_2,x_3,x_4)\\ &-\mathrm{Res}\left[\rho(h,0)\,\mathcal{N}^{\Delta}_{h,0}\mathcal{N}^{\Delta}_{\tilde{h},0}\,\Psi^{\Delta,\Delta,\Delta,\Delta}_{h,0}(x_1,x_2,x_3,x_4)\right]_{h=2\Delta}.\end{aligned} \tag{3.E.24}$$

This has the exact same form as (3.E.21), but is quite different in nature. Contrary to the previous case, it is now the functional space itself that is deviating from the original definition. In particular, convoluting (3.E.24) with the metric of $\mathcal{V}^{\mathrm{symm}}_{\Delta}$, we obtain a modified resolution of the identity:

$$\begin{aligned}\mathbb{I}_{\mathrm{symm}}(x_1,x_2,x_3,x_4) &\equiv \frac{1}{2}\left(\delta(x_1-x_3)\delta(x_2-x_4)+\delta(x_1-x_4)\delta(x_2-x_3)\right)\\ &= \sum_{J\in\mathbb{N}_0^{\mathrm{even}}}\int_{\frac{d}{2}}^{\frac{d}{2}+\mathrm{i}\infty}\frac{\mathrm{d}h}{2\pi\,\mathrm{i}}\rho(h,J)\,\mathcal{N}^{\Delta}_{h,J}\mathcal{N}^{\widetilde{\Delta}}_{\tilde{h},J}\,\Psi^{\Delta,\Delta,\widetilde{\Delta},\widetilde{\Delta}}_{h,J}(x_1,x_2,x_3,x_4)\\ &\quad-\mathrm{Res}\left[\rho(h,0)\,\mathcal{N}^{\Delta}_{h,0}\mathcal{N}^{\widetilde{\Delta}}_{\tilde{h},0}\,\Psi^{\Delta,\Delta,\widetilde{\Delta},\widetilde{\Delta}}_{h,0}(x_1,x_2,x_3,x_4)\right]_{h=2\Delta}.\end{aligned} \tag{3.E.25}$$

Since (3.E.11) has no poles, it would seem that the isolated contribution here is trivial. However, $\Psi^{\Delta,\Delta,\widetilde{\Delta},\widetilde{\Delta}}_{2\Delta,0}(x_1,x_2,x_3,x_4)$ is a singular distribution proportional to $1/|x_{34}|^d \sim \Gamma(0)\delta(x_{34})$; writing explicitly the limit involved in the definition of the residue, we find that such singularity leads to a non-trivial isolated contribution to the resolution of the identity:

$$\begin{aligned}
&-\text{Res}\left[\rho(h,0)\,\mathcal{N}^{\Delta}_{h,0}\mathcal{N}^{\widetilde{\Delta}}_{\tilde{h},0}\,\Psi^{\Delta,\Delta,\widetilde{\Delta},\widetilde{\Delta}}_{h,0}(x_1,x_2,x_3,x_4)\right]_{h=2\Delta}\\
&\quad=\lim_{\epsilon\to 0}\,2\epsilon\,\rho(2\Delta-2\epsilon,0)\,\frac{2^{d/2}}{\pi^d}\,\Psi^{\Delta,\Delta,\widetilde{\Delta},\widetilde{\Delta}}_{2\Delta-2\epsilon,0}(x_1,x_2,x_3,x_4)\\
&\quad=\lim_{\epsilon\to 0}\,c(d/2-\epsilon)\,c(2\Delta-2\epsilon)\,c(d-2\Delta+2\epsilon)\,\Psi^{\Delta,\Delta,\widetilde{\Delta},\widetilde{\Delta}}_{2\Delta-2\epsilon,0}(x_1,x_2,x_3,x_4)\\
&\quad=c(2\Delta)\,c(d-2\Delta)\int \mathrm{d}^d x_0\,\frac{1}{|x_{10}|^{2\Delta}|x_{20}|^{2\Delta}}\,\frac{1}{|x_{30}|^{d-2\Delta}|x_{40}|^{d-2\Delta}}\delta(x_{34})\,,
\end{aligned}\tag{3.E.26}$$

where we used the distributional identity $\lim_{\epsilon\to 0} c(d/2-\epsilon)/|x|^{d-2\epsilon} = \delta(x)$.

Conformal partial waves on the sphere. Everything we discussed in this appendix transcribes mutatis mutandis for CFTs on the sphere via the Weyl mapping (i.e. replacing all the distances by chordal distance and adding the adequate volume factors). By conformality of all the integrals involved (e.g. in (3.E.7), (3.E.10), and so on), the analytic properties of the conformal partial wave expansion are unchanged, and the effect of being on the sphere is only visible in the external points being multiplied by the appropriate $\Omega(x)$ factors.

However, in the evaluation of the sphere free energy we encounter traces of endomorphisms on $\mathcal{V}_\Delta$,

$$\text{Tr}(\mathcal{E}) = \int \mathrm{d}^d x_1 \mathrm{d}^d x_2\,\mathcal{E}(x_1,x_2,x_1,x_2)\,,\tag{3.E.27}$$

which are divergent due to their conformal invariance. The regularization of such traces necessarily breaks conformal invariance, and as a result $\Omega(x)$ factors survive, which play a crucial role in leading to finite results. The precise choice of regularization and its effects are described in the bulk of the chapter.

3.F The NNLO graph in Fig. 3.6

In this section we show that the contribution of the graph in Fig. 3.6 to the sphere free energy is finite. As it is not especially informative, we will not compute this contribution exactly.

The amplitude of any vacuum graph can be written as the convolution of a free covariance (representing any of its edges) and a two-point kernel (representing the amplitude of the remaining two-point amputated graph G):

$$I = \int_{x,y} C(x,y)A^G(x,y)\,.\tag{3.F.1}$$

In the case of the melon in (3.4.13) for instance $A^G(x,y) = C(x,y)^3$. Using dimensional regularization and $\Delta = \frac{d-\epsilon}{4}$, dimensional analysis leads to:

$$I = \int_{x,y} \frac{c(\Delta)}{s(x,y)^{\frac{d-\epsilon}{2}}}\,\frac{A^G(\epsilon)}{s(x,y)^{\frac{3}{2}d-b\epsilon}}\,.\tag{3.F.2}$$

The precise scaling b depends on the particular graph one considers (e.g. $b = 3/2$ for the melon). Following the same steps leading to (3.4.16) we conclude that:

$$I \sim \frac{1}{\Gamma(\frac{1+2b}{4}\epsilon)} A^G(\epsilon) \,. \tag{3.F.3}$$

For the melon $A^G(\epsilon) \sim \epsilon^0$, that is the melon does not contribute to the sphere free energy in the $\epsilon \to 0$ limit. We show below that for the graph in Fig. 3.6 opened on any of its edges, as depicted in Fig. 3.11, there exist two constants A_1 and A_2 such that:

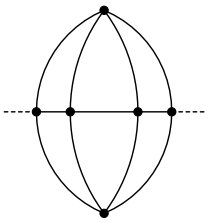

FIGURE 3.11: Amputated two-point diagram obtained by opening any edge in the graph of Fig. 3.6.

$$\frac{A_1}{\epsilon} < A^G(\epsilon) < \frac{A_2}{\epsilon} \,. \tag{3.F.4}$$

hence this graph brings a finite contribution to the sphere free energy. This contribution cancels between the different fixed points of interest as they all have the same tetrahedral coupling.

The remainder of this appendix is a rigorous proof of (3.F.4). It is quite lengthy and uses a set of techniques that, while standard, are quite apart from the ones used in the rest of the chapter.

One can of course apply the techniques we discuss here to the ladder diagrams. Graph by graph the ladder diagrams are divergent, and present increasingly singular poles in $1/\epsilon$. Accounting for the diagrams with λ_1 vertices allows one to subtract the poles and one can in principle resum the finite parts to reproduce the finite part of (3.4.32). This graph by graph computation is exceedingly difficult. The main gain of the conformal partial waves techniques we introduced in the main body of this chapter is to bypass this analysis entirely and directly give us the end result.

Going to flat space. We are interested in identifying the leading singular behavior in the $\epsilon \to 0$ limit of the amplitude $A^G(x, y)$ of amputated two-point graphs G. As already mentioned, dimensional analysis implies that, up to local terms: $A^G(x, y) = A^G(\epsilon)/s(x, y)^{\frac{3}{2}d-b\epsilon}$ where $A^G(\epsilon)$ might display poles in $1/\epsilon$. As this is an ultraviolet divergence it is insensitive to the details of the infrared regularization hence the leading divergence is the same on the sphere and on flat space. From now on we work on flat space.

Why it is non-trivial. In the long-range model two-point graphs are primitively power divergent. Once this local power divergence is dealt with (either set to zero in dimensional regularization or subtracted by a mass counterterm in other schemes) the only remaining primitively divergent graphs are the four-point ones. The latter bring $1/\epsilon$ poles that pile up if they come from subgraphs fully included in larger subgraphs (we review how this occurs below).

For two-point amputated graphs this naive power counting yields $A^G(\epsilon) \sim \epsilon^{-1}$ for the two-point melon (as it has four-point subgraphs) and $A^G(\epsilon) \sim \epsilon^{-2}$ for the two-point graph in Fig. 3.11, as it has a four-point subgraph that is a subgraph of another four-point subgraph. The non-trivial result of this section is that a detailed analysis of the sub divergences of these two graphs improves on the naive expectation, that is $A^G(\epsilon) \sim \epsilon^0$ for the melon and $A^G(\epsilon) \sim \epsilon^{-1}$ for the graph in Fig. 3.11

Structure of the amplitudes. On flat space the divergences and their subtractions are captured by the Bogoliubov–Parasiuk–Hepp–Zimmermann theorem [112, 113, 114]. For long-range models only two and four-point subgraphs are primitively divergent and they are subtracted by applying local Taylor operators.

The momentum and direct space formulation of the BPHZ theorem are reviewed for instance in [114] and the parametric space version is discussed in [115, 116]. In flat space, using Schwinger parameters, the amplitude of an amputated graph in the long-range model with external momenta p_i, V vertices and E edges is $\bar{A}^G_\mu(p_i) = (2\pi)^d \delta(\sum_i p_i) A^G_\mu(p_i)$ with:

$$\begin{aligned} A^G(p_i) &= \frac{1}{\Gamma(\zeta)^E (4\pi)^{\frac{d}{2}(E-V+1)}} \int_0^{k^{-2}} \left(\prod_{e\in G} d\alpha_e \; \alpha_e^{\zeta-1} \right) \frac{e^{-\frac{V(G)}{U(G)}}}{U(G)^{d/2}} \; , \\ U(G) &= \sum_{T\subset G} \prod_{e\notin T} \alpha_e \; , \quad V(G) = \sum_{T_1,T_2\subset G} (\sum_{i\in T_2} p_i)^2 \prod_{e\notin T_1\cup T_2} \alpha_e \; , \end{aligned} \tag{3.F.5}$$

where T runs over the spanning trees in G, respectively T_1, T_2 run over the pairs of trees, and $i \in T_2$ runs over the external vertices that belong to the tree T_2. The integral is cut-offed by and infrared cutoff k on the integration interval, but any other infrared cutoff will do. The overall factor $(2\pi)^d \delta(\sum_i p_i)$ reproduces the bare vertex. We work in dimensional regularization and we set $\zeta = \frac{d+\epsilon}{4}$. The amplitude at zero external momenta of G is, up to prefactors:

$$A^G \sim \int_0^{k^{-2}} \left(\prod_{e\in G} d\alpha_e \; \alpha_e^{\zeta-1} \right) \frac{1}{U(G)^{d/2}} = k^{-2\zeta E + d[E-V+1]} \int_0^1 \left(\prod_{e\in G} d\alpha_e \; \alpha_e^{\zeta-1} \right) \frac{1}{U(G)^{d/2}} \; . \tag{3.F.6}$$

If G is a two-point graph its amplitude in momentum space writes:

$$A^G(p) = p^{\frac{d+\epsilon}{2} - V\epsilon} A^G(\epsilon) + A^G \; , \tag{3.F.7}$$

where we denote somewhat abusively by $A^G(\epsilon)$ the coefficient of the scaling behavior in p. Note that for two-point graphs A^G is zero in dimensional regularization, as it is power divergent. This is of course not the case for four-point graphs. In principle $A^G(\epsilon)$ is a function of p/k and in the case of the melon it can be shown [17] that it has a finite limit for $k \to 0$.

Taylor operators and renormalized amplitudes. The Taylor operators acting on amplitudes are localization operators. For any γ subgraph of G we define:

$$\tau_\gamma A^G(p_i) \equiv A^\gamma \; A^{G/\gamma}(p_i) \; , \tag{3.F.8}$$

where A^γ is the amplitude of γ at zero momentum and G/γ denotes the graph obtained from G by contracting γ to a point. As we deal with the long-range case the subtraction of local parts suffices in order to render the amplitudes ultraviolet finite.

We consider amputated subgraphs γ of G. A subgraph γ contains all the vertices hooked to its edges. An inclusion forest [113] of subgraphs of G is a family $\mathcal{F}$ of subgraphs such that any two $\gamma_1, \gamma_2 \in \mathcal{F}$ are either totally disjoint (i.e. they do not share neither edges nor vertices) or one of them is fully contained in the other:

$$\mathcal{F} = \left\{ \gamma \in G \middle| \forall \gamma_1, \gamma_2 \text{ either } \gamma_1 \subset \gamma_2 \text{ , or } \gamma_2 \subset \gamma_1 \text{ , or } \gamma_1 \cap \gamma_2 = \emptyset \right\} . \tag{3.F.9}$$

The renormalization operator [112, 113, 114] R_G associated to the graph G is a sum over the inclusion forests $\mathcal{F} \subset G$ of primitively divergent subgraphs (i.e. two and four-point subgraphs in our

case) of a product of Taylor operators associated to the graphs in the forest:

$$R_G = \sum_{\mathcal{F}\subset\mathcal{G}} \prod_{\gamma\in\mathcal{F}} (-\tau_\gamma) \,. \tag{3.F.10}$$

the forests include the empty forest, which contributes a 1 to this formula.

Theorem 3. *(BPHZ [115, 114]). The renormalized amplitude $R_G A^G(p_i)$ of any graph G is ultraviolet convergent, that is $\lim_{\epsilon\to 0} R_G A^G(p_i)$ is finite.*

How we will use the BPHZ theorem. We are interested in identifying the $1/\epsilon$ behavior of the bare amplitude of a two-point graph G. Separating the empty forest in the renormalization operator we have:

$$R_G A^G(p) = A^G(p) + \sum_{\mathcal{F}\subset\mathcal{G}}^{\mathcal{F}\neq\emptyset} \prod_{\gamma\in\mathcal{F}} (-\tau_\gamma) A^G(p) \,, \tag{3.F.11}$$

and the BPHZ theorem ensures that this expression is convergent in the $\epsilon \to 0$ limit. It follows that the singular part of the coefficient $A^G(\epsilon)$ in (3.F.7) *must be entirely canceled by the subtractions*, hence it equals the divergent part of the counterterms.

The melon. Let us first consider the melon G. As primitively divergent subgraphs it has itself $\gamma = G$, and three subgraphs $\gamma_i, i = 1, 2, 3$ made of two edges. It follows that:

$$R_G A^G(p) = A^G(p) - \tau_\gamma A^G(p) - \sum_i \tau_{\gamma_i} A^G(p) + \sum_i \tau_\gamma \tau_{\gamma_i} A^G(p) = A^G(p) - A^G \,. \tag{3.F.12}$$

In this equation $\tau_\gamma A^G(p)$ is just the local part A^G of the melon (and in particular it is zero in dimensional regularization). Moreover, $\tau_\gamma \tau_{\gamma_i} A^G(p) = \tau_{\gamma_i} A^G(p)$ because G/γ_i is a tadpole graph, therefore the action of τ_γ is trivial. It follows that the two terms summed over i cancel exactly, which, together with (3.F.7), yields:

$$p^{\frac{d+\epsilon}{2} - V\epsilon} A^G(\epsilon) = A(p) - A^G = R_G A^G(p) \,. \tag{3.F.13}$$

As $R_G A^G(p)$ has a finite limit for $\epsilon \to 0$ we conclude that $A^G(\epsilon)$ has no poles in $1/\epsilon$.

The graph in Fig. 3.11. This graph has many four-point subgraphs. To identify them we label x, y the two external vertices, v_1, v_2 the top and bottom vertices and z_1, z_2 the two vertices on the horizontal (x and z_1 are connected by an edge). The list of two and four-point subgraphs of the graph in Fig. 3.11 comprises:

- two kite graphs, see Fig. 3.12, γ_x (and γ_y) obtained by cutting the edges (x, v_1), (x, z_1) and (x, v_2) (resp. (y, v_1), (y, z_2) and (y, v_2)).

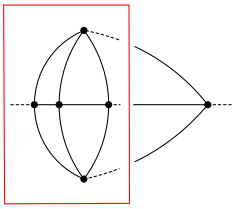

FIGURE 3.12: Kite graph obtained by cutting (y, v_1), (y, z_2) and (y, v_2).

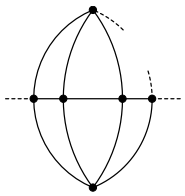

FIGURE 3.13: Example of one γ^{ab} graph, obtained by cutting one of the internal edges.

- 11 graphs γ^{ab} (see Fig. 3.13) obtained by cutting any of the internal edges (a, b) in the graph.
- itself, that is $\gamma = G$

These graphs are organized in several inclusion forests:

- the empty forest
- the one graph forests. They consist in either
  - the graph γ
  - one of the kite graphs γ_x or γ_y
  - any one of the remaining 11 graphs γ^{ab}
- the two graphs forests. They are
  - 11 of the form $\{\gamma, \gamma^{ab}\}$ for some ab.
  - three of the form $\{\gamma^{xa}, \gamma_x\}$ for the as connected to x by some edge respectively three of the form $\{\gamma^{ya}, \gamma_y\}$ for the as connected to y by some edge in G
  - two special ones $\{\gamma, \gamma_x\}$ and $\{\gamma, \gamma_y\}$
- the three graph forests. There are six of these ones
  - three of the form $\{\gamma, \gamma^{xa}, \gamma_x\}$ for some a and three of the form $\{\gamma, \gamma^{ya}, \gamma_y\}$ for some a.

Plenty of the contributions to the renormalized amplitude cancel as for any γ^{ab} , G/γ^{ab} is contracted to a tadpole hence $\tau_{\gamma^{ab}} A^G = \tau_\gamma \tau_{\gamma^{ab}} A^G$ and $\tau_{\gamma^{ab}} \tau_{\gamma_i} A^G = \tau_\gamma \tau_{\gamma^{ab}} \tau_{\gamma_i} A^G$. The renormalized amplitude is then

$$R_G A^G(p) = A^G(p) - A^G - 2A^{\gamma_x}\left[A^{G/\gamma_x}(p) - A^{G/\gamma_x}\right] . \tag{3.F.14}$$

Observe that G/γ_x is the two-point melon graph, hence incidentally $A^{G/\gamma_x}(p) - A^{G/\gamma_x}$ is nothing but the subtracted melon $R_{G/\gamma_x} A^{G/\gamma_x}(p)$ Combining this with (3.F.7) we find that:

$$p^{\frac{d+\epsilon}{2} - V\epsilon} A^G(\epsilon) = A(p) - A^G = R_G A^G(p) + 2A^{\gamma_x} R_{G/\gamma_x} A^{G/\gamma_x}(p) , \tag{3.F.15}$$

and as the renormalized amplitudes on the right hand side above have finite limits at $\epsilon \to 0$, the leading divergence of $A^G(\epsilon)$ is the same as the local part of the kite graph A^{γ_x}.

The amplitude of the kite graph. We will now conclude this section by proving that the amplitude of the kite graph has a pole of order 1 in ϵ. The amplitude of any four-point graph G with no two-point subgraphs at zero external momenta:

$$A^G = \int_0^{k^{-2}} \left(\prod_{e\in G} d\alpha_e \, \alpha_e^{\zeta-1}\right) \frac{1}{U(G)^{d/2}} = k^{-2\zeta E + d[E-V+1]} \int_0^1 \left(\prod_{e\in G} d\alpha_e \, \alpha_e^{\zeta-1}\right) \frac{1}{U(G)^{d/2}} , \tag{3.F.16}$$

is a convergent integral over α for $\zeta = \frac{d+\epsilon}{4}$ but exhibits poles in $1/\epsilon$.

For a graph with E edges, we divide the integration interval into Hepp sectors, which we denote σ, that is total orderings of the α parameters $\alpha_{e_{\sigma(1)}} \leq \alpha_{e_{\sigma(2)}} \leq \cdots \leq \alpha_{e_{\sigma(E)}}$. The edge $e_{\sigma(1)}$ is the most ultraviolet (lowest α), $e_{\sigma(2)}$ is the next most ultraviolet and so on up to $e_{\sigma(E)}$, which is the most infrared. There are $E!$ sectors, as many as there are permutations. Up to the global scaling the amplitude is:

$$A^G = k^{\epsilon - V\epsilon} \sum_\sigma A^G_\sigma \ , \quad A^G_\sigma = \int_{0 \leq \alpha_{\sigma(1)} \leq \cdots \leq \alpha_{\sigma(E)} \leq 1} \left(\prod_{e \in G} d\alpha_e \ \alpha_e^{\zeta - 1} \right) \frac{1}{U(G)^{d/2}} \ . \tag{3.F.17}$$

The polynomial $U(G)$ is a sum of positive terms. It is thus bounded from below by any of its terms, and from above by the number of terms times the largest of them. The number of trees in a graph is bounded by the number of subsets of edges, that is 2^E.

In each Hepp sector there is exactly one leading monomial corresponding to the tree T_σ built by proceeding from 1 to E and at each step adding the edge $e_{\sigma(q)}$ if it does not form a loop. We thus ensure that the edges with the lowest possible α parameters are in the tree, hence the complement of T_σ has the highest possible αs, that is in the sector σ:

$$0 \leq \alpha_{\sigma(1)} \leq \cdots \leq \alpha_{\sigma(E)} \leq 1 \Rightarrow 2^E \prod_{e \notin T_\sigma} \alpha_e \geq U(G) \geq \prod_{e \notin T_\sigma} \alpha_e \ . \tag{3.F.18}$$

Associated to a Hepp sector we have the set of "high graphs" $\gamma_q = \{e_{\sigma(1)}, \dots e_{\sigma(q)}\}$ formed by the q most ultraviolet edges. The subgraphs are considered amputated, that is they contain all the edges $\gamma_q = \{e_{\sigma(1)}, \dots e_{\sigma(q)}\}$ and the vertices hooked to them, but not the external edges (which can be either genuine external edges of G, or some of the "lower" edges $e_{\sigma(q+1)} \dots e_{\sigma(E)}$). We remark that $\gamma_E = G$ and that γ_q is not necessarily connected. By construction the leading tree T_σ is a tree in every connected component of γ_q, and it is the unique tree with this property.

At fixed Hepp sector σ we perform the diagonal change of variables:

$$\alpha_{\sigma(i)} = \prod_{j=i}^{E} t_j^2 \ , \qquad \alpha_{\sigma(E)} = t_E^2 \ , \ \ \alpha_{\sigma(E-1)} = t_{E-1}^2 t_E^2 \ , \ \ \dots \ \ \alpha_{\sigma(1)} = t_1^2 t_2^2 \dots t_E^2 \ , \tag{3.F.19}$$

and we note that all the edges of γ_q have a factor t_q^2. Now T_σ is a tree in every connected component of γ_q, hence the number of edges of γ_q not in T_σ is $E(\gamma_q) - V(\gamma_q) + C(\gamma_q)$ with $V(\gamma_q), E(\gamma_q)$ and $C(\gamma_q)$ the numbers of vertices, edges and connected components of γ_q. Every other tree T in G will be a forest (a collection of trees) in some of the connected components of some γ_qs and the number of edges of such a γ_q not belonging to T is strictly larger that $E(\gamma_q) - V(\gamma_q) + C(\gamma_q)$, hence:

$$U(G)\Big|_{\alpha_{\sigma(i)} = \prod_{j=i}^E t_j^2} = \prod_{i=1}^{E} t_i^{2[E(\gamma_i) - V(\gamma_i) + C(\gamma_i)]} \big[1 + O(t)\big] \ . \tag{3.F.20}$$

As the change of variables is diagonal we have:

$$A^G_\sigma = 2^E \int_0^1 \left(\prod_{i=1}^{E} dt_i \right) \prod_{i=1}^{E} t_i^{-1 + 2i\zeta - d[E(\gamma_i) - V(\gamma_i) + C(\gamma_i)]} \frac{1}{[1 + O(t)]^{d/2}} \ . \tag{3.F.21}$$

An upper/lower bound is obtained by using $2^E > 1 + O(t) > 1$. Denoting the convergence degree of γ_i by $\omega(\gamma_i) = 2i\zeta - d[E(\gamma_i) - V(\gamma_i) + C(\gamma_i)]$, if all the convergence degrees are positive an upper/lower

bound is:

$$\prod_{i=1}^{E}\frac{1}{\omega(\gamma_i)} \leq A_\sigma^G \leq 2^E \prod_{i=1}^{E}\frac{1}{\omega(\gamma_i)} \,. \tag{3.F.22}$$

In order to conclude it is enough to examine the possible convergence degrees for all the subgraphs of G. The number of edges of γ_i is exactly i and as we deal with quartic vertices $2i = 4V(\gamma_i) - n(\gamma_i)$ with $n(\gamma_i)$ the number of external half edges of γ_i. Denoting γ_i^ρ the connected components of γ_i, with $\rho = 1, \dots C(\gamma_i)$, and observing that the edges, vertices and external legs are distributed among the connected components, the convergence degree of γ_i is:

$$\omega(\gamma_i) = 2i\zeta - d[E(\gamma_i) - V(\gamma_i) + C(\gamma_i)] = i(2\zeta - \frac{d}{2}) + d\sum_{\rho=1}^{C(\gamma_i)}\frac{n(\gamma_i^\rho)-4}{4} = \frac{\epsilon}{2}i + d\sum_{\rho=1}^{C(\gamma_i)}\frac{n(\gamma_i^\rho)-4}{4} \,, \tag{3.F.23}$$

where we used $\zeta = \frac{d+\epsilon}{4}$. So far we have been quite general: we only assumed that there are no subgraphs with zero or negative convergence degree, that is no two-point subgraphs. For the kite graph:

- every strict subgraph (i.e. subgraph different from itself) has at least six external half-edges but less that 20 half edges hence $8\epsilon + 4d \geq \omega(\gamma_i) \geq \frac{d}{2}$.
- the wheel itself (corresponding to t_E) has 4 external half edges and 8 edges $\omega(\gamma_E) = 4\epsilon$.

Thus (recalling that there are $E!$ sectors) upper and lower bounds are:

$$\frac{1}{\epsilon}\left(\frac{1}{4(4d+8\epsilon)^E}\right) \leq A_\sigma^G \leq \frac{1}{\epsilon}\left(\frac{4^{E-1}}{d^E}\right) \;\Rightarrow\; \frac{k^{\epsilon-5\epsilon}}{\epsilon}\left(\frac{8!}{4(4d+8\epsilon)^8}\right) \leq A^G \leq \frac{k^{\epsilon-5\epsilon}}{\epsilon}\left(\frac{8!\,4^7}{d^8}\right) \,. \tag{3.F.24}$$

3.G Regularized trace of conformal partial waves

In this appendix we show how to compute $\mathcal{I}_\epsilon(J)$ (3.4.24). By homogeneity of the sphere, we can set $z = 0$, and factor out the volume of the d-sphere $V_d = \int \mathrm{d}^d z\, \Omega(z)^d$, given in (3.A.7). The most generic form of a three-point function $\langle\phi\phi O\rangle$ is fixed by conformal symmetry as in (3.E.1) and we obtain:

$$\mathcal{I}_\epsilon(J) = V_d \int \mathrm{d}^d x_1 \mathrm{d}^d x_2 \frac{(Z^{\mu_1}\cdots Z^{\mu_J} - \text{“traces"})\,(Z^{\mu_1}\cdots Z^{\mu_J} - \text{“traces"})}{(1+x_1^2)^\epsilon (1+x_2^2)^\epsilon |x_1|^{d-\epsilon}|x_2|^{d-\epsilon}|x_1-x_2|^{d-\epsilon}} \,, \tag{3.G.1}$$

where $Z^\mu = \frac{|x_1||x_2|}{|x_1-x_2|}\left(\frac{x_1^\mu}{|x_1|^2} - \frac{x_2^\mu}{|x_2|^2}\right)$ has unit norm. In order to take care of the spin structure we use the following identity (e.g. [111, 117]), which follows from the addition theorem (3.A.11):

$$(Z^{\mu_1}\cdots Z^{\mu_J} - \text{“traces"})\,(Z^{\mu_1}\cdots Z^{\mu_J} - \text{“traces"}) = \frac{(d-2)_J}{2^l(\frac{d-2}{2})_J} = \frac{\Gamma(d-2+J)\Gamma(\frac{d-2}{2})}{2^J\Gamma(d-2)\Gamma(\frac{d-2}{2}+J)} \,. \tag{3.G.2}$$

Then the relation $\mathcal{I}_\epsilon(J) = \frac{\Gamma(d-2+J)\Gamma(\frac{d-2}{2})}{2^J\Gamma(d-2)\Gamma(\frac{d-2}{2}+J)}\mathcal{I}_\epsilon(0)$ holds and it is sufficient to compute the integral at $J = 0$. Now we are ready to deal with the integral

$$\frac{\mathcal{I}_\epsilon(0)}{V_d} = (2a)^{3\epsilon-d}\int \mathrm{d}^d x_1 \mathrm{d}^d x_2 \frac{1}{(1+x_1^2)^\epsilon(1+x_2^2)^\epsilon|x_1|^{d-\epsilon}|x_2|^{d-\epsilon}|x_1-x_2|^{d-\epsilon}} \,. \tag{3.G.3}$$

It is convenient to perform the change of variable: $x^\mu = \frac{x_1^\mu}{x_1^2}$ and $y^\mu = \frac{x_2^\mu}{x_2^2}$. The Jacobian determinant of the transformation is $x^{-2d}y^{-2d}$ and the integral simplifies to:

$$\frac{\mathcal{I}_\epsilon(0)}{V_d} = (2a)^{3\epsilon-d}\int \mathrm{d}^d x \mathrm{d}^d y \frac{1}{(1+x^2)^\epsilon (1+y^2)^\epsilon (|x-y|^2+\mu^2)^{\frac{d}{2}-\frac{\epsilon}{2}}}\,, \tag{3.G.4}$$

where we have introduced another regulator μ^2 that is needed to make the integral convergent. Assuming $0<\epsilon<d$, we introduce three Schwinger parameters:

$$\begin{aligned}\frac{\mathcal{I}_\epsilon(0)}{V_d} = (2a)^{3\epsilon-d}\int \mathrm{d}^d x \mathrm{d}^d y \frac{1}{\Gamma(\epsilon)^2\Gamma(\frac{d}{2}-\frac{\epsilon}{2})}\int d\alpha_1 d\alpha_2 d\alpha_3 (\alpha_1\alpha_2)^{\epsilon-1}\alpha_3^{\frac{d}{2}-1-\frac{\epsilon}{2}} \\ \times e^{-\alpha_1(1+x^2)-\alpha_2(1+y^2)-\alpha_3(x^2+y^2-2xy)-\alpha_3\mu^2}\,.\end{aligned} \tag{3.G.5}$$

We can now perform the Gaussian integrals in x and y:

$$\frac{\mathcal{I}_\epsilon(0)}{V_d} = (2a)^{3\epsilon-d}\frac{\pi^d}{\Gamma(\epsilon)^2\Gamma(\frac{d}{2}-\frac{\epsilon}{2})}\int d\alpha_1 d\alpha_2 d\alpha_3 \frac{(\alpha_1\alpha_2)^{\epsilon-1}\alpha_3^{\frac{d}{2}-1-\frac{\epsilon}{2}}}{(\alpha_1\alpha_2+\alpha_3(\alpha_1+\alpha_2))^{d/2}} e^{-\alpha_1-\alpha_2-\mu^2\alpha_3}\,. \tag{3.G.6}$$

Using the Mellin-Barnes representation [118] we find:

$$\begin{aligned}\frac{\mathcal{I}_\epsilon(0)}{V_d} = \frac{(2a)^{3\epsilon-d}\pi^d}{\Gamma(\epsilon)^2\Gamma(\frac{d}{2}-\frac{\epsilon}{2})}\int_{x_0-i\infty}^{x_0+i\infty}\left(\frac{dz}{2\pi i}\right)\int d\alpha_1 d\alpha_2 d\alpha_3 e^{-\alpha_1-\alpha_2-\mu^2\alpha_3} \\ \times\frac{\Gamma(-z)\Gamma(z+\frac{d}{2})(\alpha_1\alpha_2)^{\epsilon+z-1}\alpha_3^{-z-\frac{\epsilon}{2}-1}}{\Gamma(\frac{d}{2})(\alpha_1+\alpha_2)^{z+d/2}}\,.\end{aligned} \tag{3.G.7}$$

Next, for $\mathrm{Re}(z)<-\epsilon/2$ we can use the integral representation of the Gamma function to integrate α_3. And if we require also $\mathrm{Re}(z)>-\epsilon$ and $\mathrm{Re}(z)+2\epsilon>d/2$ the integration over α_1 and α_2 can be found in [118]. We finally obtain:

$$\begin{aligned}\frac{\mathcal{I}_\epsilon(0)}{V_d} = \frac{(2a)^{3\epsilon-d}\pi^d}{\Gamma(\epsilon)^2\Gamma(\frac{d}{2}-\frac{\epsilon}{2})}\int_{x_0-i\infty}^{x_0+i\infty}\left(\frac{dz}{2\pi i}\right)\mu^{2z+\epsilon} \\ \times\frac{\Gamma(-z)\Gamma\left(\frac{d+2z}{2}\right)\Gamma\left(-\frac{2z+\epsilon}{2}\right)\Gamma(z+\epsilon)^2\Gamma\left(\frac{-d+2z+4\epsilon}{2}\right)}{\Gamma\left(\frac{d}{2}\right)\Gamma(2z+2\epsilon)}\,.\end{aligned} \tag{3.G.8}$$

Since we have the two conditions $\mathrm{Re}(z)<-\epsilon/2$ and $\mathrm{Re}(z)>-\epsilon$, we are free to choose $x_0\in(-\epsilon,-\epsilon/2))$. Moreover we must take $\epsilon>d/2$ in order to avoid poles of the last gamma function in this range, but of course we will then analytically continue the result to small ϵ. Closing the contour to the right we pick only the poles at $z=n$ and $z=-\epsilon/2+n$ with $n\in\mathbb{N}_0$. Computing the residues at the poles we find the result:

$$\begin{aligned}\frac{\mathcal{I}_\epsilon(0)}{V_d} = (2a)^{3\epsilon-d}\left(\frac{\pi^d\Gamma\left(\frac{\epsilon}{2}\right)^3\Gamma\left(\frac{3\epsilon}{2}-\frac{d}{2}\right)}{\Gamma\left(\frac{d}{2}\right)\Gamma(\epsilon)^3}\right)(1+\mathcal{O}(\mu^2)) \\ +\mu^\epsilon(2a)^{3\epsilon-d}\left(\frac{\pi^d\Gamma\left(-\frac{\epsilon}{2}\right)\Gamma\left(\frac{4\epsilon-d}{2}\right)}{\Gamma(2\epsilon)\Gamma\left(\frac{d}{2}-\frac{\epsilon}{2}\right)}\right)(1+\mathcal{O}(\mu^2))\,.\end{aligned} \tag{3.G.9}$$

When we remove the μ regulator, while keeping ϵ finite, only the first term coming from $z=-\epsilon/2$ survives and we find the final result (3.4.27).

3.H Large-J expansion

In this appendix we detail how the finite part from (3.4.22) is extracted. As explained in the main text, in order to regularize the sum over J it is important to consistently shift $\widetilde{\Delta} \to \widetilde{\Delta} - \epsilon$ and $\tilde{h} \to \tilde{h} - \epsilon$ everywhere. In particular, it is crucial to introduce ϵ in the product of normalization factors (3.E.11). At large J this product reduces to:

$$\mathcal{N}^{\Delta}_{h,J}\mathcal{N}^{\widetilde{\Delta}-\epsilon}_{\tilde{h}-\epsilon,J} \sim \frac{2^{3(d+\epsilon)/2+J}}{(2\pi)^d}\, J^{-3\epsilon}\,(1+\mathcal{O}(1/J))\,, \tag{3.H.1}$$

and the factor $J^{-3\epsilon}$ turns out to suffice to render the sum convergent. After setting $\Delta = \frac{d}{4}$, the regularized version of (3.4.22) reads:

$$-g\frac{\partial}{\partial g}F^{\epsilon}_{\text{NNLO}} = N^2 \sum_{J\in\mathbb{N}_0}\int_{\frac{d}{2}}^{\frac{d}{2}+\mathrm{i}\,\infty}\frac{\mathrm{d}h}{2\pi\,\mathrm{i}}\rho(h,J)\,\frac{k(h,J)^2}{1-k(h,J)}\,\mathcal{N}^{\frac{d}{4}}_{h,J}\mathcal{N}^{\frac{3d}{4}-\epsilon}_{\tilde{h}-\epsilon,J}\,\mathcal{I}_{\epsilon}(J)\,, \tag{3.H.2}$$

where $\rho(h,J)$, $k(h,J)$, $\mathcal{N}^{\Delta}_{h,J}$ and $\mathcal{I}_{\epsilon}(J)$ are all ratios of gamma functions.

Integrating numerically each term at fixed J, and using standard convergence tests, one finds that the resulting series is divergent at $\epsilon = 0$. In order to isolate and subtract the divergence, we need to identify the asymptotic behavior at large J. A naive expansion of the integrand in $1/J$ leads however to a divergent integral over h, due to the exchange of limit and integral, and a more careful analysis is needed. It turns out to be convenient to make the change of variable $h = d/2 + \mathrm{i}\,\alpha J$ in the integral, after which we can use Stirling formula on the gamma functions with J in the argument. With this procedure we find the following asymptotic behavior in J:

$$-\frac{1}{N^2}g\frac{\partial}{\partial g}F^{\epsilon}_{\text{NNLO}} \to \sum_{J\in\mathbb{N}_+}\frac{1}{J^{1+3\epsilon}}\int_0^{+\infty}\mathrm{d}\alpha\,F(\alpha,\epsilon) = \zeta(1+\epsilon)f(\epsilon)\,, \tag{3.H.3}$$

hence the series has a simple pole at $\epsilon = 0$. The precise expressions of $F(\alpha,\epsilon)$ and $f(\epsilon)$ are:

$$F(\alpha,\epsilon) = \frac{\pi^{-\frac{d}{2}}\,g^4\,2^{-2d+\frac{9\epsilon}{2}-1}\,a^{3\epsilon}\,\Gamma\left(\frac{d-2}{2}\right)\Gamma\left(\frac{\epsilon}{2}\right)^3\Gamma\left(\frac{3\epsilon}{2}-\frac{d}{2}\right)}{\Gamma(d-2)\Gamma\left(d\right)\Gamma(\epsilon)^3}\,\alpha^{d-2}\left(\alpha^2+1\right)^{1-d-\frac{3\epsilon}{2}}\,, \tag{3.H.4}$$

$$f(\epsilon) = \frac{\pi^{2-\frac{d}{2}}\,g^4\,2^{-3d+\frac{3\epsilon}{2}+4}\,a^{3\epsilon}\,\Gamma\left(\frac{3\epsilon}{2}-\frac{d}{2}\right)\Gamma\left(\frac{1}{2}(d+3\epsilon-1)\right)}{\Gamma\left(d\right)\Gamma\left(\frac{\epsilon+1}{2}\right)^3\Gamma\left(d+\frac{3\epsilon}{2}-1\right)}\,, \tag{3.H.5}$$

and they are both analytic functions at $\epsilon = 0$ (for $2 < d < 4$). For numerical computation, it is convenient to add and subtract the asymptotic contribution (3.H.3) to the original series, and write:

$$\begin{aligned}-g\frac{\partial}{\partial g}F^{\epsilon}_{\text{NNLO}} = {}& N^2\int_{\frac{d}{2}}^{\frac{d}{2}+\mathrm{i}\,\infty}\frac{\mathrm{d}h}{2\pi\,\mathrm{i}}\rho(h,0)\,\frac{k(h,0)^2}{1-k(h,0)}\,\mathcal{N}^{\Delta}_{h,0}\mathcal{N}^{\widetilde{\Delta}-\epsilon}_{\tilde{h}-\epsilon,0}\,\mathcal{I}_{\epsilon}(0)\\ &+ N^2\sum_{J\in\mathbb{N}_+}\left(\int_{\frac{d}{2}}^{\frac{d}{2}+\mathrm{i}\,\infty}\frac{\mathrm{d}h}{2\pi\,\mathrm{i}}\rho(h,J)\,\frac{k(h,J)^2}{1-k(h,J)}\,\mathcal{N}^{\Delta}_{h,J}\mathcal{N}^{\widetilde{\Delta}-\epsilon}_{\tilde{h}-\epsilon,J}\,\mathcal{I}_{\epsilon}(J) - \frac{f(\epsilon)}{J^{1+3\epsilon}}\right)\\ &+ N^2\zeta(1+\epsilon)f(\epsilon)\,,\end{aligned} \tag{3.H.6}$$

where in the first term we isolated the $J = 0$ contribution. The sum in the second line is now convergent for $\epsilon = 0$, hence it can be computed numerically. The last term expands in ϵ as:

$$N^2 f(\epsilon)\zeta(1+3\epsilon) = N^2\Big(\frac{f(0)}{3\epsilon} + \frac{1}{3}f'(0) + \gamma f(0) + \mathcal{O}(\epsilon)\Big)\,, \tag{3.H.7}$$

and after subtracting the pure pole part, it yields an additional finite contribution. Overall we get the derivative of the sphere free energy:

$$-g\frac{\partial}{\partial g}F_{\rm NNLO} = \lim_{\epsilon\to 0}\left(-g\frac{\partial}{\partial g}F^{\epsilon}_{\rm NNLO} - \frac{N^2 f(0)}{3\epsilon}\right) , \tag{3.H.8}$$

which can be evaluated numerically. For example, for $d = 3$, $g = 1$ and $a = 1$, we find:

$$-g\frac{\partial}{\partial g}F_{\rm NNLO} = 7.57 \times 10^{-4}\, N^2 . \tag{3.H.9}$$

Chapter 4

Finite-size vs. finite-temperature effects in CFT

4.1 Introduction

Quantum field theories in high energy physics are typically based on Lagrangians which only depend on the fields and their first derivatives. Higher-order derivatives in time are excluded in order to preserve unitarity, and then by Lorentz invariance higher-order derivatives in space are excluded as well. Fractional derivatives of order less than one are instead excluded by locality, or the need of having a particle interpretation. Such requirements might be dropped in Euclidean field theories, if the base space is interpreted as representing only spatial directions and the theory itself as a model of classical equilibrium statistical physics. It is within this perspective that we can frame the study of non-local models containing fractional derivatives, also known as long-range models. Such models have been realized experimentally in recent years (see [5] for a review), but have been studied from a theoretical standpoint since a long time because of several interesting features: they can violate the Mermin-Wagner theorem and admit phase transitions even in one dimension, as proved by Dyson for the long-range Ising model [119]; they typically lead to one-parameter families of universality classes (as found for example by two-loop [120, 121] and three-loop computations [118, 122]) and tuning such parameter one can study, at fixed dimension, phenomena such as the crossover from a long-range to a short-range universality class [123, 124, 125, 71]; one can rigorously construct fixed points and trajectories of the renormalization group in three dimensions [126, 127, 128, 129, 130]; and so on. Their realizations in the context of defect or boundary field theories have also contributed to renewing theoretical interest in such models [66, 32].

In this chapter, we want to address some aspects of finite-size and finite-temperature effects, which in general are very important (see for example [131]), in long-range models. In particular, we will study the long-range $O(N)$ model with one compact direction. This can be seen as a special case of finite-size effects in the corresponding classical statistical model [132]. However, by far the most common motivation for introducing only one compact direction is the fact that the quantum statistical mechanics of a d-dimensional system at finite temperature $T = 1/\beta$ can be described as a $(d+1)$-dimensional Euclidean field theory with compact Euclidean time of length β, that is, on a space-time $S^1_\beta \times \mathbb{R}^d$ with Euclidean signature (e.g. [133]). Such a description has two complementary limits: the $\beta \to \infty$ limit describing a quantum system at zero-temperature as a Euclidean field theory in $d+1$ dimensions, and the $\beta \to 0$ limit describing a classical system at equilibrium in d space dimensions. Therefore, in general with a given Euclidean field theory comes a choice of interpreting it as representing either a classical or a quantum statistical system. However, this is not always the case, as the quantum interpretation is more constrained: for example, unitarity implies that derivatives of order higher than two cannot be assigned to an imaginary-time direction. Moreover, fractional derivatives should also be interpreted with care, as the reconstruction of a quantum Hamiltonian from a Lagrangian containing fractional time derivatives poses some challenges, and it might describe a

system very different from that associated to the classical interpretation. We stress this point because of our focus on long-range models, where the fact that finite-temperature and finite-size cases are structurally different seems to be sometimes overlooked. As we will discuss below, the finite-size classical system involves a compact direction among those appearing in the non-local kernel, while the field theoretic description of the finite-temperature quantum system requires the introduction of one extra compact direction with local interaction. This observation is not really new, but with few exceptions [134, 135] it is often only left implicit in the details of numerical simulations [136, 137], and it has not been explored much at an analytical level.

In order to clarify this point, let us consider a finite but continuous system[1] with Hamiltonian:

$$H(\Pi, Q) = \frac{1}{2}\sum_{i\in\Lambda}\Pi_i^2 + U(Q)\ , \qquad U(Q) = -\sum_{i,j\in\Lambda} J_{ij}Q_iQ_j + \sum_{i\in\Lambda} V(Q_i)\ , \tag{4.1.1}$$

where $\Lambda \subset \mathbb{Z}^d$ is a finite d-dimensional lattice, and J_{ij} is not restricted to nearest neighbouring sites, but rather assumed to be of the form:

$$J_{ij} \sim \frac{1}{|i-j|^{d+2\zeta}}\ , \qquad 0 < \zeta < 1\ , \tag{4.1.2}$$

with the case $\zeta = 1$ being equivalent to the nearest-neighbour (or short-range) model.

In the classical canonical partition function, the configuration variables Q and their conjugate momenta Π are independent variables (e.g. taking values in $\mathbb{R}$), and expectation values in the canonical ensemble are computed as integrals over phase space with the Boltzmann weight. When considering a Q-dependent observable $\mathcal{A}(Q)$, the integral over Π factors out:

$$\langle \mathcal{A}(Q)\rangle_{\text{class.}} \propto \int e^{-\beta U(Q)}\mathcal{A}(Q)\prod_{i\in\Lambda} dQ_i\ . \tag{4.1.3}$$

In the formal continuum limit $\Lambda \to \mathbb{R}^d$ and $Q_i \to \phi(x)$ this becomes a Euclidean functional integral, and β is absorbed into the definition of the couplings of the action $\beta U(Q) \to S[\phi]$:

$$S[\phi] \sim -\int d^dx d^dy\,\frac{\phi(x)\phi(y)}{|x-y|^{d+2\zeta}} + \int d^dx\, V(\phi)\ . \tag{4.1.4}$$

In the quantum case, Π and Q are instead replaced by non-commuting operators $\hat\Pi$ and $\hat Q$, and expectation values computed as $\langle \mathcal{A}(\hat Q)\rangle_{\text{quant.}} \propto \text{Tr}[\mathcal{A}(Q)e^{-\beta\hat H}]$. Noticing that $e^{-\beta\hat H}$ has the form of the time evolution operator $e^{\imath t\hat H}$ with imaginary time $t = \imath\beta$, one then proceeds using the Trotter formula to split the interval $[0,\beta]$ in n steps, and introducing resolutions of the identity in both the $|\Pi\rangle$ and $|Q\rangle$ bases at each step, thus reducing again to commuting variables. Integrating over Π, one reaches:

$$\langle \mathcal{A}(\hat Q)\rangle_{\text{quant.}} \propto \int e^{-\frac{1}{2\epsilon}\sum_{<k,l>}\sum_{i\in\Lambda}(Q_{i,k}-Q_{i,l})^2 - \epsilon\sum_k U(Q_k)}\mathcal{A}(Q)\prod_{k=1}^{n}\prod_{i\in\Lambda} dQ_{i,k}\ , \tag{4.1.5}$$

where $\epsilon = \beta/n$ and the lattice now includes a (Euclidean) time direction, with periodic boundary condition $Q_{i,n+1} = Q_{i,1}$, along which the action is short-range ($< k,l >$ denotes nearest-neighbours). In the continuum limit, this becomes again a Euclidean field theory, but on a $(d+1)$-dimensional space, and with an anisotropy in the (Euclidean) time direction, if $\zeta \neq 1$.[2]

[1] See [138] for a similar story in the case of discrete spin systems.

[2] Notice that such a construction goes through in a very similar fashion for any Hamiltonian of the form $H(\Pi, Q) = K(\Pi) + U(Q)$, with the only difference that if the integral in Π is not Gaussian then the result will not be Gaussian in

The main point of this example is to highlight that given a model with long-range interactions in space, its classical and quantum partition functions do not differ just in the number of dimensions, but also in the structure of the action entering the path integral. Notice that this does not preclude the possibility of interpreting as a finite-temperature quantum system the model (4.1.4) with a compactified direction: in fact, for $\zeta \leq 1$ the model is reflection positive and the Osterwalder-Schrader theorem [140] grants the existence of an underlying quantum system. However, the construction of the corresponding quantum Hamiltonian can be very complicated and even include additional degrees of freedom. For example, it is known that an action like (4.1.4) with $d = 1$ can be obtained from a spin-boson model, i.e. a single quantum spin coupled to a dissipative bosonic bath, by a similar procedure as the one leading to (4.1.5) and by tracing out the bosonic degrees of freedom (e.g. [141]).

In this chapter, we will be interested in distinguishing and studying the same kind of long-range model in two different regimes: as a classical statistical field theory with one compact spatial direction and as a quantum statistical field theory at finite temperature (i.e. with compact Euclidean time). In other words, we will consider a continuous version of the model (4.1.5), defined in general on $S^1_\beta \times S^1_L \times \mathbb{R}^{d-1}$, with long-range interaction in the d spatial directions and standard local interaction in the imaginary-time direction, i.e. the coordinate on S^1_β (see equation (4.4.1) below for the explicit form of the action). However, we will never consider explicitly the case with both β and L finite: we will start with the classical system at $\beta \to 0$ and $0 < L < \infty$ (i.e. a purely long-range model on $S^1_L \times \mathbb{R}^{d-1}$), and then study the finite-temperature quantum system at $0 < \beta \leq \infty$ and $L \to \infty$ (i.e. a short-range in time and long-range in space model on $S^1_\beta \times \mathbb{R}^d$).

In both cases, we will focus on the critical model. As usual, this will correspond to tuning the non-compactified version of the model (i.e. on $\mathbb{R}^d$ or $\mathbb{R}^{d+1}$) to the infrared fixed point of the renormalization group, where the model is scale invariant. In the isotropic case (the classical model), it is known that such invariance is promoted to full conformal invariance [66], and as we review below, an interesting question is what happens to the conformal structure of the theory once a spatial direction is compactified. In the anisotropic case (the quantum model), the situation is more complicated, as the $SO(d+1)$ group of rotations is broken to $SO(d)$ even at zero temperature. The scaling invariance is in this case of the Lifshitz type (see below), and at present it is not clear to us whether this will be enhanced to some form of anisotropic conformal invariance (see [142] for examples of that).

Finite-size effects in CFTs. In general, a conformal field theory (CFT) in $\mathbb{R}^d$ is unambiguously defined by its CFT data, that is, the spectrum of scaling dimensions of its primary operators and the set of all the operator product expansion (OPE) coefficients. One-point functions vanish identically, two-point functions are fixed up to normalization by the spin and scaling dimensions of the operators, and three-point functions are fixed by the same data plus the OPE coefficients. For higher n-point functions no new data are needed, as in principle they can be reconstructed by repeated use of the OPE. Things change when one or more spatial directions are compactified. In fact, such compactifications obviously introduce a scale (the size L of the compact direction) that breaks both scale and rotation invariance. Luckily, not all the beauty of CFT is lost: if the system is still tuned to the same critical point corresponding to the CFT of the non-compact case, we expect that the compactification will not affect small-distance[3] properties, such as the OPE and the short-scale divergence of the two-point functions (hence the scaling dimensions). As a consequence, the reduction of n-point functions to lower correlators is still possible, at least for configurations of the n points inside a ball of radius smaller than L. On the other hand, this reasoning does not apply to one-point functions: since translations are preserved by toroidal compactifications, one-point functions have to be constant, and thus do not admit a short-distance limit. Therefore, as a consequence of the broken scale invariance, the one-point

$(Q_{i,k} - Q_{i,l})$; but it will still be short-ranged in time. For a case with mixing terms, see for example the rotor model [139].

[3] Smaller than the smallest size of the compact directions.

function of an operator $\mathcal{O}$ can acquire a non-vanishing value, proportional to $L^{-\Delta_\mathcal{O}}$, where $\Delta_\mathcal{O}$ is the scaling dimension of the operator. The non-vanishing coefficients of one-point functions thus become new CFT data, that permeate through OPE to all the higher n-point functions.

Such aspects of finite-size/temperature effects in CFTs have been discussed in [143, 144, 145, 146, 147, 148], and we follow in particular the presentation of [145]. On $S^1_L \times \mathbb{R}^{d-1}$, conformal symmetry constrains the one-point functions to take the form:

$$\langle \mathcal{O}^{\bar{\mu}}_{(\Delta_\mathcal{O},J)} \rangle = \frac{b_\mathcal{O}}{L^{\Delta_\mathcal{O}}} \left(e^{\mu_1} \cdots e^{\mu_J} - \text{traces} \right) , \tag{4.1.6}$$

where $\Delta_\mathcal{O}$ and J are the scaling dimension and spin (order of the symmetric traceless tensor representation of $SO(d)$) of the operator $\mathcal{O}$, and e is the unit vector in the compact direction. The L dependence in (4.1.6) is fixed but the coefficient $b_\mathcal{O}$ is not: it is the new CFT data we discussed above. The non-vanishing of $b_\mathcal{O}$ affects the OPE of the two-point functions, which otherwise would only include the identity operator. Indeed, starting with a two-point function in direct space:

$$G(y, \mathbf{x}) = \langle \phi(y, \mathbf{x}) \phi(0,0) \rangle , \qquad y \in S^1_L , \ \mathbf{x} \in \mathbb{R}^{d-1} , \tag{4.1.7}$$

and using the OPE for the two fields ϕ (which is convergent in the region $x^2 = y^2 + \mathbf{x}^2 < L^2$, as argued in [145]) one obtains:

$$G(y, \mathbf{x}) = \sum_{\mathcal{O} \in \phi \times \phi} \frac{f_{\phi\phi\mathcal{O}}}{c_\mathcal{O}} |x|^{\Delta_\mathcal{O} - 2\Delta_\phi - J} x_{\mu_1} \cdots x_{\mu_J} \langle \mathcal{O}^{\bar{\mu}}_{(\Delta_\mathcal{O},J)}(0) \rangle , \tag{4.1.8}$$

where $f_{\phi\phi\mathcal{O}}$ is the OPE coefficient and $c_\mathcal{O}$ is the normalization coefficient of the two-point function of $\mathcal{O}$. As the tensor structure in (4.1.6) is symmetric and traceless one can use [111, 117]:

$$|x|^{-J} x_{\mu_1} \cdots x_{\mu_J} \left(e^{\mu_1} \cdots e^{\mu_J} - \text{traces} \right) = C_J^{\left(\frac{d-2}{2}\right)}(\eta) \frac{J! \Gamma\left(\frac{d-2}{2}\right)}{2^J \Gamma\left(\frac{d-2}{2} + J\right)} , \tag{4.1.9}$$

where $\eta = y/|x|$ and $C_J^{\left(\frac{d-2}{2}\right)}(\eta)$ is a Gegenbauer Polynomial and rewrite the OPE of the two-point function as:

$$G(y, \mathbf{x}) = \sum_{\mathcal{O} \in \phi \times \phi} \frac{a_\mathcal{O}}{L^{\Delta_\mathcal{O}}} C_J^{\left(\frac{d-2}{2}\right)}(\eta) |x|^{\Delta_\mathcal{O} - 2\Delta_\phi} , \qquad a_\mathcal{O} \equiv \frac{b_\mathcal{O} f_{\phi\phi\mathcal{O}}}{c_\mathcal{O}} \frac{J! \Gamma\left(\frac{d-2}{2}\right)}{2^J \Gamma\left(\frac{d-2}{2} + J\right)} . \tag{4.1.10}$$

Note that in the infinite-size case one can go through the same steps and write an OPE expansion for the two-point function, but since only the term corresponding to the identity operator (with $\Delta_\mathcal{O} = 0$) has a non-vanishing expectation value in the limit $L \to \infty$ one recovers the standard conformal form of the two-point function.

In the finite-size case one can in principle read off the coefficients $a_\mathcal{O}$ by expanding the two-point function as a sum over terms of the form $C_J^{\left(\frac{d-2}{2}\right)}(\eta)|x|^{\Delta - 2\Delta_\phi}$. Conversely, once the $a_\mathcal{O}$ coefficients are known one can reconstruct the two-point function. In practice, both of these reconstructions are typically hard, as they require knowing exactly either the two-point function or the CFT data. However, they can become useful in special circumstances in which either of these pieces of information is available, as in the large-N limit that we will employ here.

The new data $b_\mathcal{O}$, for $\mathcal{O}$ in the OPE of two fundamental fields of the short-range $O(N)$ model, have been computed in [145, 148] at leading and subleading order of the $1/N$ expansion. Here we will tackle similar computations for the long-range case.

Fractional Lifshitz field theories. As argued above, the quantum version of a long-range model, at zero or non-zero temperature, is mapped to a Euclidean field theory with a strong anisotropy. That is, it is not just the compactification of the Euclidean time direction that breaks rotation invariance: the invariance is broken already by the local dynamics. The model that arises in such case (see our action (4.4.1), as well as [134, 135]) is a kind of Lifshitz field theory, that is, the type of theory used as Landau free energy of a Lifshitz point [149]. Lifshitz points are characterized by a distinctive phase diagram, including a modulated phase, and an anisotropic scale invariance:

$$\tau \to \Omega^z \tau, \quad x_i \to \Omega x_i \,, \tag{4.1.11}$$

where we denoted τ the Euclidean time and the exponent z is known as *dynamic critical exponent*, because of the similarity with the scale invariance of dynamic critical phenomena [150]. Typical Lifshitz field theories are scalar field theories whose kinetic term has two time derivatives[4] and $2z$ spatial derivatives, with z typically being an integer (most commonly $z = 2$). Our action will be of a similar form, but with non-integer $z = \zeta$, fixed by the corresponding classical long-range model (4.1.4), and thus we will call it *fractional Lifshitz field theory* (FLFT).

Given that most of the literature on Lifshitz field theories is focused on actions with $z = 2$, or other integer values, there are several open questions for our FLFT, even at zero temperature. For example, as we mentioned above, we do not currently know whether at the interacting fixed point scale invariance is enhanced to some form of anisotropic conformal invariance. Moreover, we do not know yet if at such fixed point the dynamic critical exponent takes a value different from ζ,[5] and we also do not know if above some $\zeta^* < 1$ there is a crossover to the short-range universality class ($\zeta = 1$), as in the isotropic long-range model. We hope to address these questions in a separate in the future (the last two require in particular to go beyond the leading order of the large-N approximation, to which we stick in the present work), while here we wish to use this model for a comparative study of some finite-temperature versus finite-size effects.

Plan of the chapter. The chapter is organised as follows. In section 4.2, we start by studying the case of a generalized free field theory on $S^1_L \times \mathbb{R}^{d-1}$, as a warm up. In the process we need to deal with higher twist operators that are absent in the short-range case. We reproduce the results of [145] for the $a_{\mathcal{O}}$ coefficients in the expansion of the two-point function for operators with arbitrary spin and twist by a different technique. In section 4.3, we study the long-range $O(N)$ model with finite size. We prove the existence of a finite-size mass and compute the coefficients $b_{\mathcal{O}}$ for spinning operators with minimal twist. We also compute the one-point functions for operators with arbitrary twist, and deduce their $a_{\mathcal{O}}$ coefficients. In section 4.4, we switch to the case of the quantum long-range model at finite temperature, described by a FLFT on $S^1_\beta \times \mathbb{R}^d$. We show that at zero temperature this model admits an interacting infrared fixed point. We then show that a thermal mass is generated when putting the model on $S^1_\beta \times \mathbb{R}^d$ and we derive the one-point functions for an infinite family of scaling operators at finite temperature.

In appendix 4.A, we give some details on the computation of the zero temperature CFT data for bilinear operators, that is the normalizations of the two-point functions and the OPE coefficients $f_{\phi\phi J}$.

4.2 Generalized free field theory

As a warm up, we first consider the case of a conformal generalized free field theory (GFFT), i.e. a massless Gaussian theory with a non-local inverse covariance, also known as mean field theory [79] or

[4] In the classical interpretation of Lifshitz points, "time" is actually one spatial direction of a spatially anisotropic classical system [149]. However, an interpretation as time has also appeared in the context of quantum Lifshitz points [151] or of Lorentz-violating quantum field theories [152].

[5] As a reminder, in the isotropic long-range model there is no anomalous dimension.

fractional Gaussian field [153]. It is worth discussing it in some detail because it is the simplest case of (non-local) CFT, and because typical long-range models can be defined as perturbations of a GFFT.

We begin by recalling some basic facts in the non-compact case, viewed as a classical statistical field theory at criticality, that is, the GFFT defined on $\mathbb{R}^d$, with Euclidean signature. By definition this is a CFT whose only non-vanishing connected n-point function is the two-point function, given by the covariance $C(x)$ of a Gaussian measure, which however has a non-canonical scaling exponent $\Delta_\phi > d/2 - 1$:

$$C(x) = \frac{c(\Delta_\phi)}{|x|^{2\Delta_\phi}} , \qquad c(\Delta_\phi) = \frac{\Gamma(\Delta_\phi)}{2^{d-2\Delta_\phi}\pi^{d/2}\Gamma(\frac{d}{2} - \Delta_\phi)} . \tag{4.2.1}$$

Writing $\Delta_\phi = d/2 - \zeta$, such GFFT can be obtained from a functional integral with the action:[6]

$$S_{\mathrm{GFFT}}[\phi] = \frac{1}{2}\int \mathrm{d}^d x\, \phi(x)(-\partial^2)^\zeta \phi(x) , \tag{4.2.2}$$

where $\partial^2 = \partial_\mu \partial^\mu$ is the Laplace operator. The fractional power of the Laplacian can be defined in many equivalent ways [90], and in particular as the inverse of the operator displayed in (4.2.1), which has a kernel of the same form, but with the replacement $\Delta_\phi \to d - \Delta_\phi$, leading to the kinetic term of (4.1.4).[7] The easiest definition is of course in Fourier space, where $(-\partial^2)^\zeta$ is defined as the multiplication operator $(p^2)^\zeta$, which is the inverse of the Fourier transform of (4.2.1) (the coefficient $c(\Delta_\phi)$ is chosen precisely to have a unit coefficient in momentum space, $\tilde{C}(p) = 1/(p^2)^\zeta$).

Since the theory is Gaussian, the scaling dimensions of local composite operators are simply given by $n_\phi \Delta_\phi + n_\partial$, where n_ϕ is the number of ϕ fields and n_∂ the number of derivatives. This is the same as in the local free field theory, but the operator content is slightly different in the two cases: in the GFFT case, objects like the energy-momentum tensor or the field equations are non-local, hence they do not appear in the algebra of local operators. As a consequence, we cannot use the Schwinger-Dyson equation:

$$\langle \frac{\delta S}{\delta \phi(x_0)} \phi(x_1) \cdots \phi(x_n) \rangle = \sum_{i=1}^{n} \delta(x_0 - x_i) \langle \prod_{j \neq i}^{1,\ldots,n} \phi(x_j) \rangle , \tag{4.2.3}$$

to conclude that insertions of $(-\partial^2)\phi$ in any n-point function (at separate points) vanish.[8]

Another consequence of Gaussianity is that in the OPE of two fundamental fields, $\phi \times \phi$, only bilinear operators in ϕ appear, that is, operators of the schematic form:

$$[\phi\phi]_{k,\mu_1\cdots\mu_J}(x) =: \phi(x)(\partial^2)^k \left(\partial_{\mu_1}\ldots\partial_{\mu_J} - \text{traces}\right)\phi(x) : , \tag{4.2.4}$$

where $J \in 2\mathbb{N}_0$, $k \in \mathbb{N}_0$, and the colon notation implies a renormalization of the composite operator (normal ordering in this case). These operators have dimension:

$$\Delta_{k,J} = 2\Delta_\phi + J + 2k . \tag{4.2.5}$$

[6] We typically assume $0 < \zeta < 1$. The restriction to $\zeta < 1$ is imposed to preserve reflection positivity (unitarity in Lorentzian signature), but also because $\zeta > 1$ would correspond to a strong short-range rather than long-range action, and moreover the operator with $\zeta = 1$ would in that case be a relevant perturbation. The restriction to $\zeta > 0$ is instead chosen to avoid a strong long-range action, with its associated unusual thermodynamic features [72].

[7] Notice that $c(d - \Delta_\phi) = c(d/2 + \zeta) < 0$ for $0 < \zeta < 1$, thus matching the minus sign in (4.1.4). Notice also that despite such minus sign, the GFFT action is positive definite, as best understood in momentum space: this is because the position space representation of the fractional Laplacian is singular and needs a subtraction, which is not written explicitly in (4.1.4) (see footnote 18 of [1]).

[8] In fact it is straightforward to check that they do not vanish: using the fact that the theory is Gaussian we reduce $\langle[\partial^2\phi](x_0)\phi(x_1)\cdots\phi(x_n)\rangle$ to products of two-point functions, and we observe that $\langle[\partial^2\phi](x_0)\phi(x_i)\rangle = \partial^2_{x_0}\langle\phi(x_0)\phi(x_i)\rangle \neq \delta(x_0 - x_i)$ for $\Delta_\phi \neq d/2 - 1$.

Introducing the twist $\tau_{k,J} = \Delta_{k,J} - J$, we see that the operators with $k = 0$ are the minimal-twist operators, also known as double-twist operators [154]. Once more, the appearance of the higher-twist operators, with $k > 0$, marks a difference with respect to the local free theory. Another way to see this difference is by using the conformal partial wave expansion [40, 155, 100, 156] of the four-point function. A conformal four-point function of identical scalars can be written as follows:

$$\begin{aligned}\langle\phi(x_1)\phi(x_2)\phi(x_3)\phi(x_4)\rangle =& \langle\phi(x_1)\phi(x_2)\rangle\langle\phi(x_3)\phi(x_4)\rangle + \\ &+ \sum_J \int_{\frac{d}{2}-\imath\infty}^{\frac{d}{2}+\imath\infty} \frac{dh}{2\pi i} \frac{1}{1-k(h,J)} \mu^d_{\Delta_\phi,J}(h,J)\, G^{\Delta_\phi}_{h,J}(x_i)\ ,\end{aligned} \tag{4.2.6}$$

where $G^{\Delta_\phi}_{h,J}(x_i)$ is the conformal block, $\mu^d_{\Delta_\phi,J}(h,J)$ is a known function[9] and $k(h,J)$ is the eigenvalue of the Bethe-Salpeter four-point kernel. In the case of a free theory, we have $k(h,J) = 0$ and one can close the contour of integration of h on the right of the complex plane and pick the poles of $\mu^d_{\Delta_\phi,J}(h,J)\, G^{\Delta_\phi}_{h,J}(x_i)$ on the right of $\frac{d}{2}$. The location of such poles are the scaling dimensions of bilinear primaries and the residues are their OPE coefficients with two ϕ. In [44] it is shown that for $\Delta_\phi > \Delta_{SR} = \frac{d-2}{2}$ the location of poles are at $h = \Delta_{k,J} = 2\Delta_\phi + J + 2k$, but in the limit $\Delta_\phi \to \Delta_{SR}$ all the residues with $k \geq 1$ go to zero, hence those poles disappear.

As written in (4.2.4), the bilinear operators are in a schematic form because we have not taken into account the primary constraint, ensuring that they transform appropriately under the full conformal group. In the short-range case the precise form of bilinear primaries has been extensively studied [40, 157, 158] and we review it in appendix 4.A. However, as we already emphasized above, in that case k is forced to be zero by the equation of motion. As a consequence, the operators with $k > 0$, relevant for the GFFT, have not been studied as much in the literature, and to the best of our knowledge their general form is not known, although a recurrence relation was derived in [159]. Below we give the explicit expressions for some primary operators with $k = 1$ and $k = 2$:

$$\begin{aligned}
\frac{[\phi\phi]_{1,0}(x)}{\mathcal{N}_{1,0}} =:& \phi\partial^2\phi(x): + \left(\frac{\Delta_{SR}}{\Delta_\phi} - 1\right) : \partial_\alpha\phi\partial_\alpha\phi(x) :\ , \\
\frac{[\phi\phi]_{2,0}(x)}{\mathcal{N}_{2,0}} =:& \phi\partial^2\partial^2\phi(x): + \left(4\frac{(\Delta_{SR} - \Delta_\phi - 1)}{\Delta_\phi}\right) : \partial_\alpha\phi\partial_\alpha\partial^2\phi(x) : \\
&+ \left(\frac{(\Delta_\phi - \Delta_{SR} + 1)\,(\Delta_\phi(\Delta_\phi + 4) + 2 - \Delta_{SR})}{\Delta_\phi(\Delta_\phi + 1)\,(\Delta_\phi - \Delta_{SR})}\right) : \partial^2\phi\partial^2\phi(x) : \\
&+ \left(\frac{2\,(\Delta_\phi - \Delta_{SR})\,(\Delta_\phi - \Delta_{SR} + 1)}{\Delta_\phi(\Delta_\phi + 1)}\right) : \partial_\alpha\partial_\beta\phi\partial_\alpha\partial_\beta\phi(x) :\ , \\
\frac{[\phi\phi]_{1,\mu_1\mu_2}(x)\xi^{\mu_1}\xi^{\mu_2}}{\mathcal{N}_{1,2}} =:& \phi\partial^2(\imath\xi\cdot\partial)^2\phi(x): + \left(\frac{(\Delta_\phi + 2)(\Delta_\phi + 3)}{\Delta_\phi(\Delta_\phi + 1)}\right) : \partial^2\phi(\imath\xi\cdot\partial)^2\phi(x) : \\
&+ \left(\frac{2\,(\Delta_{\rm SR} - \Delta_\phi)}{\Delta_\phi}\right) : \partial_\alpha\phi(\imath\xi\cdot\partial)^2\partial_\alpha\phi(x) : - \left(\frac{2(\Delta_\phi + 3)}{\Delta_\phi}\right) : \phi\partial^2(\imath\xi\cdot\partial)\phi(\imath\xi\cdot\partial)\phi(x) : \\
&+ \left(\frac{2(\Delta_\phi + 2)\,(\Delta_\phi - \Delta_{\rm SR})}{\Delta_\phi(\Delta_\phi + 1)}\right) : \partial_\alpha(\imath\xi\cdot\partial)\phi\partial_\alpha(\imath\xi\cdot\partial)\phi(x) :\ .
\end{aligned} \tag{4.2.7}$$

where we recall that $\Delta_{SR} = \frac{d-2}{2}$ is the scaling dimension of the field in the short-range case, ξ is a complex vector with $\xi^2 = 0$ and $\mathcal{N}_{k,J}$ is a normalization that we are free to fix at convenience.

We notice that for $\Delta_\phi = \Delta_{SR}$ only terms with at least one $\partial^2\phi$ survive, but, as explained above, such terms vanish in the short-range case due to the field equations. Also, we notice that the operators

[9] $\mu^d_{\Delta_J}(h,J)$ is the Plancherel weight $\rho(h,J)$ multiplied by the right normalization of three-point functions, necessary to make them an orthonormal basis of the appropriate space of bilocal functions.

with $k > 0$ do not coincide with the trace part subtracted in the spinning operators. For example, from the formulas of appendix 4.A we have:

$$\begin{aligned}\frac{[\phi\phi]_{0,\mu\nu}(x)}{\mathcal{N}_{0,2}} =& : \phi\partial_\mu\partial_\nu\phi(x) : -\frac{\Delta_\phi+1}{\Delta_\phi} : \partial_\mu\phi\partial_\nu\phi(x) : \\ &- \frac{\delta_{\mu\nu}}{d}\left(: \phi\partial^2\phi(x) : -\frac{\Delta_\phi+1}{\Delta_\phi} : \partial_\alpha\phi\partial_\alpha\phi(x) :\right) ,\end{aligned} \tag{4.2.8}$$

and we see that the trace part is a different linear combination than the one appearing in $[\phi\phi]_{1,0}(x)$.

4.2.1 Propagator on $S^1_L \times \mathbb{R}^{d-1}$

As anticipated in the introduction, we now place the model in a hyper-strip geometry with one compactified dimension of length L and periodic boundary conditions. The propagator in momentum space is just:

$$\tilde{C}_L(q_n, \mathbf{p}) = \frac{1}{(\mathbf{p}^2 + q_n^2)^\zeta} , \tag{4.2.9}$$

with $q_n = 2\pi n/L$, $n \in \mathbb{Z}$, and $\mathbf{p} \in \mathbb{R}^{d-1}$. The subscript L signifies that the covariance corresponds to a compactified strip geometry, and in the non-compact case we recover the GFFT covariance, $C_\infty \equiv C$. In order to Fourier transform back to direct space, we will introduce a fictitious integration in q via $1 = \int dq\, \delta(q - q_n)$ and use the Poisson summation formula for distributions:

$$\frac{1}{L}\sum_n \delta(q - q_n) = \frac{1}{2\pi}\sum_m e^{\imath L m q} . \tag{4.2.10}$$

Considering q as the first component of a d-dimensional continuous momentum $p = (q, \mathbf{p})$, we get:

$$C_L(y, \mathbf{x}) = \frac{1}{L}\sum_{n=-\infty}^{+\infty}\int \frac{d^{d-1}\mathbf{p}}{(2\pi)^{d-1}}\frac{e^{\imath\mathbf{p}\cdot\mathbf{x}+\imath q_n y}}{(\mathbf{p}^2+q_n^2)^\zeta} = \sum_{m=-\infty}^{+\infty}\int\frac{d^dp}{(2\pi)^d}\frac{e^{\imath p\cdot x_m}}{(p^2)^\zeta} , \tag{4.2.11}$$

where $y \in S^1_L$, $\mathbf{x} \in \mathbb{R}^{d-1}$, and $x_m = (y + mL, \mathbf{x})$. At this stage we could proceed by using a Schwinger parametrization for the denominator (as for example in [118]). However this does not generalize nicely to the massive case of the next section, hence we evaluate here the two-point function in position space by a different method.

We write the momentum space propagator as a Stieltjes transform (or Källén-Lehmann representation):

$$\frac{1}{(p^2)^\zeta} = \int_0^{+\infty} ds\, \frac{\rho(s)}{p^2+s} , \qquad \rho(s) = \frac{\sin(\pi\zeta)}{\pi}s^{-\zeta} . \tag{4.2.12}$$

The Fourier transform in (4.2.11) is then reduced to the standard one for the short-range massive scalar free propagator, and we thus obtain:

$$\begin{aligned} C_L(y,\mathbf{x}) &= \frac{\sin(\pi\zeta)}{(2\pi)^{d/2}\pi}\sum_{m=-\infty}^{+\infty}\int_0^{+\infty} ds\, s^{-\zeta}\left(\frac{\sqrt{s}}{|x_m|}\right)^{d/2-1} K_{\frac{d}{2}-1}(\sqrt{s}|x_m|) \\ &= \frac{\sin(\pi\zeta)}{(2\pi)^{d/2}\pi}\sum_{m=-\infty}^{+\infty}\frac{1}{|x_m|^{d-2\zeta}}\int_0^{+\infty} ds\, s^{-\zeta+d/4-1/2}\, K_{\frac{d}{2}-1}(\sqrt{s}) \\ &= \frac{\sin(\pi\zeta)\Gamma(1-\zeta)\Gamma(d/2-\zeta)}{2^{2\zeta}\pi^{d/2}\pi}\sum_{m=-\infty}^{+\infty}\frac{1}{|x_m|^{d-2\zeta}} \\ &= c(\Delta_\phi)\sum_{m=-\infty}^{+\infty}\frac{1}{|x_m|^{2\Delta_\phi}}\,, \end{aligned} \tag{4.2.13}$$

where $K_{\frac{d}{2}-1}(x)$ is the modified Bessel function of second kind. This might look like a useless exercise, as we knew already the result of the Fourier transform in (4.2.11), but its usefulness lies in highlighting a strategy that will be fruitful in the massive case.

4.2.2 One-point functions of the minimal-twist operators

We are now interested in computing the one-point function of bilinear primary operators introduced in (4.2.4). The most convenient way to deal with the tracelessness condition of higher-spin operators is by means of the index-free formalism of [40, 157]: define an operator $\mathcal{O}_{k,J}(x,\xi)$ by contracting each derivative with a complex null vector $\xi = (\chi, \boldsymbol{\xi})$ such that $\boldsymbol{\xi}^2 = -\chi^2$ (see appendix 4.A for more details). For now, we will consider $k = 0$.

When computing in momentum space the one-point function of the primary operator defined in (4.A.1) we just have to substitute $\overleftarrow{\partial} \to -\imath p$ and $\overrightarrow{\partial} \to \imath p$. As a result, only the $n = 0$ term in the sum (4.A.2) survives, the prefactor simplifies to one and we get:

$$\begin{aligned} \langle \mathcal{O}_{0,J}(x,\xi)\rangle &\equiv \xi^{\mu_1}\cdots\xi^{\mu_J}\langle [\phi_a\phi_a]_{0,\mu_1\cdots\mu_J}(x)\rangle \\ &= \frac{1}{L}\sum_{n=-\infty}^{+\infty}\int\frac{d^{d-1}\mathbf{p}}{(2\pi)^{d-1}}\frac{(\imath\mathbf{p}\cdot\boldsymbol{\xi}+\imath q_n\chi)^J}{(\mathbf{p}^2+q_n^2)^\zeta} - \int\frac{d^dp}{(2\pi)^d}\frac{(\imath p\cdot\xi)^J}{(p^2)^\zeta}\,, \end{aligned} \tag{4.2.14}$$

where the subtraction term comes from the normal ordering of the operator, as implemented before compactifying one direction, and an ultraviolet regularization is implicitly assumed. As written, it is not obvious that the normal ordering is sufficient in making the one-point function finite when we remove the regularization. In order to see that indeed it is finite, it is convenient to use the Poisson formula, and rewrite:

$$\begin{aligned} \langle \mathcal{O}_{0,J}(x,\xi)\rangle &= \sum_{m=-\infty}^{+\infty}\int\frac{d^dp}{(2\pi)^d}\frac{(\imath\mathbf{p}\cdot\boldsymbol{\xi}+\imath q\chi)^J\, e^{\imath Lmq}}{(\mathbf{p}^2+q^2)^\zeta} - \int\frac{d^dp}{(2\pi)^d}\frac{(\imath p\cdot\xi)^J}{(p^2)^\zeta} \\ &= \sum_{m\neq 0}\int\frac{d^dp}{(2\pi)^d}\frac{(\imath\mathbf{p}\cdot\boldsymbol{\xi}+\imath q\chi)^J\, e^{\imath Lmq}}{(\mathbf{p}^2+q^2)^\zeta}\,. \end{aligned} \tag{4.2.15}$$

The oscillating factor renders each term in the sum finite (as can be shown by deforming the contour of integration of q in the complex plane), and the normal ordering removes the only term without oscillating factor. Actually, the subtracted term vanishes for $J > 0$ in any regularization preserving rotation invariance, such as a cutoff on p^2 (via the insertion in the integrand of a cutoff function

$f(p^2/\Lambda^2)$ decaying sufficiently fast at infinity): by symmetry reasons the resulting integral over p must be proportional to a linear combination of products of $J/2$ Kronecker delta functions, which vanish when contracted with the null vector ξ. The $m \neq 0$ terms are instead not rotation invariant, due to the phase factor depending only on one momentum component, and thus are non-vanishing.

Following an idea from [148], we define a generating function for these expectations:

$$\sum_{J\geq 0} \frac{\langle \mathcal{O}_{0,J}(x,\xi)\rangle}{J!} = \sum_{m\neq 0} \int \frac{d^d p}{(2\pi)^d} \frac{e^{ip\cdot\xi_m}}{(p^2)^\zeta} \equiv C^{(0)}(\xi) \ , \tag{4.2.16}$$

where $\xi_m = (\chi + mL, \boldsymbol{\xi})$. We recognize that such a generating function is the two-point function, with the $m = 0$ term subtracted, and evaluated at the null vector ξ, $C^{(0)}(\xi) = C_L(\xi) - C(\xi)$. Therefore, it is enough to use our previous results, evaluated at $x = \xi$ and read off the coefficients of the one-point function from the expansion in powers of χ.

Note that the general OPE formula for the two-point function in (4.1.10), when evaluated at a null ξ (and subtracting the divergent contribution from the identity operator, $\Delta_\mathcal{O} = J = 0$), becomes:

$$C^{(0)}(\xi) = \sum_{J\in 2\mathbb{N}_0} \frac{1}{L^{2\Delta_\phi + J}} \frac{b^{(\text{free})}_{0,J} f_{\phi\phi J}}{c_{0,J}} \chi^J \ . \tag{4.2.17}$$

On the other hand, using the general formula (4.1.6), and contracting with our null vector ξ, we find:

$$\langle \mathcal{O}_{0,J}(x,\xi)\rangle = \frac{b^{(\text{free})}_{0,J}}{L^{2\Delta_\phi + J}} \chi^J \ . \tag{4.2.18}$$

Therefore, by comparison to (4.2.16), in our conventions it must be $f_{\phi\phi J}/c_{0,J} = 1/J!$. In appendix 4.A we prove that this is indeed the case.

After subtracting the divergent $m = 0$ term (corresponding to the contribution from the identity operator) from (4.2.13), and replacing $x \to \xi$, we have:

$$C^{(0)}(\xi) = c(\Delta_\phi) \sum_{m\neq 0} \frac{1}{|Lm|^{2\Delta_\phi} (1 + \frac{2\chi}{mL})^{\Delta_\phi}} \ . \tag{4.2.19}$$

Expanding in χ, and combining the terms with $m > 0$ and $m < 0$, the odd powers of χ cancel while the even ones reconstitute a Riemann zeta function, which we denote ζ_R, to avoid confusion with our long-range parameter:

$$C^{(0)}(\xi) = c(\Delta_\phi) \sum_{J\in 2\mathbb{N}_0} \frac{\chi^J}{L^{J+2\Delta_\phi}} \frac{\Gamma(J+\Delta_\phi)}{J!\Gamma(\Delta_\phi)} 2^{J+1} \zeta_R(J + 2\Delta_\phi) \ . \tag{4.2.20}$$

From such expansion we can extract the one-point function coefficients:

$$b^{(\text{free})}_{0,J} = c(\Delta_\phi) \frac{\Gamma(J+\Delta_\phi)}{\Gamma(\Delta_\phi)} 2^{J+1} \zeta_R(J + 2\Delta_\phi) \ . \tag{4.2.21}$$

Lastly, using the relation $f_{\phi\phi J}/c_{0,J} = 1/J!$ we find:

$$a^{(\text{free})}_{0,J} \equiv \frac{J!\Gamma(\Delta_{SR})}{2^J \Gamma(\Delta_{SR} + J)} \frac{b^{(\text{free})}_{0,J} f_{\phi\phi J}}{c_{0,J}} = c(\Delta_\phi) \frac{2\Gamma(\Delta_\phi + J)\Gamma(\Delta_{SR})}{\Gamma(\Delta_\phi)\Gamma(\Delta_{SR} + J)} \zeta_R(J + 2\Delta_\phi) \ , \tag{4.2.22}$$

which matches with the result in [145], up to the different normalization of the two-point function $c(\Delta_\phi)$.

4.2.3 One-point functions of higher-twist operators

As we already discussed, in the case of long-range models the OPE of $\phi \times \phi$ contains also higher-twist operators, of the form (4.2.4) with $k > 0$. As we do not have a general formula for the primaries with $k > 0$, we cannot explicitly compute their two-point functions, and the associated coefficient, or their OPE coefficient. However, the precise distribution of derivatives is irrelevant for the tadpole computation, as the derivatives acting on the left and right field ϕ in Fourier space both reduce to (plus or minus) the same loop momentum. Therefore, we can implicitly define the normalization to be the one such that the one-point function reduces to:[10]

$$\begin{aligned}\langle \mathcal{O}_{k,J}(x,\xi)\rangle =& \frac{1}{L}\sum_{n=-\infty}^{+\infty}\int \frac{d^{d-1}\mathbf{p}}{(2\pi)^{d-1}}\frac{(\imath \mathbf{p}\cdot\boldsymbol{\xi}+\imath q_n\chi)^J}{(\mathbf{p}^2+q_n^2)^\zeta}(\mathbf{p}^2+q_n^2)^k \\ &-\int \frac{d^dp}{(2\pi)^d}\frac{(\imath x\cdot\xi)^J}{(p^2)^\zeta}(p^2)^k\,,\end{aligned} \tag{4.2.23}$$

which is finite, by the same argument used for $k = 0$, and again the subtraction is really needed only for $J = 0$. As before, we will aim at a generating function for the corresponding coefficient $a_{k,J}$, defined as in (4.1.10), which is independent of the normalization of $\mathcal{O}_{k,J}$.

We begin by defining a generating function of such one-point functions. That is, after using again the Poisson formula, we write:

$$\begin{aligned}C^{(k)}(\chi,\boldsymbol{\xi}) \equiv& \sum_{J\geq 0}\frac{\langle \mathcal{O}_{k,J}(x,\xi)\rangle}{J!} = \sum_{m\neq 0}\int \frac{d^dp}{(2\pi)^d}\frac{e^{\imath p\cdot\xi_m}}{(p^2)^\zeta}(p^2)^k \\ =& (-\partial^2)^k C^{(0)}(x)_{|_{x=(\chi,\boldsymbol{\xi})}}\,,\end{aligned} \tag{4.2.24}$$

which unsurprisingly is the result of applying k Laplacians to the (subtracted) covariance and evaluating it at $x = \xi$. Then we can find an alternative representation of $C^{(k)}(\chi,\boldsymbol{\xi})$ just by acting with k Laplacians on (4.1.8) and evaluating at $x = \xi$, we find:

$$C^{(k)}(\chi,\boldsymbol{\xi}) = (-1)^k \sum_{J\in 2\mathbb{N}_0}\frac{\chi^J}{J!}\frac{a_{k,J}}{L^{2\Delta_\phi+2k+J}}\frac{2^{J+2k}k!\Gamma(k+J+\Delta_{SR}+1)}{(J+\Delta_{SR})\Gamma(\Delta_{SR})}\,. \tag{4.2.25}$$

On the other hand, from the Fourier representation in (4.2.24) it is clear that $C^{(k)}(\chi,\boldsymbol{\xi})$ corresponds to the replacement $\zeta \to \zeta - k$ (i.e. $\Delta_\phi \to \Delta_\phi + k$) in the subtracted covariance $C^{(0)}(\chi,\boldsymbol{\xi})$, and thus we obtain:

$$C^{(k)}(\chi,\boldsymbol{\xi}) = c(\Delta_\phi+k)\sum_{m\neq 0}\frac{1}{|\xi_m|^{2\Delta_\phi+2k}}\,, \tag{4.2.26}$$

which, after repeating the same steps as before, becomes:

$$C^{(k)}(\chi,\boldsymbol{\xi}) = c(\Delta_\phi+k)\sum_{J\in 2\mathbb{N}_0}\frac{\chi^J}{L^{J+2k+2\Delta_\phi}}\frac{\Gamma(J+\Delta_\phi+k)}{J!\Gamma(\Delta_\phi+k)}2^{J+1}\zeta_R(J+2\Delta_\phi+2k)\,. \tag{4.2.27}$$

[10] In the cases of the operators that we wrote in (4.2.7), the explicit normalizations are

$$\mathcal{N}_{1,0} = \frac{\Delta_\phi}{\Delta_{SR}}\,,\quad \mathcal{N}_{2,0} = \frac{\Delta_\phi(\Delta_\phi+1)(\Delta_\phi-\Delta_{SR})}{2\Delta_\phi(\Delta_{SR}^2+\Delta_{SR}+1)-\Delta_{SR}^2(2\Delta_{SR}+1)+\Delta_{SR}+2}\,,\quad \mathcal{N}_{1,2} = -\frac{\Delta_\phi(\Delta_\phi+1)}{2\Delta_{SR}}\,.$$

Lastly, by comparison with (4.2.25), we extract the $a_{k,J}$ coefficients:

$$a_{k,J} = c(\Delta_\phi)\frac{2(J+\Delta_{SR})\Gamma(\Delta_{SR})\Gamma(\Delta_\phi+J+k)\Gamma(\Delta_\phi-\Delta_{SR}+k)}{k!\Gamma(\Delta_\phi)\Gamma(\Delta_{SR}+J+k+1)\Gamma(\Delta_\phi-\Delta_{SR})}\zeta_R(J+2k+2\Delta_\phi)\,, \tag{4.2.28}$$

that again match with the result in [145] up to the $c(\Delta_\phi)$ factor.

4.3 Classical long-range $O(N)$ model with a finite size

The long-range $O(N)$ model is defined by the action:

$$S[\phi] = \int_{\mathbb{R}^d} d^dx \left(\frac{1}{2}\phi_a(x)(-\partial^2)^\zeta\phi_a(x) + \frac{1}{2}M^{2\zeta}_{\text{bare}}\phi^2(x) + \frac{\lambda}{4N}(\phi^2(x))^2\right)\,, \tag{4.3.1}$$

where $a = 1,\dots,N$, $\phi^2(x) \equiv \sum_a \phi_a(x)^2$, and M_{bare} is the bare mass, which we treat as a pure counterterm because we are interested in the critical theory. It is convenient to introduce also the intermediate field representation, by the usual Hubbard-Stratonovich transformation:

$$S[\phi,\sigma] = \int d^dx \left(\frac{1}{2}\phi_a(x)(-\partial^2)^\zeta\phi_a(x) + \frac{1}{2}M^{2\zeta}_{\text{bare}}\phi^2(x) + N\frac{\sigma(x)^2}{4\lambda} + \frac{\imath}{2}\sigma(x)\phi^2(x)\right)\,. \tag{4.3.2}$$

For any $\zeta \in (d/4, 1)$ one finds a non-trivial IR fixed point, most easily accessible in the large-N expansion, or in the small-ϵ expansion where $\zeta = (d+\epsilon)/4$ [120]. Characteristic features of such fixed point are the absence of anomalous dimension (that is, the two-point function scales as in the corresponding GFFT, as proved rigorously in [129]), and ζ-dependent critical exponents. Such ζ-dependent fixed points are then associated to a one-parameter family of universality classes, collectively called *long-range universality class*. An interesting crossover phenomenon actually occurs before reaching $\zeta = 1$: there exists a $\zeta^\star \in (d/4, 1)$ such that for $\zeta > \zeta^\star$ the operator $\phi_a\partial^2\phi_a$ (i.e. the local kinetic term) becomes relevant at the IR fixed point, thus destabilizing it and driving the system to the short-range universality class [123]. The value of such crossover exponent for $2 \le d < 4$ is $\zeta^\star = 1 - \eta_{SR}/2$, where η_{SR} is the anomalous dimension of the short-range model.[11] However, since $\eta_{SR} = O(1/N)$ [7], at large N there is no crossover, and our analysis will apply all the way to $\zeta = 1$.

In the large-N limit, the propagator only receives mass corrections, via tadpoles, and we thus have the following Schwinger-Dyson equation:

$$\tilde{G}(p)^{-1} = \tilde{C}(p)^{-1} + M^{2\zeta}_{\text{bare}} + \frac{\lambda}{2}\int\frac{d^dp'}{(2\pi)^d}\tilde{G}(p')\,, \tag{4.3.3}$$

where $\tilde{C}(p)$ is as in the GFFT, and we defined $\langle\phi_a(x)\phi_a(0)\rangle = \delta_{ab}G(x)$ and $\tilde{G}(p)$ the Fourier transform of $G(x)$. Since the tadpole is momentum-independent, the solution must be of the form $\tilde{G}(p)^{-1} = \tilde{C}(p)^{-1} + M^{2\zeta}$. Tuning the model to criticality requires choosing a bare mass M_{bare} such that $M = 0$, which amounts to canceling the tadpole contribution, hence we have:

$$M^{2\zeta}_{\text{bare}} = -\frac{\lambda}{2}\int\frac{d^dp}{(2\pi)^d}\frac{1}{(p^2)^\zeta} \equiv -\frac{\lambda}{2}\mathcal{T}\,. \tag{4.3.4}$$

In the same limit, the connected four-point function is given by a sum of chains of bubble diagrams, with full leading-order propagator on each edge, see Fig. 4.1.

[11] For $d = 1$ the upper limit is $\zeta^\star = 1/2$, beyond which there can be no spontaneous symmetry breaking [119].

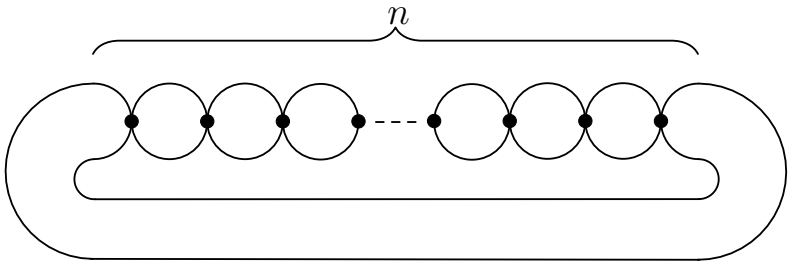

FIGURE 4.1: Chain of bubbles with $n \geq 1$ vertices. The connected four-point function is given by the sum of all such chains.

Therefore, the proper vertex in momentum space reads:

$$\Gamma^{(4)}(p) = \frac{2\lambda}{1+\lambda B(p)} , \tag{4.3.5}$$

where p is the total transferred momentum and we defined the bubble integral:

$$B(p) = \int \frac{d^d q}{(2\pi)^d} \frac{1}{q^{2\zeta}(p-q)^{2\zeta}} = \frac{c(d/2-\zeta)^2}{c(d-2\zeta)} |p|^{d-4\zeta} . \tag{4.3.6}$$

We define the renormalized dimensionless coupling g at some renormalization group scale $|p| = \mu$:

$$g = \mu^{4\Delta_\phi - d} \Gamma^{(4)}(\mu)/2 . \tag{4.3.7}$$

It follows that the beta function is:[12]

$$\beta(g) = \mu \frac{dg}{d\mu} = -(d-4\Delta_\phi)g + \frac{c(\Delta_\phi)^2}{c(2\Delta_\phi)}(d-4\Delta_\phi)g^2 . \tag{4.3.8}$$

Therefore, for $\Delta_\phi < d/4$ (i.e. $\zeta > d/4$) the beta function has a zero (i.e. a fixed point) at $g^\star = c(2\Delta_\phi)/c(\Delta_\phi)^2$. It is worth noticing that since we can trivially invert the relation between bare and renormalized coupling to get:

$$\mu^{4\Delta_\phi - d}\lambda = \frac{g}{1 - \frac{c(\Delta_\phi)^2}{c(2\Delta_\phi)} g} , \tag{4.3.9}$$

the fixed point corresponds to the limit $\lambda \to \infty$.

Another well known large-N result for the short-range $O(N)$ model, which generalizes straightforwardly to the long-range case, is the fact that at the IR fixed point the composite operator $\phi^2(x)$ (of dimension $\Delta_{0,0} = 2\Delta_\phi = d - 2\zeta$ in the GFFT) is mapped to its shadow operator (of dimension $\Delta_\sigma = d - \Delta_{0,0} = 2\zeta$), which can be identified with the intermediate field $\sigma(x)$. This is a particular realization of the general result by Gubser and Klebanov [81] on large-N flows driven by a double-trace operator (in this case, the $(\phi^2)^2$ interaction). There are many other ways to see the same result, for example by means of the conformal partial wave representation of the four-point function [1], or diagrammatically, as we will see below.

The other bilinear primaries (4.2.4) remain instead in the spectrum. In addition, in the interacting model we also have other operators, with more powers of σ or ϕ. Naively, at large N such operators are suppressed in the OPE of $\phi \times \phi$. However, the situation is more subtle: as argued in [145], in the expansion (4.1.10) it can happen that for certain $\mathcal{O}$'s while $f_{\phi\phi\mathcal{O}}/\sqrt{c_\mathcal{O}}$ is suppressed, $b_\mathcal{O}/\sqrt{c_\mathcal{O}}$ is

[12] Notice that for $d - 4\Delta_\phi = 4\zeta - d = \epsilon$ (i.e. for $\zeta = (d+\epsilon)/4$) the second term is finite (and positive) in the limit $\epsilon \to 0$, because $c(2\Delta_\phi) \sim 1/\Gamma(\epsilon/2)$, and we recover the standard one-loop result $\beta(g) = -\epsilon g + 2g^2/((4\pi)^{d/2}\Gamma(d/2))$ (see [118]).

boosted, thus resulting in a finite contribution to $a_{\mathcal{O}}$ even at large N. This in fact does happen for the operators $\sigma^n(x)$ which yield non-trivial contributions to the OPE, as we will discuss in 4.3.5.

Two-point functions of spinning operators. When evaluating at leading order in $1/N$ the two-point functions of bilinear operators of the $O(N)$ model, we need to sum chains of bubble diagrams, as for the four-point function. We now show that for the spinning operators at the fixed point the sum over the chain of bubbles reduces to the contribution of a single bubble, and thus their two-point functions (and hence scaling dimensions) are the same as in the GFFT.

First, we check once again that the ϕ^2 operator drops out of the CFT. The sum of bubbles becomes a simple geometric sum in Fourier space, hence we have:

$$\langle [\phi_a\phi_a]_0(x_1)[\phi_a\phi_a]_0(x_2)\rangle = \int \frac{d^dp}{(2\pi)^d} e^{ip\cdot x_{12}} \frac{B(p)}{1+\lambda B(p)} \,. \tag{4.3.10}$$

For $\lambda \to \infty$ the result vanishes as expected. The two-point function of $\sigma(x)$ is similar, but with the replacement $B(p) \to \lambda$ in the numerator (it coincides with the $\Gamma^{(4)}(p)$ above), hence it remains finite in the limit. We infer that ϕ^2 is replaced by its shadow operator σ at the interacting fixed point.

For higher-spin operators we have instead to distinguish the first and last bubbles:

$$\begin{aligned}\langle [\phi_a\phi_a]_{0,\mu_1\cdots\mu_J}(x_1)[\phi_a\phi_a]_{0,\nu_1\cdots\nu_J}(x_2)\rangle = \int \frac{d^dp}{(2\pi)^d} e^{ip\cdot x_{12}} \Big(&B_{\mu_1\cdots\mu_J,\nu_1\cdots\nu_J} \\ &- B_{\mu_1\cdots\mu_J} \frac{\lambda}{1+\lambda B(p)} B_{\nu_1\cdots\nu_J}\Big) \,,\end{aligned} \tag{4.3.11}$$

where $B_{\mu_1\cdots\mu_J,\nu_1\cdots\nu_J}$ is the Fourier transform of the same two-point function in the free theory, i.e. the diagram without internal vertices, while $B_{\mu_1\cdots\mu_J}$ is the Fourier transform of the two-point function of the spin-J operator with the spin-0 one, also in the free theory. However, the latter vanishes: technically because of orthogonality of the Gegenbauer polynomials [157], and conceptually because in a CFT the two-point functions of primaries of different dimensions must vanish.

The explicit computation of these two-point functions is reported in appendix 4.A.

4.3.1 Schwinger-Dyson equation in the hyper-strip geometry

We now place the model in a hyper-strip geometry with one finite dimension of length L and periodic boundary conditions. The action is as in (4.3.1) with the replacement $\mathbb{R}^d \to S^1_L \times \mathbb{R}^{d-1}$. Such setting has been extensively studied in the short-range case, and in particular in the large-N limit (e.g. [43, 160, 143, 144, 145, 146, 148]).

Like in the short-range model, also in the long-range case the propagator will acquire a mass due to the introduction of the compact direction, as we now show by reducing the Schwinger-Dyson equation to a mass gap equation.

At large N, the Schwinger-Dyson equation in momentum space is:

$$\tilde{G}(q_{n_0},\mathbf{p}_0)^{-1} = \tilde{C}_L(q_{n_0},\mathbf{p}_0)^{-1} + M^{2\zeta}_{\text{bare}} + \frac{\lambda}{2}\frac{1}{L}\sum_n \int \frac{d^{d-1}\mathbf{p}}{(2\pi)^{d-1}} \tilde{G}(q_n,\mathbf{p}) \,. \tag{4.3.12}$$

The inverse free propagator is $\tilde{C}_L(q_n,\mathbf{p})^{-1} = (\mathbf{p}^2+q_n^2)^\zeta$ as in the GFFT, $M^{2\zeta}_{\text{bare}}$ is the bare mass (4.3.4), and $q_n = 2\pi n/L$, as before. As the tadpole term in (4.3.12) does not depend on the external momentum, the full inverse two-point function is $\tilde{G}(q_n,\mathbf{p}_0)^{-1} = (\mathbf{p}_0^2+q_n^2)^\zeta + M_L^{2\zeta}$ for some M_L to be determined self-consistently.

The self-consistent gap equation for the finite-size mass is:

$$\begin{aligned} M_L^{2\zeta} &= M_{\text{bare}}^{2\zeta} + \frac{\lambda}{2}\frac{1}{L}\sum_n \int \frac{d^{d-1}\mathbf{p}}{(2\pi)^{d-1}} \frac{1}{(\mathbf{p}^2+q_n^2)^\zeta + M_L^{2\zeta}} \\ &= \frac{\lambda}{2}\left(-M_L^{2\zeta}\int \frac{d^dp}{(2\pi)^d}\frac{1}{((p^2)^\zeta + M_L^{2\zeta})(p^2)^\zeta} + \sum_{m\neq 0}\int \frac{d^dp}{(2\pi)^d}\frac{e^{\imath Lmq}}{(p^2)^\zeta + M_L^{2\zeta}}\right) \\ &\equiv \frac{\lambda}{2}\left(\mathcal{T}(M_L) - \mathcal{T}\right) , \end{aligned} \tag{4.3.13}$$

where in the second equality we used the Poisson summation formula (4.2.10), we have introduced again a d-dimensional momentum $p = (q, \mathbf{p})$, and we have combined the $m = 0$ term with the explicit expression of the bare mass. In the last step we have defined the subtracted tadpole $\mathcal{T}(M_L) - \mathcal{T}$.

The first integral in the subtracted tadpole can be computed explicitly and we find:

$$\mathcal{T}(M_L) - \mathcal{T} = \frac{\pi M_L^{d-2\zeta}}{(4\pi)^{d/2}\Gamma(d/2)\zeta \sin\left(\frac{d\pi}{2\zeta}\right)} + \sum_{m\neq 0}\int \frac{d^dp}{(2\pi)^d}\frac{e^{\imath Lmq}}{(p^2)^\zeta + M_L^{2\zeta}} . \tag{4.3.14}$$

The second term is not manifestly UV convergent, but its convergence can be inferred from the convergence of the $M_L = 0$ case of the previous section (see (4.2.13) without the $m = 0$ term, evaluated at $x_m = (Lm, \mathbf{0})$, giving $b_{0,0}^{(\text{free})}$), as the inclusion of the mass does not make the UV behavior worse.[13] Its explicit evaluation is however rather complicated, and we will take a different route to the gap equation below.

As we recalled above, at the IR fixed point the bare coupling λ flows to infinity, hence the mass gap equation corresponds to finding the value of M_L such that the subtracted tadpole (4.3.14) vanishes. We emphasize that the subtraction is essential to the existence of a solution, as otherwise the tadpole would seem positive, which of course is naive as it is in fact divergent: for $d/4 < \zeta < 1$ and $2 < d < 4$ (and for $1/4 < \zeta < \zeta^\star = 1/2$ if $d = 1$) the sine in the first term is negative, and thus a cancellation between the two terms can occur.

We will come back to this equation below, from a different perspective, and prove that it admits a solution.

4.3.2 Long-range two-point function with mass

The two-point function in direct space reads:

$$G(y, \mathbf{x}) = \frac{1}{L}\sum_{n=-\infty}^{+\infty}\int \frac{d^{d-1}\mathbf{p}}{(2\pi)^{d-1}}\frac{e^{\imath \mathbf{p}\cdot\mathbf{x} + \imath y q_n}}{(\mathbf{p}^2+q_n^2)^\zeta + M_L^{2\zeta}} . \tag{4.3.15}$$

As before, we introduce $1 = \int dq\delta(q - q_n)$ and we use the Poisson summation formula to rewrite it as:

$$G(y, \mathbf{x}) = \sum_{m=-\infty}^{+\infty}\int \frac{d^dp}{(2\pi)^d}\frac{e^{\imath p\cdot x_m}}{(p^2)^\zeta + M_L^{2\zeta}} , \tag{4.3.16}$$

where p is a d-dimensional momentum and $x_m = (y + mL, \mathbf{x})$.

In order to proceed further, we rewrite again the momentum-space propagator $\tilde{G}(p) = \left((p^2)^\zeta + M_L^{2\zeta}\right)^{-1}$ as a Stieltjes transform. While such a rewriting was trivial in the massless case because the spectral

[13] We can also explicitly show its convergence deforming the contour of integration of q to a Hankel contour in the upper (lower) complex plane for positive (negative) m.

density had to be scaling invariant, it is slightly more involved in the presence of a mass. First, as the momentum-space propagator is only a function of the squared momentum, we can define $g(p^2) = \tilde{G}(p)$, and we use Cauchy's theorem to write:

$$g(p^2) = \frac{1}{2\pi\imath} \oint_\gamma \frac{g(z)}{z - p^2} dz \,, \tag{4.3.17}$$

with γ a counterclockwise contour encircling $z = p^2$. Then, we deform the contour to infinity, and in the process we pick up poles and branch cuts of $g(z)$. Now, for $\zeta \in (0,1)$, the function $g(z) = 1/(z^\zeta + M_L^{2\zeta})$ has a branch cut on the negative axis, and no poles in the principal sheet.[14] Therefore, the deformation of the contour γ leads to a Hankel contour around the cut, which in turn leads to the standard formula for the inversion of the Stieltjes transform $\rho(s) = \frac{1}{2\pi\imath}\left(g(-s - \imath\epsilon) - g(-s + \imath\epsilon)\right)$, and we find:

$$\begin{aligned} \tilde{G}(p) &= \frac{1}{(p^2)^\zeta + M_L^{2\zeta}} = \int_0^{+\infty} ds\, \frac{\rho(s)}{p^2 + s} \,, \\ \rho(s) &= \frac{\sin(\pi\zeta)}{\pi} \frac{s^\zeta}{s^{2\zeta} + 2M_L^{2\zeta} s^\zeta \cos(\pi\zeta) + M_L^{4\zeta}} \,. \end{aligned} \tag{4.3.18}$$

Going back to position space, and setting $s = t^2$, we have:

$$G(y, \mathbf{x}) = \frac{2\sin(\pi\zeta)}{(2\pi)^{d/2}\pi} \sum_{m=-\infty}^{+\infty} \int_0^{+\infty} dt \, \left(\frac{t}{|x_m|}\right)^{d/2-1} \frac{K_{\frac{d}{2}-1}(t|x_m|) t^{1+2\zeta}}{t^{4\zeta} + 2M_L^{2\zeta} t^{2\zeta} \cos(\pi\zeta) + M_L^{4\zeta}} \,. \tag{4.3.19}$$

Because of the mass, in this case we cannot factor out of the integral the x-dependence.

At this step one might worry that for $\zeta \to 1$ everything vanishes because of the $\sin(\pi\zeta)$ factor. This is not the case because in this limit the denominator in the integrand becomes $(t^2 - M_L^2)^2$ and the integral develops a singularity (this is the analogue of the $\Gamma(1-\zeta)$ factor in the massless case of (4.2.13)). In fact in the $\zeta \to 1$ limit we recover the short-range case (4.2.13), as it can be shown by using a variation of the Plemelj–Sokhotski formula.

For later reference we write explicitly the case $d = 3$, in which the Bessel function takes a simple form:

$$G(y, x) = \frac{\sin(\pi\zeta)}{2\pi^2} \sum_{m=-\infty}^{+\infty} \int_0^{+\infty} dt \, \frac{e^{-t|x_m|}}{|x_m|} \frac{t^{1+2\zeta}}{t^{4\zeta} + 2M_L^{2\zeta} t^{2\zeta} \cos(\pi\zeta) + M_L^{4\zeta}} \,. \tag{4.3.20}$$

4.3.3 Finite-size mass solution

The $m \neq 0$ part of the subtracted tadpole (4.3.14) is the $m \neq 0$ part of the two-point function, evaluated at $x = 0$. Therefore, we can use the representation (4.3.20) to rewrite the mass gap equation in $d = 3$ as:

$$\frac{LM_L}{4\pi\zeta \sin\left(\frac{3\pi}{2\zeta}\right)} - \frac{\sin(\pi\zeta)}{\pi^2} \int_0^{+\infty} dt \, \frac{t^{2\zeta+1}}{t^{4\zeta} + 2\cos(\pi\zeta) t^{2\zeta} + 1} \ln\left(1 - e^{-LM_L t}\right) = 0 \,, \tag{4.3.21}$$

which is more suitable for a numerical evaluation, having eliminated the sum in favor of a single integral that is manifestly convergent. We find that the equation always admits a real positive solution, which we plot as a function of ζ in Fig. 4.2. The solution goes to zero at $\zeta = 3/4$, where the IR fixed point merges with the Gaussian one, and it goes to the short-range value (e.g. [160]) for $\zeta \to 1$.

[14] The poles are at $z = M_L^2 e^{\frac{\imath\pi(1+2k)}{\zeta}}$, for integer k, and it can be seen that for $0 < \zeta < 1$ none of them is in the principal sheet, which by definition corresponds to $\mathrm{Arg}(z) \in (-\pi, \pi)$.

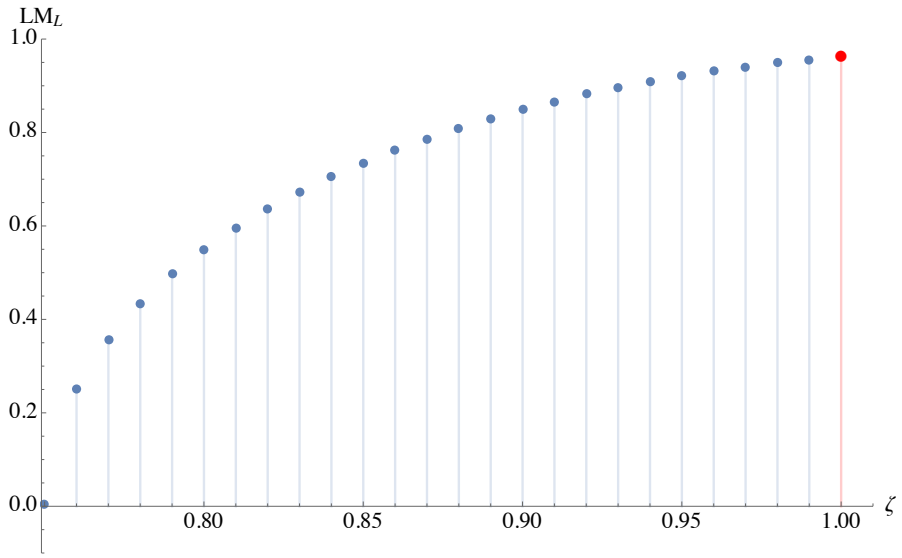

FIGURE 4.2: Numerical solutions for the mass gap equation as a function of ζ, at $d = 3$. The red dot is the value of the short-range thermal mass and it is approached in the $\zeta \to 1$ limit as expected.

4.3.4 One-point functions of the minimal-twist operators

The one-point functions of the minimal-twist operators in the hyper-strip geometry are defined similarly to the GFFT case, except for the presence of the mass and the restriction to $J > 0$, as the ϕ^2 operator is not in the spectrum:

$$\langle \mathcal{O}_{0,J}(x,\xi)\rangle = \sum_{m\neq 0}\int \frac{d^dp}{(2\pi)^d}\frac{(\imath \mathbf{p}\cdot\boldsymbol{\xi}+\imath q\chi)^J\, e^{\imath Lmq}}{(\mathbf{p}^2+q^2)^\zeta + M_L^{2\zeta}}\,. \tag{4.3.22}$$

Notice that the restriction to $m \neq 0$ comes from the fact that the $m = 0$ term vanishes in any rotationally invariant regularization, due to the contraction with ξ, and as before the other terms do not need any subtraction.

As in the previous section, following [148], we can evaluate the subtracted two-point function at a null vector $\xi = (\chi, \boldsymbol{\xi})$ and interpret it as the generating function of the one-point functions:

$$\begin{aligned} G^{(0)}(\chi,\boldsymbol{\xi}) = \sum_{J>0}\frac{\langle \mathcal{O}_{0,J}(x,\xi)\rangle}{J!} &= \sum_{m\neq 0}\int \frac{d^dp}{(2\pi)^d}\frac{e^{\imath p\cdot\xi_m}}{(p^2)^\zeta + M_L^{2\zeta}} \\ &\quad - M_L^{2\zeta}\int\frac{d^dp}{(2\pi)^d}\frac{1}{((p^2)^\zeta+M_L^{2\zeta})(p^2)^\zeta}\,. \end{aligned} \tag{4.3.23}$$

Notice that in order to get an exponential in the last step we had to include a spurious $J = 0$ term, which however we cancel with the last term, thanks to the mass gap equation imposing the vanishing of the subtracted tadpole (4.3.14).

An alternative explanation for the $J = 0$ subtraction in (4.3.23) is obtained by considering the general expansion of the two-point function in (4.1.10). As we know, at large N the spectrum of the $\phi \times \phi$ OPE contains the identity operator (with $\Delta_{\text{id}} = 0$), the intermediate field (with $\Delta_\sigma = 2\zeta$), and the bilinear operators with $\Delta_{k,J} = 2\Delta_\phi + J + 2k$, the $J = k = 0$ operator being excluded.[15] When

[15] As discussed earlier in the text (and originally pointed out in [145]), one-point functions can have a positive scaling in N that boosts operators whose OPE is suppressed in $1/N$, thus introducing new operators in (4.1.10) even at large

setting $x = \xi$, since $|\xi| = 0$ and the Gegenbauer polynomial is of order J, all the bilinear operators with $k > 0$ drop from the expansion, and so does also σ, since $2\zeta > 2\Delta_\phi$ for $\zeta > d/4$. Therefore, we should find only the $\Delta_{0,J>0}$ contributions plus a divergent one from the identity operator. The latter corresponds to the massless propagator in the non-compact case, but the $m = 0$ term we have removed in the first term of (4.3.23) is the massive propagator. In order to get the right operator content of (4.1.10), we should thus add back this massive propagator, and then subtract the massless one, which is precisely what the last term in (4.3.23) does, since:

$$\int \frac{d^d p}{(2\pi)^d} \frac{e^{\imath p\cdot x}}{((p^2)^\zeta + M_L^{2\zeta}} - \int \frac{d^d p}{(2\pi)^d} \frac{e^{\imath p\cdot x}}{(p^2)^\zeta} = -M_L^{2\zeta} \int \frac{d^d p}{(2\pi)^d} \frac{e^{\imath p\cdot x}}{((p^2)^\zeta + M_L^{2\zeta})(p^2)^\zeta} , \tag{4.3.24}$$

is a function of $|x|$, convergent at $|x| = 0$, and thus its value at $x = \xi$ is the same as at $x = 0$.

Subsequently we can extract the $b_{k,J}$ coefficients from the formal series expansion in χ. In $d = 3$, we have:

$$G^{(0)}(\chi, \boldsymbol{\xi}) = \frac{\pi M_L^{3-2\zeta}}{4\pi\zeta \sin\left(\frac{3\pi}{2\zeta}\right)} + \frac{\sin(\pi\zeta)}{2\pi^2} \sum_{m\neq 0} \int_0^{+\infty} dt \, \frac{e^{-t|\xi_m|}}{|\xi_m|} \frac{t^{1+2\zeta}}{t^{4\zeta} + 2M_L^{2\zeta} t^{2\zeta} \cos(\pi\zeta) + M_L^{4\zeta}} , \tag{4.3.25}$$

and the expansion in χ inside the integral takes the same form as in [148], but with t replacing the mass of the short-range case. We thus get an integral representation for the one-point functions of the $J > 0$ spinning operators:[16]

$$b_{0,J} = \frac{\sin(\pi\zeta)}{2\pi^2} \sum_{n=0}^{J} \frac{2^{n-J+1}(2J-n)!}{n!(J-n)!} \int_0^{+\infty} dt \, \mathrm{Li}_{J+1-n}\left(e^{-tLM_L}\right) \frac{t^{1+2\zeta+n}(LM_L)^{n+2-2\zeta}}{t^{4\zeta} + 2t^{2\zeta}\cos(\pi\zeta) + 1} . \tag{4.3.26}$$

Unfortunately the integral above can not be evaluated in terms of usual special functions and needs to be evaluated numerically. We compare results to the short-range case by means of a plot in Fig. 4.3.

4.3.5 One-point functions of higher-twist operators

As in the GFFT, we define the one-point functions of the higher-twist bilinear operators with an implicit choice of normalization such that:

$$\langle \mathcal{O}_{k,J}(x,\xi)\rangle = \frac{1}{L} \sum_n \int \frac{d^{d-1}\mathbf{p}}{(2\pi)^{d-1}} \frac{(\imath \mathbf{p}\cdot\boldsymbol{\xi} + \imath q_n \chi)^J}{(\mathbf{p}^2 + q_n^2)^\zeta + M_L^{2\zeta}} (\mathbf{p}^2 + q_n^2)^k - \text{counterterms} . \tag{4.3.27}$$

In order to make explicit the structure of divergences and related counterterms we make use again of the Poisson formula, and we write:

$$\langle \mathcal{O}_{k,J}(x,\xi)\rangle = \sum_{m\neq 0} \int \frac{d^d p}{(2\pi)^d} \frac{(\imath p\cdot\xi)^J \, (p^2)^k \, e^{\imath Lmq}}{(p^2)^\zeta + M_L^{2\zeta}} + \delta_{J,0}\mathcal{C}_k , \tag{4.3.28}$$

where:

$$\mathcal{C}_k \equiv \int \frac{d^d p}{(2\pi)^d} \frac{(p^2)^k}{(p^2)^\zeta + M_L^{2\zeta}} - \sum_{n=0}^{\lfloor \frac{d+2k-2\zeta}{2\zeta} \rfloor} (-M_L^{2\zeta})^n \int \frac{d^d p}{(2\pi)^d} (p^2)^{k-(n+1)\zeta} . \tag{4.3.29}$$

N. However, such operators have larger scaling dimension (at fixed spin) than those we are considering here, so they do not affect this argument.

[16] Again we can use $f_{\phi\phi J}/c_{0,J} = 1/J!$ and easily compute $a_{0,J}$ from $b_{0,J}$

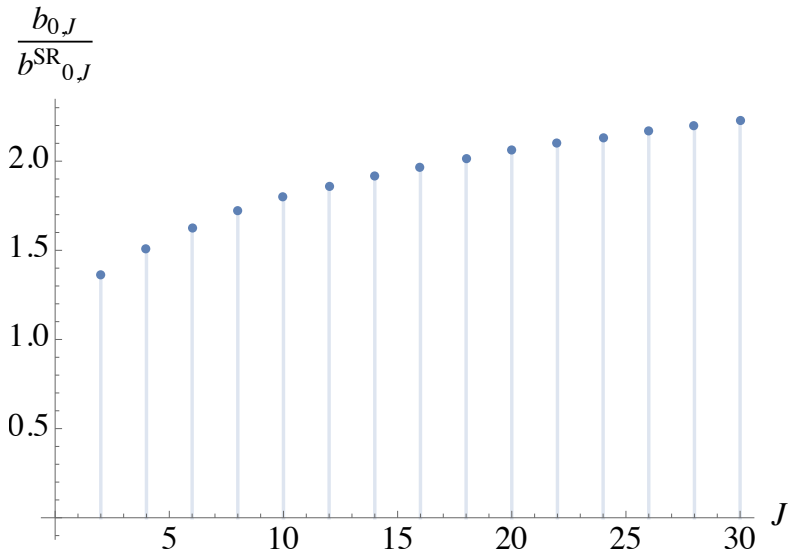

FIGURE 4.3: Plot of the ratio between $b_{0,J}$ for $\zeta = 0.8$ and the corresponding short-range value.

We have used again the fact that for $J > 0$ the $m = 0$ term vanishes in any rotationally invariant regularization. For $J = 0$ we have subtracted instead the purely divergent parts of the $m = 0$ term. Alternatively, we could drop such explicit subtractions and evaluate the $m = 0$ term by analytic continuation in k from a region of convergence (i.e. $-d/2 < k < -d/2 + \zeta$). It is however interesting, and actually useful, to keep them explicit as we will see that they have a direct interpretation in terms of (4.1.10).

We are going to define again a generating function for these one-point functions, as:

$$\begin{aligned} G^{(k)}(\chi, \boldsymbol{\xi}) &\equiv \sum_{J\geq 0} \frac{\langle \mathcal{O}_{k,J}(x,\xi)\rangle}{J!} = \sum_{m\neq 0} \int \frac{d^d p}{(2\pi)^d} \frac{e^{\imath p\cdot \xi_m}}{(p^2)^\zeta + M_L^{2\zeta}} (p^2)^k + \mathcal{C}_k \\ &= \Big((-\partial^2)^k G(x) - \mathcal{L}_k(x) \Big)_{x=\xi} , \end{aligned} \tag{4.3.30}$$

where:

$$\begin{aligned} \mathcal{L}_k(x) &= \sum_{n=0}^{\lfloor \frac{d+2k-2\zeta}{2\zeta} \rfloor} (-M_L^{2\zeta})^n \int \frac{d^d p}{(2\pi)^d} (p^2)^{k-(n+1)\zeta}\, e^{\imath p\cdot x} \\ &= \sum_{n=0}^{\lfloor \frac{d+2k-2\zeta}{2\zeta} \rfloor} \frac{(-M_L^{2\zeta})^n\, c(d/2+k-(n+1)\zeta)}{|x|^{d+2k-2(n+1)\zeta}} . \end{aligned} \tag{4.3.31}$$

The interpretation of $\mathcal{L}_k(x)$ is the following. When acting k times with a Laplacian on (4.1.10) and setting $x = \xi$, we have a similar structure as in the GFFT from the bilinear operators and the identity operator. In addition, we have other operators that at fixed k give vanishing contributions (see footnote 15), but we also have operators that give new divergent contributions from some k on: these are operators $\mathcal{O}$ with $\Delta_\mathcal{O} - 2\Delta_\phi < 2k$ not even. For example, the intermediate field σ, having $J = 0$ and non-integer dimension $\Delta_\sigma = 2\zeta$, gives vanishing contribution at $k = 0$, but a diverging one as soon as $k \geq 1$ if $d \geq 2$: indeed $\partial^2 |x|^{\Delta_\sigma - 2\Delta_\phi} = \partial^2 |x|^{4\zeta - d} = (4\zeta - d)(4\zeta - 2)|x|^{4\zeta - d - 2}$, and $4\zeta - d - 2 < 0$ for $\zeta < 1$ and $d \geq 2$. More in general, we see by comparing (4.3.31) with (4.1.10), that the operators leading to singularities in $(-\partial^2)^k G(\xi)$ have dimension $\Delta_{\sigma^n} = 2n\zeta$, and thus correspond

to the composite fields σ^n:[17]

$$(-\partial^2)^k \frac{a_{\sigma^n}}{L^{2n\zeta}}|x|^{2n\zeta-2\Delta_\phi} = \frac{a_{\sigma^n}}{L^{2n\zeta}} \frac{(-4)^k\Gamma(n\zeta-\Delta_\phi+1)\Gamma(d/2+n\zeta-\Delta_\phi)}{\Gamma(n\zeta-\Delta_\phi+1-k)\Gamma(d/2+n\zeta-\Delta_\phi-k)}|x|^{2n\zeta-2\Delta_\phi-2k} . \quad (4.3.32)$$

Therefore, we need to subtract these dangerous terms from $(-\partial^2)^k G(x)$ before setting $x=\xi$, which is what we are doing with $\mathcal{L}_k(x)$. Equivalently, we can introduce a regularization, subtract $\mathcal{L}_k^{\text{reg.}}(\xi)$, and then remove the regulator, which is what we are doing with the subtractions of $\mathcal{C}_k$.

The above discussion has an important consequence: evaluating $(-\partial^2)^k G(x)$ allows us to extract not only the $a_{k,J}$ coefficients (from the finite part at $x=\xi$, as we did in the GFFT), but also the a_{σ^m} coefficients (from the divergent part). The latter is obtained straightforwardly by comparing (4.3.31) and (4.3.32):

$$\begin{aligned} a_{\sigma^n} &= (-1)^{n+k}(LM_L)^{2n\zeta}\frac{c(\Delta_\phi+k-n\zeta)}{4^k}\frac{\Gamma(n\zeta-\Delta_\phi+1-k)\Gamma(d/2+n\zeta-\Delta_\phi-k)}{\Gamma(n\zeta-\Delta_\phi+1)\Gamma(d/2+n\zeta-\Delta_\phi)} \\ &= (-1)^n\frac{(LM_L)^{2n\zeta}}{4^{(n+1)\zeta}\pi^{d/2}}\frac{\pi}{\sin(\pi(\Delta_\phi-n\zeta))\Gamma(n\zeta-\Delta_\phi+1)\Gamma(d/2+n\zeta-\Delta_\phi)} . \end{aligned} \quad (4.3.33)$$

Notice that any dependence on k has dropped out, and the result is valid for all $n\geq 1$. In the limit $\zeta\to 1$ this yields the short-range result:

$$a_{\sigma^n}^{SR} = (LM_L)^{2n}\, c(\Delta_{SR})\frac{\Gamma(1-\Delta_{SR})}{4^n\Gamma(n+1)\Gamma(n-\Delta_{SR}+1)} , \quad (4.3.34)$$

which in $d=3$ matches the result of [145]. However, notice that while in the short-range case in integer dimensions there are degeneracies (essentially all operators have integer canonical dimension), this is not the case for general $\zeta<1$, and therefore we can safely identify (4.3.33) with the one-point function coefficient of σ^n.

Finally, we are ready to set $x=\xi$ in (4.3.30) and extract the $a_{k,J}$ coefficients. This can be easily done as we did in section (4.2.3), that is, by comparing the Taylor expansion of (4.3.30) in χ with equation (4.2.25) and matching order by order the coefficients of the powers of χ. The reason is that equation (4.2.25) was derived starting from (4.1.10) assuming that the dimension of operators appearing in the OPE of $\phi\times\phi$ are $\Delta_{k,J}=2\Delta_\phi+2k+J$, and this is also the case for the interacting large-N theory up to the σ^n operators that we subtracted explicitly in (4.3.30). To this purpose it is convenient to write $\frac{(p^2)^k}{(p^2)^\zeta+M_L^{2\zeta}}$ as a Stieltjes transform:

$$\frac{p^{2k}}{(p^2)^\zeta+M_L^{2\zeta}} = \int_0^{+\infty} ds\,\frac{\rho(s)}{p^2+s} , \qquad \rho(s)=\frac{\sin(\pi\zeta)}{\pi}\frac{s^{\zeta+k}}{s^{2\zeta}+2M_L^{2\zeta}s^\zeta\cos(\pi\zeta)+M_L^{4\zeta}} . \quad (4.3.35)$$

Then specializing to $d=3$ we find:

$$G^{(k)}(\chi,\boldsymbol{\xi}) = \frac{\sin(\pi\zeta)}{2\pi^2}\sum_{m\neq 0}\int_0^{+\infty} dt\,\frac{e^{-t|x_m|}}{|x_m|}\frac{t^{1+2\zeta+2k}}{t^{4\zeta}+2M_L^{2\zeta}t^{2\zeta}\cos(\pi\zeta)+M_L^{4\zeta}}+\mathcal{C}_k , \quad (4.3.36)$$

[17] It can be shown that spinning operators involving σ or higher powers of ϕ^2 are subleading in the $1/N$ expansion (remember that we compute $b_{\mathcal{O}}$ at finite L, but $f_{\phi\phi\mathcal{O}}$ and $c_{\mathcal{O}}$ at infinite L). This explains why we only find contributions from σ^n, which has $a_{\sigma^n}\sim O(N^0)$.

where $\mathcal{C}_k$ contributes to the $J = 0$ term only, while the sum over m will contribute to any J. After performing the small χ expansion we get:

$$\begin{aligned} G^{(k)}(\chi, \boldsymbol{\xi}) = &- \frac{1}{L^{3-2\zeta+2k}} \left(\frac{\sin(\pi\zeta)}{\pi^2} \int_0^{+\infty} dt \ln\left(1 - e^{-LM_L t}\right) \frac{t^{1+2\zeta+2k} (LM_L)^{2-2\zeta+2k}}{t^{4\zeta} + 2t^{2\zeta}\cos(\pi\zeta) + 1} \right) + \mathcal{C}_k \\ &+ \sum_{J>0} \frac{\chi^J}{J! L^{3-2\zeta+2k+J}} \left(\frac{\sin(\pi\zeta)}{2\pi^2} \sum_{n=0}^{J} \frac{2^{n-J+1}(2J-n)!}{n!(J-n)!} \right. \\ &\left. \times \int_0^{+\infty} dt \ \mathrm{Li}_{J+1-n}\left(e^{-tLM_L}\right) \frac{t^{1+2\zeta+n+2k} (LM_L)^{n+2-2\zeta+2k}}{t^{4\zeta} + 2t^{2\zeta}\cos(\pi\zeta) + 1} \right) , \end{aligned} \tag{4.3.37}$$

where the first line corresponds to spin-zero operator and the sum to all the spinning operators. Comparing with (4.2.25) we finally find:

$$\begin{aligned} a_{k,0} = &\frac{-\sin(\pi\zeta)}{(2k+1)!\pi^2} \int_0^{+\infty} dt \ln\left(1 - e^{-tLM_L}\right) \frac{t^{1+2\zeta+2k} (LM_L)^{2-2\zeta+2k}}{t^{4\zeta} + 2t^{2\zeta}\cos(\pi\zeta) + 1} \\ &+ \frac{(LM_L)^{3-2\zeta+2k}}{(2k+1)! 4\pi\zeta \sin\left(\pi \frac{2k+3}{2\zeta}\right)} , \\ a_{k,J} = &\frac{4^{-k-J}(J+\frac{1}{2})\sin(\pi\zeta)}{\pi^{3/2}\Gamma(J+k+\frac{3}{2})k!} \sum_{n=0}^{J} \frac{2^n (2J-n)!}{n!(J-n)!} \\ &\times \int_0^{+\infty} dt \ \mathrm{Li}_{J+1-n}\left(e^{-tLM_L}\right) \frac{t^{1+2\zeta+n+2k} (LM_L)^{n+2-2\zeta+2k}}{t^{4\zeta} + 2t^{2\zeta}\cos(\pi\zeta) + 1} , \end{aligned} \tag{4.3.38}$$

where we used the fact that $\mathcal{C}_k$ in $d = 3$ evaluates to:

$$\mathcal{C}_k = \frac{M_L^{3-2\zeta+2k}}{4\pi\zeta \sin\left(\pi \frac{2k+3}{2\zeta}\right)} . \tag{4.3.39}$$

4.4 Quantum long-range $O(N)$ model at finite temperature

The simplest example of an interacting fractional Lifshitz field theory (FLFT), of the type discussed in the introduction is described by the action:

$$\begin{aligned} S[\phi] = \int d\tau \int d^d x \Big(&\frac{1}{2}\phi_a(\tau, x)(-\partial_\tau^2)\phi_a(\tau, x) + \frac{1}{2}\phi_a(\tau, x)(-\partial_i\partial_i)^\zeta \phi_a(\tau, x) \\ &+ \frac{1}{2} M_{\text{bare}}^{2\zeta} \phi^2(\tau, x) + \frac{\lambda}{4N} (\phi^2(\tau, x))^2 \Big) , \end{aligned} \tag{4.4.1}$$

where ∂_τ is the ordinary derivative with respect to the Euclidean time τ, $(-\partial_i\partial_i)^\zeta$ is the fractional Laplacian for the d spatial directions and, as before, $a = 1, \ldots, N$, $\phi^2(\tau, x) \equiv \sum_a \phi_a(\tau, x)^2$, and M_{bare} is the bare mass. As argued in the introduction, we can view this model, when defined on $\mathbb{R}^{d+1}$ or $S^1_\beta \times \mathbb{R}^d$, as describing the quantum long-range $O(N)$ model at zero or finite temperature, respectively. With the same perspective, a similar model has been considered in [134, 135], where it has been studied at finite N by other means. Alternatively, one could view it as a classical anisotropic model with short-range interactions in one direction (compact or not) and long-range interactions in the remaining (non-compact) ones (see also [161] for a previous study of anisotropic long-range models).

We notice first of all that dimensional analysis of the quadratic part of the action implies that we have the mass dimensions $[x] = -1$, $[\tau] = -\zeta$, and therefore $[\phi] = \Delta_\phi$ given by:

$$2\Delta_\phi + 2\zeta - \zeta - d = 0 \quad \Rightarrow \quad \Delta_\phi = \frac{d-\zeta}{2} \,. \tag{4.4.2}$$

As a consequence, the quartic interaction in (4.4.1) is marginal (i.e. $[\lambda] = 0$) for $4\Delta_\phi = d + \zeta$, that is, $\zeta = d/3$. The model we are interested in has $\zeta < 1$ and a relevant quartic interaction, therefore we will concentrate on $d = 2$ and $2/3 < \zeta < 1$, but for now we keep d and ζ unspecified.

The action (4.4.1) is invariant under global $O(N)$ transformations with ϕ transforming in the fundamental representation. Moreover, it is clearly translation invariant, both in time and space, while for $\zeta \neq 1$ it has rotation invariance only in space. We will be interested in the limiting cases in which it has also a scaling symmetry, namely, the ultraviolet Gaussian fixed point and an infrared interacting fixed point. Due to the anisotropic nature of the model we expect a Lifshitz type of scaling invariance, that is:

$$\tau \to \Omega^\zeta \tau, \qquad x \to \Omega x, \qquad \phi(\tau, x) \to \phi(\Omega^\zeta \tau, \Omega x) = \Omega^{-\Delta_\phi} \phi(\tau, x) \,, \tag{4.4.3}$$

for any constant $\Omega > 0$. This symmetry is in general not promoted to a generalized form of conformal invariance.[18] The anisotropy and lack of conformal invariance imply that even at fixed points the correlators are much less restricted than in the isotropic case. One-point functions are still vanishing (for non-compact space-time), because of translation and scale invariance. However, for the two-point function we have:

$$\langle \phi(\tau, x) \phi(0, 0) \rangle = |x|^{-2\Delta_\phi} f_x \left(\frac{|\tau|^{1/\zeta}}{|x|} \right) = |\tau|^{-\frac{2\Delta_\phi}{\zeta}} f_\tau \left(\frac{|x|}{|\tau|^{1/\zeta}} \right) \,, \tag{4.4.4}$$

where we have expressed it in two equivalent ways, and we expect the $f_x(u)$ and $f_\tau(u)$ to be two functions that are regular in zero and vanishing at infinity as $u^{-2\Delta_\phi}$, but otherwise completely unconstrained.

Even if the fixed-point theories are not conformally invariant, we can still make use of the OPE, although in this case we expect it to be only an asymptotic expansion (see for example [164]). Indeed, assuming that a fixed-point Lifshitz field theory admits a basis in the space of operators consisting in scaling operators $\mathcal{O}_i$ with dimensions Δ_i, such that $\mathcal{O}_i(\Omega^\zeta \tau, \Omega x) = \Omega^{-\Delta_i} \mathcal{O}_i(\tau, x)$, the OPE expansion writes:

$$\mathcal{O}_{i_1}(\tau_1, x_1) \mathcal{O}_{i_2}(\tau_2, x_2) = \sum_k f_{i_1 i_2 k}(\tau_{12}, x_{12}) \, \mathcal{O}_k(\tau_2, x_2) \,, \tag{4.4.5}$$

[18] In the case $\zeta = 2$, when formulated as a dynamic critical model (or stochastic partial differential equation problem), it has been shown in [162] that there is a larger symmetry, namely the Schrödinger group (see [142] and references therein), but only for the response function, not the correlator. This result has been generalized in [163] to the case $\zeta = 2/n$, for $n \in \mathbb{N}$, but this does not include our interesting $d = 2$ case with $\zeta \in (2/3, 1)$.

where $\tau_{12} = \tau_1 - \tau_2$ and $x_{12} = x_1 - x_2$, and the equality should be understood to be only in the asymptotic sense. Applying a scaling transformation and the OPE in either order we have:

$$\begin{aligned}
\mathcal{O}_{i_1}(\Omega^\zeta \tau_1, \Omega x_1)\mathcal{O}_{i_2}(\Omega^\zeta \tau_2, \Omega x_2) &= \Omega^{-\Delta_{i_1}-\Delta_{i_2}} \mathcal{O}_{i_1}(\tau_1, x_1)\mathcal{O}_{i_2}(\tau_2, x_2) \\
&= \Omega^{-\Delta_{i_1}-\Delta_{i_2}} \sum_k f_{i_1 i_2 i}(\tau_{12}, x_{12})\ \mathcal{O}_k(\tau_2, x_2)\ , \\
\mathcal{O}_{i_1}(\Omega^\zeta \tau_1, \Omega x_1)\mathcal{O}_{i_2}(\Omega^\zeta \tau_2, \Omega x_2) &= \sum_k f_{i_1 i_2 k}(\Omega^\zeta \tau_{12}, \Omega x_{12})\ \mathcal{O}_k(\Omega^\zeta \tau_2, \Omega x_2) \\
&= \sum_k f_{i_1 i_2 k}(\Omega^\zeta \tau_{12}, \Omega x_{12}) \Omega^{-\Delta_k} \mathcal{O}_k(\tau_2, x_2)\ ,
\end{aligned} \tag{4.4.6}$$

hence the OPE coefficient is a scaling function $f_{i_1 i_2 k}(\Omega^\zeta \tau, \Omega x) = \Omega^{\Delta_k - \Delta_{i_1} - \Delta_{i_2}} f_{i_1 i_2 k}(\tau, x)$, that is, we can always write:

$$f_{ijk}(\tau, x) = |\tau|^{\frac{\Delta_k - \Delta_i - \Delta_j}{\zeta}} f_{ijk}\left(\frac{|x|}{|\tau|^{1/\zeta}}\right)\ . \tag{4.4.7}$$

This will be useful in the finite-temperature case (compact time), in order to relate the two-point function to the one-point functions via the zero-temperature OPE coefficients.

We will first discuss the free theory as a warm up, and then move on to the interacting case.

4.4.1 The massless free fractional Lifshitz field theory at zero temperature

The action of the massless free FLFT at zero temperature is (we suppress the $O(N)$ indices here as the N fields are decoupled in this case):

$$S[\phi] = \int_{-\infty}^{+\infty} d\tau \int_{\mathbb{R}^d} d^d x \left(\frac{1}{2}\phi(\tau, x)(-\partial_0^2)\phi(\tau, x) + \frac{1}{2}\phi(\tau, x)(-\partial_i \partial_i)^\zeta \phi(\tau, x)\right)\ . \tag{4.4.8}$$

It is trivial to check that this action is invariant under Lifshitz scaling (4.4.3). This implies that the two-point function, or covariance $C(\tau, x)$ of the Gaussian measure, must have the form (4.4.4). Indeed, writing the direct space covariance as a Fourier transform:

$$C(\tau, x) = \int \frac{d^d p}{(2\pi)^d} \int \frac{d\omega}{2\pi}\ \frac{e^{\imath p\cdot x + \imath \omega \tau}}{(p^2)^\zeta + \omega^2}\ , \tag{4.4.9}$$

the integral over ω can be performed easily, by deforming the contour and picking up a pole:

$$C(\tau, x) = \int \frac{d^d p}{(2\pi)^d} e^{\imath p\cdot x} \frac{e^{-|\tau|(p^2)^{\zeta/2}}}{2(p^2)^{\zeta/2}}\ , \tag{4.4.10}$$

where the integral is convergent for $\zeta < d$. Simple rescalings reproduce (4.4.4) and, recalling that $2\Delta_\phi = d - \zeta$, we have the limit cases:[19]

$$\begin{aligned} C(\tau,0) &= |\tau|^{-\frac{2\Delta_\phi}{\zeta}} \int \frac{d^dp}{(2\pi)^d} \frac{e^{-(p^2)^{\zeta/2}}}{2(p^2)^{\zeta/2}} = \frac{\Gamma\left(\frac{d-\zeta}{\zeta}\right)}{(4\pi)^{d/2}\zeta\Gamma\left(\frac{d}{2}\right)} |\tau|^{-\frac{2\Delta_\phi}{\zeta}} , \\ C(0,x) &= \int \frac{d^dp}{(2\pi)^d} e^{\imath p\cdot x} \frac{1}{2(p^2)^{\zeta/2}} = \frac{c(\Delta_\phi)}{2} |x|^{-2\Delta_\phi} , \end{aligned} \tag{4.4.11}$$

and we notice that $C(0,x)$ is (half) the GFFT covariance of section 4.2, with the replacement $\zeta \to \zeta/2$.

Bilinear operators. As the theory is Gaussian and massless, we expect again that in the (non-conformal) OPE of two fundamental fields, $\phi\times\phi$, only bilinear operators in ϕ appear, that is, operators of the schematic form:

$$[\phi\phi]_{k,l,\mu_1\cdots\mu_J}(\tau,x) =: \phi(\tau,x)(\partial_\tau)^k(\partial_i\partial_i)^l \left(\partial_{i_1}...\partial_{i_J} - \text{traces}\right)\phi(\tau,x) : , \tag{4.4.12}$$

whose scaling dimension is

$$\Delta_{k,l,J} = 2\Delta_\phi + J + 2l + k\zeta . \tag{4.4.13}$$

Notice that while we have the usual degeneracy for a fixed integer n such that $J + 2l = 2n$, the time derivatives are in general (for non-rational ζ) unambiguously identifiable. On the other hand, lacking special conformal transformations to select primary operators, the distribution of derivatives on the two fields is rather arbitrary.

4.4.2 The massless free fractional Lifshitz field theory at finite temperature

The massless free FLFT at finite temperature is defined by the action:

$$S[\phi] = \int_0^\beta d\tau \int_{\mathbb{R}^d} d^dx \left(\frac{1}{2}\phi(\tau,x)(-\partial_\tau^2)\phi(\tau,x) + \frac{1}{2}\phi(\tau,x)(-\partial_i\partial_i)^\zeta\phi(\tau,x)\right) . \tag{4.4.14}$$

In this case, the covariance, or two-point function, is:

$$C_\beta(\tau,x) = \frac{1}{\beta}\sum_{n=-\infty}^{+\infty} \int \frac{d^dp}{(2\pi)^d} \frac{e^{\imath p\cdot x + \imath\omega_n\tau}}{p^{2\zeta}+\omega_n^2} , \tag{4.4.15}$$

where $\omega_n = 2\pi n/\beta$ and the subscript β tracks the inverse temperature. In this notation, the covariance at zero temperature of the previous section is denoted $C_\infty(\tau,x)$. After using the Poisson summation formula, C_β becomes:

$$C_\beta(\tau,x) = \sum_{m=-\infty}^{+\infty} \int \frac{d^dp}{(2\pi)^d} \int \frac{d\omega}{(2\pi)} \frac{e^{\imath p\cdot x + \imath\omega\tau_m}}{p^{2\zeta}+\omega^2} , \tag{4.4.16}$$

[19] Keeping both τ and x different from zero, we can reduce to single integral representations in various ways. For instance, we can use spherical coordinates in (4.4.10), perform the angular integral and remain with an integral over the radial part, involving an hypergeometric function. Alternatively, and perhaps more interestingly, we can use again a spectral representation of the integrand, that is, perform a Stieltjes transform with respect to p^2 and then use the standard result for the short-range massive propagator, to obtain:

$$C(\tau,x) = \int_0^{+\infty} \frac{ds}{(2\pi)^{d/2+1}} \left(\frac{\sqrt{s}}{|x|}\right)^{\frac{d-2}{2}} K_{\frac{d-2}{2}}(\sqrt{s}|x|)\, s^{-\frac{\zeta}{2}}\, \mathrm{Im}\left(e^{\frac{\imath\pi}{2}\zeta}\, e^{-|\tau|s^{\frac{\zeta}{2}}e^{-\frac{\imath\pi}{2}\zeta}}\right) .$$

where $\tau_m = \tau + \beta m$. Following the same steps as in the previous section we get the massless covariance at finite temperature:

$$C_\beta(\tau, x) = \sum_{m=-\infty}^{+\infty} \int \frac{d^d p}{(2\pi)^d} e^{ip\cdot x} \frac{e^{-|\tau_m|(p^2)^{\zeta/2}}}{2(p^2)^{\zeta/2}} , \tag{4.4.17}$$

which becomes, after summing over m (restricting to the fundamental domain $0 \leq \tau < \beta$):[20]

$$C_\beta(\tau, x) = \int \frac{d^d p}{(2\pi)^d} e^{ip\cdot x} \frac{1}{2(p^2)^{\zeta/2}} \left(e^{-\tau (p^2)^{\frac{\zeta}{2}}} + \frac{e^{\tau (p^2)^{\frac{\zeta}{2}}} + e^{-\tau (p^2)^{\frac{\zeta}{2}}}}{e^{\beta (p^2)^{\frac{\zeta}{2}}} - 1} \right) . \tag{4.4.18}$$

The first term in parentheses is the $m = 0$ mode and reproduces the zero-temperature result. This is the only surviving term in the $\beta \to \infty$ limit. The second term captures the finite temperature effects.

As in the case of the GFFT at finite size, the two-point function can be seen as the generating function for the one-point functions of scaling operators. For example if we set $x = 0$ and Taylor expand in τ in (4.4.15) we find:

$$C_\beta(\tau, 0) = \sum_{k\geq 0} \frac{(-1)^k \tau^{2k}}{(2k)!} \left(\frac{1}{\beta} \sum_{n=-\infty}^{+\infty} \int \frac{d^d p}{(2\pi)^d} \frac{\omega_n^{2k}}{p^{2\zeta} + \omega_n^2} \right) , \tag{4.4.19}$$

and the coefficient of τ^{2k} is the one-point function of the bilinear scaling operator $\mathcal{O}_k(\tau', x) =: \phi \partial_\tau^{2k} \phi(\tau', x) :$ at finite temperature.[21] As the integral in (4.4.19) is divergent, one needs to regularize it by an explicit subtraction. This is fairly straightforward in this case: in order to cure all the ultraviolet divergences it is enough to subtract the zero-temperature two-point function:

$$\begin{aligned} \sum_{k\geq 0} \frac{(-1)^k \tau^{2k}}{(2k)!} \langle \mathcal{O}_k(\tau', x) \rangle &= C_\beta(\tau, 0) - C_\infty(\tau, 0) \\ &= \sum_{k\geq 0} \frac{(-1)^k \tau^{2k}}{(2k)!} \left(\frac{1}{\beta} \sum_{n=-\infty}^{+\infty} \int \frac{d^d p}{(2\pi)^d} \frac{\omega_n^{2k}}{p^{2\zeta} + \omega_n^2} - \int \frac{d\omega}{2\pi} \int \frac{d^d p}{(2\pi)^d} \frac{\omega^{2k}}{p^{2\zeta} + \omega^2} \right) , \end{aligned} \tag{4.4.20}$$

which comes to subtracting the $m = 0$ mode after Poisson summation.

This subtraction can be understood directly from the representation (4.4.18), which we now rewrite in $d = 2$ and at $x = 0$, with the change of variables $t = p^2$:

$$C_\beta(\tau, 0) = \frac{1}{8\pi} \int_0^\infty dt \; t^{-\frac{\zeta}{2}} \left(e^{-\tau t^{\frac{\zeta}{2}}} + \frac{e^{\tau t^{\frac{\zeta}{2}}} + e^{-\tau t^{\frac{\zeta}{2}}}}{e^{\beta t^{\frac{\zeta}{2}}} - 1} \right) . \tag{4.4.21}$$

A naive Taylor expansion of the integrand yields ultraviolet (large t) divergent terms at every order, coming form the first term (the zero-temperature $m = 0$ mode):

$$\frac{1}{8\pi} \int_0^\infty dt \sum_{k\geq 0} \frac{(-1)^k}{k!} \tau^k \; t^{\frac{\zeta}{2}(k-1)} . \tag{4.4.22}$$

[20] For $0 \leq \tau < \beta$, we have $\sum_m e^{-a|\tau+\beta m|} = e^{-a\tau} + \sum_{m\geq 1} e^{-a\tau - a\beta m} + \sum_{m\geq 1} e^{a\tau - a\beta m} = e^{-a\tau} + \frac{e^{a\tau} + e^{-a\tau}}{e^{a\beta} - 1}$ for any a with positive real part.

[21] Operators with odd number of time derivatives vanish even at finite temperature, due to time-reversal symmetry.

However, once they are summed over k they reconstitute $C_\infty(\tau,0)$ (compare to (4.4.11)):

$$\frac{1}{8\pi}\int_0^\infty dt\ t^{-\frac{\zeta}{2}}\ e^{-\tau t^{\frac{\zeta}{2}}} = \tau^{-\frac{2\Delta_\phi}{\zeta}}\ \frac{\Gamma(2/\zeta-1)}{4\pi\zeta} \equiv \tau^{-\frac{2\Delta_\phi}{\zeta}}\ \tilde{d}_{-2\Delta_\phi/\zeta}\ , \tag{4.4.23}$$

which is unsurprising as the divergence came from expanding in τ the $m=0$ mode.

Subtracting these terms in the spectral representation and Taylor expanding the second term in τ we identify the one-point functions of the scaling operators $\mathcal{O}_k$:

$$(-1)^k\,\langle \mathcal{O}_k(\tau',x)\rangle = \frac{1}{4\pi}\int_0^\infty dt\ \frac{t^{\zeta(k-\frac{1}{2})}}{e^{\beta t^{\frac{\zeta}{2}}}-1} = \frac{\Gamma(2\Delta_\phi/\zeta+2k)\ \mathrm{Li}_{2\Delta_\phi/\zeta+2k}(1)}{2\pi\zeta\,\beta^{2\Delta_\phi/\zeta+2k}} \equiv \beta^{-\frac{2\Delta_\phi}{\zeta}-2k}\ d_{2k}\ . \tag{4.4.24}$$

Observe that the counterterm part $C_\infty(\tau,0)\sim\tau^{-2\Delta_\phi/\zeta}$ is non-analytic at $\tau=0$, that is, the two-point function is:

$$C_\beta(\tau,0) = \tau^{-\frac{2\Delta_\phi}{\zeta}}\ \tilde{d}_{-2\Delta_\phi/\zeta} + \sum_{k\geq 0}\frac{\tau^{2k}}{(2k)!}\ \beta^{-\frac{2\Delta_\phi}{\zeta}-2k} d_{2k}\ , \tag{4.4.25}$$

and the subtraction is designed to take out the non-analytic piece of the two-point function, corresponding to the identity operator's contribution to the OPE.

4.4.3 The interacting fractional Lifshitz field theory at zero temperature

We now turn on the quartic interaction in the zero-temperature theory, that is, we consider the full model (4.4.1) on $\mathbb{R}^{d+1}$, and we are going to show that at large N the theory exhibits an interacting infrared fixed point, much like its isotropic counterpart.

The Schwinger-Dyson equation at zero temperature relates the free covariance $\tilde{C}^{-1}(\omega,p)=\omega^2+(p^2)^\zeta$ and the full interacting propagator (two-point function). As the combinatorics is the same as in the usual $O(N)$ model, at large N we have the usual dominance of cactus diagrams, and thus the Schwinger-Dyson equation reads:

$$\tilde{G}(\omega_0,p_0)^{-1} = \tilde{C}(\omega_0,p_0)^{-1} + M^{2\zeta}_{\text{bare}} + \frac{\lambda}{2}\int\frac{d^dp}{(2\pi)^d}\int\frac{d\omega}{2\pi}\,\tilde{G}(\omega,p)\,, \tag{4.4.26}$$

which as usual gives only a mass correction to the free propagator. Like in the isotropic case, we tune the bare mass in order to cancel such mass correction and obtain a massless propagator $\tilde{G}^{-1}(\omega,p)=\omega^2+(p^2)^\zeta$, that is, we impose the condition:

$$0 = M^{2\zeta}_{\text{bare}} + \frac{\lambda}{2}\int\frac{d^dp}{(2\pi)^d}\int\frac{d\omega}{2\pi}\,\frac{1}{\omega^2+(p^2)^\zeta} \equiv M^{2\zeta}_{\text{bare}} + \frac{\lambda}{2}\mathcal{T}\ , \tag{4.4.27}$$

where of course a ultraviolet regularization is implicit for the massless tadpole $\mathcal{T}=C(0,0)$.

In order to show that the model exhibits an infrared fixed point in the large-N limit, we derive the beta function of the quartic coupling. As usual in the vector large-N limit, the beta function is one-loop exact and at one loop only the bubble graph contributes. We regularize the infrared by performing a subtraction at a non-zero external momentum $(\omega_0,0)$ such that $\omega_0=\mu^\zeta$.[22] The bubble

[22] Alternatively we can subtract at an external momentum $(0,p)$ such that $p^2=\mu^2$. The computation in this case is slightly more involved but leads to the same result, as expected.

integral with massless propagator is then:

$$\begin{aligned} B &= \int \frac{d\omega}{2\pi} \int \frac{d^d q}{(2\pi)^d} \frac{1}{(\omega^2 + (q^2)^\zeta)((\omega+\omega_0)^2 + (q^2)^\zeta)} \\ &= \int \frac{d^d q}{(2\pi)^d} \frac{(q^2)^{-\zeta/2}}{4(q^2)^\zeta + \omega_0^2} = -\frac{2^{1-\frac{d}{\zeta}} \pi \omega_0^{\frac{d}{\zeta}-3}}{(4\pi)^{\frac{d}{2}} \Gamma(\frac{d}{2}) \zeta \cos(\frac{\pi d}{2\zeta})} , \end{aligned} \tag{4.4.28}$$

where we integrated over ω by deforming the contour and using the residue theorem. In the weakly relevant case $\zeta = \frac{d+\epsilon}{3}$, this integral exhibits a pole $B = \frac{\mu^{-\epsilon}}{2(4\pi)^{d/2}\Gamma(d/2)\epsilon}$. The large-$N$ proper vertex at the subtraction point is:

$$\Gamma^{(4)}(\omega_0, 0) = \frac{2\lambda}{1+\lambda B} , \tag{4.4.29}$$

and defining the running coupling $g = \mu^{-\epsilon}\Gamma^{(4)}(\omega_0, 0)/2$, we obtain the large-$N$ beta function:

$$\beta(g) = \mu \partial_\mu g = -\epsilon g + \frac{g^2}{2(4\pi)^{d/2}\Gamma(d/2)} . \tag{4.4.30}$$

This beta function displays a non-trivial fixed point $g^\star = 2(4\pi)^{d/2}\Gamma(d/2)\epsilon$, corresponding to a bare coupling λ flowing to infinity.

4.4.4 The interacting fractional Lifshitz field theory at finite temperature

At last, we turn on also the temperature, that is, we compactify the Euclidean time direction and study the full model (4.4.1) on $S^1_\beta \times \mathbb{R}^d$, and we are going to discuss the thermal mass and one-point functions of the scaling operators.

The model is tuned to the same fixed point, still at large N, but the compactification of time implies that the tadpole is no longer canceled by the bare mass in (4.4.27), and therefore we have a solution of the Schwinger-Dyson equation of the form $\tilde{G}^{-1}_\beta(\omega_n, p) = \omega_n^2 + (p^2)^\zeta + M_{th}^{2\zeta}$, with $\omega_n = 2\pi n/\beta$ and non-vanishing thermal mass M_{th}. The thermal mass is fixed self-consistently by the mass gap equation:

$$\begin{aligned} M_{th}^{2\zeta} &= M_{\text{bare}}^{2\zeta} + \frac{\lambda}{2} \frac{1}{\beta} \sum_n \int \frac{d^d p}{(2\pi)^d} \frac{1}{\omega_n^2 + (p^2)^\zeta + M_{th}^{2\zeta}} \\ &= \frac{\lambda}{2} \Bigg(\sum_{m \neq 0} \int \frac{d^d p}{(2\pi)^d} \int \frac{d\omega}{2\pi} \frac{e^{\imath \beta m \omega}}{\omega^2 + (p^2)^\zeta + M_{th}^{2\zeta}} \\ &\qquad - M_{th}^{2\zeta} \int \frac{d^d p}{(2\pi)^d} \int \frac{d\omega}{2\pi} \frac{1}{(\omega^2 + (p^2)^\zeta + M_{th}^{2\zeta})(\omega^2 + (p^2)^\zeta)} \Bigg) \\ &\equiv \frac{\lambda}{2} \left(\mathcal{T}(M_{th}) - \mathcal{T} \right) , \end{aligned} \tag{4.4.31}$$

where in the second equality we used the Poisson summation formula (4.2.10), and we have combined the $m = 0$ term with the explicit expression of the bare mass. In the last step we have defined the subtracted thermal tadpole $\mathcal{T}(M_{th}) - \mathcal{T} = G_\beta(0,0) - C_\infty(0,0)$.

At the fixed point, the bare coupling λ diverges, and thus the mass gap equation becomes:

$$\mathcal{T}(M_{th}) - \mathcal{T} = 0 . \tag{4.4.32}$$

We are going to show that it admits a unique non-vanishing solution for $\zeta \in (d/3, 1)$.

First, we write the two-point function at finite temperature in position space in the Fourier representation:

$$G_\beta(\tau,x)=\frac{1}{\beta}\sum_{n=-\infty}^{+\infty}\int\frac{d^dp}{(2\pi)^d}\,\frac{e^{\imath p\cdot x+\imath\omega_n\tau}}{p^{2\zeta}+\omega_n^2+M_{th}^{2\zeta}}=\sum_{m=-\infty}^{+\infty}\int\frac{d^dp}{(2\pi)^d}\int\frac{d\omega}{2\pi}\frac{e^{\imath p\cdot x+\imath\omega\tau_m}}{p^{2\zeta}+\omega^2+M_{th}^{2\zeta}}\,, \tag{4.4.33}$$

with $\tau_m=\tau+\beta m$. The integral over ω is evaluated again by the residue theorem and restricting to the fundamental domain $\tau\in[0,\beta)$ the sum over m is just a geometric series (see footnote 20), leading to:

$$\begin{aligned}G_\beta(\tau,x)=\int\frac{d^dp}{(2\pi)^d}e^{\imath p\cdot x}\frac{1}{2\sqrt{M_{th}^{2\zeta}+(p^2)^\zeta}}\Bigg(&e^{-\tau\sqrt{M_{th}^{2\zeta}+(p^2)^\zeta}}\\&+\frac{e^{\tau\sqrt{M_{th}^{2\zeta}+(p^2)^\zeta}}+e^{-\tau\sqrt{M_{th}^{2\zeta}+(p^2)^\zeta}}}{e^{\beta\sqrt{M_{th}^{2\zeta}+(p^2)^\zeta}}-1}\Bigg)\,,\end{aligned} \tag{4.4.34}$$

where the first term in parentheses is the $m=0$ term.

Setting $d=2$, taking $\tau=x=0$, and changing variables to $p^2=t$, we arrive at the following integral form of the mass gap equation:

$$\mathcal{T}(M_{th})-\mathcal{T}=\frac{1}{8\pi}\int_0^\infty dt\,\left[\frac{1}{\sqrt{M_{th}^{2\zeta}+t^\zeta}}\left(1+\frac{2}{e^{\beta\sqrt{M_{th}^{2\zeta}+t^\zeta}}-1}\right)-\frac{1}{\sqrt{t^\zeta}}\right]=0\,, \tag{4.4.35}$$

that always admits a unique solution.[23] We have plotted a numerical solution as a function of ζ in Fig. 4.4.

Keeping $\tau\neq0$, we obtain instead:

$$G_\beta(\tau,0)=\frac{1}{8\pi}\int_0^\infty dt\,\frac{1}{\sqrt{M_{th}^{2\zeta}+t^\zeta}}\left(e^{-\tau\sqrt{M_{th}^{2\zeta}+t^\zeta}}+\frac{e^{\tau\sqrt{M_{th}^{2\zeta}+t^\zeta}}+e^{-\tau\sqrt{M_{th}^{2\zeta}+t^\zeta}}}{e^{\beta\sqrt{M_{th}^{2\zeta}+t^\zeta}}-1}\right)\,, \tag{4.4.37}$$

and we are interested in its small τ expansion, which again we relate to the one-point function of the bilinear scaling operator $\mathcal{O}_k(\tau',x)=:\phi\partial_\tau^{2k}\phi(\tau',x):$ at finite temperature:

$$\sum_{k\geq0}\frac{(-1)^k\tau^{2k}}{(2k)!}\langle\mathcal{O}_k(\tau',x)\rangle=G_\beta(\tau,0)-\text{counterterms}\,. \tag{4.4.38}$$

As in the isotropic case, the $k=0$ operator will actually drop from this equation, as it is not in the spectrum of the interacting fixed point, where it is replaced by the intermediate field σ. Moreover, as in section 4.3.5, the counterterms will contain useful information about other operators in the spectrum.

The need for counterterms comes from the first term in parentheses in (4.4.37), i.e. the $m=0$ mode: its naive Taylor expansion in τ exhibits ultraviolet divergent terms at each order. Such divergences

[23] We rewrite the mass gap equation as $f_1(M_{th})=f_2(M_{th})$ with:

$$f_1(M_{th})=\int_0^\infty dt\,\frac{1}{\sqrt{M_{th}^{2\zeta}+t^\zeta}}\left(\frac{2}{e^{\beta\sqrt{M_{th}^{2\zeta}+t^\zeta}}-1}\right)\,,\qquad f_2(M_{th})=\int_0^\infty dt\,\left[\frac{1}{\sqrt{t^\zeta}}-\frac{1}{\sqrt{M_{th}^{2\zeta}+t^\zeta}}\right]\,, \tag{4.4.36}$$

and f_2 is convergent for $\zeta>\frac{2}{3}$ as $f_2\sim\int^\infty dt\,t^{-3\zeta/2}$. We note that $f_1(0)>0$ and f_1 is strictly decreasing with M_{th} while $f_2(0)=0$ and f_2 is strictly increasing with M_{th}.

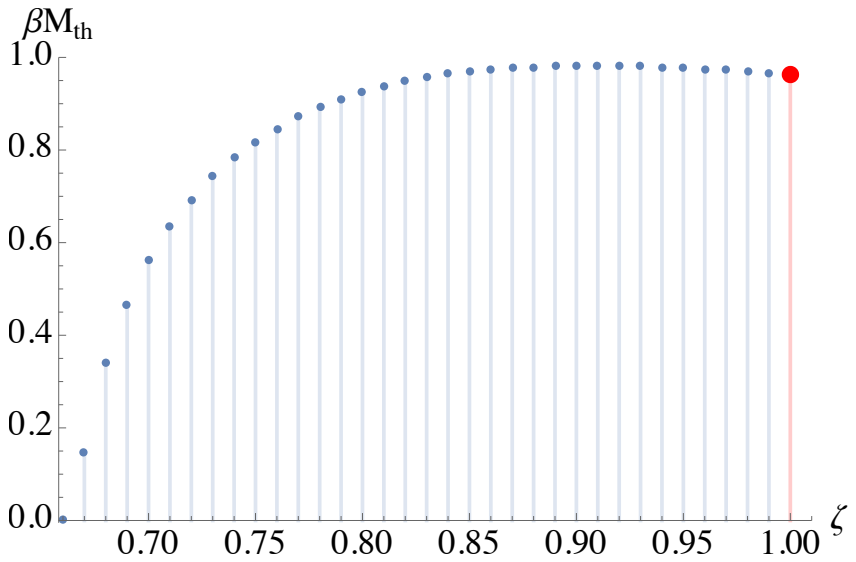

FIGURE 4.4: Numerical solutions for the thermal mass as a function of ζ in $2+1$ dimensions. The red dot is the value of the short-range thermal mass, and it is approached in the $\zeta \to 1$ limit, while the solution goes to zero for $\zeta \to 2/3$.

are renormalized by subtracting the beginning of the Taylor expansion in $M^{2\zeta}$ up to the appropriate order:

$$\frac{1}{8\pi}\int_0^\infty dt \sum_{q\geq 0}\frac{(-\tau)^q}{q!}\left[(M_{th}^{2\zeta}+t^\zeta)^{\frac{q-1}{2}} - \sum_{n=0}^{\lfloor \frac{q}{2}\rfloor}\frac{\Gamma(\frac{q+1}{2})}{n!\Gamma(\frac{q+1}{2}-n)}(M_{th}^{2\zeta})^n t^{\zeta(\frac{q-1}{2}-n)}\right]. \tag{4.4.39}$$

The odd $q = 2k+1$ terms are entirely subtracted, since $(M_{th}^{2\zeta}+t^\zeta)^k$ is a polynomial in $M^{2\zeta}$, while for even $q = 2k$ only the terms containing a power of t larger than -1 are subtracted:

$$\frac{1}{8\pi}\frac{\tau^{2k}}{(2k)!}\int_0^\infty dt\left[(M_{th}^{2\zeta}+t^\zeta)^{k-\frac{1}{2}} - \sum_{n=0}^{k}\frac{\Gamma(k+\frac{1}{2})}{n!\Gamma(k-n+\frac{1}{2})}(M_{th}^{2\zeta})^n t^{\zeta(k-n-\frac{1}{2})}\right], \tag{4.4.40}$$

resulting in an expression that is both ultraviolet ($t\to\infty$) and infrared ($t\to 0$) convergent for $\zeta > 2/3$. Indeed, convergence in the infrared is obvious term by term; convergence in the ultraviolet follows by noting that the subtracted integrand behaves like $t^{-\frac{3}{2}\zeta}$ at large t. Grouping the counterterms by their power in M_{th}, we obtain the following small-τ expansion of the massive two-point function in finite temperature (recall that $2\Delta_\phi = 2-\zeta$):

$$G_\beta(\tau,0) = \tau^{-\frac{2\Delta_\phi}{\zeta}}\left(\sum_{n=0}^{\infty}(\tau M_{th}^\zeta)^{2n}\tilde{d}_{-2\Delta_\phi/\zeta+2n} + \sum_{k\geq 0}\frac{(\tau M_{th}^\zeta)^{2k+\frac{2\Delta_\phi}{\zeta}}}{(2k)!}d_{2k}^{(\beta M_{th}^\zeta)}\right), \tag{4.4.41}$$

exhibiting the finite-temperature scaling behavior $G_\beta(\tau,0) = \tau^{-2\Delta_\phi/\zeta}\,h\left(\tau M_{th}^\zeta\right)$ for a function $h(u)$ that is finite, but non-analytic, at $u=0$. Taking into account the prefactor, the non-analytic part in τ of $G_\beta(\tau,0)$ is the first term in parentheses in (4.4.41), while the second term gives the analytic part.

The coefficients of the non-analytic part of $G_\beta(\tau,0)$ are:

$$\begin{aligned}\tilde{d}_{-2\Delta_\phi/\zeta+2n} &= \int_0^\infty \frac{dt}{8\pi} \sum_{q\geq 2n} \frac{(-1)^q}{q!} \frac{\Gamma(\frac{q+1}{2})}{n!\Gamma(\frac{q+1}{2}-n)} t^{\zeta(\frac{q-1}{2}-n)} \\ &= \int_0^\infty \frac{dt}{8\pi} \left(\frac{{}_1F_2\left(1;\frac{1}{2},n+1;\frac{t^\zeta}{4}\right)}{4^n\, t^{\zeta/2}(n!)^2} - \frac{{}_0F_1\left(;n+\frac{3}{2};\frac{t^\zeta}{4}\right)}{(2n+1)!} \right) ,\end{aligned} \tag{4.4.42}$$

and, although each term at q fixed is ultraviolet divergent, performing the sum over q first we obtain a convergent integral expression due to the alternating sign (the linear combination of hypergeometric functions decays like $t^{-\zeta(n+1)/2}e^{-t^{\zeta/2}}$ for $t\to+\infty$).

The analytic part of $G(\tau,0)$ comprises effects due to both the finite temperature and the presence of a non-zero thermal mass:

$$\begin{aligned} d_{2k}^{(\beta M_{th}^\zeta)} &= \int_0^\infty \frac{dt}{8\pi} \left[(1+t^\zeta)^{k-\frac{1}{2}} - \sum_{n=0}^{k} \frac{\Gamma(k+\frac{1}{2})}{n!\Gamma(k-n+\frac{1}{2})} t^{\zeta(k-n-\frac{1}{2})} + \frac{2\left(1+t^\zeta\right)^{k-\frac{1}{2}}}{e^{\beta M_{th}^\zeta\sqrt{1+t^\zeta}}-1} \right] \\ &= \int_0^\infty \frac{dt}{8\pi} \left[-\frac{\Gamma\left(k+\frac{1}{2}\right)\,{}_2F_1\left(1,\frac{3}{2};k+2;-t^{-\zeta}\right)}{2\sqrt{\pi}\,(k+1)!\,t^{3\zeta/2}} + \frac{2\left(1+t^\zeta\right)^{k-\frac{1}{2}}}{e^{\beta M_{th}^\zeta\sqrt{1+t^\zeta}}-1} \right] , \end{aligned} \tag{4.4.43}$$

and we stress again that this is a convergent integral for $\zeta > 2/3$.

As in the CFT case, the coefficients of the small-τ expansion can be related to the one-point functions of composite operators. Indeed, from (4.4.5) and (4.4.7), we have:

$$\phi(\tau,0)\phi(0,0) = \sum_{\mathcal{O}} f_{\phi\phi\mathcal{O}}(0)\, |\tau|^{\frac{\Delta_\mathcal{O}-2\Delta_\phi}{\zeta}}\, \mathcal{O}(0,0) , \tag{4.4.44}$$

where $\mathcal{O}$ runs over all the scaling operators in the theory. Taking the expectation value of (4.4.44), we conclude that the two-point function is a generating function for the one-point functions of the operators $\mathcal{O}$ having $f_{\phi\phi\mathcal{O}}(0)\neq 0$. Notice that the operators in (4.4.44) are not primaries, as we do not have conformal invariance here, hence they include also total derivatives of composite operators. However, the latter have vanishing one-point functions even at finite temperature, due to translation invariance.

Seen from such an OPE perspective, we recognize that (4.4.41) is indexed by two classes of operators. First, we have operators with momentum dimensions $\frac{\Delta_\mathcal{O}-2\Delta_\phi}{\zeta} = 2k$, i.e. $\Delta_\mathcal{O} = 2\Delta_\phi + 2k\zeta$. These are identified with the operators $\mathcal{O}_k(\tau,x) =: \phi\partial_\tau^{2k}\phi(\tau,x) :$. By consistency with (4.4.38), we must have that with our choices of normalizations $f_{\phi\phi\mathcal{O}}(0) = (-1)^k/(2k)!$, and thus we conclude that:

$$(-1)^k \langle \mathcal{O}_k(\tau',x)\rangle = M_{th}^{2\Delta_\phi+2k\zeta} d_{2k}^{(\beta M_{th}^\zeta)} . \tag{4.4.45}$$

Notice that the mass gap equation corresponds to $d_0^{(\beta M_{th})} = 0$.

Second, we have a family of operators with momentum dimension $\frac{\Delta_\mathcal{O}-2\Delta_\phi}{\zeta} = 2n - \frac{2\Delta_\phi}{\zeta}$, i.e. $\Delta_\mathcal{O} = 2n\zeta$. As in the isotropic case, the intermediate field $\sigma(x)$, which can be introduced as in (4.3.2), is identified with the shadow of $\phi^2(x)$ and has momentum dimension $\Delta_\sigma = d+\zeta-2\Delta_\phi = 2\zeta$. Therefore, the second class of operators contributing to the OPE of the two-point function correspond to composite σ^n operators:

$$f_{\phi\phi\sigma^n}(0)\,\langle\sigma^n(\tau',x)\rangle = M_{th}^{2n\zeta}\ \tilde{d}_{-2\Delta_\phi/\zeta+2n} . \tag{4.4.46}$$

4.5 Conclusions

We have studied classical and quantum versions of the long-range $O(N)$ model at large N, focusing on the effects of having one compact spatial direction in the former or finite temperature in the latter. The quantum model is mapped as usual to a Euclidean field theory with one extra (time) dimension, along which the action is local, thus resulting in an anisotropic action, which at criticality has a Lifshitz scale invariance, but no conformal invariance. This should be contrasted to the short-range case, where the classical and quantum model are described by the same field theory, in d and $d+1$ dimensions, respectively, and therefore they are both conformal at criticality. Therefore, in the long-range model also the finite-size and finite-temperature compactifications are quite different: the finite-size geometry corresponds to compactifying a direction along which the model has long-range interaction, while the finite temperature corresponds to compactifying the local Euclidean time direction.

In both cases, the non-compact versions of the model exhibit an ultraviolet Gaussian fixed point and an interacting infrared fixed point. Upon compactification, the fixed-point data (conformal data in the classical case, or simply fixed-point data in the quantum one) of the non-compact theories needs to be supplemented with the non-zero values of one-point functions of primary (respectively scaling) operators.

We have focused on the operators arising in the OPE of two fundamental fields. The corresponding new data can be inferred from the small argument behaviour of the two-point function, and consequently our main technical tool consists in finding suitable expansions of the latter. Our results are:

- for the free (ultraviolet) compactified theories, we obtained the one-point functions of bilinear operators. In the finite-size case we obtained such data for all the bilinear primaries, with arbitrary spin and twist. In the finite-temperature case we computed this data only for scalar bilinears with time derivatives.

- in the case of the compactified interacting (infrared) theories, at large N, the effect of the interaction is encoded in the appearance of a dynamically generated mass scale which we determined self-consistently. We obtained the fixed-point data for the same set of bilinear operators as in the free case. Moreover, in the interacting cases, a second infinite family of operators contributes to the OPE, consisting in arbitrary powers of the Hubbard–Stratonovich intermediate field. We computed also the one-point functions of such operators.

A natural extension of this work would be to consider other configurations of the background geometry, for example considering the classical model with more or all directions compactified, or the quantum model with compact spatial directions, either at zero or finite temperature.

Another important future direction would be the inclusion of subleading corrections in $1/N$. In the short-range case, the effect of next-to-leading corrections on the new finite-temperature data has been studied in [148]. In the long-range case, we expect further complications. In the classical isotropic case, we have seen that even in the leading-order we considered here, the non-standard propagator makes analytic computations much harder, and certainly this will affect the loop integrals that are needed for subleading orders. In the anisotropic (quantum) case, computations are harder even at zero temperature; in fact, as we mentioned in the introduction, the fractional Lifshitz field theory we considered here has not been studied much before, and there are several open directions even at zero temperature. In particular, it would be interesting to determine the deviation of the dynamic critical exponent z, characterizing the Lifshitz scaling at the fixed point, from its leading order value $z = \zeta$, and to ascertain the existence of a crossover (or transition) to isotropic short-range behavior above some critical value of ζ. Such aspects of the zero-temperature FLFT require at least the next-to-leading order in $1/N$, therefore we postpone them to future work.

4.A Minimal twist bilinear operators

The most general bilinear primary operator with spin J is generated by acting with a precise combination of derivatives on the two fields. The combination is fixed by requiring that the operator is annihilated by the generator of special conformal transformations. The result of imposing such constraint on minimal twist operators was obtained in [40, 157] (see also [158, 165]), and it is most easily expressed by introducing a complex polarization vector ξ^μ such that $\xi^2 = 0$ with which to form a scalar:

$$\mathcal{O}_{0,J}(x,\xi) \equiv [\phi_a\phi_a]_{0,\mu_1\cdots\mu_J}(x)\xi^{\mu_1}\cdots\xi^{\mu_J} = \frac{1}{N} : \phi_a(x) f_J\left(\xi\cdot\overleftarrow{\partial}, \xi\cdot\overrightarrow{\partial}\right)\phi_a(x) : , \tag{4.A.1}$$

where the colon notation stands as usual for normal (or Wick) ordering (e.g. [166]), which serves to cancel the divergence in the one-point function. The function $f_J(u,v)$ is found to be

$$f_J(u,v) = \frac{J!\,\Gamma\left(\nu^{(\zeta)}\right)}{4^J\,\Gamma\left(\nu^{(\zeta)}+J\right)}(u+v)^J\,C_J^{\nu^{(\zeta)}}\left(\frac{u-v}{u+v}\right) = \sum_{n=0}^{J/2}\gamma_{n,J}\,(u+v)^{2n}\,(u-v)^{J-2n} , \tag{4.A.2}$$

with $C_J^{\nu^{(\zeta)}}(z)$ being a Gegenbauer polynomial with $\nu^{(\zeta)} = \frac{d-2\zeta-1}{2}$, and

$$\gamma_{n,J} = (-1)^n \frac{J!}{2^J\,\Gamma\left(\nu^{(\zeta)}+J\right)}\frac{\Gamma\left(J+\nu^{(\zeta)}-n\right)}{2^{2n}\,n!(J-2n)!} . \tag{4.A.3}$$

The normalization is chosen for convenience as in [157] (in particular it gives finite coefficients for $J>0$ in $d=3$).

4.A.1 Normalization of two-point functions

The two-point function at zero temperature can be computed in the free theory by applying the above formula to the (formal) spin-0 case [157]

$$\langle\mathcal{O}_{0,J}(x_1,\xi_1)\mathcal{O}_{0,J}(x_2,\xi_2)\rangle = \frac{2}{N}C(x_{12})f_J\left(\xi_1\cdot\overleftarrow{\partial}_1, \xi_1\cdot\overrightarrow{\partial}_1\right) f_J\left(\xi_2\cdot\overleftarrow{\partial}_2, \xi_2\cdot\overrightarrow{\partial}_2\right) C(x_{12}) . \tag{4.A.4}$$

In order to extract the normalization constant $c_{0,J}$ in

$$\langle\mathcal{O}_{0,J}(x,\xi_1)\mathcal{O}_{0,J}(0,\xi_2)\rangle = c_{0,J}\frac{\left(\xi_1^\mu\left(\delta_{\mu\nu}-2\frac{x_\mu x_\nu}{x^2}\right)\xi_2^\nu\right)^J}{(x^2)^{d-2+J}} , \tag{4.A.5}$$

it is enough to choose $\xi_1=\xi_2=\xi$, in which case the Kronecker delta terms drop out. The derivatives can be evaluated explicitly using the representation

$$C(x) = \frac{\Gamma(d/2-\zeta)}{2^{2\zeta}\pi^{d/2}\Gamma(\zeta)}\frac{1}{(x^2)^{d/2-\zeta}} = \frac{1}{2^{2\zeta}\pi^{d/2}\Gamma(\zeta)}\int_0^{+\infty} d\alpha\,\alpha^{d/2-\zeta-1}e^{-\alpha x^2} , \tag{4.A.6}$$

and the differential formula

$$(\xi\cdot\partial)^k e^{-\alpha x^2} = (-2\,\alpha\,\xi\cdot x)^k e^{-\alpha x^2} . \tag{4.A.7}$$

Noticing that $\partial_1 C(x_{12}) = -\partial_2 C(x_{12})$ and remembering that J is even, we find

$$\begin{aligned}
\langle \mathcal{O}_{0,J}(x,\xi)\mathcal{O}_{0,J}(0,\xi)\rangle &= \frac{2}{N}\left(\frac{1}{2^{2\zeta}\pi^{d/2}\Gamma(\zeta)}\right)^2 \int_0^{+\infty} d\alpha_1\, \alpha_1^{d/2-\zeta-1} \int_0^{+\infty} d\alpha_2\, \alpha_2^{d/2-\zeta-1} \\
&\quad \times f_J(-2\,\alpha_1\,\xi\cdot x, -2\,\alpha_2\,\xi\cdot x)^2 e^{-(\alpha_1+\alpha_2)x^2} \\
&= \frac{2}{N}\left(\frac{1}{2^{2\zeta}\pi^{d/2}\Gamma(\zeta)}\frac{J!\,\Gamma\left(\nu^{(\zeta)}\right)}{4^J\,\Gamma\left(\nu^{(\zeta)}+J\right)}\right)^2 \frac{(-2\,\xi\cdot x)^{2J}}{(x^2)^{d-2\zeta+2J}} \int_0^{+\infty} d\alpha_1\, \alpha_1^{d/2-\zeta-1} \int_0^{+\infty} d\alpha_2\, \alpha_2^{d/2-\zeta-1} \\
&\quad \times (\alpha_1+\alpha_2)^{2J}\, C_J^{\nu^{(\zeta)}}\left(\frac{\alpha_1-\alpha_2}{\alpha_1+\alpha_2}\right)^2 e^{-(\alpha_1+\alpha_2)} \\
&= \frac{2}{N}\left(\frac{1}{2^{2\zeta}\pi^{d/2}\Gamma(\zeta)}\frac{J!\,\Gamma\left(\nu^{(\zeta)}\right)}{4^J\,\Gamma\left(\nu^{(\zeta)}+J\right)}\right)^2 \frac{(-2\,\xi\cdot x)^{2J}}{(x^2)^{d-2\zeta+2J}} 2^{2\zeta+1-d} \int_0^{+\infty} ds\, s^{d-2\zeta+2J-1}\, e^{-s} \\
&\quad \times \int_{-1}^{+1} dt\,(1-t^2)^{\nu^{(\zeta)}-\frac{1}{2}} C_J^{\nu^{(\zeta)}}(t)^2 \\
&= \frac{2}{N}\frac{\Gamma(d-2\zeta+2J)}{2^{4\zeta}\pi^d\Gamma(\zeta)^2}\left(\frac{J!\,\Gamma\left(\nu^{(\zeta)}\right)}{4^J\,\Gamma\left(\nu^{\zeta}+J\right)}\right)^2 2^J \frac{\pi 2^{1-4\nu^{(\zeta)}}\Gamma(J+2\nu^{(\zeta)})}{J!(J+\nu^{(\zeta)})\Gamma(\nu^{(\zeta)})^2}\frac{(2\,(\xi\cdot x)^2)^J}{(x^2)^{d-2\zeta+2J}}\,,
\end{aligned} \tag{4.A.8}$$

where we used the change of variables $\alpha_1 = s(1+t)/2$, $\alpha_2 = s(1-t)/2$, and the orthogonality of Gegenbauer polynomials

$$\int_{-1}^{+1} dt\,(1-t^2)^{\alpha-1/2} C_J^{\alpha}(t)^2 = \frac{\pi 2^{1-2\alpha}\Gamma(J+2\alpha)}{J!(J+\alpha)\Gamma(\alpha)^2}\,. \tag{4.A.9}$$

We thus find

$$\begin{aligned}
c_{0,J} &= \frac{2}{N}\frac{\Gamma(d-2\zeta+2J)}{2^{4\zeta}\pi^d\Gamma(\zeta)^2}\left(\frac{J!\,\Gamma\left(\nu^{(\zeta)}\right)}{4^J\,\Gamma\left(\nu^{(\zeta)}+J\right)}\right)^2 \frac{\pi 2^{1-4\nu^{(\zeta)}+J}\Gamma(J+2\nu^{(\zeta)})}{J!(J+\nu^{(\zeta)})\Gamma(\nu^{(\zeta)})^2} \\
&= \frac{2}{N}\frac{\pi^{\frac{1}{2}-d} J! 2^{-d-2\zeta-J+2}\Gamma(d+J-2\zeta-1)\Gamma\left(\frac{d}{2}+J-\zeta\right)}{\Gamma(\zeta)^2\Gamma\left(\frac{d}{2}+J-\zeta-\frac{1}{2}\right)}\,.
\end{aligned} \tag{4.A.10}$$

This result agrees in the limit $\zeta = 1$ with [158] up to the $\left(\frac{J!\,\Gamma\left(\nu^{(1)}\right)}{4^J\,\Gamma\left(\nu^{(1)}+J\right)}\right)^2$ factor from the normalization of [157].

4.A.2 OPE coefficient $f_{\phi\phi J}$

Now we compute the OPE coefficient between a spinning operator of the kind $\mathcal{O}_{0,J}$ and two fundamental fields. The functional form of the three-point function is constrained by conformal symmetry to be

$$\langle \mathcal{O}_{0,J}(x_0,\xi)\phi_i(x_1)\phi_j(x_2)\rangle = \delta_{ij} f_{\phi\phi J}\left(\frac{\xi\cdot x_{20}}{x_{20}^2} - \frac{\xi\cdot x_{10}}{x_{10}^2}\right)^J \frac{1}{(x_{02}^2)^{\frac{d}{2}-\zeta}(x_{01}^2)^{\frac{d}{2}-\zeta}}\,. \tag{4.A.11}$$

We can compute the three-point function explicitly by Wick theorem as we did for the two-point function and extract the OPE coefficient by comparing with (4.A.11). We have

$$\begin{aligned}\langle \mathcal{O}_{0,J}(x_0,\xi)\phi_i(x_1)\phi_i(x_2)\rangle =& \frac{2}{N}\left(\frac{1}{2^{2\zeta}\pi^{d/2}\Gamma(\zeta)}\right)^2 \int_0^{+\infty} d\alpha_1\, \alpha_1^{\frac{d}{2}-\zeta-1} \int_0^{+\infty} d\alpha_2\, \alpha_2^{\frac{d}{2}-\zeta-1} \\ & \times f_J(-2\,\alpha_1\,\xi\cdot(x_0-x_1), -2\,\alpha_2\,\xi\cdot(x_0-x_2)) e^{-\alpha_1 x_{01}^2-\alpha_2 x_{02}^2}\,.\end{aligned} \tag{4.A.12}$$

Without loss of generality we can set $x_0 = 0$ and we get to

$$\begin{aligned}\langle \mathcal{O}_{0,J}(0,\xi)\phi_i(x_1)\phi_i(x_2)\rangle =& \frac{2}{N}\frac{J!\,\Gamma(\nu^{(\zeta)})}{4^{2\zeta+J}\pi^d\Gamma(\zeta)^2\Gamma(\nu^{(\zeta)}+J)} \int_0^{+\infty} d\alpha_1\, \alpha_1^{\frac{d}{2}-\zeta-1} \int_0^{+\infty} d\alpha_2\, \alpha_2^{\frac{d}{2}-\zeta-1} \\ & \times \left(2\alpha_1\frac{\xi\cdot x_1}{x_1^2}+2\alpha_2\frac{\xi\cdot x_2}{x_2^2}\right)^J C_J^{(\nu^{(\zeta)})}\left(\frac{2\alpha_1\frac{\xi\cdot x_1}{x_1^2}+2\alpha_2\frac{\xi\cdot x_2}{x_2^2}}{2\alpha_1\frac{\xi\cdot x_1}{x_1^2}-2\alpha_2\frac{\xi\cdot x_2}{x_2^2}}\right)\frac{e^{-\alpha_1-\alpha_2}}{(x_1^2)^{d/2-\zeta}(x_2^2)^{d/2-\zeta}}\,.\end{aligned} \tag{4.A.13}$$

Considering the region $x_2^2 \gg x_1^2$ the argument the argument of the Gegenbauer polynomials become 1 and it is easy to extract

$$\begin{aligned} f_{\phi\phi J} &= \frac{2}{N}\frac{J!\,\Gamma(\nu^{(\zeta)})}{4^{2\zeta+J}\pi^d\Gamma(\zeta)^2\Gamma(\nu^{(\zeta)}+J)} 2^J\Gamma\left(\frac{d}{2}-\zeta\right)\Gamma\left(\frac{d}{2}-\zeta+J\right)\frac{\Gamma(2\nu^{(\zeta)}+J)}{\Gamma(2\nu^{(\zeta)})J!} \\ &= \frac{2}{N}\frac{\Gamma\left(\frac{d-1}{2}-\zeta\right)\Gamma\left(\frac{d}{2}-\zeta\right)\Gamma(d+J-2\zeta-1)\Gamma\left(\frac{d}{2}+J-\zeta\right)}{\pi^d 2^{4\zeta+J}\Gamma(\zeta)^2\Gamma(d-2\zeta-1)\Gamma\left(J+\frac{d-1}{2}-\zeta\right)}\,. \end{aligned} \tag{4.A.14}$$

Now it is simple to check by a direct computation that in our conventions

$$\frac{f_{\phi\phi J}}{c_{0,J}} = \frac{1}{J!}\,. \tag{4.A.15}$$

Chapter 5

Dynamic critical exponent in quantum long-range models

5.1 Introduction

Systems with long-range interactions appear in a large variety of physical situations [72]. Among the many possible instances, a particularly interesting class of systems is the one described by models with a two-body interaction that decays with distance according to a power law, with sufficiently slow decay. The paradigmatic example in such a class is the long-range Ising model, associated to the classical Hamiltonian

$$H_I = -J \sum_{i,j\in\mathcal{L}} \frac{\sigma_i\,\sigma_j}{|i-j|^{d+2\zeta}} \ , \tag{5.1.1}$$

where $\mathcal{L} \subset \mathbb{Z}^d$ is a finite d-dimensional lattice, $\sigma_i = \pm 1$ are the Ising variables at site $i \in \mathcal{L}$, $J > 0$ is their coupling, and the long-range exponent is in the range $0 < \zeta < 1$, with the limiting case $\zeta = 1$ being equivalent to the nearest-neighbour (or short-range) model. Such model, and its extensions with internal $O(N)$ symmetry, has been extensively studied, both in its lattice version and in its field theoretic Ginzburg-Landau formulation [119, 120, 123, 167, 126, 127, 128, 129, 124, 66, 71, 32, 118, 122], and several related experimental systems have been constructed in recent years (see [5] for a review).

We emphasize that $\mathcal{L}$ in (5.1.1) represents space only, time being frozen, as is always the case in classical equilibrium statistical mechanics. When considering instead quantum versions of long-range models, a short-range temporal interaction arises after the standard quantum-to-classical mapping [138, 139], as explicitly emphasized in [3] (see also [134, 135]).[1] Keeping with the Ising example, the quantum model is obtained by replacing the classical Ising variables σ_i with Pauli matrices $\hat{\sigma}_i^z$ at each site, and adding to the Hamiltonian a transverse field interaction $h\sum_i \hat{\sigma}_i^x$, in order to induce a nontrivial quantum dynamics:

$$\hat{H}_{qI} = -J \sum_{i,j\in\mathcal{L}} \frac{\hat{\sigma}_i^z\,\hat{\sigma}_j^z}{|i-j|^{d+2\zeta}} - \gamma \sum_{i\in\mathcal{L}} \hat{\sigma}_i^x \ . \tag{5.1.2}$$

The quantum statistical partition function at inverse temperature β can then be mapped to a classical one by applying the Trotter formula to $e^{-\beta\hat{H}_{qI}}$, and after some manipulations [138] obtain:

$$\begin{aligned} \mathcal{Z}_{qI} &= \mathrm{Tr}[e^{-\beta\hat{H}_{qI}}] \\ &\sim \lim_{n\to\infty} \sum_{\{\sigma_{i,t}=\pm 1\}_{i\in\mathcal{L},t=1\ldots n}} \exp\left\{ \frac{\beta J}{n} \sum_{i,j,t} \frac{\sigma_{i,t}\,\sigma_{j,t}}{|i-j|^{d+2\zeta}} + \frac{\beta}{2} \ln\coth(\frac{\gamma}{n}) \sum_{i,t} \sigma_{i,t}\sigma_{i,t+1} \right\} , \end{aligned} \tag{5.1.3}$$

[1] Models with long-range temporal dynamics can also be conceived, for example in the presence of dissipation, impurities, or memory effects (e.g. [141, 168]), but we will not consider them here.

where the classical Ising variables now have a second index, interpreted as discrete Euclidean time, and periodic boundary conditions are assumed: $\sigma_{i,n+1} = \sigma_{i,1}$. One then concludes that the Ginzburg-Landau description of the quantum long-range Ising model must be an anisotropic scalar field theory, long-range in space and short-range in time. In chapter 4 we called such a theory a fractional Lifshitz field theory, and the scope of this chapter is to further study its critical properties.

Scalar Lifshitz field theories were first studied in [169] to describe tri-critical points in the presence of paramagnetic, ferromagnetic, and modulated phases. Denoting the time coordinate τ and the d-dimensional spatial coordinates x, a standard example is an action of the form:[2]

$$S[\phi] = \int d^d x d\tau \left\{ \frac{1}{2}(\partial_\tau \phi)^2 + \frac{\rho_0}{2} \sum_j (\partial_j \phi)^2 + \frac{1}{2} \Big(\sum_j \partial_j \partial_j \phi \Big)^2 + V[\phi] \right\} , \tag{5.1.4}$$

with j ranging over the spatial dimensions. Usual ordered and disordered phases can be reached by tuning the potential, while a spatially modulated phase, breaking translation invariance, can be obtained by choosing $\rho_0 < 0$. The Lifshitz point [169] is by the definition the critical point at the intersection of such phases, and one is interested in computing the associated critical exponents. For example, this has been done for a model in this family with a quartic interaction, using either perturbative methods up to two loops [170, 171, 172] or the functional renormalization group approach [173], while in [174, 175, 176] the anisotropic quartic $O(N)$ vector model was studied by means of the $1/N$ expansion. Notice that in the original setting of Lifshitz points, “time" is actually one spatial direction of a spatially anisotropic classical system, but it can have an interpretation as (real or imaginary) time in other contexts, such as Lorentz-violating quantum field theories with improved ultraviolet behavior [152, 177, 178], or quantum Lifshitz points [151].

One interesting feature of Lifshitz field theories is that while they break explicitly Lorentz or rotation invariance, they exhibit anisotropic scale invariance at fixed points of the renormalization group. An anisotropic scaling transformation of an operator $\mathcal{O}$ writes:

$$\mathcal{O}(\tau, x) = l^{\Delta_\mathcal{O}} \mathcal{O}(l^z \tau, l x) , \tag{5.1.5}$$

with $\Delta_\mathcal{O}$ the scaling dimension of $\mathcal{O}$, and $z \neq 1$ the anisotropy exponent, also known as dynamic critical exponent due to its similar role in dynamic critical phenomena [150]. Typical Lifshitz field theories in the literature are constructed as perturbations of a Gaussian theory with an integer anisotropy exponent, as in the example above, which has $z = 2$. However, a non-integer z generally appears at interacting fixed points. The way this happens in practice is that in the renormalized theory the operators $(\partial_\tau \phi)^2$ and $(\sum_j \partial_j \partial_j \phi)^2$ get different anomalous dimensions, say η_2 and η_4, respectively, and one finds the relation [172, 173]:

$$z = \frac{4 - \eta_4}{2 - \eta_2} . \tag{5.1.6}$$

Here, we will study a Lifshitz type of model in which a nonlocal operator, known as fractional Laplacian, replaces the higher-order spatial derivative terms.[3] In other words, we will consider a continuum version of the model (5.1.3), with the long-range kernel corresponding to the integral representation of a Laplacian to power ζ, with $0 < \zeta < 1$. As a consequence of that, the standard short-range term $(\partial_j \phi)^2$ is in this case irrelevant,[4] and thus there is no modulated phase in these

[2] From now on, when discussing the field-theoretic approach to these models we will talk about actions rather than Hamiltonians.

[3] From the point of view of our motivation the time direction has the interpretation of imaginary time in the classical description of a quantum statistical model. However, a spatial interpretation of an anisotropic classical statistical model is also possible (see for example [161] for a more general model with this interpretation).

[4] However, beyond some value of the long-range exponent it might become a dangerously irrelevant operator, as in the isotropic case [123, 71].

models. Moreover, the nonlocal nature of the spatial term implies that it needs no renormalization, and hence its anomalous dimension vanishes. Therefore, we expect to find $z = 2\zeta/(2-\eta_2)$, which we will confirm.

We will consider models with either a cubic or a quartic interaction in the regime in which they are weakly relevant, that is, for ζ slightly above its lower critical value (i.e. the value below which the infrared fixed point is non-interacting, and thus mean field theory applies). We will show that they exhibit a nontrivial infrared renormalization group fixed point, and we will compute explicitly the corrections to the canonical value of z (i.e. $z = \zeta$) at leading order in the perturbative expansion.

The model with quartic interaction has $\mathbb{Z}_2$ invariance, and it can be interpreted as the Ginzburg-Landau theory for the quantum long-range Ising model, as explained above. The cubic model instead will require an imaginary coupling, and thus it can be interpreted as describing the Yang-Lee edge singularity at imaginary magnetic field for the same model, similarly to the usual Yang-Lee model [179] (recently reviewed in [180]).

We will start from the cubic model in section 5.2, as calculations in this case are slightly easier, and as such it provides a useful benchmark for general renormalization aspects. Moreover, such model has never been studied before. We will then move to the quartic case in section 5.3. The latter has been studied also in [134, 135], but with methods and results that are complementary to ours.

5.2 The cubic model

The free model. The free fractional Lifshitz theory in $d+1$ dimensions with Euclidean signature is defined by the action:

$$S[\phi] = \frac{1}{2}\int d\tau d^d x\, \phi(\tau,x)\left[(-\partial^2)^\zeta - \partial_\tau^2\right]\phi(\tau,x)\,, \tag{5.2.1}$$

where τ is the Euclidean time coordinate, x the d-dimensional position, and $(-\partial^2)^\zeta = \left(-\sum_{i=1}^d \partial_i\partial^i\right)^\zeta$ stands for the fractional Laplacian in the d spatial dimensions [90]. In position space, the latter is given by a nonlocal integral kernel which corresponds to the continuum version of (5.1.1):

$$\int d^d x\, \phi(\tau,x)\,(-\partial^2)^\zeta\,\phi(\tau,x) \propto \int d^d x\, d^d y\, \frac{\phi(\tau,x)\phi(\tau,y)}{|x-y|^{d+2\zeta}}\,. \tag{5.2.2}$$

For the sake of conciseness, and for stressing the analogy to ordinary Lifshitz field theories, in the rest of the chapter we will use the derivative notation when writing the action.

The covariance of the model, written as Fourier transform, is:

$$C(\tau,x) = \int \frac{d^d p\, d\omega}{(2\pi)^{d+1}}\,\frac{e^{\imath\omega\tau+\imath px}}{\omega^2+(p^2)^\zeta}\,, \tag{5.2.3}$$

and it enjoys the anisotropic Lifshitz scale invariance:

$$C(\tau,x) = l^{2\Delta_\phi}\, C(l^\zeta\tau, lx)\,, \tag{5.2.4}$$

with $\Delta_\phi = \frac{d-\zeta}{2}$ the mass dimension of the field under anisotropic scaling. As the model is free, the correlators are computed by the Wick theorem and obey the scaling law:

$$\begin{aligned} F^{(n)}(\tau_1,x_1;\dots;\tau_n,x_n) &= \frac{\int[d\phi]e^{-S(\phi)}\;\phi(\tau_1,x_1)\dots\phi(\tau_n,x_n)}{\int[d\phi]e^{-S(\phi)}} \\ &= l^{n\Delta_\phi}\, F^{(n)}(l^\zeta\tau_1, lx_1;\dots;l^\zeta\tau_n,lx_n)\,, \end{aligned} \tag{5.2.5}$$

reflecting the invariance of the action under a field change of variable $\phi(\tau,x) = l^{\Delta_\phi}\phi'(l^\zeta\tau, lx)$, where we took into account the fact that the Jacobian of this change of variable is field independent.

Only the correlators with even n are non zero, and if one restricts to connected correlation functions $G^{(n)}$, only the two point function is nontrivial and it equals the covariance:

$$G^{(2)}(\tau_1,x_1;\tau_2,x_2) = C(\tau_1-\tau_2, x_1-x_2)\ . \tag{5.2.6}$$

The interacting model: bare theory and scaling. For the interacting theory one needs to distinguish between the bare and the renormalized versions of the model. We start by discussing the bare theory, defined by the action:

$$S_b[\phi_b] = \int d\tau d^dx \left\{ \frac{1}{2}\phi_b(\tau,x)\left[\left(-\partial^2\right)^\zeta - \partial_\tau^2\right]\phi_b(\tau,x) + \imath\frac{\lambda_b}{3!}\phi_b(\tau,x)^3 \right\}, \tag{5.2.7}$$

which depends on the bare field $\phi_b(\tau,x)$. Depending on the regularization scheme, additional linear and quadratic terms might be needed for renormalization, but we can view the above action as representing our target scale-invariant theory. No couplings are introduced in the kinetic term, as they can always be set to 1 by a rescaling of ϕ_b, τ, and λ_b. Note that we have explicitly factored an imaginary unit in the interaction, which is standard for cubic interactions. We will also assume $\lambda_b > 0$, since the two choices of sign are related by a field redefinition $\phi_b \to -\phi_b$.

The critical value of ζ for which the cubic interaction is marginal, that is such that the interaction is invariant under the field change of variable $\phi_b(\tau,x) = l^{\Delta_\phi}\phi_b'(l^\zeta\tau, lx)$, respects $3\Delta_\phi - d - \zeta = 0$, that is $\zeta = \frac{d}{5}$. The weakly relevant case is obtained by setting $\zeta = \frac{d+\epsilon}{5}$, with $\epsilon > 0$ small, leading to the mass dimension of the coupling $[\lambda_b] = d+\zeta-3\Delta_\phi = \frac{\epsilon}{2}$. In order to have an interesting renormalization group flow towards the infrared, and keep $\zeta < 1$, which is needed for the long-range interpretation and for avoiding the need of a relevant $\phi_b\partial_x^2\phi_b$ term in the action, we must stick to $d < 5$.

With the above choices, the action is invariant under the simultaneous change of field variables and coupling:

$$\phi_b(\tau,x) = l^{\Delta_\phi}\phi_b'(l^\zeta\tau, lx)\ , \qquad \lambda_b = l^{\epsilon/2}\lambda_b' \qquad \Rightarrow \qquad S_b[\phi_b,\lambda_b] = S_b[\phi_b',\lambda_b']\ . \tag{5.2.8}$$

We stress that this is essentially dimensional analysis, not a a true invariance of the theory, because the actions above are evaluated at different values of the coupling.

For $\epsilon > 0$, using analytical continuation when needed, the correlation functions of the theory are finite order by order in the perturbative expansion, and they display the following behaviour under rescaling (we denote the arguments of the correlators collectively by τ, x):

$$F_b^{(n)}(\tau,x|\lambda_b) = \frac{\int[d\phi_b]e^{-S_b[\phi_b,\lambda_b]}\ \phi_b(\tau_1,x_1)\dots\phi(\tau_n,x_n)}{\int[d\phi_b]e^{-S_b[\phi_b,\lambda_b]}} = l^{n\Delta_\phi}F_b^{(n)}(l^\zeta\tau, lx|l^{-\epsilon/2}\lambda_b)\ . \tag{5.2.9}$$

Equivalently, the bare correlation functions respect the differential equation:

$$\left[n\Delta_\phi - \frac{\epsilon}{2}\lambda_b\partial_{\lambda_b} + \zeta D_\tau + D_x\right]F_b^{(n)}(\tau,x|\lambda_b) = 0\ , \tag{5.2.10}$$

where $D_\tau = \sum_i \tau_i\partial_{\tau_i}$ is the time and $D_x = \sum_{i,\nu} x_i^\nu\partial_{x_i^\nu}$ the space dilatation operator. Formally, the bare correlators are eigenfunctions of the anisotropic dilatation operator $\zeta D_\tau + D_x$ in the marginal $\epsilon = 0$ case, and slightly break it in the weakly relevant case.

This is however formal because, as usual, the bare correlation functions display poles in $1/\epsilon$ which we will eliminate by passing to renormalized ones.

The effective action. One often considers the effective action of the model, that is minus the generating function of amputated one-particle irreducible (1PI) correlators. For the bare theory this writes (somewhat formally):

$$e^{-\Gamma_b[\Phi_b]} = \int_{1\mathrm{PI}} d\varphi \; e^{-S_b[\Phi_b+\varphi]} \; . \tag{5.2.11}$$

The transformation of the bare action under scaling implies that:

$$\Gamma_b[\Phi_b|\lambda_b]\Big|_{\Phi_b = l^{\Delta_\phi}\Phi'_b(l^\zeta\tau, lx); \lambda_b = l^{\epsilon/2}\lambda'_b} = \Gamma_b[\Phi'_b|\lambda'_b] \; , \tag{5.2.12}$$

and it follows that under a rescaling the bare amputated 1PI correlators behave as:[5]

$$\begin{aligned} &\Gamma^{(n)}_b(\tau, x|\lambda_b) = l^{n(\zeta+d-\Delta_\phi)}\Gamma^{(n)}_b(l^\zeta\tau, lx|l^{-\epsilon/2}\lambda_b) \; , \\ &\left[n(\zeta+d-\Delta_\phi) - \frac{\epsilon}{2}\lambda_b\partial_{\lambda_b} + \zeta D_\tau + D_x\right]\Gamma^{(n)}_b(\tau, x|\lambda_b) = 0 \; . \end{aligned} \tag{5.2.13}$$

In momentum space the scaling transformation becomes

$$\Gamma^{(n)}_b(\omega, p|\lambda_b) = l^{-n\Delta_\phi}\Gamma^{(n)}_b(l^{-\zeta}\omega, l^{-1}p|l^{-\epsilon/2}\lambda_b) \; , \tag{5.2.14}$$

but we note that there is one subtlety: this scaling relation concerns the *full* n-point amputated correlators. Such correlators contain a global conservation of momentum and frequency:

$$\begin{aligned} \Gamma^{(n)}_b(\omega, p|\lambda_b) &= \delta(\sum \omega)\delta(\sum p)\; \bar\Gamma^{(n)}_b(\omega, p|\lambda_b) \; , \\ \bar\Gamma^{(n)}_b(\omega, p|\lambda_b) &= l^{\zeta+d}l^{-n\Delta_\phi}\bar\Gamma^{(n)}_b(l^{-\zeta}\omega, l^{-1}p|l^{-\epsilon/2}\lambda_b) \; , \end{aligned} \tag{5.2.15}$$

where we denoted $\bar\Gamma^{(n)}$ the momentum space n-point kernels of the effective action.[6]

The one loop order. At one loop order, denoting $\mathbf{x} = (\tau, x)$ and $d\mathbf{x} = d\tau d^d x$, the bare effective action is expanded in powers of the field as follows:

$$\begin{aligned} \Gamma_b[\Phi_b] =& S_b[\Phi_b] + \imath\frac{\lambda_b}{2}\int d\mathbf{x}\; \Phi_b(\mathbf{x})C(0) + \frac{\lambda_b^2}{4}\int d\mathbf{x}d\mathbf{x}'\; \Phi_b(\mathbf{x})\Phi_b(\mathbf{x}')C(\mathbf{x}-\mathbf{x}')^2 \\ &- \imath\frac{\lambda_b^3}{3!}\int d\mathbf{x}d\mathbf{x}'d\mathbf{x}''\; \Phi_b(\mathbf{x})\Phi_b(\mathbf{x}')\Phi_b(\mathbf{x}'')C(\mathbf{x}-\mathbf{x}')C(\mathbf{x}'-\mathbf{x}'')C(\mathbf{x}''-\mathbf{x}) + O(\Phi^4) \; . \end{aligned} \tag{5.2.16}$$

The 1PI bare two and three point functions in momentum space, where we factored out the global momentum and frequency conservation, are at this order:

$$\begin{aligned} \bar\Gamma^{(2)}_b(\omega_0, p_0) &= \omega_0^2 + (p_0^2)^\zeta + \frac{1}{2}\lambda_b^2\; \mathcal{B}(\omega_0, p_0) \; , \\ \bar\Gamma^{(3)}_b(\omega_1, p_1; \omega_2, p_2) &= \imath\lambda_b - \imath\lambda_b^3\; \mathcal{T}(\omega_1, p_1; \omega_2, p_2) \; , \end{aligned} \tag{5.2.17}$$

where $\mathcal{B}$ and $\mathcal{T}$ are respectively the bubble and the triangle diagrams depicted in Fig. 5.1 with

[5] We use $\int d\tau dx\; \Phi_b(\tau, x)^n\Gamma^{(n)}_b(\tau, x|\lambda_b) = \int d\tau' dx'\; \left(l^{-\Delta_\phi}\Phi_b(l^{-\zeta}\tau', l^{-1}x')\right)^n \Gamma^{(n)}_b(\tau', x'|l^{-\epsilon/2}\lambda_b)$.

[6] In order to underline the distinction between $\Gamma^{(n)}$ and $\bar\Gamma^{(n)}$, observe that for an isotropic long range free theory we have the two point amputated correlator $\Gamma^{(2)}(p, q) = p^{2\zeta}\delta(p+q)$, $d = 2\zeta + 2\Delta_\phi$ which obeys the scaling law $l^{-2\Delta_\phi}[l^{-2\zeta}p^{2\zeta}\delta(l^{-1}p + l^{-1}q)] = p^{2\zeta}\delta(p+q)$, while $\bar\Gamma^{(2)}(p) = p^{2\zeta}$ obeys the scaling law $l^{d-2\Delta_\phi}(l^{-2\zeta}p^{2\zeta}) = p^{2\zeta}$.

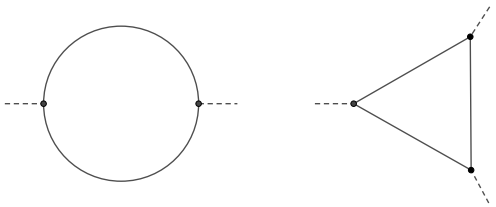

FIGURE 5.1: Left: bubble diagram $\mathcal{B}(\omega_0, p_0)$. Right: triangle diagram $\mathcal{T}(\omega_1, p_1; \omega_2, p_2)$.

amplitudes:

$$\begin{aligned}\mathcal{B}(\omega_0, p_0) &= \int \frac{d^d q\, d\omega}{(2\pi)^{d+1}} \frac{1}{\omega^2 + (q^2)^\zeta} \frac{1}{(\omega_0+\omega)^2 + [(p_0+q)^2]^\zeta} ,\\ \mathcal{T}(\omega_1, p_1; \omega_2, p_2) &= \int \frac{d^d q\, d\omega}{(2\pi)^{d+1}} \frac{1}{\omega^2 + (q^2)^\zeta} \frac{1}{(\omega_1+\omega)^2 + [(p_1+q)^2]^\zeta} \\ &\qquad \times \frac{1}{(\omega_1+\omega_2+\omega)^2 + [(p_1+p_2+q)^2]^\zeta} ,\end{aligned} \tag{5.2.18}$$

where we have labelled all the momenta as incoming.

Power counting. At arbitrary orders, the effective action writes as the sum over 1PI amputated Feynman graphs with amplitude:

$$\mathcal{A}(\omega_E, q_E) = \int \prod_L d\omega_L d^d q_L \prod_e \frac{1}{\omega_e^2 + (q_e^2)^\zeta} , \tag{5.2.19}$$

where q_L, ω_L are the independent loop momenta and frequencies, q_e, ω_e are the momenta and frequencies of the internal edges, that is linear combinations of loop momenta and frequencies and external momenta and frequencies q_E, ω_E. Note that we have factored a global conservation of frequency and momentum.

The power counting of a graph with P propagators (edges), V vertices and n external points is obtained by taking $q_L \sim \Lambda$ and $\omega_L \sim \Lambda^\zeta$, leading to $\Lambda^{(d+\zeta)(P-V+1)-2\zeta P}$. Taking into account that $2P = 3V - n$, this is:

$$\Lambda^{d+\zeta-(d+\zeta)V+(d-\zeta)P} = \Lambda^{d+\zeta-\frac{n}{2}(d-\zeta)+V(\frac{d}{2}-\frac{5}{2}\zeta)} , \tag{5.2.20}$$

which for $\zeta = \frac{d}{5}$ becomes $\Lambda^{\frac{d}{5}(6-2n)}$. We conclude that, at $\epsilon = 0$:

- vacuum and one-point graphs ($n = 0, 1$) are power divergent: the vacuum graphs play no role and the one-point graphs are not 1PI, except for a generalized amputated tadpole. A linear counterterm will be added in order to cancel this term and ensure that $\Phi = 0$ is a stationary point for the effective action.
- two-point graphs ($n = 2$) are power divergent, $\mathcal{A}(\omega_0) \sim \Lambda^{\frac{2d}{5}}$, and $\partial_{\omega_0^2}\mathcal{A}(\omega_0) \sim \Lambda^0$ is logarithmically divergent. Two counterterms bilinear in the field will be added in order to subtract the divergent parts.
- three-point graphs ($n = 3$) are logarithmically divergent. A cubic counterterm will be added to subtract their divergent part.

Observe that, as long-range models do not exhibit a wave function renormalization,[7] the coefficient of the $(p_0^2)^\zeta$ term in the two point function is not divergent.

Renormalization. In order to subtract the divergences we consider the renormalized action

$$S_r[\phi] = \int d\tau d^d x \Big\{ \frac{1}{2}\phi(\tau,x)\left[(-\partial^2)^\zeta - Z\,\partial_\tau^2\right]\phi(\tau,x) + \delta\kappa\,\phi(\tau,x) + \frac{1}{2}\delta m^{2\zeta}\,\phi(\tau,x)^2 + \frac{\imath}{3!}\lambda\,\phi(\tau,x)^3 \Big\}\,, \tag{5.2.21}$$

and the associated renormalized correlators for the renormalized field ϕ.

We will parameterize $\lambda = \mu^{\frac{\epsilon}{2}} g Z_g$, with g the dimensionless renormalized coupling and Z_g a multiplicative renormalization factor. The renormalization functions $Z = 1 + \delta Z(g)$, $Z_g = 1 + \delta Z_g(g)$ and $\delta m^{2\zeta}(g)$ and $\delta\kappa(g)$ are chosen so as to ensure that the renormalized correlators have no divergences. The precise form of the counterterms depends on the renormalization scheme. For example, we could fix them by imposing four BPHZ-like renormalization conditions, one for each class of divergent graphs. However, as usual for a massless theory, such conditions must be imposed at a nonvanishing subtraction momentum scale μ. In this respect, we note that it is more practical to chose a configuration of external momenta in which the spatial momentum is set to zero and the external frequency acts as cutoff:[8]

$$\bar\Gamma_r^{(1)} = 0\,, \quad \bar\Gamma_r^{(2)}(0,0) = 0\,, \quad \partial_{\omega_0^2}\bar\Gamma_r^{(2)}(\mu^\zeta,0) = 1\,, \quad \bar\Gamma_r^{(3)}(\mu^\zeta,0;-(1+c)\mu^\zeta,0) = \imath\mu^{\frac{\epsilon}{2}} g\,. \tag{5.2.22}$$

The constant c should be chosen so that the configuration is nonexceptional [181], in our case meaning $c \neq 0$, and it is otherwise an arbitrary choice of the renormalization scheme, not affecting any observable quantity, such as the critical exponents. However, at one loop we encounter no problem at $c = 0$, and as calculations are easier in this case, we will make such exceptional choice in the following.

The first two conditions are automatically guaranteed in analytic regularization, because the propagator being massless, the amplitudes of the corresponding diagrams give pure power divergences (in the momentum cutoff), which are set to zero in analytic regularization. With other choices of regularization, we would instead fix $\delta m^{2\zeta}(g)$ and $\delta\kappa(g)$ so as to completely subtract the power divergent amplitudes. Either way we can safely ignore them from now on.

The remaining two conditions require in general subtractions of both divergent and finite terms. In minimal subtraction we instead only subtract the divergent parts, hence $\partial_{\omega_0^2}\bar\Gamma_r^{(2)}(\mu^\zeta,0)$ and $\bar\Gamma_r^{(3)}(\mu^\zeta,0;-\mu^\zeta,0)$ will be more complicated functions of the renormalized coupling, but the structure of counterterms and renormalization group functions is simplified. In the following we will use minimal subtraction.

We go to the weakly relevant case $\zeta = \frac{d+\epsilon}{5}$ and compute the amplitudes in analytic continuation in ϵ. Besides setting the power divergences to zero, this has the effect of converting the logarithmic divergences in poles in $\frac{1}{\epsilon}$. Although ϵ is now to be kept finite, the same renormalization procedure as for the $\epsilon = 0$ theory is to be carried out, as otherwise we would not be entitled to trust the small ϵ expansion. In minimal subtraction the counterterms $\delta Z(g)$ and $\delta Z_g(g)$ are series in $1/\epsilon$ (that is they have no finite part) which are tuned so that the renormalized correlators have a well defined $\epsilon \to 0$

[7] In order to separate the divergent part of a graph we Taylor expand it at small momentum; but in a Taylor expansion only the integer powers of the momentum appear, hence the divergences are subtracted by counterterms for bilinear operators with an integer number of derivatives $\phi(-\partial^2)^m\phi$.

[8] Due to the anisotropy of the problem, it is not obvious that this choice will prevent infrared divergence at all orders, but we conjecture that it is true.

limit:[9]

$$\delta Z(g) = \sum_{\ell \geq 1} \frac{\alpha_\ell(g)}{\epsilon^\ell} , \quad \delta Z_g(g) = \sum_{\ell \geq 1} \frac{\gamma_\ell(g)}{\epsilon^\ell} . \tag{5.2.23}$$

The coefficients $\alpha_\ell(g)$ and $\gamma_\ell(g)$ are power series in g, starting at order $g^{2\ell}$,[10] with finite coefficients independent of ϵ or μ.

The counterterms are treated as additional vertices $\delta Z(g)$ and $\delta Z_g(g)$, and in the presence of such vertices the renormalized two and three point 1PI functions write at first nontrivial order in g as:

$$\begin{aligned} \bar{\Gamma}^{(2)}_r(\omega_0, p_0) &= [1 + \delta Z(g)]\ \omega_0^2 + (p_0^2)^\zeta + \frac{\mu^\epsilon}{2} g^2\ \mathcal{B}(\omega_0, p_0) , \\ \bar{\Gamma}^{(3)}_r(\omega_1, p_1; \omega_2, p_2) &= \imath \mu^{\epsilon/2} g [1 + \delta Z_g(g)] - \imath \mu^{3\epsilon/2} g^3\ \mathcal{T}(\omega_1, p_1; \omega_2, p_2) . \end{aligned} \tag{5.2.24}$$

Note that $\mathcal{B}$, $\mathcal{T}$, and all the other graph amplitudes arising in these expansions are computed with the bare propagator $\omega^2 + (p^2)^\zeta$. The point is that the bare expansion generates divergences and these divergences are subtracted order by order by adding the counterterms: there is never any reason to compute amplitudes of graphs using the renormalized propagator $[1 + \delta Z(g)]\ \omega^2 + (p^2)^\zeta$. Indeed, using the renormalized propagator corresponds to resummations of infinite families of bare graphs with arbitrary insertions of the counterterm vertex $\delta Z(g)$ on all the edges.

For the bubble and the triangle graphs we have the following singular behaviour:

$$\partial_{\omega_0^2} \mathcal{B}(\mu^\zeta, 0) = -\mu^{-\epsilon} \frac{b}{\epsilon} + \text{finite} , \qquad \mathcal{T}(\mu^\zeta, 0; -\mu^\zeta, 0) = \mu^{-\epsilon} \frac{t}{\epsilon} + \text{finite} . \tag{5.2.25}$$

where b and t are given in Appendix 5.A, hence the minimal subtraction counterterms that ensure that the one-loop divergences are subtracted are:

$$\delta Z(g) = \frac{1}{2} g^2\ \frac{b}{\epsilon} , \qquad \delta Z_g(g) = g^2\ \frac{t}{\epsilon} . \tag{5.2.26}$$

Renormalized theory from the bare theory. Up to terms which we can ignore, the renormalized theory is described by the action:

$$S[\phi] = \int d\tau d^d x \left\{ \frac{1}{2} \phi(\tau, x) \left[\left(-\partial^2\right)^\zeta - Z \partial_\tau^2 \right] \phi(\tau, x) + \imath \frac{\lambda}{3!} \phi(\tau, x)^3 \right\} , \tag{5.2.27}$$

[9] In practice this is enforced at a renormalization point, as above, but once the pole is taken out in such a way, the correlators $\Gamma^{(n)}_r(\omega, p)$ have a well defined $\epsilon \to 0$ limit for arbitrary external frequencies and momenta ω, p.

[10] In order to show this, first one notices that order-ℓ poles appear first at ℓ loops, which in turn can for example be derived by the finiteness of beta function and anomalous dimension, as in [182]. Next, remembering that for an n-point graph with P internal propagators, V vertices and ℓ loops we have the relations $3V = 2P + n$ and $\ell = P - V + 1$, we find $V = 2\ell + n - 2$, from which, choosing $n = 2$ and 3 and remembering that vertex counterterms are multiplied by an extra factor of g, our statement follows.

and maps onto the bare one by a field redefinition and change of couplings:[11]

$$\phi(\tau,x) = Z^{-\frac{1}{4}}\phi_b(Z^{-\frac{1}{2}}\tau,x)\ ,\quad \lambda Z^{-\frac{1}{4}} = \lambda_b \qquad \Rightarrow \qquad S[\phi;\lambda,Z] = S_b[\phi_b,\lambda_b]\ . \tag{5.2.28}$$

The renormalized correlators are related to the bare correlators by:

$$F_r^{(n)}(\tau,x|\lambda,Z) = \frac{\int [d\phi] e^{-S(\phi)}\ \phi(\tau_1,x_1)\dots\phi(\tau_n,x_n)}{\int [d\phi] e^{-S(\phi)}} = Z^{-\frac{n}{4}}\ F_b^{(n)}(Z^{-\frac{1}{2}}\tau,x|\lambda Z^{-\frac{1}{4}})\ , \tag{5.2.29}$$

and we note that, contrary to the more familiar isotropic case, one needs to rescale the time argument with an appropriate power of Z.

One computes the renormalized amputated 1PI correlators of the theory using the renormalized action $S[\phi]$, or by a change of variables in terms of the bare one:

$$\begin{aligned} e^{-\Gamma_r[\Phi]} &= \int_{1\mathrm{PI}} d\varphi\ e^{-S[\Phi+\varphi;\lambda,Z]} = \int_{1\mathrm{PI}} d\varphi\ e^{-S_b[\Phi_b+\varphi;\lambda Z^{-\frac{1}{4}}]}\ , \\ \Phi(\tau,x) &= Z^{-\frac{1}{4}}\Phi_b(Z^{-\frac{1}{2}}\tau,x)\ , \end{aligned} \tag{5.2.30}$$

that is the relation between the bare and renormalized effective actions reproduces the relation between the classical actions, $\Gamma_r[\Phi|\lambda,Z] = \Gamma_b[\Phi_b|\lambda Z^{-\frac{1}{4}}]\big|_{\Phi_b(\tau,x)=Z^{\frac{1}{4}}\Phi(Z^{1/2}\tau,x)}$. This implies that the amputated correlators transform like:[12]

$$\Gamma_r^{(n)}(\tau,x|\lambda,Z) = Z^{-\frac{n}{4}}\Gamma_b^{(n)}(Z^{-\frac{1}{2}}\tau,x|\lambda Z^{-\frac{1}{4}})\ , \tag{5.2.31}$$

or in momentum space:

$$\begin{aligned} \Gamma_r^{(n)}(\omega,p|\lambda,Z) &= Z^{\frac{n}{4}}\Gamma_b^{(n)}(Z^{\frac{1}{2}}\omega,p|\lambda Z^{-\frac{1}{4}})\ , \\ \bar\Gamma_r^{(n)}(\omega,p|\lambda,Z) &= Z^{\frac{n}{4}-\frac{1}{2}}\bar\Gamma_b^{(n)}(Z^{\frac{1}{2}}\omega,p|\lambda Z^{-\frac{1}{4}})\ . \end{aligned} \tag{5.2.32}$$

As a sanity check, we can compute the amplitudes of graphs reorganizing the renormalized theory, that is including the full coupling Z in the propagator. The amplitudes of amputated graphs contributing to the renormalized amputated correlators write as:

$$\begin{aligned} \tilde{\mathcal{A}}(\omega_E,q_E) &= \int \prod_L d\omega_L d^dp_L\ \prod_e \frac{1}{Z\,\omega_e^2 + (q_e^2)^\zeta} \overset{\omega_L=\omega'_L Z^{-1/2}}{=\!=\!=\!=} \left(Z^{-1/2}\right)^{P-V+1} \mathcal{A}(Z^{1/2}\omega_E,q_E) \\ &= Z^{-V/4+n/4-1/2}\mathcal{A}(Z^{1/2}\omega_E,q_E)\ , \\ \mathcal{A}(\omega_E,q_E) &= \int \prod_L d\omega_L d^dp_L\ \prod_e \frac{1}{\omega_e^2 + (p_e^2)^\zeta}\ , \end{aligned} \tag{5.2.33}$$

[11] In fact, because of the scale invariance of the free theory, a one parameter family of mappings onto different bare theories exist, involving a rescaling also of τ and x:

$$\phi(\tau,x) = Z^{-\frac{1}{4}+\alpha\Delta_\phi}\phi_b^{(1)}(Z^{-\frac{1}{2}+\zeta\alpha}\tau, Z^\alpha x)\ ,\quad \lambda Z^{-\frac{1}{4}-(d+\zeta-3\Delta_\phi)\alpha} = \lambda_b^{(\alpha)} \qquad S[\phi;\lambda,Z] = S_b[\phi_b^{(\alpha)},\lambda_b^{(\alpha)}]\ .$$

We can interpret this as a family of renormalization schemes, which is more evident if we keep fixed the bare coupling. Remembering that $d+\zeta-3\Delta_\phi = \epsilon/2$, only the $\alpha=0$ scheme corresponds to a true minimal subtraction, in the sense that the relation between λ and λ_b does not involve finite redefinitions of the coupling, $\lambda_b = \mu^{\epsilon/2} g\left(1+\sum_{n\geq 1}\frac{\tilde\gamma_n(g)}{\epsilon^n}\right)$. For $\alpha\neq 0$, the expansion in powers of g of the factor $Z^{-\alpha\epsilon/2}$ leads to positive powers of ϵ that introduce in the above relation new terms that are finite or vanishing in the $\epsilon\to 0$ limit.

[12] We use $\int d\tau dx\ \Phi(\tau,x)^n\Gamma_r^{(n)}(\tau,x|\lambda,Z) = \int d\tau' dx'\ \left(Z^{\frac{1}{4}}\Phi(Z^{1/2}\tau',x')\right)^n \Gamma_b^{(n)}(\tau',x'|\lambda Z^{-\frac{1}{4}})$ and change variable.

with $\mathcal{A}(\omega_E, q_E)$ being the bare amplitude with $Z = 1$. Since each such amplitude is multiplied by λ^V, we recover the above relation between bare and renormalized proper vertices:

$$\bar{\Gamma}_r^{(n)}(\omega_E, q_E|\lambda, Z) = Z^{\frac{n}{4}-\frac{1}{2}}\, \bar{\Gamma}_b^{(n)}(Z^{1/2}\omega_E, q_E|\lambda Z^{-1/4}) \,. \tag{5.2.34}$$

We note that, contrary to the more familiar isotropic case, the relation between the bare and renromalized versions of the general correlators and of the amputated one particle irreducible ones is the same.

The renormalization group flow. The renormalized correlators $F_r^{(n)}(\tau, x|\mu^{\frac{\epsilon}{2}} g Z_g, Z)$ are functions only of g and μ (and of course τ and x) and are free of divergences. To emphasize this fact, and to follow common practice, we will write the renormalized correlators as $F_r^{(n)}(\tau, x|g, \mu)$, with a slight abuse of notation. In terms of such new notation, we rewrite equation (5.2.29) as:

$$F_r^{(n)}(\tau, x|g, \mu) = Z^{-\frac{n}{4}} F_b^{(n)}(Z^{-\frac{1}{2}}\tau, x|\mu^{\frac{\epsilon}{2}} g Z_g Z^{-\frac{1}{4}}) \,, \tag{5.2.35}$$

where at fixed g and $\epsilon > 0$ both the renormalized and the bare correlators depend on μ via the explicit combination on the right-hand side of the equation. At $\epsilon = 0$, due to the poles in $1/\epsilon$ of the bare correlators and renormalization functions, a logarithmic dependence on μ survives.

The renormalization group is designed to capture the μ-dependence of renormalized correlators for a fixed bare theory, and it does so with the introduction of beta function and anomalous dimension. The beta function $\beta = \mu \frac{dg}{d\mu}$ is obtained by tuning g with μ so that the bare coupling stays fixed:

$$\mu \frac{d}{d\mu}\left[\mu^{\frac{\epsilon}{2}} g Z_g Z^{-\frac{1}{4}}\right] = 0 \qquad \Rightarrow \qquad \beta(g) = -\frac{\frac{\epsilon}{2} g}{1 + g\frac{Z_g'}{Z_g} - \frac{1}{4} g \frac{Z'}{Z}} \,, \tag{5.2.36}$$

where a prime denotes a derivative with respect to g. Using the expansion (5.2.23) in powers of $1/\epsilon$ for the counterterms, we find

$$\beta(g) = -\frac{\epsilon}{2} g + \frac{g^2}{2}\left(\gamma_1'(g) - \frac{\alpha_1'(g)}{4}\right) \,, \tag{5.2.37}$$

and all the contributions from α_n and γ_n with $n > 1$, as well as higher powers of the $n = 1$ terms, must cancel for consistency. At one loop we have $\alpha_1(g) = \frac{1}{2} g^2\, b$ and $\gamma_1(g) = g^2\, t$ hence we get:[13]

$$\beta(g) = -\frac{\epsilon}{2} g + g^3 (t - \frac{b}{8}) + O(g^5) \,. \tag{5.2.38}$$

Such beta function has a zero, i.e. a fixed point, at (note that $t = 3b$ according to Appendix 5.A):

$$g_\star = \sqrt{\frac{\epsilon}{2t - \frac{b}{4}}} = 2^{\frac{d+5}{2}} \pi^{d/4} \sqrt{\frac{\epsilon\, \Gamma\left(\frac{d}{2}\right)}{23}} \,, \tag{5.2.39}$$

which is infrared attractive, as the corresponding correction-to-scaling exponent is positive:

$$\partial_g \beta(g)|_{g=g^\star} = \epsilon \,. \tag{5.2.40}$$

[13] In the α-dependent scheme of footnote 11 we would obtain $\beta = -\frac{\epsilon}{2} g + g^3 (t - b(1 + 2\epsilon\alpha)/8)$. The scheme dependence of the one-loop term is not surprising as it is scheme-independent only in the marginal case, $\epsilon = 0$. The critical exponents are instead α-independent, as they should.

For the anomalous dimension $\eta = \mu\frac{d}{d\mu}\ln Z = \beta Z'/Z$, at one loop we find $\eta = -g^2 b$, which at the fixed point becomes:

$$\eta^\star = -\frac{\epsilon b}{2t - \frac{b}{4}} = -\frac{4\epsilon}{23} \,. \tag{5.2.41}$$

The Callan-Symanzik equation encapsulates the change of the renormalized correlators with the renormalization scale. It is obtained by taking into account that the bare correlators do not depend on the renormalization scale, $\mu\frac{d}{d\mu}F_b^{(n)}(\tau, x|\mu^{\frac{\epsilon}{2}} g Z_g Z^{-\frac{1}{4}}) = 0$, and using (5.2.35). Due to the time rescaling between the renormalized and the bare correlator, one gets an additional term with respect to the usual Callan-Symanzik equation:

$$\mu\frac{d}{d\mu}F_r^{(n)} = -\frac{n}{4}\eta\, F_r^{(n)} - \frac{1}{2}\eta D_\tau F_r^{(n)} \quad \Rightarrow \quad \left[\mu\partial_\mu + \beta\partial_g + \frac{n}{4}\eta + \frac{\eta}{2}D_\tau\right] F_r^{(n)} = 0 \tag{5.2.42}$$

where $D_\tau = \sum_i \tau_i \partial_{\tau_i}$ is the time dilatation operator. We note that, contrary to the isotropic case, one gets the exact same form of the Callan-Symanzik for the one particle irreducible amputated correlator.

Lifshitz scaling at fixed point. In order to understand the behaviour of the renormalized correlators (amputated or not) under rescaling we combine (5.2.35) and (5.2.9) to conclude:

$$F_r^{(n)}(\tau, x|g, \mu) = l^{n\Delta_\phi} F_r^{(n)}(l^\zeta \tau, lx|g, l^{-1}\mu) \,, \tag{5.2.43}$$

which again is just a statement about engineering dimensions. In order to deduce scaling dimensions, we act on both sides with the derivative $l\frac{d}{dl}$, evaluated at $l = 0$, and we combine it with the Callan-Symanzik equation, obtaining:[14]

$$\left[n\Delta_\phi + \zeta D_\tau + D_x - \mu\partial_\mu\right] F_r^{(n)} = 0 \quad \Rightarrow \quad \left[n(\Delta_\phi + \frac{\eta}{4}) + (\zeta + \frac{\eta}{2})D_\tau + D_x + \beta\partial_g\right] F_r^{(n)} = 0 \,. \tag{5.2.44}$$

At the fixed point, the correlators are eigenfunctions of the anisotropic scaling operator $zD_\tau + D_x$, with the following dynamic exponent and scaling dimension:

$$\begin{aligned} z &= \zeta + \frac{\eta_\star}{2} = \frac{d}{5} + \frac{13\epsilon}{115} \,, \\ \Delta_\star &= \Delta_\phi + \frac{\eta_\star}{4} = \frac{2d}{5} - \frac{33\epsilon}{230} \,. \end{aligned} \tag{5.2.45}$$

That is, they have the following Lifshitz scale invariance:

$$F_r^{(n)}(\tau, x|g_\star, \mu) = l^{n\Delta_\star} F_r^{(n)}(l^z \tau, lx|g_\star, \mu) \,. \tag{5.2.46}$$

For example, at $n = 2$ the solution of the fixed point scaling equation is:

$$F_r^{(2)}(\tau, x|g_\star, \mu) = |x|^{-2\Delta_\star} \mu^{-\eta_\star/2} f\left(\frac{\tau^2}{\mu^{\eta_\star}|x|^{2z}}\right) \,, \tag{5.2.47}$$

where the function $f(u)$ is regular in zero and vanishes at infinity as $u^{-\Delta_\star/z}$, and otherwise it is completely unconstrained. The explicit factors of μ in (5.2.47) are there to make it compatible with canonical dimensional analysis, summarized in (5.2.43), but play no role for the more interesting scaling given by (5.2.46).

[14] Taking into account that the amputated correlator changes under rescaling according to (5.2.13), an equation similar to (5.2.44) with Δ_ϕ replaced by $d + \zeta - \Delta_\phi$ holds in that case. The two equations are consistent as $d + \zeta - \Delta_\phi + \frac{\eta}{4} = d + (\zeta + \frac{\eta}{2}) - (\Delta_\phi + \frac{\eta}{4})$.

In order to compare to existing literature on Lifshitz field theories, it is instructive to repeat the above analysis for the proper vertices in momentum space. Recalling that the renormalized vertices are written in terms of the bare ones as:

$$\bar{\Gamma}_r^{(n)}(\omega, p|g, \mu) = Z^{\frac{n}{4}-\frac{1}{2}} \bar{\Gamma}_b^{(n)}(Z^{\frac{1}{2}}\omega, p|\mu^{\frac{\epsilon}{2}} g Z_g Z^{-\frac{1}{4}}) \,, \tag{5.2.48}$$

we deduce the Callan-Symanzik equation:

$$\left[\mu\partial_\mu + \beta\partial_g + \Big(\frac{1}{2} - \frac{n}{4}\Big)\eta - \frac{\eta}{2}\omega\partial_\omega\right] \bar{\Gamma}_r^{(n)}(\omega, p|g, \mu) = 0 \,. \tag{5.2.49}$$

Dimensional analysis gives instead:

$$\bar{\Gamma}_r^{(n)}(\omega, p|g, \mu) = l^{\zeta+d} l^{-n\Delta_\phi} \bar{\Gamma}_r^{(n)}(l^{-\zeta}\omega, l^{-1}p|g, l^{-1}\mu) \,, \tag{5.2.50}$$

which combined with the Callan-Symanzik equation leads to:

$$\begin{aligned} &\left[(\zeta + d - n\Delta_\phi) - \zeta D_\omega - D_p - \mu\partial_\mu\right] \bar{\Gamma}_r^{(n)}(\omega, p|g, \mu) = 0 \\ &\quad \Rightarrow \quad \left[\zeta + d + \frac{\eta}{2} - n(\Delta_\phi + \frac{\eta}{4}) - (\zeta + \frac{\eta}{2})D_\omega - D_p + \beta\partial_g\right] \bar{\Gamma}_r^{(n)}(\omega, p|g, \mu) = 0 \,. \end{aligned} \tag{5.2.51}$$

For $n = 2$, at the fixed point, this becomes:

$$\left[2\zeta - zD_\omega - D_p\right] \bar{\Gamma}_r^{(2)}(\omega, p|g_\star, \mu) = 0 \,, \tag{5.2.52}$$

whose solution is:

$$\bar{\Gamma}_r^{(2)}(\omega, p|g_\star, \mu) = |p|^{2\zeta} f\left(\frac{\omega^2}{\mu^{-\eta_\star}|p|^{2z}}\right) \,, \tag{5.2.53}$$

where the function $f(u)$ is regular in zero and blows up at infinity as $u^{\zeta/z}$. Therefore, we have:

$$\begin{aligned} \bar{\Gamma}_r^{(2)}(0, p|g_\star, \mu) &\sim |p|^{2\zeta} \equiv |p|^{2\zeta-\eta_{2\zeta}} \,, \\ \bar{\Gamma}_r^{(2)}(\omega, 0|g_\star, \mu) &\sim \omega^{2\zeta/z} \equiv \omega^{2-\eta_2} \,, \end{aligned} \tag{5.2.54}$$

where we introduced the standard definition of correlation exponents η_2 and $\eta_{2\zeta}$, for which we read off:

$$\eta_2 = 2 - \frac{2\zeta}{z} = \frac{\eta_\star}{\zeta + \eta_\star/2} \,, \qquad \eta_{2\zeta} = 0 \,. \tag{5.2.55}$$

Lastly, we obtain the following expression for the dynamic exponent:

$$z = \frac{2\zeta - \eta_{2\zeta}}{2 - \eta_2} \,, \tag{5.2.56}$$

which holds also for integer values of $\zeta > 1$, but with a nonvanishing $\eta_{2\zeta}$.

As a final remark, we notice that for integer ζ, besides the additional counterterms that need to be introduced, a different renormalization scheme is typically employed [170, 171], in which the bare and renormalized fields are simply related by $\phi(\tau, x) = Z_\phi^{-\frac{1}{2}} \phi_b(\tau, x)$, with no rescaling of τ. However, a further rescaling is later performed on ϕ and x in order to remove the redundant coupling associated to the spatial higher-derivative operator (σ in the notation of [170, 171]). It can be shown that the net effect of such operations corresponds to the choice $\alpha = 1/(2\zeta)$ in the α-dependent scheme of footnote 11. Therefore, universal quantities are not affected by such choice.

5.3 The quartic model

The results generalize mutatis mutandis to a model with quartic potential:

$$S_b[\phi_b] = \int d\tau d^d x \left\{ \frac{1}{2}\phi_b(\tau,x)\left[\left(-\partial^2\right)^\zeta - \partial_\tau^2\right]\phi_b(\tau,x) + \frac{\lambda_b}{4!}\phi_b(\tau,x)^4 \right\}, \tag{5.3.1}$$

While the field dimension is still $\Delta_\phi = \frac{d-\zeta}{2}$, the coupling has dimension $d+\zeta-4\Delta_\phi$. Therefore, the quartic interaction is marginal for $\zeta = \frac{d}{3}$ and weakly relevant for $\zeta = \frac{d+\epsilon}{3}$, corresponding to $d+\zeta-4\Delta_\phi = \epsilon$. Therefore, in order to have an interesting renormalization group flow, and keep $\zeta < 1$, we must stick to $d < 3$.

We can rephrase the statement about marginality from the point of view of power counting, which leads like before to the superficial divergence $\Lambda^{(d+\zeta)(P-V+1)-2\zeta P}$. However, this time we have $2P = 4V - n$, and thus the superficial divergence is $\Lambda^{d+\zeta-\frac{n}{2}(d-\zeta)+V(d-3\zeta)}$, which for $\zeta = \frac{d+\epsilon}{3}$ becomes $\Lambda^{\frac{d}{3}(4-n)-\epsilon(V-\frac{2+n}{6})}$. Therefore, for $\epsilon = 0$ the theory is renormalizable, with logarithmically-divergent four-point point graphs, while for $\epsilon > 0$ it is super-renormalizable, with finite four-point graphs.

The bare full correlators behave under rescaling as:

$$\begin{aligned} &F_b^{(n)}(\tau,x|\lambda_b) = l^{n\Delta_\phi} F_b^{(n)}(l^\zeta\tau, lx|l^{-\epsilon}\lambda_b) \\ &\quad\Rightarrow \quad \left[n\Delta_\phi - \epsilon\lambda_b\partial_{\lambda_b} + \zeta D_\tau + D_x\right] F_b^{(n)}(\tau,x|\lambda_b) = 0 \,, \end{aligned} \tag{5.3.2}$$

while the bare 1PI correlators behave as:

$$\begin{aligned} &\Gamma_b^{(n)}(\tau,x|\lambda_b) = l^{n(\zeta+d-\Delta_\phi)} \Gamma_b^{(n)}(l^\zeta\tau, lx|l^{-\epsilon}\lambda_b) \\ &\quad\Rightarrow \quad \left[n(\zeta+d-\Delta_\phi) - \epsilon\lambda_b\partial_{\lambda_b} + \zeta D_\tau + D_x\right] \Gamma_b^{(n)}(\tau,x|\lambda_b) = 0 \end{aligned} \tag{5.3.3}$$

Due to $\mathbb{Z}_2$ invariance of the model, only the correlators with even n are non-vanishing. For the $n = 2$ and 4 correlators in momentum space, with the global momentum and frequency conservation factored out, we have at one loop:

$$\begin{aligned} \bar\Gamma_b^{(2)}(\omega_0,p_0) &= \omega_0^2 + (p_0^2)^\zeta - \frac{1}{6}\lambda_b^2\, \mathcal{M}(\omega_0,p_0) \,, \\ \bar\Gamma_b^{(4)}(\omega_1,p_1;\omega_2,p_2;\omega_3,p_3) &= \lambda_b - \frac{1}{2}\lambda_b^2 \Big(\mathcal{B}(\omega_1+\omega_2,p_1+p_2) \\ &\qquad + \mathcal{B}(\omega_1+\omega_3,p_1+p_3) + \mathcal{B}(\omega_2+\omega_3,p_2+p_3) \Big) \,, \end{aligned} \tag{5.3.4}$$

where $\mathcal{M}$ and $\mathcal{B}$ are respectively the melon and the bubble diagrams depicted in Fig. 5.2 with amplitudes:

$$\begin{aligned} \mathcal{M}(\omega_0,p_0) &= \int \frac{d^dq_1\, d\omega_1}{(2\pi)^{d+1}} \int \frac{d^dq_2\, d\omega_2}{(2\pi)^{d+1}} \frac{1}{\omega_1^2+(q_1^2)^\zeta} \frac{1}{\omega_2^2+(q_2^2)^\zeta} \\ &\qquad \times \frac{1}{(\omega_0+\omega_1+\omega_2)^2 + [(p_0+q_1+q_2)^2]^\zeta} \,, \\ \mathcal{B}(\omega_0,p_0) &= \int \frac{d^dq\, d\omega}{(2\pi)^{d+1}} \frac{1}{\omega^2+(q^2)^\zeta} \frac{1}{(\omega_0+\omega)^2+[(p_0+q)^2]^\zeta} \,. \end{aligned} \tag{5.3.5}$$

As renormalization point we will take $(\omega_1,p_1) = (\omega_2,p_2) = (\omega_3,p_3) = (\mu^\zeta/2,0)$ and $(\omega_4,p_4) = (-\frac{3}{2}\mu^\zeta,0)$, so that $\omega_1+\omega_2 = \omega_1+\omega_3 = \omega_2+\omega_3 = \mu^\zeta$ and $\sum_i \omega_i = 0$.

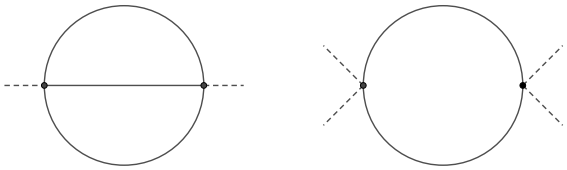

FIGURE 5.2: Left: melon diagram $\mathcal{M}(\omega_0, p_0)$. Right: bubble diagram $\mathcal{B}(\omega_1+\omega_2, p_1+p_2)$.

Notice that the bubble integral is exactly as the one we encountered for the two-point function of the cubic model, but in the present case it is to be evaluated in a different range of ζ, and it is now associated to a four-point function. The net effect is that in the quartic model we are not interested in $\partial_{\omega_0^2}\mathcal{B}(\mu^\zeta, 0)$, which in this case converges for $\epsilon \to 0$, but rather in $\mathcal{B}(\mu^\zeta, 0)$ itself, which has a $1/\epsilon$ pole.

The renormalized action is:

$$S_r[\phi] = \int d\tau d^d x \left\{ \frac{1}{2}\phi(\tau,x)\left[(-\partial^2)^\zeta - Z\,\partial_\tau^2\right]\phi(\tau,x) + \frac{1}{2}\delta m^{2\zeta}\,\phi(\tau,x)^2 + \frac{1}{4!}\lambda\,\phi(\tau,x)^4 \right\}, \tag{5.3.6}$$

with $\lambda = \mu^\epsilon g Z_g$ and counterterms $\delta Z(g) = Z - 1$, $\delta m^{2\zeta}$ and $\delta Z_g(g) = Z_g - 1$. We will again employ analytic regularization and ignore the mass counterterm. For the other two counterterms we have, in the minimal subtraction scheme, an expression like (5.2.23), where however the coefficients $\alpha_\ell(g)$ and $\gamma_\ell(g)$ are now starting at order $g^{\ell+1}$ and g^ℓ, respectively.[15]

The renormalized 1PI two and four-point functions write at first nontrivial order in g:

$$\begin{aligned}
\bar\Gamma_r^{(2)}(\omega_0, p_0) &= [1+\delta Z(g)]\;\omega_0^2 + (p_0^2)^\zeta - \frac{1}{6}\mu^{2\epsilon} g^2\;\mathcal{M}(\omega_0, p_0)\;, \\
\bar\Gamma_r^{(4)}(\omega_1,p_1;\omega_2,p_2;\omega_3,p_3) &= \mu^\epsilon g[1+\delta Z_g(g)] - \frac{1}{2}\mu^{2\epsilon} g^2\;\Big(\mathcal{B}(\omega_1+\omega_2, p_1+p_2) \\
&\qquad + \mathcal{B}(\omega_1+\omega_3, p_1+p_3) + \mathcal{B}(\omega_2+\omega_3, p_2+p_3)\Big)\;,
\end{aligned} \tag{5.3.7}$$

with singular behaviour:

$$\partial_{\omega_0^2}\mathcal{M}(\mu^\zeta, 0) = -\mu^{-2\epsilon}\frac{M}{\epsilon} + \text{finite}\;, \qquad \mathcal{B}(\mu^\zeta, 0) = \mu^{-\epsilon}\frac{B}{\epsilon} + \text{finite}\;, \tag{5.3.8}$$

with B and M given in appendix 5.A, hence the minimal subtraction counterterms that ensure that the divergences are subtracted are:

$$\delta Z(g) = -\frac{1}{6}\,g^2\,\frac{M}{\epsilon}\;, \qquad \delta Z_g(g) = \frac{3}{2}\,g\,\frac{B}{\epsilon}\;. \tag{5.3.9}$$

[15] In this case order-ℓ poles appear first at $\ell+1$ loops, for $\partial_{\omega^2}\bar\Gamma_b^{(2)}$, and at ℓ loops, for $\bar\Gamma_b^{(4)}$. Moreover, the topological relation is now $4V = 2P + n$.

The renormalized theory maps onto the bare one by the following field redefinition and change of couplings:

$$\phi(\tau,x) = Z^{-\frac{1}{4}}\phi_b(Z^{-\frac{1}{2}}\tau,x)\ , \qquad \lambda Z^{-\frac{1}{2}} = \lambda_b\ . \tag{5.3.10}$$

The structure of the beta function is slightly altered with respect to the cubic case:

$$\mu\frac{d}{d\mu}\left[\mu^\epsilon g Z_g Z^{-\frac{1}{2}}\right] = 0 \qquad \Rightarrow \qquad \beta = -\frac{\epsilon g}{1+g\frac{Z'_g}{Z_g}-\frac{1}{2}g\frac{Z'}{Z}}\ , \qquad \eta = \beta\frac{Z'}{Z}\ , \tag{5.3.11}$$

where again a prime denotes a derivative with respect to g. Using the expansion (5.2.23) in powers of $1/\epsilon$ for the counterterms, we find:

$$\beta(g) = -\frac{\epsilon}{2}g + \frac{g^2}{2}\left(\gamma'_1(g) - \frac{\alpha'_1(g)}{2}\right)\ , \tag{5.3.12}$$

and all the contributions from α_n and γ_n with $n>1$, as well as higher powers of the $n=1$ terms, must cancel for consistency. At leading order we have $\alpha_1(g) = -\frac{1}{6}g^2\,M$ and $\gamma_1(g) = \frac{3}{2}\,g\,B$, hence we get:[16]

$$\beta(g) = -\epsilon g + \frac{3}{2}g^2 B + O(g^3)\ , \qquad \eta(g) = \frac{1}{3}\,g^2 M + O(g^3)\ , \tag{5.3.13}$$

with fixed point $g_\star = \frac{2\epsilon}{3B}$, and anomalous dimension $\eta_\star = \frac{4\epsilon^2 M}{27B^2}$.

The renormalized correlators write in terms of bare ones as:

$$F_r^{(n)}(\tau,x|g,\mu) = Z^{-\frac{n}{4}}F_b^{(n)}(Z^{-\frac{1}{2}}\tau,x|\mu^\epsilon g Z_g Z^{-\frac{1}{2}})\ , \tag{5.3.14}$$

and hence the Callan-Symanzik equation is unchanged. In particular, we find again:

$$\left[n(\Delta_\phi+\frac{\eta}{4}) + (\zeta+\frac{\eta}{2})D_\tau + D_x + \beta\partial_g\right]F_r^{(n)} = 0\ . \tag{5.3.15}$$

Recalling that $\Delta_\phi = \frac{d-\zeta}{2}$, we conclude as in the cubic case that at the fixed point the correlators are eigenfucntions of the anisotropic scaling operator $zD_\tau + D_x$, with the following dynamic exponent and scaling dimension:

$$\begin{aligned} z &= \zeta + \frac{\eta_\star}{2} = \frac{d+\epsilon}{3} + \frac{2\epsilon^2 M}{27B^2}\ , \\ \Delta_\star &= \Delta_\phi + \frac{\eta_\star}{4} = \frac{2d-\epsilon}{6} + \frac{\epsilon^2 M}{27B^2}\ , \end{aligned} \tag{5.3.16}$$

with the constants B and M given in (5.A.6) and (5.A.19), respectively.

[16] The melon contribution, corresponding to a two-loops diagram, does not enter the beta function in our leading-order approximation: it would contribute at order g^3, together with contributions from two-loops four-point diagrams. It is common to consider a strict one-loop approximation, so that the anomalous dimension is vanishing; however, because of such vanishing, it is also consistent to consider $\beta(g)$ and $\eta(g)$ at the same order in g, as we do here, rather than at the same loop order.

5.A Integrals

5.A.1 The bubble integral, $\mathcal{B}$

The bubble integral writes:

$$\mathcal{B}(\omega_0, p_0) = \int \frac{d^d q\, d\omega}{(2\pi)^{d+1}} \frac{1}{\omega^2 + (q^2)^\zeta} \frac{1}{(\omega_0+\omega)^2 + [(p_0+q)^2]^\zeta} . \tag{5.A.1}$$

The integral is in general quite challenging, but when $p_0 = 0$ one can integrate ω by deforming the contour in the complex plane and using the residue theorem, and then use the spherical symmetry of the spacial momentum integral to obtain:

$$\mathcal{B}(\omega_0, 0) = \int \frac{d^d q}{(2\pi)^d} \frac{(q^2)^{-\zeta/2}}{4(q^2)^\zeta + \omega_0^2} = -\frac{2^{1-\frac{d}{\zeta}} \pi \omega_0^{\frac{d}{\zeta}-3}}{(4\pi)^{\frac{d}{2}} \Gamma(\frac{d}{2}) \zeta \cos(\frac{\pi d}{2\zeta})} . \tag{5.A.2}$$

In the evaluation of the spatial integral we have assumed $\zeta \in (d/3, d)$, where it is convergent. Analytic regularization amounts to analytically continuing the result to the region of interest.

In the cubic model we are interested in $0 < \zeta - d/5 \ll 1$. In order to extract the coefficient b of equation (5.2.25) we take a derivative with respect to ω_0^2, and set $\omega_0 = \mu^\zeta$ and $\zeta = \frac{d+\epsilon}{5}$. We find:

$$\partial_{\omega_0^2} \mathcal{B}(\mu^\zeta, 0) = -\mu^{-\epsilon} \frac{2^{-d-3} \pi^{-\frac{d}{2}}}{\epsilon \Gamma\left(\frac{d}{2}\right)} + O(1) , \tag{5.A.3}$$

and therefore:

$$b = \frac{2^{-d-3} \pi^{-\frac{d}{2}}}{\Gamma\left(\frac{d}{2}\right)} . \tag{5.A.4}$$

In the quartic model, we are instead interested in $0 < \zeta - d/3 \ll 1$, which lies in the range of convergence. In this case, in order to extract the coefficient B of equation (5.3.8) we do not take any derivative, and we directly set $\omega_0 = \mu^\zeta$ and $\zeta = \frac{d+\epsilon}{3}$. We find:

$$\mathcal{B}(\mu^\zeta, 0) = \mu^{-\epsilon} \frac{2^{-d-1} \pi^{-\frac{d}{2}}}{\epsilon \Gamma\left(\frac{d}{2}\right)} + O(1) , \tag{5.A.5}$$

and therefore:

$$B = \frac{2^{-d-1} \pi^{-\frac{d}{2}}}{\Gamma\left(\frac{d}{2}\right)} = 4b . \tag{5.A.6}$$

5.A.2 The triangle integral, $\mathcal{T}$

The triangle integral at the subtraction point writes:

$$\mathcal{T}(\mu^\zeta, 0; -\mu^\zeta, 0) = \int \frac{d\omega d^d q}{(2\pi)^{d+1}} \frac{1}{[\omega^2 + (q^2)^\zeta]^2} \frac{1}{(\omega+\mu^\zeta)^2 + (q^2)^\zeta} . \tag{5.A.7}$$

Using again the residue theorem we find:

$$\mathcal{T}(\mu^\zeta, 0; -\mu^\zeta, 0) = \int \frac{d^d q}{(2\pi)^d} \frac{q^{-3\zeta}\left(12 q^{2\zeta} + \mu^{2\zeta}\right)}{4\left(4q^{2\zeta} + \mu^{2\zeta}\right)^2} = \frac{\pi^{1-\frac{d}{2}} 2^{1-\frac{d(\zeta+1)}{\zeta}} (d-2\zeta) \mu^{d-5\zeta}}{\zeta^2 \Gamma\left(\frac{d}{2}\right) \cos\left(\frac{\pi d}{2\zeta}\right)} , \tag{5.A.8}$$

where the spatial momentum integral is convergent in the interval $\zeta \in (d/5, d/3)$, which includes $\zeta = \frac{d+\epsilon}{5}$. For small ϵ we find:

$$\mathcal{T}(\mu^\zeta, 0; -\mu^\zeta, 0) = \mu^{-\epsilon}\, 3\, \frac{2^{-d-3}\pi^{-\frac{d}{2}}}{\epsilon\Gamma\left(\frac{d}{2}\right)} + O(1)\,, \tag{5.A.9}$$

and therefore, the coefficient t of equation (5.2.25) is:

$$t = 3\, \frac{2^{-d-3}\pi^{-\frac{d}{2}}}{\Gamma\left(\frac{d}{2}\right)} = 3b\,. \tag{5.A.10}$$

We can also verify that the above result is independent of the choice of c in (5.2.22). For general c we have:

$$\mathcal{T}(\mu^\zeta, 0; -(1+c)\mu^\zeta, 0) = \int \frac{d\omega d^d q}{(2\pi)^{d+1}}\, \frac{1}{\omega^2 + (q^2)^\zeta}\, \frac{1}{(\omega+\mu^\zeta)^2 + (q^2)^\zeta}\, \frac{1}{(\omega - c\mu^\zeta)^2 + (q^2)^\zeta}\,. \tag{5.A.11}$$

The integration of the frequency can be performed again by residue theorem, and the remaining integral in spherical coordinates is:

$$\mathcal{T}(\mu^\zeta, 0; -(1+c)\mu^\zeta, 0) = \frac{2^{1-d}\pi^{-\frac{d}{2}}}{\Gamma\left(\frac{d}{2}\right)} \int_0^{+\infty} dq\, \frac{q^{d-1-\zeta}(12q^{2\zeta} + (1+c+c^2)\mu^{2\zeta})}{(4q^{2\zeta}+\mu^{2\zeta})(4q^{2\zeta}+c^2\mu^{2\zeta})(4q^{2\zeta}+(1+c)^2\mu^{2\zeta})}\,, \tag{5.A.12}$$

which we could not evaluate explicitly. However, we can extract the $1/\epsilon$ pole by the following reasoning. The integral is convergent for $\zeta \in (d/5, d)$. At $\zeta = \frac{d}{5}$, it is logarithmically divergent, and as it does not contain sub-divergences, in analytic regularization it diverges as a simple pole in ϵ. Moreover, the coefficient of such pole does not depend on the infrared regulator. Since the ultraviolet divergence that generates the $1/\epsilon$ pole arises at large momenta, we can set $\mu = 0$ in the integrand and compute the integral with a sharp cut-off instead to extract the universal coefficient of the ϵ pole. We find as before:

$$\mathcal{T}(\mu^\zeta, 0; -(1+c)\mu^\zeta, 0) = \mu^{-\epsilon}\, 3\, \frac{2^{-d-3}\pi^{-\frac{d}{2}}}{\epsilon\Gamma\left(\frac{d}{2}\right)} + O(1)\,. \tag{5.A.13}$$

5.A.3 The melon integral, $\mathcal{M}$

The melon integral writes:

$$\begin{aligned}\mathcal{M}(\omega_0, 0) = \int \frac{d^d q_1\, d\omega_1}{(2\pi)^{d+1}} \int \frac{d^d q_2\, d\omega_2}{(2\pi)^{d+1}}\, &\frac{1}{\omega_1^2 + (q_1^2)^\zeta} \\ &\times \frac{1}{(\omega_0+\omega_1+\omega_2)^2 + [(q_1+q_2)^2]^\zeta}\,,\end{aligned} \tag{5.A.14}$$

which becomes, using the Schwinger parametrization:

$$\begin{aligned}\mathcal{M}(\omega_0,0) &= \int \frac{d^dq_1\,d\omega_1}{(2\pi)^{d+1}} \int \frac{d^dq_2\,d\omega_2}{(2\pi)^{d+1}} \int_0^{+\infty} d\alpha_1 d\alpha_2 d\alpha_3 \\ &\qquad \times\ e^{-\alpha_1(\omega_1^2+(q_1^2)^\zeta)-\alpha_2(\omega_2^2+(q_2^2)^\zeta)-\alpha_3((\omega_0+\omega_1+\omega_2)^2+[(q_1+q_2)^2]^\zeta)} \\ &= \int \frac{d^dq_1}{(2\pi)^d} \int \frac{d^dq_2}{(2\pi)^d} \int_0^{+\infty} d\alpha_1 d\alpha_2 d\alpha_3 \\ &\qquad \times\ e^{-\alpha_1(q_1^2)^\zeta-\alpha_2(q_2^2)^\zeta-\alpha_3[(q_1+q_2)^2]^\zeta} \frac{e^{-\frac{\alpha_1\alpha_2\alpha_3\omega_0^2}{\alpha_1\alpha_2+\alpha_1\alpha_3+\alpha_2\alpha_3}}}{4\pi\sqrt{\alpha_1\alpha_2+\alpha_1\alpha_3+\alpha_2\alpha_3}}\,.\end{aligned} \tag{5.A.15}$$

Next, taking the derivative with respect to ω_0^2 and setting the latter to zero, we obtain:

$$\begin{aligned}\partial_{\omega_0^2}\mathcal{M}(0,0) &= -\int_{|q_1|\geq\mu} \frac{d^dq_1}{(2\pi)^d} \int_{|q_2|\geq\mu} \frac{d^dq_2}{(2\pi)^d} \int_0^{+\infty} d\alpha_1 d\alpha_2 d\alpha_3 \\ &\qquad \times\ e^{-\alpha_1(q_1^2)^\zeta-\alpha_2(q_2^2)^\zeta-\alpha_3[(q_1+q_2)^2]^\zeta} \frac{\alpha_1\alpha_2\alpha_3}{4\pi(\alpha_1\alpha_2+\alpha_1\alpha_3+\alpha_2\alpha_3)^{3/2}}\,.\end{aligned} \tag{5.A.16}$$

The subscript on the momentum integrals signals that, as we have set $\omega_0 = 0$, the integral is infrared divergent and needs a cutoff μ. As we are only interested in the leading ultraviolet divergence, the precise form of the infrared regulator is irrelevant.

In the sector $\alpha_3 > \alpha_1, \alpha_2$, we make the redefinition $\alpha_i = t_i\alpha_3$ for $i = 1, 2$, and integrate over α_3. Taking into account that we have 3 sectors, we obtain:

$$\begin{aligned}\partial_{\omega_0^2}\mathcal{M}(0,0) &= -\frac{3}{2\pi}\int_0^1 dt_1 dt_2 \frac{t_1t_2}{(t_1+t_2+t_1t_2)^{3/2}} \\ &\qquad \times \int_{|q_1|\geq\mu} \frac{d^dq_1}{(2\pi)^d} \int_{|q_2|\geq\mu} \frac{d^dq_2}{(2\pi)^d} \frac{1}{(t_1(q_1^2)^\zeta + t_2(q_2^2)^\zeta + [(q_1+q_2)^2]^\zeta)^3}\,.\end{aligned} \tag{5.A.17}$$

In order to extract the residue of $1/\epsilon$ pole we use the following strategy. For $d > 1$, we go to spherical coordinates and integrate out the angular coordinates, except the angle between q_1 and q_2, which we denote θ. Then, we define a vector with the moduli of q_1 and q_2 as components $q = (|q_1|, |q_2|)$, and we switch to polar coordinates $q \to (p, \varphi)$, with $p = |q|$ and $\varphi \in (0, \pi/2)$. We get:

$$\begin{aligned}\partial_{\omega_0^2}\mathcal{M}(0,0) &= -\frac{3S_{d-1}S_{d-2}}{(2\pi)^{2d+1}} \int_0^1 dt_1 dt_2 \frac{t_1t_2}{(t_1+t_2+t_1t_2)^{3/2}} \int_{\sqrt{2}\mu}^\infty dp \frac{p^{2d-1}}{p^{6\zeta}} \\ &\times \int_0^\pi d\theta \int_0^{\pi/2} d\varphi \frac{\sin^{d-2}(\theta)\sin^{d-1}(\varphi)\cos^{d-1}(\varphi)}{\left(t_1\left(\cos^2(\varphi)\right)^\zeta + t_2\left(\sin^2(\varphi)\right)^\zeta + [1+2\cos(\theta)\sin(\varphi)\cos(\varphi)]^\zeta\right)^3}\,,\end{aligned} \tag{5.A.18}$$

where S_n is the volume of the n-sphere.

The integral over p is convergent for $\zeta = \frac{d+\epsilon}{3} > d/3$ and it has a $1/\epsilon$ pole, $\int_{\sqrt{2}\mu}^\infty p^{-1-2\epsilon} = \frac{\mu^{-2\epsilon}}{2^{1+\epsilon}\epsilon}$. It follows that the coefficient M in (5.3.8) is:

$$\begin{aligned}M &= \frac{3S_{d-1}S_{d-2}}{2(2\pi)^{2d+1}} \int_0^1 dt_1 dt_2 \frac{t_1t_2}{(t_1+t_2+t_1t_2)^{3/2}} \\ &\times \int_0^\pi d\theta \int_0^{\pi/2} d\varphi \frac{\sin^{d-2}(\theta)\sin^{d-1}(\varphi)\cos^{d-1}(\varphi)}{\left(t_1\left(\cos^2(\varphi)\right)^{d/3} + t_2\left(\sin^2(\varphi)\right)^{d/3} + [1+2\cos(\theta)\sin(\varphi)\cos(\varphi)]^{d/3}\right)^3}\,,\end{aligned} \tag{5.A.19}$$

and the remaining integrals are convergent and can be evaluated numerically.

For $d = 1$, there is no angular integration for the two momenta, and performing directly the change of variables $(q_1, q_2) \to (p, \varphi)$, where now $\varphi \in (0, 2\pi)$, we get:

$$M = \frac{3}{2(2\pi)^3} \int_0^1 dt_1 dt_2 \frac{t_1 t_2}{(t_1 + t_2 + t_1 t_2)^{3/2}} \times \int_0^{2\pi} d\varphi \frac{1}{\left(t_1 \left(\cos^2(\varphi)\right)^{1/3} + t_2 \left(\sin^2(\varphi)\right)^{1/3} + \left[1 + 2\sin(\varphi)\cos(\varphi)\right]^{1/3} \right)^3} . \tag{5.A.20}$$

A numerical evaluation with 1% precision gives:

$$M \simeq \begin{cases} 3.19 \times 10^{-4} & \text{for } d = 2 \\ 2.66 \times 10^{-3} & \text{for } d = 1 \end{cases} . \tag{5.A.21}$$

Chapter 6

The small N series of zero-dimensional $O(N)$ model

The most famous problem of the perturbative expansion in quantum field theory is the existence of ultraviolet divergences in the amplitudes of Feynman diagrams. This is successfully dealt with using the theory of perturbative renormalization. However, even in one and zero dimensions (quantum mechanics and combinatorial models, respectively), where renormalization is not needed, perturbation theory poses another notorious challenge: in most cases the perturbative series is only an asymptotic series, with zero radius of convergence. Borel resummation is the standard strategy to address this problem, but this comes with its own subtleties. From a practical standpoint, we are often only able to compute just the first few terms in the perturbative expansion. At a more fundamental level, singularities are present in the Borel plane, associated to instantons (and renormalons in higher dimensions). The instanton singularities are not accidental: they stem from the factorial growth of the number of Feynamn diagrams with the perturbation order, which is also the origin of the divergence of the perturbation series.[1]

From the resummation point of view, the most inconvenient feature of perturbation theory is that it does not naively capture contributions from non-analytical terms. For example, it is well known that instanton contributions of the type $e^{-1/g}$ ($g > 0$ being the coupling constant) can be present in the evaluation of some quantity of interest, but they are missed in the perturbative series as their Taylor expansion at $g = 0$ vanishes identically.

Such exponentially suppressed terms are the archetypal example of nonperturbative effects, and their evaluation poses an interesting challenge. Aiming to include them, but still relying for practical reasons on perturbative methods, one ends up with a more general form of asymptotic expansion, known as *transseries*, which is roughly speaking a sum of perturbative and nonperturbative sectors, for example:

$$F(g) \simeq \sum_{n\geq 0} a_n\, g^n + \sum_i e^{\frac{c_i}{g}}\, g^{\gamma_i} \sum_{n\geq 0} b_{i,n}\, g^n \,. \tag{6.0.1}$$

Over time it became increasingly clear that, in many examples of interest, using the theory of Borel summation for the perturbative sector it is possible to reconstruct some information about the nonperturbative ones. This relation between the perturbative and nonperturbative sectors is known as *resurgence*, and it was originally developed by Écalle in the context of ordinary differential equations [21] (see [183] for a modern review). Ideas coming from resurgence theory were extensively used in quantum field theory: for recent reviews with a quantum field theory scope, see [184, 185, 186], and in particular [187], which contains also a comprehensive list of references to applications and other reviews.

[1] The renormalon singularities specific to higher dimensions, are different. They are located on the positive real axis and stem from the factorial growth of the renormalized amplitude of a family of diagrams consisting in essentially one diagram per perturbation order.

Zero-dimensional quantum field theoretical models, which are purely combinatorial models,[2] are useful toy models for the study of transseries expansions. Most conveniently, they allow one to set aside all the complications arising from the evaluation and renormalization of Feynman diagrams. Moreover, their partition functions and correlations typically satisfy ordinary differential equations, thus fitting naturally in the framework of Écalle's theory of resurgence. The zero dimensional ϕ^4, or more generally ϕ^{2k} with $k \geq 2$, models in zero dimensions have been exhaustively studied [187, 190]. From a physics perspective, the current mathematical literature on resurgence deals mainly with such zero dimensional models.

At the opposite end, the rigorous study of the Borel summability in fully fledged quantum field theory is the object of constructive field theory [191, 114, 192]. It should come as no surprise that the generalization of results on resurgence in zero dimensions to the higher dimensional setting is very much an open topic: while Écalle's theory can serve as good inspiration, as in [184, 185, 186, 187], the rigorous study of resurgence in higher dimensional quantum field theory is much more involved. First of all, in higher dimensions the partition function (and correlators) does not obey an ordinary differential equation, and one cannot simply invoke Écalle's theory. Moreover, the coefficients of the perturbative series are given by divergent Feynman amplitudes, which need to be renormalized, leading to a running coupling. Incorporating the effects of renormalization in the resurgence analysis is an open question (see for instance [193] for an investigation of resurgence in the Callan–Symanzik renormalization group equation). One thing is clear: in order to answer such questions it is insufficient to simply invoke the current theory of resurgence, and one needs to develop new techniques adapted to the more general context of quantum field theory.

From this perspective, revisiting the resurgence in zero dimensional models using techniques inspired by constructive field theory can be of great use. Following such route, we consider the zero-dimensional $O(N)$ model with quartic potential.[3] Denoting $\phi = (\phi_a)_{a=1,\dots N} \in \mathbb{R}^N$ a vector in $\mathbb{R}^N$ and $\phi^2 = \sum_{a=1}^N \phi_a \phi_a$ the $O(N)$ invariant, the partition function of the model is:[4]

$$Z(g,N) = \int_{-\infty}^{+\infty} \left(\prod_{a=1}^{N} \frac{d\phi_a}{\sqrt{2\pi}} \right) e^{-S[\phi]} , \qquad S[\phi] = \frac{1}{2}\phi^2 + \frac{g}{4!}(\phi^2)^2 . \tag{6.0.2}$$

The $N = 1$ case has been extensively studied in [187]. One can analytically continue $Z(g,1)$, regarded as a function of the coupling constant g, to a maximal domain in the complex plane. Subsequently, one discovers that $Z(g,1)$ displays a branch cut at the real negative axis and that the nonperturbative contributions to $Z(g,1)$ are captured by its discontinuity at the branch cut. A resurgent transseries is obtained when one considers g as a point on a Riemann surface with a branch point at $g = 0$. From now on we parameterize this Riemann surface as $g = |g|e^{\imath\varphi}$ and we choose as principal sheet $\varphi \in (-\pi, \pi)$.

An approach to the study of the partition function in (6.0.2) in the case $N = 1$ is to use the steepest-descent method [195, 196]. We concisely review this in Appendix 6.A. One notes that on the principal sheet only one Lefschetz thimble contributes. As g sweeps through the principal sheet the thimble is smoothly deformed, but not in the neighborhood of the saddle point: the asymptotic evaluation of the integral is unchanged. When g reaches the negative real axis there is a discontinuous jump in the relevant thimbles and a pair of thimbles (passing through a pair of conjugated non trivial

[2] These are for example of interest in the context of random geometry, see for example [188, 14, 189].

[3] The same model has been considered in a similar context in [194], where the problem of constructing Lefschetz thimbles in the N-dimensional space have been studied. By using the intermediate field formalism we will bypass such problem here.

[4] Note that we do not use the usual normalization $g/4$ of the interaction in the $O(N)$ model, but stick to $g/4!$ in order to facilitate the comparison with the literature on transseries which deals mostly with the $N = 1$ case for which the normalization $g/4!$ is standard. Also, we do not use the 't Hooft coupling $\lambda = gN$, which is needed for a well defined $1/N$ expansion: in this chapter we keep N small.

saddle points of the action) starts contributing, giving rise to a one-instanton sector in the transseries of $Z(g,1)$.

Another approach to the transseries expansion of $Z(g,1)$ is to use the theory of ordinary differential equations [187, 190]. It turns out that $Z(g,1)$ obeys a second-order homogeneous linear ordinary differential equation for which $g=0$ is an irregular singular point (e.g. [195]), giving another perspective on why the expansion one obtains is only asymptotic.

More interestingly, one can wonder what can be said about the nonperturbative contributions to the free energy, that is, the logarithm of the partition function $W(g,1)=\ln Z(g,1)$, or to the connected correlation functions. If we aim to study the free energy, the steepest-descent method does not generalize straightforwardly as we lack a simple integral representation for $W(g,1)$. One can formally write $Z(g,1)$ as a transseries and then expand the logarithm in powers of the transseries monomial $e^{\frac{c}{g}}$, thus obtaining a multi-instanton transseries. However this is very formal, as the transseries is only an asymptotic expansion, and we would like to have a direct way to obtain the asymptotic expansion of $W(g,1)$. The closest one can get to an integral formula for the free energy is to use the Loop Vertex Expansion (LVE) [22]. This constructive field theory expansion is a combination of the intermediate field representation with the Brydges-Kennedy-Abdesselam-Rivasseau (BKAR) formula and has successfully been used in higher dimensional quantum field theory [25] to prove Borel summability results and even study the decay of the correlations (note however that the results of [25] concern a theory with fixed UV and IR cutoffs, bypassing the issue of the renormalization group flow). However, deriving directly the transseries expansion of $W(g,1)$ using the steepest-descent method on the LVE expansion proved so far impractical. One can study the transseries expansion of $W(g,1)$ using again the theory of ordinary differential equations as $W(g,1)$ obeys a nonlinear ordinary differential equation [187] but this can not be directly generalized to higher dimensions.

In this chapter, we consider a general N and we revisit both the partition function $Z(g,N)$ and the free energy $W(g,N)$ from a different angle. We focus in particular on the small-N expansion, which provides a natural interpretation for the LVE. Such expansion could be physically interesting in higher dimensions, where the $N\to 0$ limit of the model is related to self-avoiding random walks [197], an active area of investigation in modern statistical physics [198]. However, it should be noticed that our results will not be confined to infinitesimal N, as such expansion has a finite radius of convergence (Proposition 2 below).

The aim of our analysis is not to "solve the problem" of computing the transseries expansion of $Z(g,N)$ or $W(g,N)$: this can be done almost immediately using known results about special functions and classical results in resurgence theory. Our aim is to analyze these objects using techniques one can then employ in the interesting case of quantum field theory in higher dimensions. Our main results are the use of the Hubbard-Stratonovich intermediate field formulation to introduce a small-N expansion (Section 6.1.2), the application of the LVE to prove analyticity and Borel summability results for the free energy (Section 6.2.1), *in N and g*, and the study of the resurgence properties of the LVE expansion. The results of our study provide a proof of concept for a set of techniques which can be employed in higher dimensions, starting in the quantum mechanical case and then moving on to quantum field theory.

The chapter is organized as follows. In Section 6.1, we study $Z(g,N)$ in the intermediate field representation. This allows us to quickly prove its Borel summability along all the rays in the cut complex plane $\mathbb{C}_\pi=\mathbb{C}\setminus\mathbb{R}_-$. More importantly, the intermediate field representation provides a new perspective on the origin of the instanton contributions: in this representation, the steepest-descent contour never changes, but when g reaches the negative real axis a singularity traverses it and detaches a Hankel contour around a cut. We insist that this Hankel contour is *not* a steepest-descent contour, but it *does* contribute to the asymptotic evaluation of the integral, because the cut is an obstruction when deforming the contour of integration towards the steepest-descent path. It is precisely the Hankel contour that yields the one-instanton contribution. We then build the analytic continuation of $Z(g,N)$

to the whole Riemann surface, identify a second Stokes line, compute the Stokes data encoding the jumps in the analytic continuation at the Stokes lines and discuss the monodromy of $Z(g,N)$. Next we observe that, because in the intermediate field representation N appears only as a parameter in the action, we can perform a small-N expansion:

$$Z(g,N) = \sum_{n\geq 0} \frac{1}{n!} \left(-\frac{N}{2}\right)^n Z_n(g) \,. \tag{6.0.3}$$

We thus study $Z_n(g)$ for all integer n, proving its Borel summability in $\mathbb{C}_\pi$ and computing its transseries expansion in an extended sector of the Riemann surface, with $\arg(g) \in (-3\pi/2, 3\pi/2)$, which we denote $\mathbb{C}_{3\pi/2}$.

In Section 6.2, we proceed to study $W(g,N) = \ln(Z(g,N))$. We first establish its Borel summability along all the rays in $\mathbb{C}_\pi$ using constructive field theory techniques. We then proceed to the small-N expansion of this object:

$$W(g,N) = \sum_{n\geq 1} \frac{1}{n!} \left(-\frac{N}{2}\right)^n W_n(g) \,, \tag{6.0.4}$$

and prove that this is an absolutely convergent series in a subdomain of $\mathbb{C}_{3\pi/2}$ and that both $W(g,N)$ and $W_n(g)$ are Borel summable along all the rays in $\mathbb{C}_\pi$. Finally, in order to obtain the transseries expansion of $W_n(g)$ and $W(g,N)$ we note that $W_n(g)$ can be written in terms of $Z_n(g)$ using the Möbius inversion formula relating moments and cumulants. Because of the absolute convergence of the small-N series, it makes sense to perform the asymptotic expansion term by term, and thus we rigorously obtain the transseries for $W(g,N)$ in a subdomain of $\mathbb{C}_{3\pi/2}$. In the Appendices we gather some technical results, and the proofs of our propositions.

Ultimately, we obtain less information on the Stokes data for $W(g,N)$ than for $Z(g,N)$. While for $Z(g,N)$ we are able to maintain analytic control in the whole Riemann surface of g, the constructive field theory techniques we employ here allow us to keep control over $W(g,N)$ as an analytic function on the Riemann surface only up to $\varphi = \pm 3\pi/2$, that is past the first Stokes line, but not up to the second one. The reason for this is that close to $\varphi = \pm 3\pi/2$ there is an accumulation of Lee-Yang zeros, that is zeros of $Z(g,N)$, which make the explicit analytic continuation of $W(g,N)$ past this sector highly non trivial. New techniques are needed if one aims to recover the Stokes data for $W(g,N)$ farther on the Riemann surface: an analysis of the differential equation obeyed by $W(g,N)$ similar to the one of [199] could provide an alternative way to access it directly.

One can naturally ask what is the interplay between our results at small N and the large-N nonperturbative effects, first studied for the zero-dimensional $O(N)$ model in [200] (see also [184] for a general review, and [201] for a more recent point view). This is a very interesting question: indeed, the relation between the two expansions is a bit more subtle than the relation between the small coupling and the large coupling expansions for instance. The reason is that, when building the large-N series, one needs to use the 't Hooft coupling, which is a rescaling of the coupling constant by a factor of N. This changes the N-dependence of the partition function and free energy, making the relation between small-N and large-N expansions nontrivial. A good news on this front is that the analyticity domains in g becomes uniform in N when recast in terms of the 't Hooft coupling [202]. But there is still quite some work to do in order to connect the transseries analysis at small N with that at large N. However, we stress once more that, while the large-N expansion is asymptotic, the small-N expansion is convergent.

Main results. Our main results are the following:

- In Proposition 1, we study $Z(g,N)$. While most of the results in this proposition are known for $N = 1$, we recover them using the intermediate field representation (which provides a new point

of view) and generalize them to arbitrary $N \in \mathbb{R}$. In particular we uncover an interplay between $Z(g, N)$ and $Z(-g, 2-N)$ in the transseries expansion of the partition function for general N.

- Proposition 2 deals with the function $Z_n(g)$, notably its Borel summability, transseries, and associated differential equation. To our knowledge, $Z_n(g)$ has not been studied before and all of the results presented here are new.
- Proposition 3 and 4 generalize previous results in the literature [203] on the analyticity and Borel summability of $W(g, 1)$ to $W(g, N)$ and furthermore derive parallel results for $W_n(g)$.
- Proposition 5 contains the transseries expansion of $W_n(g)$, which has not been previously considered in the literature. We also give a closed formula for the transseries expansion of $W(g, N)$.
- Lastly, in Proposition 6, we derive the tower of recursive differential equations obeyed by $W_n(g)$. This serves as an invitation for future studies of the transseries of $W_n(g)$ from an ordinary differential equations perspective.

The natural next step is to explore how this picture is altered in higher dimensions. While this is a wide open question, several lessons can be learned from our present work. First, the small N series for the free energy W obtained via the LVE expansion will very likely be convergent, hence one should be able to study the resurgence properties of W by first studying such properties for the "cumulants" W_n, which can be done by studying the "moments Z_n" and using Möbius inversion. Second, for the moments Z_n, the steepest descent contour in the intermediate σ field representation will be insensitive to the coupling constant, hence in this representation the Stokes phenomenon will correspond to singularities crossing this fixed contour.

6.1 The partition function $Z(g, N)$

In this Section we collect some facts about the asymptotic expansion of the partition function (6.0.2). Most of them are known, or derivable from the expression of the $Z(g, N)$ in terms of special functions, whose asymptotic expansions are to a large degree known [204]. Nonetheless we present a "path integral–like" derivation and rather explicit formulae for the coefficients that should be useful, as they are more directly generalizable, in applications to proper field theories.

We study $Z(g, N)$ by means of the Hubbard-Stratonovich intermediate field formulation [205, 206], which is crucial to the Loop Vertex Expansion [22] of the free energy $W(g, N)$ that we will study below. This is based on rewriting the quartic term of the action as a Gaussian integral over an auxiliary variable σ (or field, in higher dimensions):

$$e^{-\frac{g}{4!}(\phi^2)^2} = \int_{-\infty}^{+\infty} [d\sigma]\; e^{-\frac{1}{2}\sigma^2 + \imath\sqrt{\frac{g}{12}}\sigma\phi^2}\;, \tag{6.1.1}$$

where the Gaussian measure over σ is normalized, i.e. $[d\sigma] = d\sigma/\sqrt{2\pi}$ and $\imath = e^{\imath\frac{\pi}{2}}$. Note that σ is a real number, not a vector. With this trick, the integral over ϕ becomes Gaussian and can be performed for $g > 0$, leading to a rewriting of the partition function (6.0.2) as:

$$Z(g, N) = \int_{-\infty}^{+\infty} [d\sigma]\; e^{-\frac{1}{2}\sigma^2} \frac{1}{\left(1 - \imath\sqrt{\frac{g}{3}}\sigma\right)^{N/2}}\;. \tag{6.1.2}$$

Although the original partition function is defined only for integer N and we have assumed that $g > 0$, in the σ representation (6.1.2) it becomes transparent that $Z(g, N)$ can be analytically continued both in N and in g.

6.1.1 Analytic continuation and transseries

As a matter of notation, we denote $\varphi \equiv \arg(g)$, and, in order to label some sets that will appear repeatedly in the rest of the chapter, we define:

$$\mathbb{C}_\psi \equiv \{g \in \mathbb{C},\ g = |g|e^{\imath\varphi} :\ \varphi \in (-\psi, \psi)\}\ . \tag{6.1.3}$$

In particular, $\mathbb{C}_\pi = \mathbb{C} \setminus \mathbb{R}_-$ is the cut complex plane. For $\psi > \pi$, the set $\mathbb{C}_\psi$ should be interpreted as a sector of a Riemann sheet, extending the principal sheet $\mathbb{C}_\pi$ into the next sheets.

Our first aim is to understand the analytic continuation of the partition function in the maximal possible domain of the Riemann surface. For later convenience, we introduce the following function, not to be confused with the partition function $Z(g, N)$:

$$Z^{\mathbb{R}}(g,N) = \int_{-\infty}^{+\infty} [d\sigma]\ e^{-\frac{1}{2}\sigma^2} \frac{1}{\left(1 - \imath\, e^{\imath\frac{\varphi}{2}}\sqrt{\frac{|g|}{3}}\sigma\right)^{N/2}}\ , \qquad \forall \varphi \neq (2k+1)\pi\ ,\ k \in \mathbb{Z}\ , \tag{6.1.4}$$

which is an absolutely convergent integral for any $|g|$ and any $\varphi \neq (2k+1)\pi$. We have used a superscript $\mathbb{R}$ to distinguish it from $Z(g, N)$ and to emphasize that the integral is performed on the real line, irrespective of the value of $\varphi \neq (2k+1)\pi$. Moreover, for $N/2 \notin \mathbb{Z}$, the integrand is computed using the principal branch of the logarithm:

$$\ln\left(1 - e^{\imath\frac{\pi+\varphi}{2}}\sqrt{\frac{|g|}{3}}\sigma\right) = \frac{1}{2}\ln\left[(\cos\tfrac{\varphi}{2})^2 + (\sin\tfrac{\varphi}{2} + \sqrt{\tfrac{|g|}{3}}\sigma)^2\right] + \imath\ \mathrm{Arg}(1 - e^{\imath\frac{\pi+\varphi}{2}}\sqrt{\tfrac{|g|}{3}}\sigma)\ , \tag{6.1.5}$$

where the Arg function is the principal branch of the argument, valued in $(-\pi, \pi)$. In particular, a change of variables $\sigma \to -\sigma$ shows that $Z^{\mathbb{R}}(g, N) = Z^{\mathbb{R}}(e^{2\pi\imath}g, N)$, which is thus a single-valued function on $\mathbb{C}_\pi$, with a jump at $\mathbb{R}_-$. The analytic continuation of the partition function $Z(g, N)$ will instead be a multi-valued function on $\mathbb{C}$, and thus require the introduction of a Riemann surface. We can view $Z^{\mathbb{R}}(g, N)$ as a periodic function on the same Riemann surface, with of course $Z(g, N) = Z^{\mathbb{R}}(g, N)$ for $g \in \mathbb{C}_\pi$, and $Z(g, N) \neq Z^{\mathbb{R}}(g, N)$ once one steps out of the principal Riemann sheet.

We collect all the relevant result concerning the partition function in Proposition 1. For now we restrict to N real, but the proposition can be extended to complex N with little effort.[5] We will drop this assumption later.

Proposition 1 (Properties of $Z(g, N)$)**.** *Let $N \in \mathbb{R}$ be a fixed parameter. The partition function $Z(g, N)$ satisfies the following properties:*

1. *for every $g \in \mathbb{C}_\pi$, the integral in (6.1.2) is absolutely convergent and bounded from above by*

$$|Z(g,N)| \leq \begin{cases} \left(\cos\frac{\varphi}{2}\right)^{-N/2}\ , & N \geq 0 \\ 2^{|N|/2} + \frac{2^{3|N|/4}}{\sqrt{\pi}}\frac{|g|^{N/4}}{3^{|N|/4}}\Gamma(\frac{|N|+2}{4})\ , & N < 0 \end{cases}\ , \tag{6.1.6}$$

   hence $Z(g, N)$ is analytic in $\mathbb{C}_\pi$.

2. *For $g \in \mathbb{C}_\pi$, the partition function is $Z(g, N) = Z^{\mathbb{R}}(g, N)$ and has the perturbative expansion:*

$$Z(g,N) \simeq \sum_{n=0}^{\infty} \frac{\Gamma(2n + N/2)}{2^{2n} n!\, \Gamma(N/2)} \left(-\frac{2g}{3}\right)^n\ , \tag{6.1.7}$$

[5] For N complex with positive real part, for instance, one uses the inequality $|z^{-N/2}| \leq |\mathrm{Re}(z)|^{-\mathrm{Re}(N)/2} e^{\pi|\mathrm{Im}(N)|/2}$.

where $\simeq$ means that the equation has to be interpreted in the sense of asymptotic series, i.e.:

$$\lim_{\substack{g\to 0\\ g\in\mathbb{C}_\pi}} g^{-n_{\max}} \left| Z(g,N) - \sum_{n=0}^{n_{\max}} \frac{\Gamma(2n+N/2)}{2^{2n} n!\,\Gamma(N/2)} \left(-\frac{2g}{3}\right)^n \right| = 0 \,, \qquad \forall n_{\max} \geq 0 \,. \tag{6.1.8}$$

3. *The function $Z(g,N)$ is Borel summable along all the directions in $\mathbb{C}_\pi$.*

4. *$Z(g,N)$ can be continued past the cut, on the entire Riemann surface. However, $\mathbb{R}_-$ is a Stokes line, that is, the anticlockwise and clockwise analytic continuations $Z_+(g,N)$ and $Z_-(g,N)$ are not equal and cease to be Borel summable at $\mathbb{R}_-$. A second Stokes line is found at $\mathbb{R}_+$ on the second sheet. For $\varphi \notin \pi\mathbb{Z}$, the analytic continuation of the partition function to the whole Riemann surface writes:*

$$\begin{aligned}
&2k\pi < |\varphi| < (2k+1)\pi : \\
&\quad Z(g,N) = \omega_{2k}\; Z(e^{\imath(2k)\tau\pi} g, N) \\
&\qquad\qquad + \eta_{2k}\; \frac{\sqrt{2\pi}}{\Gamma(N/2)}\; e^{\imath\tau\frac{\pi}{2}}\; e^{\frac{3}{2g}}\; \left(e^{\imath(2k+1)\tau\pi}\frac{g}{3}\right)^{\frac{1-N}{2}}\; Z(e^{\imath(2k+1)\tau\pi} g, 2-N) \\
&\qquad\qquad = \omega_{2k}\; Z^{\mathbb{R}}(g,N) + \eta_{2k}\; \frac{\sqrt{2\pi}}{\Gamma(\frac{N}{2})}\; e^{\imath\tau\frac{\pi}{2}}\; e^{\frac{3}{2g}}\; \left(e^{\imath(2k+1)\tau\pi}\frac{g}{3}\right)^{\frac{1-N}{2}}\; Z^{\mathbb{R}}(-g, 2-N) \,, \\
&(2k+1)\pi < |\varphi| < (2k+2)\pi : \\
&\quad Z(g,N) = \omega_{2k+1}\; Z(e^{\imath(2k+2)\tau\pi} g, N) \\
&\qquad\qquad + \eta_{2k+1}\; \frac{\sqrt{2\pi}}{\Gamma(N/2)} e^{\imath\tau\frac{\pi}{2}} e^{\frac{3}{2g}}\; \left(e^{\imath(2k+1)\tau\pi}\frac{g}{3}\right)^{\frac{1-N}{2}}\; Z(e^{\imath(2k+1)\tau\pi} g, 2-N) \\
&\qquad\qquad = \omega_{2k+1}\; Z^{\mathbb{R}}(g,N) + \eta_{2k+1}\; \frac{\sqrt{2\pi}}{\Gamma(\frac{N}{2})} e^{\imath\tau\frac{\pi}{2}} e^{\frac{3}{2g}}\; \left(e^{\imath(2k+1)\tau\pi}\frac{g}{3}\right)^{\frac{1-N}{2}}\; Z^{\mathbb{R}}(-g, 2-N) \,,
\end{aligned} \tag{6.1.9}$$

where $\tau = -\mathrm{sgn}(\varphi)$ and the Stokes parameters (ω,η) are defined recursively as:

$$(\omega_0,\eta_0) = (1,0) \,, \qquad \begin{cases} \omega_{2k+1} &= \omega_{2k} \\ \eta_{2k+1} &= \eta_{2k} + \omega_{2k} \end{cases} \,, \qquad \begin{cases} \omega_{2(k+1)} &= \omega_{2k+1} + \tilde{\tau}\;\eta_{2k+1} \\ \eta_{2(k+1)} &= e^{\imath\tau\pi(N-1)}\eta_{2k+1} \end{cases} \,, \tag{6.1.10}$$

with $\tilde{\tau} = e^{\imath\tau\pi\frac{N+1}{2}}\; 2\sin\frac{N\pi}{2}$. The recursion gives:

$$(\omega_{2k},\eta_{2k}) = \begin{cases} e^{\imath\tau\pi N\frac{k}{2}}\;(1,0) & ,\, k \text{ even} \\ e^{\imath\tau\pi N\frac{k+1}{2}}\;(1,-1) & ,\, k \text{ odd} \end{cases} \,. \tag{6.1.11}$$

The monodromy group of $Z(g,N)$ is of order 4 if N is odd, and of order 2 if N is even. More generally, we have a monodromy group of finite order if N is a rational number, and an infinite monodromy otherwise.

5. *From Properties 2 and 4 we obtain that for g in the sector $k\pi < |\varphi| < (k+1)\pi$ of the Riemann surface the partition function has the following transseries expansion:*

$$\begin{aligned} Z(g,N) \simeq & \omega_k \sum_{n=0}^{\infty} \frac{\Gamma(2n+N/2)}{2^{2n} n!\,\Gamma(N/2)} \left(-\frac{2g}{3}\right)^n \\ & + \eta_k\, e^{\imath\tau\pi(1-\frac{N}{2})}\, \sqrt{2\pi} \left(\frac{g}{3}\right)^{\frac{1-N}{2}} e^{\frac{3}{2g}} \sum_{q\geq 0} \frac{1}{2^{2q} q!\,\Gamma(\frac{N}{2}-2q)} \left(\frac{2g}{3}\right)^q , \end{aligned} \tag{6.1.12}$$

where we used:

$$\Gamma(2q+1-N/2)\Gamma(N/2-2q) = \frac{\pi}{\sin(\pi\frac{N}{2}-2\pi q)} = \Gamma(1-N/2)\Gamma(N/2)\,. \tag{6.1.13}$$

The transseries displays an additional property: the instanton series is obtained from the perturbative one by substituting $N \to 2-N$ and $g \to -g$ and vice versa.

6. *From Property 5, the discontinuity of the partition function at the negative real axis:*

$$\mathrm{disc}_\pi\big(Z(g,N)\big) \equiv \lim_{g\to\mathbb{R}_-} \Big(Z_-(g,N) - Z_+(g,N)\Big)\,, \tag{6.1.14}$$

has the following asymptotic expansion:

$$\begin{aligned} \mathrm{disc}_\pi\big(Z(g,N)\big) \simeq & \imath\sqrt{2\pi} \left(\frac{|g|}{3}\right)^{\frac{1-N}{2}} e^{-\frac{3}{2|g|}} \sum_{q\geq 0} \frac{1}{2^{2q} q!\,\Gamma(\frac{N}{2}-2q)} \left(-\frac{2|g|}{3}\right)^q \\ = & \imath\sqrt{\frac{2}{\pi}} \sin\frac{N\pi}{2} \left(\frac{|g|}{3}\right)^{\frac{1-N}{2}} e^{-\frac{3}{2|g|}} \sum_{q\geq 0} \frac{\Gamma(2q+\frac{2-N}{2})}{2^{2q}\,q!} \left(-\frac{2|g|}{3}\right)^q , \end{aligned} \tag{6.1.15}$$

where for N even integer the sum truncates at $q = N/4-1$, if N is a multiple of 4, and at $q = \lfloor N/4 \rfloor$ otherwise.

7. *The partition function obeys an homogenous linear ordinary differential equation:*

$$16g^2 Z''(g,N) + ((8N+24)g+24)\,Z'(g,N) + N(N+2)Z(g,N) = 0\,, \tag{6.1.16}$$

which can be used to reconstruct the resurgent transseries expansion of $Z(g,N)$.

Proof. See Appendix 6.B.1. □

The proof of this proposition is quite technical. The most interesting points come at Property 4. While the full details can be found in Appendix 6.B.1, we discuss here how the Stokes phenomenon arises in the intermediate field representation.

In order to obtain the asymptotic approximation of an integral we need to deform the integration contour to steepest-descent contours (or Lefschetz thimbles) where the Laplace method can be applied. An integration contour will in principle intersect several steepest-ascent (upwards) paths of several saddle points and it must then be deformed (i.e. relaxed under the gradient flow) to run along the thimbles of these saddle points [196, 187]. When varying some parameter continuously the relevant thimbles can collide and change discontinuously leading to discontinuous changes of the asymptotic regimes at Stokes lines. This is exactly the picture in the ϕ representation of the partition function, which we recall in Appendix 6.A.

In the σ representation the picture is different. Let us go back to (6.1.2) expressing $Z(g,N)$ as an integral over the real line. The partition function $Z(g,N)$ is analytically continued to the extended Riemann sheet $\mathbb{C}_{3\pi/2}$ by tilting the integration contour to $e^{-\imath\theta}\sigma$ respectively $e^{\imath\theta}\sigma$ with $\theta>0$ for its anticlockwise respectively clockwise analytic continuations $Z_+(g,N)$ and $Z_-(g,N)$.

In this representation, the Lefshetz thimble is always the real axis, irrespective of g. In fact, as g goes to zero, the Laplace method instructs us to look for the saddle point of the exponent in the integrand (the function $f(x)$ in (6.A.1)), which in this case is a simple quadratic function,[6] while the subexponential function (the function $a(x)$ in (6.A.1)) is irrelevant for the determination of the saddle points. However, what happens is that the integrand has a branch point (or pole for N a positive even integer) and this point crosses the thimble at the Stokes line. This is depicted in Fig. 6.1.

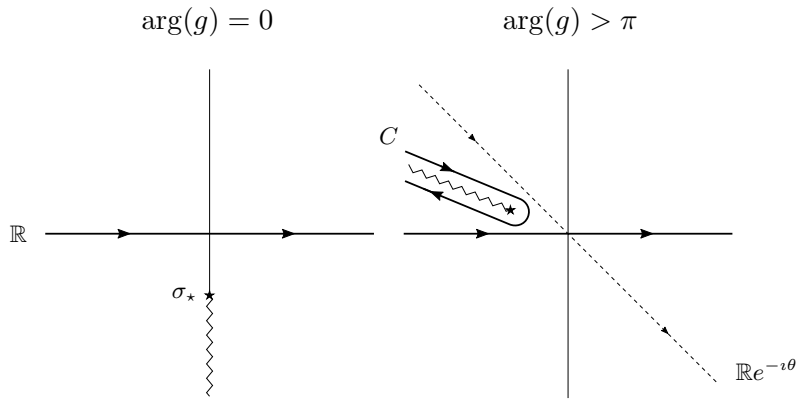

FIGURE 6.1: As $\arg(g)$ increases, the branch cut moves clockwise in the complex σ-plane. When g crosses the negative real axis the tilted contour is equivalent to a Hankel contour C plus the original contour along the real line (6.1.17).

In detail, as long as $g=|g|e^{\imath\varphi}\in\mathbb{C}_\pi$, the integral converges because the branch point $\sigma_\star=-\imath\sqrt{3/g}$ with branch cut $\sigma_\star\times(1,+\infty)$, lies outside the integration contour. As g approaches $\mathbb{R}_-$, the branch point hits the contour of integration: for $\varphi\nearrow\pi$ the branch point hits the real axis at $-\sqrt{3/|g|}$. The analytic continuation $Z_+(g,N)$ consists in tilting the contour of integration in σ to avoid the collision with the branch point. However, in order to derive the asymptotic behaviour of $Z_+(g,N)$, we need to deform the integration contour back to the thimble, which is always the real axis. Once g passes on the second Riemann sheet ($\varphi>\pi$), when deforming the tilted contour to the the real axis we generate an additional Hankel contour (see Fig. 6.1):

$$\begin{aligned}
&Z_\pm(g,N)\big|_{\varphi\gtrless\pm\pi}=\int_{e^{\mp\imath\theta}\mathbb{R}}[d\sigma]\,\frac{e^{-\frac12\sigma^2}}{\left(1-\imath\sqrt{\frac{g}{3}}\sigma\right)^{N/2}}=Z^{\mathbb{R}}(g,N)+Z^C_\pm(g,N)\ ,\\
&Z^{\mathbb{R}}(g,N)=\int_{\mathbb{R}}[d\sigma]\,e^{-\frac12\sigma^2}\frac{1}{\left(1-\imath\sqrt{\frac{g}{3}}\sigma\right)^{N/2}}\ ,\qquad Z^C_\pm(g,N)=\int_C[d\sigma]\,e^{-\frac12\sigma^2}\frac{1}{\left(1-\imath\sqrt{\frac{g}{3}}\sigma\right)^{N/2}}\ ,
\end{aligned}\tag{6.1.17}$$

where the Hankel contour C turns clockwise around the cut $\sigma_\star\times(1,+\infty)$, i.e. starting at infinity with argument $\frac{3\pi}{2}-\frac{\varphi}{2}$ and going back with argument $-\frac{\pi}{2}-\frac{\varphi}{2}$ after having encircled the branch point $\sigma_\star$. We kept a subscript $\pm$ for the contribution of the Hankel contour, because, even though the definition of $Z^C_\pm(g,N)$ and C might suggest that it is one single function of g, in fact the integral around the cut is divergent for $|\varphi|<\pi/2$, and therefore the integrals at $\pi<\varphi<3\pi/2$ and at $-\pi>\varphi>-3\pi/2$ are *not*

[6] This is perhaps more clear after rescaling σ by $1/\sqrt{g}$ to cast our integral in the same form as (6.A.1).

the analytic continuation of each other. This fact is reflected in the τ-dependence of the asymptotic expansion in (6.1.12).

The appearance of the Hankel contour marks a discontinuity of the contour of integration in σ as a function of the argument of g, which translates into a discontinuity of the asymptotic expansion of $Z(g,N)$, that is, a Stokes phenomenon. We insist that the Hankel contour is *not* a thimble for the integral in (6.1.2), but it *contributes* to the asymptotic evaluation of the integral, providing the one-instanton contribution in the transseries of $Z(g,N)$.

In order to go beyond $|\varphi| = 3\pi/2$, one notices that we can analytically continue separately $Z^{\mathbb{R}}(g,N)$ and $Z^C_{\pm}(g,N)$. The first is analytic in the range $|\varphi| \in (\pi, 3\pi)$, where its asymptotic expansion is just the standard perturbative series. The analytic continuation of $Z^C_{\pm}(g,N)$ is not immediate in the Hankel contour representation, which is only convergent for $\pi/2 < |\varphi| < 3\pi/2$, but after resolving the discontinuity at the cut and using again the Hubbard-Stratonovich trick (as detailed in Appendix 6.B.1), it turns out that it can be rewritten as:

$$Z^C_{\pm}(g,N) = e^{\imath\tau\pi(1-\frac{N}{2})}\left(\frac{g}{3}\right)^{\frac{1-N}{2}} e^{\frac{3}{2g}} \frac{\sqrt{2\pi}}{\Gamma(N/2)}\, Z(e^{\imath\tau\pi}g, 2-N)\,. \tag{6.1.18}$$

with $\tau = -\mathrm{sgn}(\varphi)$. In this form it is manifest that $Z^C_{\pm}(g,N)$ is analytic in g as long as $e^{\imath\tau\pi}g$ belongs to the principal sheet of the Riemann surface, that is for $\pi < |\varphi| < 2\pi$. We have thus shown that, when going from $|\varphi| < \pi$ to $\pi < |\varphi| < 2\pi$ our analytic continuation of $Z(g,N)$ switches:

$$\begin{aligned} Z(g,N) \xrightarrow{|\varphi|\nearrow\pi_+} & Z^{\mathbb{R}}(g,N) + \frac{\sqrt{2\pi}}{\Gamma(N/2)}\, e^{\imath\tau\frac{\pi}{2}}\, e^{\frac{3}{2g}} \left(e^{\imath\tau\pi}\frac{g}{3}\right)^{\frac{1-N}{2}} Z^{\mathbb{R}}(-g, 2-N) \\ &= Z(e^{\imath(2\tau\pi)}g, N) + \frac{\sqrt{2\pi}}{\Gamma(N/2)}\, e^{\imath\tau\frac{\pi}{2}}\, e^{\frac{3}{2g}} \left(e^{\imath\tau\pi}\frac{g}{3}\right)^{\frac{1-N}{2}} Z(e^{\imath\tau\pi}g, 2-N)\,, \end{aligned} \tag{6.1.19}$$

where we explicitly exhibited the argument at which the switching takes place. In the second line above, for $\pi < |\varphi| < 2\pi$, both arguments $e^{\imath(2\tau\pi)}g$ and $e^{\imath\tau\pi}g$ belong to the principal sheet of the Riemann surface, where $Z(g,N)$ has already been constructed and proven to be analytic. The first term in (6.1.19) is regular up to $|\varphi| = 3\pi$, but the second one has a problem when $e^{\imath\tau\pi}g$ reaches the negative real axis and retracing our steps we conclude that the analytic continuation switches again:

$$\begin{aligned} Z(e^{\imath\tau\pi}g, 2-N) \xrightarrow{|\varphi|\nearrow 2\pi_+} & Z(e^{\imath(3\tau\pi)}g, 2-N) \\ &+ \frac{\sqrt{2\pi}}{\Gamma(1-N/2)}\, e^{\imath\tau\frac{\pi}{2}}\, e^{\frac{3}{2ge^{\imath\tau\pi}}} \left(e^{\imath(2\tau\pi)}\frac{g}{3}\right)^{\frac{N-1}{2}} Z(e^{\imath(2\tau\pi)}g, N)\,, \end{aligned} \tag{6.1.20}$$

where this time the arguments at which Z is evaluated on the right hand side stay in the principal sheet for $2\pi < |\varphi| < 3\pi$. Iterating, one obtains the analytic continuation to the whole Riemann surface.

Remark 1. The differential equation (6.1.16) can be solved in terms of special functions. For $N = 1$, setting $Z(g,1) = \sqrt{\frac{3}{2\pi g}} e^{\frac{3}{4g}} f(\frac{3}{4g})$, we find that the equation reduces to a modified Bessel's equation for $f(z)$:

$$z^2 f''(z) + z f'(z) - (z^2 + \frac{1}{16}) f(z) = 0\,. \tag{6.1.21}$$

Its two linearly independent solutions are the modified Bessel functions of the first and second kind of order $1/4$. However, only the second, $K_{1/4}(z)$, decays for $z \to \infty$, hence the initial condition $Z(0,1) = 1$ fixes $f(z) = K_{1/4}(z)$.

Similarly, for general N, we find that setting $Z(g,N) = (\frac{3}{2g})^{N/4} f(\frac{3}{2g})$ the differential equation reduces to Kummer's equation for $f(z)$:

$$z f''(z) + (\frac{1}{2} - z) f'(z) - \frac{N}{4} f(z) = 0 \,. \tag{6.1.22}$$

With the addition of the initial condition condition $Z(0,N) = 1$, we find that the solution is given by the Tricomi confluent hypergeometric function $f(z) = U(N/4, 1/2, z)$, whose transseries expansion can easily be obtained order by order. However, such expressions of the partition function in terms of special functions do not generalize to quantum field theory. Similarly, even the more general resurgence theory for formal solutions of ordinary differential equations will be of limited use in that context, as the partition function of a quantum field theory model does not satisfy an ordinary differential equation. For this reason, while displaying for completeness the relevant ordinary differential equations, in this work we do not make use of them, and rather refer to the literature (see references in [187]).

Our result (6.1.12) provides a useful repackaging of the transseries expansion of the partition function and an alternative derivation that should be more easily generalizable to quantum field theory.

6.1.2 Convergent small-N series of $Z(g,N)$ and transseries of its coefficients $Z_n(g)$

We will now study the discontinuity of $Z(g,N)$ from a different perspective. We expand the integrand of (6.1.2) in powers of N and exchange the order of summation and integration:

$$Z(g,N) = \sum_{n\geq 0} \frac{1}{n!} \left(-\frac{N}{2}\right)^n Z_n(g) \,, \quad Z_n(g) = \int_{-\infty}^{+\infty} [d\sigma] e^{-\frac{1}{2}\sigma^2} \left(\ln(1 - \imath\sqrt{\frac{g}{3}}\sigma)\right)^n \,. \tag{6.1.23}$$

Unlike the usual perturbative expansions in g, this is a convergent expansion: from the bound in Property 1 of Proposition 2 below, the Gaussian integral and the sum can be commuted due to Fubini's Theorem. As a function of N, we can regard $Z(g,N)$ as a generating function of "moments": unlike the usual moments, we are dealing with expectations of powers of the logarithm.

Proposition 2 (Properties of $Z_n(g)$)**.** *The $Z_n(g)$, $n \in \mathbb{N}_{\geq 0}$ satisfy the following properties:*

1. *$Z_n(g)$ is analytic in the cut plane $\mathbb{C}_\pi$. Indeed, for every $g \in \mathbb{C}_\pi$, the integral (6.1.23) is absolutely convergent and bounded from above by:*

$$|Z_n(g)| \leq K^n \frac{\left(|\ln(\cos\frac{\varphi}{2})| + 1\right)^n}{\varepsilon^n} \left(1 + |g|^{\frac{n\varepsilon}{2}} \Gamma(\tfrac{n\varepsilon+1}{2})\right) , \tag{6.1.24}$$

   for any $\varepsilon > 0$ and with K some g-independent constant. Using this bound with some fixed $\varepsilon < 2$ shows that, $\forall g \in \mathbb{C}_\pi$ the series in (6.1.23) has infinite radius of convergence in N.

2. *For $g \in \mathbb{C}_\pi$, $Z_n(g)$ has the perturbative expansion:*

$$Z_n(g) \simeq \sum_{m \geq n/2} \left(-\frac{2g}{3}\right)^m \frac{(2m)!}{2^{2m} m!} \sum_{\substack{m_1,\dots,m_{2m-n+1}\geq 0 \\ \sum k m_k = 2m,\, \sum m_k = n}} \frac{(-1)^n n!}{\prod_k k^{m_k} m_k!} \equiv Z_n^{\text{pert.}}(g) \,. \tag{6.1.25}$$

3. *The functions $Z_n(g)$ are Borel summable along all the directions in $\mathbb{C}_\pi$.*

4. *$Z_n(g)$ can be continued past the cut on the extended Riemann sheet $\mathbb{C}_{3\pi/2}$, and the small-N series has infinite radius of convergence in N in this domain. However, $\mathbb{R}_-$ is a Stokes line and the*

anticlockwise and clockwise analytic continuations $Z_{n+}(g)$ and $Z_{n-}(g)$ are not equal and cease to be Borel summable at $\mathbb{R}_-$.

5. *For $g \in \mathbb{C}_{3\pi/2}$, $Z_n(g)$ has a the following transseries expansion:*

$$Z_n(g) \simeq Z_n^{\text{pert.}}(g) + \eta\, e^{\frac{3}{2g}} Z_n^{(\eta)}(g) \,, \tag{6.1.26}$$

with $Z_n^{\text{pert.}}(g)$ as in (6.1.25), and:

$$\begin{aligned} Z_n^{(\eta)}(g) =& \frac{\imath}{\sqrt{2\pi}} \sqrt{\frac{g}{3}} \sum_{q=0}^{\infty} \sum_{p=0}^{n} \frac{1}{q!} \left(\frac{g}{6}\right)^q \binom{n}{p} \frac{d^p \Gamma(z)}{dz^p}\Big|_{z=2q+1} \\ & \left[\left(\ln(e^{\imath\tau\pi} \frac{g}{3}) - \imath\pi \right)^{n-p} - \left(\ln(e^{\imath\tau\pi} \frac{g}{3}) + \imath\pi \right)^{n-p} \right] \,, \end{aligned} \tag{6.1.27}$$

with $\tau = -\text{sgn}(\varphi)$ and η a transseries parameter which is zero on the principal Riemann sheet and one if $|\varphi| > \pi$. Proceeding in parallel to Proposition 1, one can study the full monodromy of $Z_n(g)$.

6. *The discontinuity on the negative axis has the following asymptotic expansion:*

$$\begin{aligned} \text{disc}_\pi\big(Z_n(g)\big) \simeq & \frac{e^{-\frac{3}{2|g|}}}{\sqrt{2\pi}} \sqrt{\frac{|g|}{3}} \sum_{q=0}^{\infty} \sum_{p=0}^{n} \frac{1}{q!} \left(-\frac{|g|}{6}\right)^q \binom{n}{p} \frac{d^p \Gamma(z)}{dz^p}\Big|_{z=2q+1} \\ & \left[\left(\ln|\frac{g}{3}| - \imath\pi \right)^{n-p} - \left(\ln|\frac{g}{3}| + \imath\pi \right)^{n-p} \right] \,. \end{aligned} \tag{6.1.28}$$

Summing over n, the discontinuity of the partition function (6.1.15) is recovered.

7. *The functions $Z_n(g)$ obey a tower of linear, inhomogeneous ordinary differential equations:*

$$\begin{aligned} & Z_0(g) = 1 \,, \\ & 4g^2 Z_1''(g) + 6\,(g+1)\, Z_1'(g) = 1 \,, \\ & 4g^2 Z_n''(g) + 6\,(g+1)\, Z_n'(g) = n\left(4g Z_{n-1}'(g) + Z_{n-1}(g)\right) - n(n-1) Z_{n-2}(g) \,. \end{aligned} \tag{6.1.29}$$

which can be used to reconstruct the resurgent transseries expansion of $Z_n(g)$.

Proof. See Appendix 6.B.2 □

As with Proposition 1, the most interesting points are Properties 4 and 5. Again the analytic continuations $Z_{n\pm}(g)$ of $Z_n(g)$ to the extended Riemann sheet $\mathbb{C}_{3\pi/2}$ are obtained by tilting the integration contour to $e^{\mp\imath\theta}\sigma$ with $\theta > 0$. The branch point $\sigma_\star$ of the integrand in (6.1.23) crosses the real axis when g reaches $\mathbb{R}_-$, and deforming the tilted contours back to the real axis detaches Hankel contours around the cut $\sigma_\star \times (1, +\infty)$:

$$\begin{aligned} & Z_{n\pm}(g)\big|_{\substack{\varphi > \pi \\ < -\pi}} = \int_{e^{\mp\imath\theta}\mathbb{R}} [d\sigma]\; e^{-\frac{1}{2}\sigma^2} \left(\ln(1 - \imath\sqrt{\frac{g}{3}}\sigma) \right)^n = Z_n^{\mathbb{R}}(g) + Z_{n\pm}^{C}(g) \\ & Z_n^{\mathbb{R}}(g) = \int_{\mathbb{R}} [d\sigma]\; e^{-\frac{1}{2}\sigma^2} \left(\ln(1 - \imath\sqrt{\frac{g}{3}}\sigma) \right)^n \,, \qquad Z_{n\pm}^{C}(g) = \int_{C} [d\sigma]\; e^{-\frac{1}{2}\sigma^2} \left(\ln(1 - \imath\sqrt{\frac{g}{3}}\sigma) \right)^n \,. \end{aligned} \tag{6.1.30}$$

The transeries of $Z_n(g)$ is obtained by summing the asymptotic expansions of the two pieces:

$$Z_n^{\mathbb{R}}(g) \simeq Z_n^{\text{pert.}}(g) \,, \qquad Z_{n\pm}^{C}(g) \simeq e^{\frac{3}{2g}} Z_n^{(\eta)}(g)\big|_{\tau=\mp 1} \,.$$

Notice that the homogeneous equation in Property 7 in Proposition 2 is the same for all $n \geq 1$, and it admits an exact solution in the form of a constant plus an imaginary error function:

$$4g^2 Z_1''(g) + 6(g+1)Z_1'(g) = 0 \qquad \Rightarrow \qquad Z_1(g) = c_1 + c_2 \int_0^{\imath\sqrt{\frac{3}{2g}}} e^{-t^2} dt \,. \tag{6.1.31}$$

The asymptotic expansion of the error function reproduces the one-instanton contribution of (6.1.26) for $n = 1$. For $n > 1$, instead, this is only part of the instanton contribution, the rest being generated by the recursive structure of the inhomogeneous equations. Similarly, the perturbative expansion comes from the special solution to the inhomogeneous equation, even at $n = 1$, as for those we cannot match exponential terms with the right-hand side. For $n > 1$ the homogeneous equation remains the same, but the inhomogeneous part depends on the solutions to previous equations, and thus it can also contain exponential terms.

6.2 The free energy $W(g,N)$

We now turn to the free energy $W(g,N) = \ln Z(g,N)$. Our aim is find the equivalent of the results listed in Proposition 1, in the case of $W(g,N)$. Taking the logarithm has drastic effects: the nonperturbative effects encountered in $W(g,N)$ are significantly more complicated than the ones encountered for $Z(g,N)$. One can understand this from the fact that the linear differential equation satisfied by $Z(g,N)$ translates into a nonlinear one for $W(g,N)$, leading to an infinite tower of multi-instanton sectors in the transseries [187]. Here we will follow a different route, based on the small-N expansion.

Much like the partition function $Z(g,N)$, its logarithm $W(g,N)$ can also be expanded in N:

$$W(g,N) = \ln(Z(g,N)) \equiv \sum_{n\geq 1} \frac{1}{n!} \left(-\frac{N}{2}\right)^n W_n(g) \,. \tag{6.2.1}$$

The coefficients $W_n(g)$ can be computed in terms of $Z_n(g)$. As already mentioned, $Z_n(g)$ are the moments of the random variable $\ln(1 - \imath\sqrt{g/3}\,\sigma)$, hence W_n are the cumulants of the same variable and can be computed in terms of $Z_n(g)$ by using the Möbius inversion formula (which in this case becomes the moments-cumulants formula). Let us denote π a partition of the set $\{1, \dots n\}$, $b \in \pi$ the parts in the partition, $|\pi|$ the number of parts of π and $|b|$ the cardinal of b. Then:

$$Z_n(g) = \sum_{\pi} \prod_{b\in\pi} W_{|b|}(g) \,, \qquad W_n(g) = \sum_{\pi} \lambda_\pi \prod_{b\in\pi} Z_{|b|}(g) \,, \tag{6.2.2}$$

where $\lambda_\pi = (-1)^{|\pi|-1}(|\pi|-1)!$ is the Möbius function on the lattice of partitions. Grouping together the partitions having the same number n_i of parts of size i this becomes:[7]

$$\begin{aligned} Z_n(g) &= \sum_{\substack{n_1,\dots,n_n\geq 0 \\ \sum i n_i = n}} \frac{n!}{\prod_i n_i!(i!)^{n_i}} \prod_{i=1}^{n} W_i(g)^{n_i} \ , \\ W_n(g) &= \sum_{k=1}^{n} (-1)^{k-1}(k-1)! \sum_{\substack{n_1,\dots,n_{n-k+1}\geq 0 \\ \sum i n_i = n, \sum n_i = k}} \frac{n!}{\prod_i n_i!(i!)^{n_i}} \prod_{i=1}^{n-k+1} Z_i(g)^{n_i} \ . \end{aligned} \tag{6.2.3}$$

Equation (6.2.3) relates $W_n(g)$ and $Z_n(g)$ as analytic functions of g. However, this translates into a relation between $W(g,N)$ and $Z(g,N)$ which holds only *in the sense of formal power series in* N. Even though $Z(g,N)$ is analytic in some domain, one cannot conclude that $W(g,N)$ is also analytic in the same domain: convergence of the series defining $Z(g,N)$ does not imply convergence of the series defining $W(g,N)$ in (6.2.1). This can most readily be seen at the zeros of the partition function, the so-called Lee-Yang zeros, which are singular points for the free energy. In order to study the analyticity properties of $W(g,N)$ one needs to use a completely different set of tools. However, as we will see below, the Möbius inversion has its own uses: it is the most direct way to access the transseries expansion of $W(g,N)$.

6.2.1 Constructive expansion

The following Proposition 3 is a slight variation on the Loop Vertex Expansion (LVE) introduced in [22] (see also [203] for more details). It gives an integral representation for $W_n(g)$ in (6.2.1) which allows us to prove that $W(g,N)$ is convergent (hence analytic) in a bounded domain on the extended Riemann sheet $\mathbb{C}_{3\pi/2}$, wrapping around the branch point at the origin.

In Proposition 1 we fixed N to be a real parameter. However, equation (6.1.23) writes $Z(g,N)$ as an expansion in N with a nonzero (infinite!) radius of convergence in N, as long as $|\varphi| < 3\pi/2$ (note that the bound in Property 1 of Proposition 2 suffices only for $|\varphi| < \pi$; in order to reach $|\varphi| < 3\pi/2$, one needs to use the improved bound in (6.B.42)). We can therefore extend N to a larger domain in the complex plane. As the following proposition shows, something similar applies also to $W(g,N)$, but with a finite radius of convergence.

Notation. Let us denote T_n the set of combinatorial trees with n vertices labeled $1,\dots n$. There are $\frac{(n-2)!}{\prod_{i=1}^n (d_i-1)!}$ trees over n labelled vertices with coordination d_i at the vertex i and $\sum_i d_i = 2(n-1)$. The total number of trees in T_n is n^{n-2}. Let $\mathcal{T} \in T_n$ be such a tree. We denote $P^{\mathcal{T}}_{k-l}$ the (unique) path in the tree $\mathcal{T}$ connecting the vertices k and l. If we associate to each edge $(k,l) \in \mathcal{T}$ a variable u_{kl} between 0 and 1, we can define the $n \times n$ matrix $w^{\mathcal{T}}$:

$$w^{\mathcal{T}}_{kl} \equiv \begin{cases} 1 \ , & \text{if } \ k = l \\ \inf_{(i,j)\in P^{\mathcal{T}}_{k-l}} \{u_{ij}\} \ , & \text{else} \end{cases} \ . \tag{6.2.4}$$

[7] This can also be obtained directly from Faà di Bruno's formula:

$$\frac{d^n}{du^n} \ln Z|_{u=0} = \sum_{\substack{n_1,\dots n_n\geq 0 \\ \sum i n_i = n}} \frac{n!}{\prod_i n_i!(i!)^{n_i}} \ (n_1+\dots+n_n-1)! \ \frac{(-1)^{n_1+\dots+n_n-1}}{Z^{n_n+\dots+n_n}} \prod_{i\geq 1} [Z^{(i)}]^{n_i}|_{u=0} \ ,$$

noticing that for $u = -N/2$, we have $Z^{(i)} = Z_i$.

The matrix $w^{\mathcal{T}}$ is a positive matrix for any choice of u parameters, and is strictly positive outside a set of measure 0 (see Appendix 2.5.2 for more details). Of course the matrix w depends on u but we suppress this in order to simplify the notation.

Proposition 3 (The LVE expansion, analyticity)**.** *Let N be a fixed* complex *parameter and let us denote $g = |g|e^{\imath\varphi}$. The cumulants $W_n(g)$ can be written as:*

$$\begin{aligned} W_1(g) &= Z_1(g) = \int_{-\infty}^{+\infty} [d\sigma]\; e^{-\frac{1}{2}\sigma^2} \ln\left[1 - \imath\sqrt{\tfrac{g}{3}}\sigma\right] , \\ W_n(g) &= -\left(\frac{g}{3}\right)^{n-1} \sum_{\mathcal{T}\in T_n} \int_0^1 \prod_{(i,j)\in\mathcal{T}} du_{ij} \int_{-\infty}^{+\infty} \frac{\prod_i [d\sigma_i]}{\sqrt{\det w^{\mathcal{T}}}}\; e^{-\frac{1}{2}\sum_{i,j}\sigma_i (w^{\mathcal{T}})^{-1}_{ij}\sigma_j} \\ &\qquad \times \prod_i \frac{(d_i-1)!}{\left(1 - \imath\sqrt{\frac{g}{3}}\sigma_i\right)^{d_i}} , \end{aligned} \tag{6.2.5}$$

where we note that the Gaussian integral over σ is well defined, as $w^{\mathcal{T}}$ is positive, and normalized. Furthermore:

1. *The functions $W_n(g), n \geq 2$ are bounded by:*

$$|W_n(g)| \leq \frac{(2n-3)!}{(n-1)!} \left|\frac{g}{3(\cos\frac{\varphi}{2})^2}\right|^{n-1} . \tag{6.2.6}$$

   Therefore, they are analytic in the cut plane $\mathbb{C}_\pi$.

2. *The series*

$$W(g,N) = \sum_{n\geq 1} \frac{1}{n!} \left(-\frac{N}{2}\right)^n W_n(g) , \tag{6.2.7}$$

   is absolutely convergent in the following cardioid domain:

$$\mathbb{D}_0 = \left\{ g \in \mathbb{C},\; g = |g|e^{\imath\varphi} :\; |g| < \frac{1}{|N|}\,\frac{3}{2}(\cos\frac{\varphi}{2})^2 \right\} . \tag{6.2.8}$$

3. *$W_n(g)$ can be analytically continued to a subdomain of the extended Riemann sheet $\mathbb{C}_{3\pi/2}$ by tilting the integration contours to $\sigma \in e^{-\imath\theta}\mathbb{R}$:*

$$\begin{aligned} W_{1\theta}(g) =& e^{-\imath\theta} \int_{-\infty}^{+\infty} [d\sigma]\; e^{-\frac{1}{2}e^{-2\imath\theta}\sigma^2} \ln\left(1 - \imath\sqrt{\tfrac{g}{3}}e^{-\imath\theta}\sigma\right) , \\ W_{n\theta}(g) =& -\left(\frac{g}{3}\right)^{n-1} \sum_{\mathcal{T}\in T_n} \int_0^1 \prod_{(i,j)\in\mathcal{T}} du_{ij} \\ & \int_{\mathbb{R}} \frac{\prod_i e^{-\imath\theta}[d\sigma_i]}{\sqrt{\det w^{\mathcal{T}}}}\; e^{-\frac{1}{2}e^{-2\imath\theta}\sum_{i,j}\sigma_i (w^{\mathcal{T}})^{-1}_{ij}\sigma_j} \prod_i \frac{(d_i-1)!}{\left(1 - \imath\sqrt{\frac{g}{3}}e^{-\imath\theta}\sigma_i\right)^{d_i}} . \end{aligned} \tag{6.2.9}$$

4. *For $n \geq 2$ we have the following bound:*

$$|W_{n\theta}(g)| \leq \frac{(2n-3)!}{(n-1)!} \frac{1}{\sqrt{\cos(2\theta)}} \left|\frac{g}{3\sqrt{\cos(2\theta)}\left(\cos\frac{\varphi-2\theta}{2}\right)^2}\right|^{n-1} . \tag{6.2.10}$$

5. The series

$$W_\theta(g,N) = \sum_{n\geq 1} \frac{1}{n!} \left(-\frac{N}{2}\right)^n W_{n\theta}(g) \,, \tag{6.2.11}$$

is absolutely convergent in the following domain:

$$\mathbb{D}_\theta = \left\{ g\in\mathbb{C},\ g=|g|e^{i\varphi} :\ |g| < \frac{1}{|N|}\,\frac{3}{2}\left(\cos\frac{\varphi-2\theta}{2}\right)^2 \sqrt{\cos(2\theta)} \right\} . \tag{6.2.12}$$

Consequently, $W_n(g)$ and $W(g,N)$ can be analytically extended to the following respective domains:

$$\begin{aligned} W_n(g):&\quad |2\theta| < \frac{\pi}{2}\,,\ \ |\varphi-2\theta|<\pi\,,\\ W(g,N):&\quad |2\theta| < \frac{\pi}{2}\,,\ \ |\varphi-2\theta|<\pi\,,\qquad |g| < \frac{1}{|N|}\,\frac{3}{2}\left(\cos\frac{\varphi-2\theta}{2}\right)^2 \sqrt{\cos(2\theta)}\,. \end{aligned} \tag{6.2.13}$$

Pushing $\theta\to\pm\pi/4$ allows us to write a convergent expansion for all $|\varphi|<\frac{3\pi}{2}$.

Proof. See Appendix 6.B.3 □

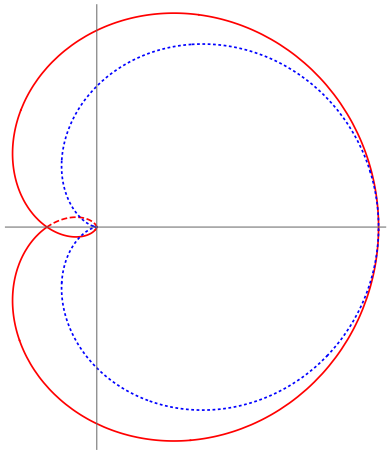

FIGURE 6.2: The cardioid domain $\mathbb{D}_0$ of (6.2.8) (dotted blue line) and the extended cardioid $\mathbb{D}_\theta$ of (6.2.12) (red line), for $\theta=\varphi/6$, which is similar to the optimal domain $\mathbb{D}_{\rm opt}$, in the complex g-plane. The branch cut is on the negative real axis, thus the portions of $\mathbb{D}_\theta$ going beyond it are to be understood as being on different Riemann sheets.

The main point of the proposition is that by constructive methods we can prove analyticity of $W(g,N)$ in a nontrivial domain. In a first step, without touching the integration contours, we prove that such domain is the cardioid of equation (6.2.8). However, the cardioid does not allow us to reach (and cross) the branch cut. Tilting the integration contours by θ, we are able to extend the original cardioid domain to the larger domain of (6.2.12) (see Fig. 6.2), going beyond the cut on a subdomain of the extended Riemann sheet $\mathbb{C}_{3\pi/2}$. The optimal domain $\mathbb{D}_{\rm opt}$ can be found by maximizing the right-hand side of (6.2.12) with respect to θ, at fixed φ, but a simpler and qualitatively similar choice is to take $\theta=\varphi/6$.

Note that the domain of analyticity of $W(g,N)$, (6.2.12), depends on N and shrinks to zero for $N\to\infty$. Results uniform in N can only be established if one keeps the 't Hooft coupling $g_t=gN$ fixed [203]. On the other hand, for any g on the extended Riemann sheet $\mathbb{C}_{3\pi/2}$, the radius of convergence of the LVE expansion in N is nonzero.

Remark 2. It is also worth noticing that the explicit expressions for the partition function in terms of special functions, discussed around (6.1.21), provide us with some useful information about the zeros of $Z(g,N)$ (Lee-Yang zeros), and hence about the singularities of $W(g,N)$. For example, in the case $N=1$, the partition function is expressed in terms of a modified Bessel function of the second kind, whose zeros have been studied in some depth. In particular, from what is known about $K_\nu(z)$ (e.g. [207]) we deduce that $Z(g,1)=\sqrt{\frac{3}{2\pi g}}e^{\frac{3}{4g}}K_{1/4}(\frac{3}{4g})$ has no zeros in the principal sheet $\mathbb{C}_\pi$, while on each of the two following sheets it has an infinite sequence of zeros approaching the semiaxis at $|\varphi|=3\pi/2$ from the left, and accumulating towards $g=0$ (see Fig. 6.3). Therefore, it should come as no surprise that $W(g,N)$ cannot be analytically continued around the origin beyond $|\varphi|=3\pi/2$.

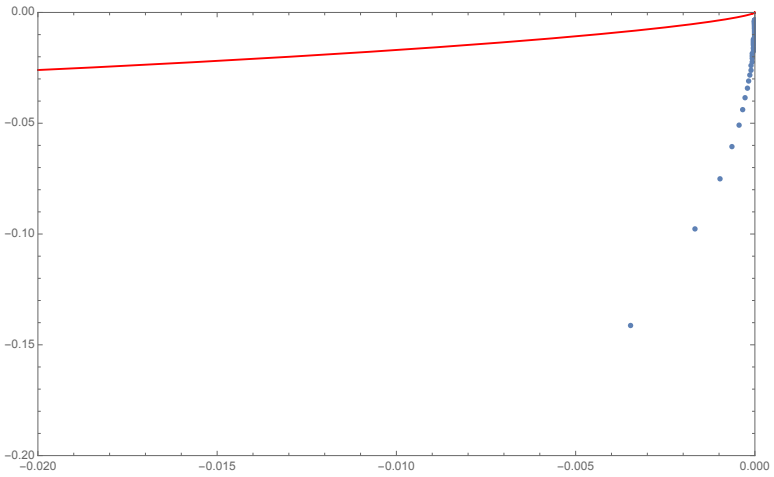

FIGURE 6.3: Approximate location (see [207]) of the Lee-Yang zeros of $Z(g,1)$ (blue dots) in the quadrant $\pi<\varphi<3\pi/2$ of $\mathbb{C}_{3\pi/2}$, together with the boundary of the domain $\mathbb{D}_\theta$ (in red).

Remark 3. Integrating out the u parameters and performing the sum over trees, one should be able to prove that integral expressions (6.2.9) reproduce the moment-cumulant relation in (6.2.3). In particular this would provide an alternative proof that the moment cumulant relation holds in the sense of analytic functions on the Riemann surface. The proof that this indeed happens is involved as the summation over trees requires the use of combinatoiral techniques similar to the ones discussed in Section 2.5.2. We postpone this for future work.

In [22] the LVE is used to prove the Borel summability of $W(g,1)$ along the positive real axis. Building on the techniques introduced in [22], we now generalize this result.

Proposition 4 (Borel summability of $W_n(g)$ and $W(g,N)$ in $\mathbb{C}_\pi$)**.** *The cumulants $W_n(g)$ and the free energy $W(g,N)$ at any fixed complex N are Borel summable along all the directions in the cut complex plane $\mathbb{C}_\pi$.*

Proof. See Appendix 6.B.4. □

6.2.2 Transseries expansion

It is well known that the (perturbative) asymptotic series of $W(g,N)$ at $g=0$ is a sum over connected Feynman graphs. The connection between the LVE expansion of $W(g,N)$ presented in Proposition 3 and the Feynman graphs is discussed in Appendix 6.C. On the other hand, the power series in each multi-instanton sector of the transseries of $W(g,N)$ has no simple diagrammatic interpretation; they

can be constructed from the nonlinear differential equation obeyed by $W(g,N)$, or more formally by expanding the logarithm of the transseries expansion of $Z(g,N)$ in powers of the transseries monomial $\exp\{3/(2g)\}$ (e.g. [187]). The latter is however only a meaningful operation in the sense of formal power series.

In this Section we take a different route and derive rigorously the transseries expansion of $W(g,N)$ by exploiting the analytical control we have on the small-N expansion. We first notice that, from Propositions 2 and 3, $W_n(g)$ and $Z_n(g)$ are analytic functions on the extended Riemann sheet $\mathbb{C}_{3\pi/2}$. Next, we use (6.2.3) to construct $W_n(g)$ as a finite linear combination of finite products of $Z_i(g)$'s. Each such product is in fact a (factored) multidimensional integral, hence we can apply to it the steepest descent method to obtain its asymptotic expansion. In $\mathbb{C}_\pi$, the asymptotic expansion of each factor $Z_i(g)$ is of the perturbative type, equation (6.1.25), and $W_n(g)$ is just a finite linear combination of Cauchy products of such series.

When turning g past the negative real axis, each integration contour in this multidimensional integral must be deformed past a cut and each $Z_{i\pm}(g) = Z_i^{\mathbb{R}}(g) + Z_{i\pm}^{C}(g)$ (see the discussion below Proposition 2). It follows that $W_i(g)$ is a linear combination of products involving $Z_i^{\mathbb{R}}(g)$'s and $Z_{i\pm}^{C}(g)$, and this representation holds in the sense of analytic functions on the Riemann surface. In order to obtain the transseries of $W_n(g)$, one needs to build the transseries expansion of each of the terms in the linear combinations. As the multidimensional integrals are factored, this is just the Cauchy product of the transseries $Z_i^{\text{pert.}}(g)$ and $e^{\frac{3}{2g}} Z_i^{(\eta)}(g)$ corresponding to $Z_i^{\mathbb{R}}(g)$ and $Z_{i\pm}^{C}(g)$, respectively.

The summation over n is more delicate, as it is an infinite series. As we have seen in Proposition 3, the small-N series of $W(g,N)$ converges in the domain $\mathbb{D}_0$ of (6.2.12), thus yielding $W(g,N)$ in terms of $W_n(g)$ as an analytic function on such domain. Therefore, we can apply the steepest descent method term by term to the small-N series, and hence the transseries of $W(g,N)$ is rigorously reconstructed by substituting the transseries for $W_n(g)$ in (6.2.1).

Unsurprisingly, at the end we recover the formal transseries of $W(g,N)$ which can be obtained by direct substitution of the transseries expansion of $Z(g,N)$, taking formally its logarithm, and then expanding in powers of $Z_i^{(\eta)}(g)$ and $Z_i^{\text{pert.}}(g) - 1$. What we gained in the process is that we replaced a formal manipulation on transseries with a rigorous manipulation on analytic functions.

Proposition 5. *The cumulant $W_n(g)$ and the full free energy $W(g,N)$ have transseries expansions, that can be organized into instanton sectors. The instanton counting parameter is denoted by p.*

1. *For $g \in \mathbb{C}_{3\pi/2}$, the cumulant $W_n(g)$ has the transseries expansion:*

$$W_n(g) = \sum_{p=0}^{n} e^{\frac{3}{2g}p} \left(\eta\sqrt{2\pi}\sqrt{\frac{g}{3}}\right)^p \sum_{l'=0}^{n-p} \left(\ln\left(\tfrac{g}{3}\right)\right)^{l'} \sum_{l\geq 0} g^l\, W_{n;l,l'}^{(p)}\,, \tag{6.2.14}$$

where $\mathbb{R}_-$ is a Stokes line, $\tau = -\text{sgn}(\varphi)$ and η is a transseries parameter which is zero on the principal Riemann sheet and is one when $|\varphi| > \pi$. The g-independent coefficient $W_{n;l,l'}^{(p)}$ is given

by the following nested sum:

$$W^{(p)}_{n;l,l'} = \sum_{\substack{k=p\\ k+p\geq 1}}^{n} (-1)^{k-1}(k-1)! \sum_{\substack{n_1,\dots,n_{n-k+1}\geq 0\\ \sum i n_i = n,\ \sum n_i = k}} \sum_{\substack{\{0\leq p_i\leq n_i\}_{i=1,\dots,n-k+1}\\ \sum p_i = p}} \frac{n!}{\prod_i (n_i-p_i)!\, p_i!\, (i!)^{n_i}}$$
$$\times \sum_{\substack{\{a^i_j\geq 0\}^{i=1,\dots,n-k+1}_{j=1,\dots,n_i}\\ \sum_i\sum_j a^i_j = l}} \sum_{\substack{\{0\leq c^i_j\leq i-1\}^{i=1,\dots,n-k+1}_{j=1,\dots,p_i}\\ \sum_i\sum_j c^i_j = l'}} \left(\frac{1}{6}\right)^{\sum_{i=1}^{n-k+1}\sum_{j=1}^{p_i} a^i_j} \left(-\frac{2}{3}\right)^{\sum_{i=1}^{n-k+1}\sum_{j=p_i+1}^{n_i} a^i_j} \tag{6.2.15}$$
$$\times \prod_{i=1}^{n-k+1} \left(\prod_{j=1}^{p_i} G(a^i_j, c^i_j; i)\right)\left(\prod_{j=p_i+1}^{n_i} G(a^i_j; i)\right),$$

with

$$G(a;i) = \frac{(2a)!}{2^{2a}a!} \sum_{\substack{a_1,\dots,a_{2a-i+1}\geq 0\\ \sum k a_k = 2a,\ \sum a_k = i}} \frac{(-1)^i i!}{\prod_k k^{a_k} a_k!},$$
$$G(a,c;i) = \sum_{b=0}^{i-1} (\imath\tau 2\pi)^{i-1-b-c} \frac{i!}{a!\, b!\, c!\, (i-b-c)!} \frac{d^b\Gamma(z)}{dz^b}\Big|_{z=2a+1}. \tag{6.2.16}$$

2. *For $g\in\mathbb{D}_\theta$, the full free energy $W(g,N)$ has the transseries expansion:*

$$W(g,N) = \sum_{n\geq 1} \frac{1}{n!}\left(-\frac{N}{2}\right)^n W_n(g)$$
$$= \sum_{p\geq 0} e^{\frac{3}{2g}p} \left(\eta\sqrt{2\pi} e^{\imath\tau\frac{\pi}{2}} \left(\frac{e^{\imath\tau\pi} g}{3}\right)^{\frac{1-N}{2}}\right)^p \sum_{l\geq 0}\left(-\frac{2g}{3}\right)^l W^{(p)}_l(N), \tag{6.2.17}$$

where

$$W^{(p)}_l(N) = \sum_{\substack{q\geq 0\\ p+q\geq 1}} (-1)^{p+q-1} \frac{(p+q-1)!}{p!q!}$$
$$\sum_{\substack{n_1,\dots,n_q\geq 1\\ m_1,\dots,m_p\geq 0\\ \sum n_i + \sum m_j = l}} \left(\prod_{i=1}^{q} \frac{\Gamma(2n_i+N/2)}{2^{2n_i} n_i!\,\Gamma(N/2)}\right)\left(\prod_{j=1}^{p} \frac{(-1)^{m_j}}{2^{2m_j} m_j!\,\Gamma(\frac{N}{2}-2m_j)}\right). \tag{6.2.18}$$

Proof. See Appendix 6.B.5 □

While the expressions in Proposition 5 are not the most amenable to computations, one feature is striking. Expanding the cumulant $W_n(g)$ into p instanton sectors, we observe that only the first n instantons contribute to W_n, that is the sum in (6.2.14) truncates to $p=n$. The n instanton contribution to W_n comes from $n=p=k$ in (6.2.15) which implies $n_1=n$ and all the others 0, hence:[8]

$$W^{(n)}_n(g) \simeq e^{\frac{3}{2g}n}\left(\eta\sqrt{2\pi}\sqrt{\frac{g}{3}}\right)^n (-1)^{n-1}(n-1)! \left(\sum_{q=0}^{\infty}\frac{(2q)!}{q!}\left(\frac{g}{6}\right)^q\right)^n. \tag{6.2.19}$$

[8] This formula is most easily derived from (6.B.74).

This is genuinely new phenomenon. Usually, for quantities that are interesting for physics, one either deals with functions having only one instanton, like $Z(g,N)$ (or $Z_n(g)$) or with function receiving contributions from all the instanton sectors, like $W(g,N)$. This is, to our knowledge, the first instance when some physically relevant quantity receiving contributions from a finite number of instantons strictly larger than one is encountered. The n instanton contribution comes from $n_1 = n$ and all the others 0, such that effectively:

$$W_n^{(n)}(g) \approx (Z_1(g))^n \ ,$$

and, for all n, $Z_n(g)$ has just a single instanton.

6.2.3 Differential equations

The exotic behaviour of $W_n(g)$ can also be understood in terms of differential equations. By rewriting the partition function as $Z(g,N) = e^{W(g,N)}$ it is straightforward to turn (6.1.16) into a differential equation for $W(g,N)$, which in turn implies a tower of equations for $W_n(g)$.

Proposition 6. *The function $W(g,N)$ obeys the nonlinear differential equation:*

$$16g^2W''(g,N) + 16g^2\left(W'(g,N)\right)^2 + \left((8N+24)g+24\right)W'(g,N) + N(N+2) = 0 \ . \tag{6.2.20}$$

The functions $W_n(g)$ obey the tower of differential equations:

$$\begin{aligned}
&4g^2W_1''(g) + 6(g+1)W_1'(g) - 1 = 0,\\
&4g^2W_2''(g) + 6(g+1)W_2'(g) + 8g^2\left(W_1'(g)\right)^2 - 8gW_1'(g) + 2 = 0,\\
&4g^2W_n''(g) + 6(g+1)W_n'(g) + 4g^2\sum_{k=1}^{n-1}\binom{n}{k}W_{n-k}'W_k' - 4ngW_{n-1}'(g) = 0 \ .
\end{aligned} \tag{6.2.21}$$

The differential equation for $W_1(g)$ is, unsurprisingly, identical to the one for $Z_1(g)$ (the connected one-point function equals to the full one-point function). Note that although the differential equation for $W(g,N)$ is nonlinear, the one for $W_n(g)$ is linear. In fact, since $W_0(g) = 0$, the nonlinear term $(W'(g,N))^2$ produces only source terms in (6.2.21). The linearity of the equations provides another point of view on why only a finite number of instantons arise in each $W_n(g)$.

6.A Asymptotic expansions

Analytic continuations of exponential integrals like $Z(g,N)$ can be carried out by deforming the original real integration cycles in the complex plane. Complex Morse theory (Picard-Lefschetz-Theory) provides a systematic framework for decomposing the original integration cycle $\mathcal{C}$ into a sum of more convenient cycles $\mathcal{J}_i$ called Lefschetz thimbles:

$$I(g) = \int_{\mathcal{C}} dx\ e^{\frac{1}{g}f(x)}a(x) = \sum_i \int_{\mathcal{J}_i} dx\ e^{\frac{1}{g}f(x)}a(x) \ . \tag{6.A.1}$$

Generically, each thimble intersects one critical (or saddle) point $x_i^* \in \mathbb{C}^m$ and consists of the union of downward flows with respect to the real part of $f(x)$ originating at x_i^*. From a topological point of view $\{\mathcal{J}_i\}$ generate the m'th relative homology group of the underlying $2m$-dimensional space. Crucially, the imaginary part of $f(x)$ is constant along each $\mathcal{J}_i$ and the integral along a thimble is absolutely convergent. Since the individual integrals are non-oscillating, it is possible to apply Laplace's method

to each term, expanding the integrand around the critical points:

$$I(g) = \sum_i e^{\frac{1}{g} f(x_i^*)} \Phi^{(i)}(g) \,, \tag{6.A.2}$$

where $\Phi^{(i)}(g)$ is an asymptotic series, possibly containing logarithms and non-integer powers of g. As g is varied, the thimbles are deformed and the number of thimbles appearing in the decomposition of the original contour $\mathcal{C}$ may vary discontinuously. These discrete changes, happening at values of g for which different thimbles intersect each other, are connected to the so called Stokes jumps.

Lefschetz thimble techniques are standard tool in resurgence analysis [208, 186, 187] and have many other applications to path integrals [209, 210, 211, 212, 194, 213]. More details and a nice pedagogical introduction can be found in [196].

In the following we review the derivation of the asymptotic expansions around the critical points of the zero-dimensional ϕ^4 theory for $N = 1$.

6.A.1 The ϕ representation of the partition function

The vacuum expansion. Our starting point is the partition function of the model in the ϕ representation. We set $N = 1$ and consider:

$$Z(g) = \int_{-\infty}^{+\infty} [d\phi]\, e^{-S[\phi]} \,, \qquad S[\phi] = \frac{1}{2}\phi^2 + \frac{g}{4!}\phi^4 \,, \tag{6.A.3}$$

where again we set $[d\phi] = d\phi/\sqrt{2\pi}$. There are three solutions of the equations of motions, i.e. critical points $S'[\phi_\star] = 0$, namely $\phi_0 = 0$ and $\phi_\pm = \pm\imath\sqrt{\frac{6}{g}}$, and each of them has an attached thimble, $\mathcal{J}_0$ and $\mathcal{J}_\pm$ (see Fig. 6.4). For symmetry reasons it is clear that $Z_{\mathcal{J}_+}(g) = Z_{\mathcal{J}_-}(g)$, thus there are only two asymptotic expansions.

Equation (6.A.3) is absolutely convergent if g is in the right half complex plane $\mathrm{Re}(g) > 0$, hence in this domain it defines an analytic function $Z(g)$. In order to analytically continue this function we turn in the complex plane and parameterize $g = |g|e^{\imath\varphi}$ but we tilt the contour of integration by $e^{-\imath\theta}$ to compensate. In detail, we define:

$$Z_\theta(g) = \int_{\mathbb{R}e^{-\imath\theta}} [d\phi]\, e^{-\frac{1}{2}\phi^2 - \frac{|g|e^{\imath\varphi}}{4!}\phi^4} = e^{-\imath\theta} \int_{\mathbb{R}} [d\phi]\, e^{-\frac{1}{2}\phi^2 e^{-2\imath\theta} - \frac{|g|e^{\imath(\varphi-4\theta)}}{4!}\phi^4} \,, \tag{6.A.4}$$

which is absolutely convergent if both $\varphi - 4\theta \in (-\pi/2, \pi/2)$ and $-2\theta \in (-\pi/2, \pi/2)$, and is independent of θ as long as it converges. As $Z_0(g) = Z(g)$, it follows that $Z_\theta(g)$ is the analytic continuation of $Z(g)$ and it is easy to check that the integral in (6.A.4) defines it for all $-3\pi/2 \le \varphi < 3\pi/2$. We denote:

$$Z_+(g) = Z_\theta(g) \text{ for } \theta > 0 \,, \qquad Z_-(g) = Z_\theta(g) \text{ for } \theta < 0 \,, \tag{6.A.5}$$

the anticlockwise respectively clockwise analytic continuations. Both $Z_+(g)$ and $Z_-(g)$ are defined for any g with $\mathrm{Re}(g) < 0$, but they are not equal. That is $Z_\theta(g)$ is a multi-valued function in the complex g-plane, with a branch point at the origin. We chose the range $-\pi < \varphi < \pi$ for the principle Riemann sheet, with a cut along the negative real axis.

For $|\varphi| < \pi$ the integration contour in (6.A.4) is homotopic to just the perturbative thimble $\mathcal{J}_0$, which at the origin is tangent to the real axis. In this case, the Laplace method applied to $Z_{\mathcal{J}_0}(g)$

amounts to Taylor expanding the quartic interaction and computing the Gaussian integral:[9]

$$\begin{aligned} Z(g) = Z_{\mathcal{J}_0}(g) &= \int_{\mathcal{J}_0} [d\phi] e^{-\frac{1}{2}\phi^2 - \frac{g}{4!}\phi^4} = \sum_{n=0}^{\infty} \frac{1}{n!} \left(-\frac{g}{4!}\right)^n \int_{-\infty}^{\infty} [d\phi] e^{-\frac{1}{2}\phi^2} \phi^{4n} \\ &= \sum_{n=0}^{\infty} \left(-\frac{2}{3}\right)^n \frac{(4n)!}{2^{6n}(2n)!n!} g^n \equiv \sum_{n=0}^{\infty} A_n^{\text{pert.}} g^n \ . \end{aligned} \tag{6.A.6}$$

The instanton sector. At $\varphi = \pm\pi$, i.e. at $g < 0$, the perturbative thimble intersects the instanton thimbles. At $|\varphi| > \pi$ they split again, but on the opposite side, so that the perturbative thimble effectively has a jump at $|\varphi| = \pi$, leading to a jump in the decomposition of the original contour $\mathcal{C}$.

As the evaluation of of the integrals along the instanton thimbles, $Z_{\mathcal{J}_\pm}$, is well behaved and continuous across the Stokes line at $\varphi = \pi$, for the asymptotic expansion around the instanton, we consider the case $g < 0$. In this case the thimbles $\mathcal{J}_\pm$ are described by $\text{Re}(\phi) = \pm\sqrt{(\text{Im}(\phi))^2 + \frac{6}{|g|}}$. Since we know the analytic expression of the thimbles, we take an explicit parametrization of the curve and use it to compute the integral. For example we can chose:

$$\gamma_\pm : \ t \in (-\infty, \infty) \to \left(\pm\sqrt{t^2 + \frac{6}{|g|}} \right) + \imath\, t \ . \tag{6.A.7}$$

and the integral reads:

$$\begin{aligned} Z_{\mathcal{J}_+} &= \int_{\mathcal{J}_+} [d\phi] e^{-S(\phi)} = \int_{-\infty}^{\infty} [dt]\ \dot{\gamma}_+(t) e^{-S(\gamma_+(t))} \\ &= \int_0^{\infty} [dt]\ \dot{\gamma}_+(t) e^{-S(\gamma_+(t))} + \int_0^{\infty} [dt]\ \dot{\gamma}_+(-t) e^{-S(\gamma_+(-t))} \ . \end{aligned} \tag{6.A.8}$$

The imaginary part of the action is zero along the thimbles. Also we have that $\dot{\gamma}_\pm(-t) = \frac{\mp t}{\sqrt{t^2 + \frac{6}{|g|}}} + \imath$, and thus the real parts of the two integrals cancel. In the end we find:

$$Z_{\mathcal{J}_+} = 2\imath \int_0^{\infty} [dt]\, e^{-\frac{3}{2|g|} - t^2 - \frac{|g|}{6}t^4} = \imath e^{\frac{3}{2g}} \int_{-\infty}^{+\infty} [dt]\, e^{-t^2 + \frac{g}{6}t^4} \ . \tag{6.A.9}$$

Now we can rescale the t by $\frac{1}{\sqrt{2}}$ and find the same integral as for $\mathcal{J}_0$ but with the opposite sign for g. In the end we have:

$$Z_{\mathcal{J}_\pm} = \frac{\imath}{\sqrt{2}} e^{\frac{3}{2g}} \sum_{p=0}^{\infty} (-1)^p A_p^{\text{pert.}} g^p \ . \tag{6.A.10}$$

Discontinuity. The discontinuity at the cut can be computed as:

$$Z_-(-|g|) - Z_+(-|g|) = \int_{\mathbb{R}e^{\imath\pi/8}} \frac{d\phi}{\sqrt{2\pi}}\ e^{-\frac{1}{2}\phi^2 + \frac{|g|}{4!}\phi^4} - \int_{\mathbb{R}e^{-\imath\pi/8}} \frac{d\phi}{\sqrt{2\pi}}\ e^{-\frac{1}{2}\phi^2 + \frac{|g|}{4!}\phi^4} \ , \tag{6.A.11}$$

where we tilted the contours by the θ of minimal absolute value which ensures convergence. Each of the two contours can be deformed to the perturbative thimble alone for $|\varphi| < \pi$. However, in the limit

[9] As explained for example in [195], in the Laplace method we restrict the integration to a small neighborhood of the saddle point, we expand the integrand, keeping only the first nontrivial term in the exponent while expanding the rest, and lastly exchange sum and integral, extending the integration domain to an infinite line along which the integrals are convergent and computable.

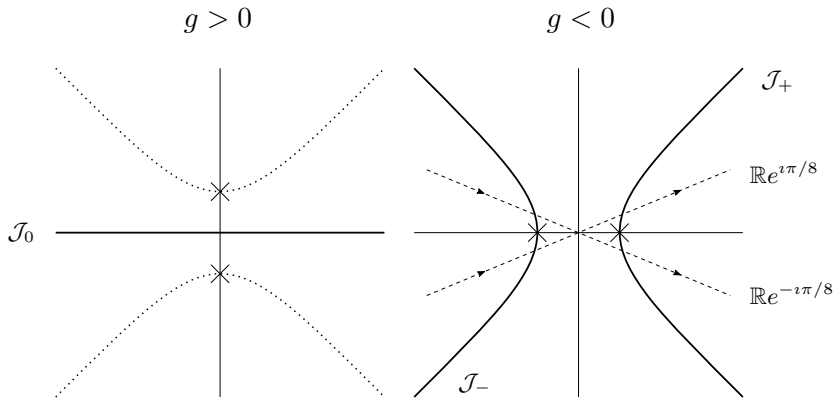

FIGURE 6.4: Critical points and thimbles (thick lines) in the complex ϕ-plane. The crosses mark the positions of the instantons and the dashed lines are the tilted contours of (6.A.11).

of $|\varphi| \nearrow \pi$ the difference of the two perturbative thimbles approaches the sum of the two instanton thimbles (see Fig. 6.5), leading to the asymptotic expansion in (6.1.15), with $N = 1$.

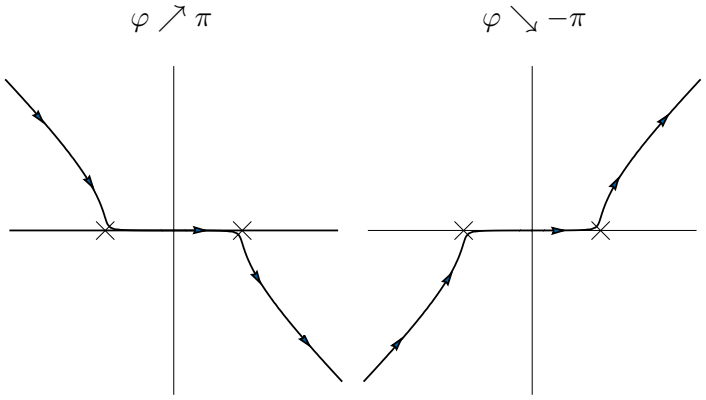

FIGURE 6.5: The thimble $\mathcal{J}_0$ for $Z_+(-|g|)$ (left) and $Z_-(-|g|)$ (right) as $|\varphi| \nearrow \pi$.

6.B Proofs of Propositions

In this appendix we gather the proofs of various Propositions in the main body of the chapter.

6.B.1 Properties of $Z(g, N)$

Proof of Proposition 1. The proof of this proposition is linear.

Property 1. This follows by bounding the square root and taking into account that the Gaussian integral is normalized to 1. For $N \geq 0$ and $g = |g|e^{\imath\varphi}$ with $-\pi < \varphi < \pi$, we have the uniform bound:

$$|1 - \imath\sqrt{\tfrac{g}{3}}\sigma| = |e^{-\imath\frac{\varphi}{2}} - \imath\sqrt{\tfrac{|g|}{3}}\sigma| \geq \cos\frac{\varphi}{2} \,. \tag{6.B.1}$$

For $N < 0$ we use $|1 - \imath\sqrt{\frac{g}{3}}\sigma| \leq 1 + \sqrt{\frac{|g|}{3}}|\sigma|$ and splitting the integration interval in regions where $\sqrt{\frac{|g|}{3}}|\sigma| \leq 1$ respectively $\sqrt{\frac{|g|}{3}}|\sigma| \geq 1$ and then re-extending the integration intervals to cover $(-\infty, \infty)$

we get:

$$|Z(g,N)| \leq \int_{-\infty}^{\infty} [d\sigma]\; e^{-\frac{1}{2}\sigma^2}(1+\sqrt{\tfrac{|g|}{3}}|\sigma|)^{|N|/2} \leq 2^{|N|/2} + \frac{2^{3|N|/4}}{\sqrt{\pi}}\frac{|g|^{N/4}}{3^{|N|/4}}\Gamma(\tfrac{|N|+2}{4})\;. \tag{6.B.2}$$

Property 2. The perturbative expansion is obtained using $(1-x)^{-N/2} = \sum_{q\geq 0}\binom{q+N/2-1}{q}x^q$ and commuting (formally) the sum and integral:

$$Z(g,N) = \sum_{n=0}^{\infty}\binom{2n+\frac{N}{2}-1}{2n}\left(-\frac{g}{3}\right)^n \int_{\mathbb{R}}[d\sigma]\; e^{-\frac{1}{2}\sigma^2}\sigma^{2n} = \sum_{n=0}^{\infty}\frac{\Gamma(2n+N/2)}{2^{2n}n!\,\Gamma(N/2)}\left(-\frac{2g}{3}\right)^n\;. \tag{6.B.3}$$

For the case $N=1$ for instance we have $\frac{\Gamma(2n+1/2)}{\Gamma(1/2)} = \frac{(4n)!}{4^{2n}(2n)!}$ (see also (6.A.6) in Appendix 6.A).

Property 3. Properties 3, 4, 5 and 6 are closely related and require that we deal carefully with the integration contour. We define:

$$\begin{aligned} Z_\theta(g,N) &= \int_{e^{-\imath\theta}\mathbb{R}}[d\sigma]\; e^{-\frac{1}{2}\sigma^2}\frac{1}{\left(1-\imath\sqrt{\frac{g}{3}}\sigma\right)^{N/2}} \\ &= \int_{\mathbb{R}} e^{-\imath\theta}[d\sigma]\; e^{-\frac{1}{2}e^{-2\imath\theta}\sigma^2}\frac{1}{\left(1-\imath\sqrt{\frac{|g|}{3}}e^{\imath\frac{\varphi-2\theta}{2}}\sigma\right)^{N/2}}\;, \end{aligned} \tag{6.B.4}$$

which is absolutely convergent if both $\varphi - 2\theta \in (-\pi,\pi)$ and $-2\theta \in (-\pi/2,\pi/2)$. Moreover, as long as it converges, it is independent of θ, as can be verified by noticing that the derivative with respect to θ can be rewritten as the integral of a total derivative in σ. Thus $Z_\theta(g,N)$ is the analytic continuation of $Z(g,N)$ and optimizing on θ the partition function can be continued to the extended Riemann sheet $\mathbb{C}_{3\pi/2}$ with a branch point at 0.

Using a Taylor formula with integral rest we have $Z_\theta(g,N) - \sum_{k=0}^{q-1}\frac{1}{k!}Z_\theta^{(k)}(0,N)g^k = R_\theta^q(g,N)$ with:

$$\begin{aligned} R_\theta^q(g,N) &= \int_0^1 du\frac{(1-u)^{2q-1}}{(2q-1)!}\int_{\mathbb{R}} e^{-\imath\theta}[d\sigma]e^{-\frac{1}{2}e^{-2\imath\theta}\sigma^2}\left(\frac{d}{du}\right)^{2q}\left(\frac{1}{\left(1-\imath\sqrt{\frac{|g|}{3}}e^{\imath\frac{\varphi-2\theta}{2}}\sigma u\right)^{\frac{N}{2}}}\right) \\ &= \int_0^1 du\frac{(1-u)^{2q-1}}{(2q-1)!}\int_{\mathbb{R}} e^{-\imath\theta}[d\sigma]e^{-\frac{1}{2}e^{-2\imath\theta}\sigma^2}\left.\frac{\left(-\imath\sqrt{\frac{|g|}{3}}e^{\imath\frac{\varphi-2\theta}{2}}\sigma\right)^n(-1)^n\frac{\Gamma(n+\frac{N}{2})}{\Gamma(\frac{N}{2})}}{\left(1-\imath\sqrt{\frac{|g|}{3}}e^{\imath\frac{\varphi-2\theta}{2}}\sigma u\right)^{\frac{2n+N}{2}}}\right|_{n=2q}\;, \end{aligned} \tag{6.B.5}$$

where for $N<0$ we need to chose $q>-N/4$. Using $|1-\imath\sqrt{\frac{|g|}{3}}e^{\imath\frac{\varphi-2\theta}{2}}\sigma u|\geq\cos\frac{\varphi-2\theta}{2}$ the rest term is bounded as:[10]

$$|R^q_\theta(g,N)|\leq\frac{1}{(\cos(2\theta))^{\frac{1}{2}+q}}\,\frac{\left(\frac{|g|}{3}\right)^q}{\left(\cos\frac{\varphi-2\theta}{2}\right)^{2q+N/2}}\,\frac{1}{(2q)!}\,\frac{\Gamma(2q+N/2)}{\Gamma(N/2)}\,\frac{(2q)!}{2^q q!}\;, \tag{6.B.6}$$

and using the Stirling formula as upper/lower bound for the Γ function[11] we have for q large enough (larger than $\max\{1,N\}$):

$$\begin{aligned}\frac{\Gamma(2q+\frac{N}{2})}{2^q q!}&\leq K\frac{(2q+\frac{N}{2}-1)^{\frac{1}{2}+2q+\frac{N}{2}-1}e^{-(2q+\frac{N}{2}-1)}}{2^q q^{\frac{1}{2}+q}e^{-q}}\\&\leq K\,2^q\,q^{q+\frac{N}{2}-1}e^{-q}\left(1+\frac{\frac{N}{2}-1}{2q}\right)^{\frac{4q+N-1}{2}}\leq K\,q!\,q^{\frac{N-3}{2}}\,2^q\;,\end{aligned} \tag{6.B.8}$$

for K some q independent constant.[12] Conveniently choosing $\theta=\varphi/6$, we get the following bounds on $Z_{\varphi/6}(g,N)$ and $R^q_{\varphi/6}(g,N)$:

$$|R^q_{\varphi/6}(g,N)|\leq\frac{K}{\left(\cos\frac{\varphi}{3}\right)^{\frac{N+1}{2}}}\,q!\,q^{\frac{N-3}{2}}\left(\frac{1}{\frac{3}{2}\left(\cos\frac{\varphi}{3}\right)^3}\right)^q|g|^q\;,\qquad|Z_{\varphi/6}(g,N)|\leq\frac{1}{\left(\cos\frac{\varphi}{3}\right)^{\frac{N+1}{2}}}\;. \tag{6.B.9}$$

Observe that $Z_\theta(g,N)$ is independent on θ only as long as φ and θ are independent, but the choice $\theta=\varphi/6$ fixes θ in terms of the argument of g and $Z_{\varphi/6}(g,N)$ depends on φ.

We are now in the position to prove that $Z(g,N)$ is Borel summable along all the directions in the cut plane $\mathbb{C}_\pi$ by verifying the conditions of Theorem 1, Appendix 2.A. This comes about as follows:

- let us fix some $\alpha\in(-\pi,\pi)$. As already noted in Properties 1 and 2, $Z(g,N)$ is analytic in $\mathbb{C}_\pi$, hence in particular at $|g|e^{\imath\alpha}$ and its asymptotic expansion at 0 is known.
- $Z(g,N)$ is analytically continued to any g in a Sokal disk (with 0 on its boundary) tilted by α, that is $g\in\mathrm{Disk}^\alpha_R=\{z\mid\mathrm{Re}(e^{\imath\alpha}/z)>1/R\}$ via $Z_{\varphi/6}(g,N)$. Note that this Sokal disk extends up to g with argument $\varphi=\alpha\pm\pi/2$. In the entire Sokal disk the rest term obeys the bound:

$$|R^q_{\varphi/6}(g,N)|\leq K\,q!\,q^{\frac{N-3}{2}}\,|g|^q\,\max_\pm\left\{\frac{1}{\left(\cos\frac{\alpha\pm\frac{\pi}{2}}{3}\right)^{\frac{N+1}{2}}}\left(\frac{1}{\frac{3}{2}\left(\cos\frac{\alpha\pm\frac{\pi}{2}}{3}\right)^3}\right)^q\right\}. \tag{6.B.10}$$

  For any fixed $\alpha\in(-\pi,\pi)$, $\min_\pm\left\{\frac{3}{2}\left(\cos\frac{\alpha\pm\frac{\pi}{2}}{3}\right)^3\right\}=\rho>0$ for some ρ hence the Taylor rest obeys the bound in (2.5.4).

[10] The factor $1/(\cos(2\theta))^q$ can be improved to 1 by Taylor expanding in the Gaussian measure along the lines of the proof of Proposition 4.

[11] In detail:

$$1\leq\frac{\Gamma(x+1)}{\sqrt{2\pi x}(x/e)^x}\leq e^{\frac{1}{12x}}\leq e^{1/12}\;,\qquad x\in[1,\infty)\;. \tag{6.B.7}$$

[12] Note that $\left(1+\frac{\frac{N}{2}-1}{2q}\right)^{\frac{4q+N-1}{2}}\leq\exp\{\frac{4q+N-1}{2}\ln(1+\frac{\frac{N}{2}-1}{2q})\}\leq\exp\{\frac{(4q+N-1)(\frac{N}{2}-1)}{4q}\}\leq K$ for $q\geq1$.

Property 4. Although this point is discussed in the main body of the chapter, we include it also here for completeness. We denote the analytic continuation of $Z(g,N)$ to the extended Riemann sheet $\mathbb{C}_{3\pi/2}$ by:

$$\theta > 0: \qquad Z_+(g,N) = Z_\theta(g,N)\,, \qquad\qquad Z_-(g,N) = Z_{-\theta}(g,N)\,. \tag{6.B.11}$$

Observe that the factorial bound on the Taylor rest term cannot be satisfied (for any choice of θ) when $\varphi \to \pm 3\pi/2$. As Borel summability along a direction α requires analytic continuation and bound on the rest term in a Sokal disk centred on that direction, hence extending up to $\alpha \pm \pi/2$, $Z(g,N)$ looses Borel summability at $g \in \mathbb{R}_-$.

We start from (6.1.2) which we quote here again:

$$Z(g,N) = \int_{-\infty}^{+\infty} [d\sigma]\; e^{-\frac{1}{2}\sigma^2} \frac{1}{\left(1 - e^{\imath\frac{\pi}{2}}\sqrt{\frac{g}{3}}\sigma\right)^{N/2}}\,, \tag{6.B.12}$$

and the Lefschetz thimble of the integral is the real axis irrespective of g (comparing to (6.A.1), we see that in the present case thimbles are defined by the saddle points of σ^2). As long as $g = |g|e^{\imath\varphi} \in \mathbb{C}_\pi$, the integral converges as the singularity at

$$\sigma_\star = -\imath\sqrt{\frac{3}{g}} = e^{-\imath\frac{\pi}{2} - \imath\frac{\varphi}{2}}\sqrt{\frac{3}{|g|}}\,, \tag{6.B.13}$$

lies outside the integration contour. Notice that the singularity is a pole for N even, and otherwise it is a branch point with branch cut $\sigma_\star \times (1, +\infty)$. We will discuss in detail the general case with a branch cut, as the case of even N turns out to be readable as a special case of the results at general N.

As g approaches $\mathbb{R}_-$ the branch point hits the contour of integration: for $\varphi \nearrow \pi$ (that is we approach the cut in the g-plane counterclockwise) the branch point hits the real axis at $-\sqrt{3/|g|}$ while for $\varphi \searrow -\pi$ (that is we approach the cut in the g-plane clockwise) the branch point hits the real axis at $\sqrt{3/|g|}$. The analytic continuation $Z_+(g,N)$ (resp. $Z_-(g,N)$) consists in tilting the contour of integration in σ by some clockwise rotation $-\theta < 0$ (resp. counterclockwise, $\theta > 0$) to avoid the collision with the branch point. However, once g passes on the second Riemann sheet $\varphi > \pi$ (resp. $\varphi < -\pi$) the tilted contour is no longer a thimble and in order to derive the asymptotic behaviour of $Z_\pm(g,N)$ we need to to rotate it back to the real axis. This costs us a Hankel contour C along the cut (see Fig. 6.1):

$$\begin{aligned} Z_\pm(g,N)\big|_{\substack{\varphi > \pi \\ \varphi < -\pi}} &= \int_{e^{\mp\imath\theta}\mathbb{R}} [d\sigma]\; \frac{e^{-\frac{1}{2}\sigma^2}}{\left(1 - \imath\sqrt{\frac{g}{3}}\sigma\right)^{N/2}} = Z^{\mathbb{R}}(g,N) + Z^C_\pm(g,N)\,, \\ Z^C_\pm(g,N) &= \int_C [d\sigma]\; e^{-\frac{1}{2}\sigma^2} \frac{1}{\left(1 - \imath\sqrt{\frac{g}{3}}\sigma\right)^{N/2}}\,. \end{aligned} \tag{6.B.14}$$

The integral $Z^{\mathbb{R}}(g,N)$, defined in (6.1.4), is absolutely convergent, and hence analytic, in the range $|\varphi| \in (\pi, 3\pi)$, where it is bounded from above as in (6.1.6).

The Hankel contour C turns clockwise around the cut $\sigma_\star \times (1, +\infty)$, i.e. starting at infinity with argument $\frac{3\pi}{2} - \frac{\varphi}{2}$ and going back with argument $-\frac{\pi}{2} - \frac{\varphi}{2}$ after having encircled the branch point $\sigma_\star$. We kept a subscript $\pm$ for the contribution of the Hankel contour, because, even though the definition of $Z^C_\pm(g,N)$ and C might suggest that it is one single function of g, in fact the integral around the

cut is divergent for $|\varphi| < \pi/2$ and therefore the integrals at $\pi < \varphi < 3\pi/2$ and at $-\pi > \varphi > -3\pi/2$ are not the analytic continuation of each other.

We will now rewrite $Z^C_\pm(g,N)$ in a more useful form. With the change of variables $\sigma = e^{-\imath\frac{\pi}{2}-\imath\frac{\varphi}{2}}\sqrt{3/|g|}\,\sigma'$ the contour C becomes a Hankel contour C' turning clockwise around $(1,+\infty)$ and a shift to $\sigma' = 1+t$ brings C' to C'', a clockwise oriented Hankel contour around the positive real axis, starting at infinity with argument 2π and going back with vanishing argument after having encircled the origin:

$$\begin{aligned} Z^C_\pm(g,N) &= \int_C [d\sigma]\; e^{-\frac{1}{2}\sigma^2}\,\frac{1}{\left(1-e^{\frac{\imath\pi}{2}}\sqrt{\frac{g}{3}}\sigma\right)^{N/2}} = \left(\frac{3}{e^{\imath\pi}g}\right)^{1/2}\int_{C'}[d\sigma']\; e^{\frac{3}{2g}(\sigma')^2}\,\frac{1}{(1-\sigma')^{N/2}} \\ &= \frac{1}{\sqrt{2\pi}}\left(\frac{3}{e^{\imath\pi}g}\right)^{1/2}\int_{C''} dt\;(e^{-\imath\pi}t)^{-\frac{N}{2}}\; e^{\frac{3}{2g}(1+t)^2}\;, \end{aligned} \tag{6.B.15}$$

where we have made explicit the choice of branch by expressing minus signs as phases. Notice that the integral converges because for $\pi < |\varphi| < \frac{3\pi}{2}$ the exponent has a negative real part.

Next, we make the change of variables $t = e^{\imath\tau\pi}\frac{g}{3}u$, with $\tau = -\mathrm{sgn}(\varphi)$ (i.e. $\tau = -$ for $\varphi > \pi$, that is for $Z^C_+(g)$ and $\tau = +$ for $\varphi < -\pi$ i.e. for $Z^C_-(g)$), obtaining:

$$Z^C_\pm(g,N) = \frac{e^{\imath\tau\pi(1-\frac{N}{2})}}{\imath\sqrt{2\pi}}\left(\frac{g}{3}\right)^{\frac{1-N}{2}} e^{\frac{3}{2g}}\int_{e^{-\imath\tau\pi-\imath\varphi}C''} du\;(e^{-\imath\pi}u)^{-\frac{N}{2}}e^{-u+\frac{g}{6}u^2}\;. \tag{6.B.16}$$

The two choices of τ are dictated by the fact that for $\pi < |\varphi| < 3\pi/2$ the contour of integration should stay in the domain of convergence continuously connected to C''. The fact that this entails two different choices of τ reflects what we anticipated about the need of keeping a $\pm$ subscript. Lastly, the contour of integration can be deformed back to C'', where we easily evaluate the discontinuity (for $N < 2$) as:[13]

$$\begin{aligned} Z^C_\pm(g,N) &= \frac{e^{\imath\tau\pi(1-\frac{N}{2})}}{\sqrt{2\pi}}\left(\frac{g}{3}\right)^{\frac{1-N}{2}} e^{\frac{3}{2g}}\;2\sin(\pi\frac{N}{2})\int_0^{+\infty} du\; e^{-u+\frac{g}{6}u^2}u^{-\frac{N}{2}} \\ &= \frac{e^{\imath\tau\pi(1-\frac{N}{2})}}{\sqrt{2\pi}}\left(\frac{g}{3}\right)^{\frac{1-N}{2}} e^{\frac{3}{2g}}\;2^{1+N/2}\sin(\pi\frac{N}{2})\int_0^{+\infty} d\rho\; e^{-\frac{1}{2}\rho^2+\frac{g}{24}\rho^4}\rho^{1-N}\;. \end{aligned} \tag{6.B.17}$$

In the last step, we performed the change of variables $u = \rho^2/2$ in order to make explicit that for $N = 1$ we reproduce (6.A.9) (times two, because the Hankel contour is only one, while there are two instanton thimbles in the ϕ representation). For general N, the integral resembles that of the $O(N)$ model in polar coordinates, except that in that case we would have the opposite sign for the power of the insertion, i.e. ρ^{N-1}. This also explains the relation between the coefficients of the perturbative and nonperturbative series in (6.1.12), which are related by the transformation $N \to 2-N$ (up to an area of S^{N-1} of the missing angular integration in (6.B.17)).

[13] This is obtained by writing, for $\mathrm{Re}(z) < 1$,

$$\int_{C''} du\; e^{-S(u)}\,(e^{-\imath\pi}u)^{-z} = \int_{+\infty}^0 du\; e^{-S(u)}\,e^{-z(\ln|u|+\imath\pi)} + \int_0^{+\infty} du\; e^{-S(u)}\,e^{-z(\ln|u|-\imath\pi)} = 2\imath\sin(\pi z)\int_0^{+\infty} du\; e^{-S(u)}\,u^{-z}\;.$$

The integral over u (or ρ) in (6.B.17) is convergent as long as $\mathrm{Re}(g) < 0$, i.e. for $\pi/2 < |\varphi| < 3\pi/2$. One can use again the Hubbard-Stratonovich trick to write (for $N < 2$):

$$\begin{aligned}\int_0^{+\infty} du\, e^{-u+\frac{g}{6}u^2} u^{-\frac{N}{2}} &= \int_{-\infty}^{+\infty} [d\sigma]\, e^{-\frac{\sigma^2}{2}} \int_0^{+\infty} du\, e^{-u(1+\sqrt{\frac{g}{3}}\sigma)} u^{-\frac{N}{2}} \\ &= \Gamma(1-N/2) \int_{-\infty}^{+\infty} [d\sigma]\, e^{-\frac{\sigma^2}{2}} \left(1+\sqrt{\frac{g}{3}}\sigma\right)^{\frac{N}{2}-1} ,\end{aligned} \tag{6.B.18}$$

where, in order to ensure uniform convergence of the u integral, we keep $|\varphi| = \pi$. Note that the integral is independent of choice of branch of $\sqrt{g}$, as a sign can be absorbed in σ. The reader will note that this is proportional to our integral in (6.1.4) with arguments $Z^{\mathbb{R}}(-g, 2-N)$, which is unambiguous as $Z^{\mathbb{R}}(g, N)$ is periodic with period 2π in the argument of g, hence one can chose any determination of $-g$. The advantage of the manipulation above is that the integral over σ now converges for $0 < |\varphi| < 2\pi$, hence it allows us to analytically continue $Z^C_{\pm}(g, N)$ beyond $|\varphi| = 3\pi/2$ up to $|\varphi| \nearrow 2\pi$.

Using Euler's reflection formula, $\Gamma(1-z)\sin(\pi z) = \pi/\Gamma(z)$, we get:[14]

$$\begin{aligned}Z^C_{\pm}(g, N) &= \frac{e^{\imath\tau\pi(1-\frac{N}{2})}}{\sqrt{2\pi}} \left(\frac{g}{3}\right)^{\frac{1-N}{2}} e^{\frac{3}{2g}} \frac{2\pi}{\Gamma(N/2)} \int_{-\infty}^{+\infty} [d\sigma]\, e^{-\frac{\sigma^2}{2}} \left(1-\imath\sqrt{\frac{-g}{3}}\sigma\right)^{\frac{N}{2}-1} \\ &= e^{\imath\tau\pi(1-\frac{N}{2})} \left(\frac{g}{3}\right)^{\frac{1-N}{2}} e^{\frac{3}{2g}} \frac{\sqrt{2\pi}}{\Gamma(N/2)}\, Z^{\mathbb{R}}(-g, 2-N) \\ &= e^{\imath\tau\pi(1-\frac{N}{2})} \left(\frac{g}{3}\right)^{\frac{1-N}{2}} e^{\frac{3}{2g}} \frac{\sqrt{2\pi}}{\Gamma(N/2)}\, Z(e^{\imath\tau\pi} g, 2-N) .\end{aligned} \tag{6.B.19}$$

In the last line above we have chosen a determination of -1 such that $e^{\imath\tau\pi} g$ belongs to the principal sheet of the Riemann surface, where $Z = Z^{\mathbb{R}}$, hence $Z(e^{\imath\tau\pi} g, 2-N) = Z^{\mathbb{R}}(e^{\imath\tau\pi} g, 2-N) = Z^{\mathbb{R}}(-g, 2-N)$, where in the last equality we used the fact that $Z^{\mathbb{R}}$ is single-valued. We have thus shown that, when going from $|\varphi| < \pi$ to $\pi < |\varphi| < 2\pi$ our analytic continuation of $Z(g, N)$ switches:

$$\begin{aligned}Z(g, N) &\xrightarrow{|\varphi|\nearrow\pi_+} Z^{\mathbb{R}}(g, N) + \frac{\sqrt{2\pi}}{\Gamma(N/2)}\, e^{\imath\tau\frac{\pi}{2}}\, e^{\frac{3}{2g}} \left(e^{\imath\tau\pi}\frac{g}{3}\right)^{\frac{1-N}{2}} Z^{\mathbb{R}}(-g, 2-N) \\ &= Z(e^{\imath(2\tau\pi)} g, N) + \frac{\sqrt{2\pi}}{\Gamma(N/2)}\, e^{\imath\tau\frac{\pi}{2}}\, e^{\frac{3}{2g}} \left(e^{\imath\tau\pi}\frac{g}{3}\right)^{\frac{1-N}{2}} Z(e^{\imath\tau\pi} g, 2-N) ,\end{aligned} \tag{6.B.20}$$

where $|\varphi| \nearrow \pi_+$ signifies that the switching takes place when $|\varphi|$ crosses the value π coming from below. In the second line above, for $\pi < |\varphi| < 2\pi$, both arguments $e^{\imath(2\tau\pi)} g$ and $e^{\imath\tau\pi} g$ belong to the principal sheet of the Riemann surface , where $Z(g, N)$ has already been constructed and proven to be analytic.

The first term in (6.B.20) is regular up to $|\varphi| = 3\pi$, but the second one has a problem when $e^{\imath\tau\pi} g$ reaches the negative real axis (which is $\varphi \to -2\tau\pi$). Note that $Z(e^{\imath\tau\pi} g, 2-N)$ approaches the cut singularity in the principal sheet of the Riemann surface, as its argument is $e^{\imath\tau\pi} g$. But we already know what happens with $Z(g', N')$ when g' traverses the cut singularity in the principal Riemann sheet: a branch point crosses the integration contour, one detaches a Hankel contour and the analytic continuation switches again:

$$\begin{aligned}Z(e^{\imath\tau\pi} g, 2-N) &\xrightarrow{|\varphi|\nearrow 2\pi_+} Z(e^{\imath(3\tau\pi)} g, 2-N) \\ &\quad + \frac{\sqrt{2\pi}}{\Gamma(1-N/2)}\, e^{\imath\tau\frac{\pi}{2}}\, e^{\frac{3}{2ge^{\imath\tau\pi}}} \left(e^{\imath(2\tau\pi)}\frac{g}{3}\right)^{\frac{N-1}{2}} Z(e^{\imath(2\tau\pi)} g, N) ,\end{aligned} \tag{6.B.21}$$

[14] Notice that this allows us also to analytically continue the result to $N \geq 2$.

where this time the arguments at which Z is evaluated on the right hand side stay in the principal sheet for $2\pi < |\varphi| < 3\pi$.

We iterate this and build the analytic continuation of $Z(g,N)$ in terms of $Z^{\mathbb{R}}$ on the whole Riemann surface. The first few steps in this continuation are:

$$\begin{aligned}
|\varphi| < \pi : \quad & Z(g,N) = Z^{\mathbb{R}}(g,N) \,, \\
\pi < |\varphi| < 2\pi : \quad & Z(g,N) = Z(e^{\imath(2\tau\pi)}g,N) + \frac{\sqrt{2\pi}}{\Gamma(\frac{N}{2})}\, e^{\imath\tau\frac{\pi}{2}}\, e^{\frac{3}{2g}}\, \left(e^{\imath\tau\pi}\frac{g}{3}\right)^{\frac{1-N}{2}}\, Z(e^{\imath\tau\pi}g, 2-N) \\
& \qquad = Z^{\mathbb{R}}(g,N) + \frac{\sqrt{2\pi}}{\Gamma(\frac{N}{2})}\, e^{\imath\tau\frac{\pi}{2}}\, e^{\frac{3}{2g}}\, \left(e^{\imath\tau\pi}\frac{g}{3}\right)^{\frac{1-N}{2}}\, Z^{\mathbb{R}}(-g, 2-N) \,, \\
2\pi < |\varphi| < 3\pi : \quad & Z(g,N) = (1+\tilde{\tau})\, Z(e^{\imath(2\tau\pi)}g,N) \\
& \qquad + e^{\imath\tau\pi(N-1)}\frac{\sqrt{2\pi}}{\Gamma(\frac{N}{2})}\, e^{\imath\tau\frac{\pi}{2}}\, e^{\frac{3}{2g}}\, \left(e^{\imath(3\tau\pi)}\frac{g}{3}\right)^{\frac{1-N}{2}}\, Z(e^{\imath(3\tau\pi)}g, 2-N) \\
& \qquad = (1+\tilde{\tau})\, Z^{\mathbb{R}}(g,N) \\
& \qquad + e^{\imath\tau\pi(N-1)}\frac{\sqrt{2\pi}}{\Gamma(\frac{N}{2})}\, e^{\imath\tau\frac{\pi}{2}}\, e^{\frac{3}{2g}}\, \left(e^{\imath(3\tau\pi)}\frac{g}{3}\right)^{\frac{1-N}{2}}\, Z^{\mathbb{R}}(-g, 2-N) \,,
\end{aligned} \tag{6.B.22}$$

where we denoted:

$$\begin{aligned}
\tilde{\tau} &= \frac{\sqrt{2\pi}}{\Gamma(N/2)}\, e^{\imath\tau\frac{\pi}{2}}\, e^{\frac{3}{2g}}\, \left(e^{\imath\tau\pi}\frac{g}{3}\right)^{\frac{1-N}{2}}\, \frac{\sqrt{2\pi}}{\Gamma(1-N/2)}\, e^{\imath\tau\frac{\pi}{2}}\, e^{\frac{3}{2ge^{\imath\tau\pi}}}\, \left(e^{\imath(2\tau\pi)}\frac{g}{3}\right)^{\frac{N-1}{2}} \\
&= 2\sin(\tfrac{N\pi}{2})\, e^{\imath\tau\pi\frac{N+1}{2}} \,.
\end{aligned} \tag{6.B.23}$$

In order to iterate equation (6.B.20), we must make sure that at each step the arguments of the functions Z involved in the analytic continuation are brought back to the principal sheet. We denote the analytic continuation of the partition function to the Riemann surface by:

$$\begin{aligned}
& 2k\pi < |\varphi| < (2k+1)\pi : \\
& \quad Z(g,N) = \omega_{2k}\, Z(e^{\imath(2k)\tau\pi}g,N) \\
& \qquad\qquad + \eta_{2k}\, \frac{\sqrt{2\pi}}{\Gamma(N/2)}\, e^{\imath\tau\frac{\pi}{2}}\, e^{\frac{3}{2g}}\, \left(e^{\imath(2k+1)\tau\pi}\frac{g}{3}\right)^{\frac{1-N}{2}}\, Z(e^{\imath(2k+1)\tau\pi}g, 2-N) \,, \\
& (2k+1)\pi < |\varphi| < (2k+2)\pi : \\
& \quad Z(g,N) = \omega_{2k+1}\, Z(e^{\imath(2k+2)\tau\pi}g,N) \\
& \qquad\qquad + \eta_{2k+1}\, \frac{\sqrt{2\pi}}{\Gamma(N/2)}\, e^{\imath\tau\frac{\pi}{2}}\, e^{\frac{3}{2g}}\, \left(e^{\imath(2k+1)\tau\pi}\frac{g}{3}\right)^{\frac{1-N}{2}}\, Z(e^{\imath(2k+1)\tau\pi}g, 2-N) \,,
\end{aligned} \tag{6.B.24}$$

a general recursion relation for the (ω_q, η_q) is obtained from (6.B.20) and (6.B.21) generalized to the Riemann surface:[15]

$$(\omega_0, \eta_0) = (1, 0) \ , \qquad \begin{cases} \omega_{2k+1} &= \omega_{2k} \\ \eta_{2k+1} &= \eta_{2k} + \omega_{2k} \end{cases} \ , \qquad \begin{cases} \omega_{2(k+1)} &= \tilde{\tau}\ \eta_{2k+1} + \omega_{2k+1} \\ \eta_{2(k+1)} &= e^{\imath\tau\pi(N-1)}\eta_{2k+1} \end{cases} \ . \tag{6.B.25}$$

The recursion can easily been solved by introducing a transfer matrix:

$$\begin{pmatrix} \omega_{2k} \\ \eta_{2k} \end{pmatrix} = A^k \begin{pmatrix} 1 \\ 0 \end{pmatrix} \ , \qquad A = \begin{pmatrix} 1+\tilde{\tau} & \tilde{\tau} \\ e^{\imath\tau\pi(N-1)} & e^{\imath\tau\pi(N-1)} \end{pmatrix} \ , \tag{6.B.26}$$

which leads to (6.1.11). Since the eigenvalues of A are $\pm e^{\imath\tau\pi\frac{N}{2}}$, we have that A^k equals the identity matrix for $k = 4$ if N is odd, and for $k = 2$ if N is even. Therefore, in these two cases we have a monodromy group of order 4 and 2, respectively. More generally, we have a monodromy group of finite order if N is a rational number, and an infinite monodromy otherwise.

Property 5. This follows by combining Property 2, which gives the asymptotic expansion of $Z^{\mathbb{R}}(g, N)$, with (6.B.19) using $(1+x)^{N/2-1} = \sum_{q\geq 0} \frac{\Gamma(N/2)}{q!\Gamma(N/2-q)} x^q$:

$$Z^C_{\pm}(g, N) = e^{\imath\tau\pi(1-\frac{N}{2})}\sqrt{2\pi}\left(\frac{g}{3}\right)^{\frac{1-N}{2}} e^{\frac{3}{2g}} \sum_{q\geq 0} \frac{1}{2^{2q} q!\ \Gamma(\frac{N}{2}-2q)} \left(\frac{2g}{3}\right)^q \ . \tag{6.B.27}$$

Property 6. In order to compute the discontinuity of the partition function, let us consider g in the complex plane of the coupling constant slightly below the negative real axis, $\mathrm{Re}(g), \mathrm{Im}(g) < 0$. This g can be reached either counterclockwise with Z_+ or clockwise with Z_-. There is a subtlety here: if we denote this point as $g = |g|e^{\imath\varphi}$ with $\varphi \in (\pi, 3\pi/2)$ in the clockwise direction, it corresponds to $g = |g|e^{\imath(\varphi-2\pi)}$ in the counterclockwise direction. While only the real axis contributes to $Z_-(g, N)$ (as turning clockwise we do not cross the cut to reach it), $Z_+(g, N)$ has the additional contribution of the Hankel contour (as turning counterclockwise we cross the cut):

$$Z_+(g, N) = Z^{\mathbb{R}}(g, N) + Z^C_+(g, N) \ , \qquad Z_-(g, N) = Z^{\mathbb{R}}(e^{-2\pi\imath}g, N) = Z^{\mathbb{R}}(g, N) \ , \tag{6.B.28}$$

where we used the fact that $Z^{\mathbb{R}}$ is single-valued. When taking the difference, the $Z^{\mathbb{R}}$ pieces cancel and the discontinuity is given by the Hankel contour contribution, $Z_-(g, N) - Z_+(g, N) = -Z^C_+(g, N)$. In particular, at the negative real axis we have:

$$\mathrm{disc}_{\pi}\big(Z(g, N)\big) = \lim_{\varphi \searrow \pi} \big(Z_-(e^{-2\pi\imath}g, N) - Z_+(g, N)\big) = -Z^C_+(e^{\imath\pi}|g|, N) \ . \tag{6.B.29}$$

Lastly, notice that the computation done on the other side of the cut, $\lim_{\varphi \nearrow -\pi} \big(Z_-(g, N) - Z_+(e^{2\pi\imath}g, N)\big)$, gives the same result, because $Z^C_-(e^{-\imath\pi}|g|, N) = -Z^C_+(e^{\imath\pi}|g|, N)$.

[15] In detail, we use:

$$Z(e^{\imath(2k)\tau\pi}g, N) \xrightarrow{|\varphi|\nearrow(2k+1)\pi_+} Z(e^{\imath(2k+2)\tau\pi}g, N) + \tfrac{\sqrt{2\pi}}{\Gamma(N/2)}\, e^{\imath\tau\frac{\pi}{2}}\, e^{\frac{3}{2g}} \left(e^{\imath(2k+1)\tau\pi}\tfrac{g}{3}\right)^{\frac{1-N}{2}} Z(e^{\imath(2k+1)\tau\pi}g, 2-N) \ ,$$

$$Z(e^{\imath(2k+1)\tau\pi}g, 2-N) \xrightarrow{|\varphi|\nearrow(2k+2)\pi_+} Z(e^{\imath(2k+3)\tau\pi}g, 2-N) + \tfrac{\sqrt{2\pi}}{\Gamma(1-N/2)}\, e^{\imath\tau\frac{\pi}{2}}\, e^{-\frac{3}{2g}} \left(e^{\imath(2k+2)\tau\pi}\tfrac{g}{3}\right)^{\frac{N-1}{2}} Z(e^{\imath(2k+2)\tau\pi}g, N) \ ,$$

$$\tfrac{\sqrt{2\pi}}{\Gamma(N/2)}\, e^{\imath\tau\frac{\pi}{2}}\, e^{\frac{3}{2g}} \left(e^{\imath(2k+1)\tau\pi}\tfrac{g}{3}\right)^{\frac{1-N}{2}} \left[\tfrac{\sqrt{2\pi}}{\Gamma(1-N/2)}\, e^{\imath\tau\frac{\pi}{2}}\, e^{-\frac{3}{2g}} \left(e^{\imath(2k+2)\tau\pi}\tfrac{g}{3}\right)^{\frac{N-1}{2}}\right] = \tilde{\tau} \ .$$

Property 7. From the intermediate field expression (6.1.2) of the partition function we find straightforwardly that $(N+4g\partial_g)Z(g,N) = NZ(g,N+2)$. Applying this twice, we have:

$$(N+2+4g\partial_g)(N+4g\partial_g)Z(g,N) = N(N+2)Z(g,N+4)\ . \tag{6.B.30}$$

Integrating by parts in (6.1.2) with $N \to N+4$, we find $N(N+2)Z(g,N+4) = -4!Z'(g,N)$, and thus we arrive at the equation:

$$N(N+2)Z(g,N) + ((8N+24)g+24)\,Z'(g,N) + 16g^2Z''(g,N) = 0\ . \tag{6.B.31}$$

This concludes the proof of Proposition 1. □

6.B.2 Properties of $Z_n(g)$

Proof of Proposition 2. The proof is similar to the one of Proposition 1.

Property 1. We start from:

$$Z_n(g) = \int_{-\infty}^{+\infty}[d\sigma]e^{-\frac{1}{2}\sigma^2}\left(\ln(1-\imath\sqrt{\frac{g}{3}}\sigma)\right)^n = \int_{-\infty}^{+\infty}[d\sigma]e^{-\frac{1}{2}\sigma^2}\left(\ln(1-\imath e^{\imath\frac{\varphi}{2}}\sqrt{\frac{|g|}{3}}\sigma)\right)^n\ , \tag{6.B.32}$$

where we parameterized $g = |g|e^{\imath\varphi}$ with $\varphi \in (-\pi,\pi)$. For any real x we have $1+|x| \geq |1-\imath e^{\imath\frac{\varphi}{2}}x| \geq \cos\frac{\varphi}{2}$, hence we can bound the logarithm as:

$$\begin{aligned} |\ln(1-\imath e^{\imath\frac{\varphi}{2}}x)|^2 &\leq \pi^2 + \max\left\{[\ln(\cos\tfrac{\varphi}{2})]^2, \left[\ln(1+|x|)\right]^2\right\} \\ &\leq 2\left[\left(|\ln(\cos\tfrac{\varphi}{2})|+1\right)\ln(e^\pi+|x|)\right]^2\ , \end{aligned} \tag{6.B.33}$$

which implies:

$$|Z_n(g)| \leq \left|2^{1/2}\left(|\ln(\cos\tfrac{\varphi}{2})|+1\right)\right|^n \int [d\sigma]e^{-\frac{1}{2}\sigma^2}\left[\ln(e^\pi+\sqrt{\frac{|g|}{3}}|\sigma|)\right]^n\ . \tag{6.B.34}$$

We have $\ln(e^\pi+\sqrt{\frac{|g|}{3}}|\sigma|) \leq \frac{1}{\varepsilon}(e^\pi+\sqrt{\frac{|g|}{3}}|\sigma|)^\varepsilon$ for any $\varepsilon > 0$. Cutting the integration interval into regions where $e^\pi < \sqrt{\frac{|g|}{3}}|\sigma|$ and regions where $e^\pi > \sqrt{\frac{|g|}{3}}|\sigma|$ and extending each piece back to the entire real line we get a bound:

$$\begin{aligned} |Z_n(g)| &\leq \frac{\left|2^{1/2}\left(|\ln(\cos\frac{\varphi}{2})|+1\right)\right|^n}{\varepsilon^n}\left[(2e^\pi)^{n\varepsilon} + \left(\frac{4|g|}{3}\right)^{\frac{n\varepsilon}{2}}\int[d\sigma]e^{-\frac{1}{2}\sigma^2}|\sigma|^{n\varepsilon}\right] \\ &\leq K^n\frac{\left(|\ln(\cos\frac{\varphi}{2})|+1\right)^n}{\varepsilon^n}\left(1+|g|^{\frac{n\varepsilon}{2}}\Gamma(\tfrac{n\varepsilon+1}{2})\right)\ . \end{aligned} \tag{6.B.35}$$

Property 2. In order to derive the asymptotic expansion of $Z_n(g)$, we use Faà di Bruno's formula:[16] to expand:

$$\left(\ln(1-\imath\sqrt{\frac{g}{3}}\sigma)\right)^n = \sum_{m\geq n}\left(\imath\sqrt{\frac{g}{3}}\right)^m \sigma^m \sum_{\substack{m_1,\dots,m_m\geq 0\\ \sum km_k=m,\,\sum m_k=n}} \frac{(-1)^n n!}{\prod_k k^{m_k} m_k!}\,, \tag{6.B.36}$$

and integrate the Gaussian term by term. As a cross check, we can (formally) resum:[17]

$$\begin{aligned}\sum_{n\geq 0}\frac{1}{n!}\left(-\frac{N}{2}\right)^n Z_n(g) &\simeq \sum_{n\geq 0}\frac{1}{n!}\left(-\frac{N}{2}\right)^n \sum_{m\geq n/2}\left(-\frac{2g}{3}\right)^m \frac{(2m)!}{2^{2m}m!}\\ &\qquad\times \sum_{\substack{m_1,\dots,m_{2m}\geq 0\\ \sum km_k=2m,\sum m_k=n}} \frac{(-1)^n n!}{\prod_k k^{m_k} m_k!}\\ &= \sum_{m=0}^{\infty}\left(-\frac{2g}{3}\right)^m \frac{(2m)!}{2^{2m}m!}\sum_{\substack{m_1,\dots,m_{2m}\geq 0\\ \sum km_k=2m}}\prod_{k=1}^{2m}\left(\frac{N}{2k}\right)^{m_k}\frac{1}{m_k!}\\ &= \sum_{m=0}^{\infty}\frac{\Gamma(2m+N/2)}{2^{2m}m!\Gamma(N/2)}\left(-\frac{2g}{3}\right)^m,\end{aligned} \tag{6.B.37}$$

reproducing the asymptotic expansion of $Z(g,N)$ in (6.1.7).

Property 3. We analytically continue $Z_n(g)$ to the extended Riemann sheet $\mathbb{C}_{3\pi/2}$ as in Property 3, Proposition 2, by turning the integration contour by $e^{-\imath\theta}$:

$$Z_{n\theta}(g) = \int_{-\infty}^{+\infty} e^{-\imath\theta}[d\sigma]e^{-\frac{1}{2}e^{-2\imath\theta}\sigma^2}\left(\ln(1-\imath e^{\imath\frac{\varphi-2\theta}{2}}\sqrt{\frac{|g|}{3}}\sigma)\right)^n. \tag{6.B.38}$$

Using a Taylor formula with integral rest, the reminder $R^q_{n\theta}(g)$ writes:

$$\begin{aligned}R^q_{n\theta}(g) &= \int_0^1 du\,\frac{(1-u)^{2q-1}}{(2q-1)!}\int_{\mathbb{R}} e^{-\imath\theta}[d\sigma]\,e^{-\frac{1}{2}e^{-2\imath\theta}\sigma^2}\left(\frac{d}{du}\right)^{2q}\left(\ln(1-\imath e^{\imath\frac{\varphi-2\theta}{2}}\sqrt{\frac{|g|}{3}}\sigma u)\right)^n\\ &= \int_0^1 du\,\frac{(1-u)^{2q-1}}{(2q-1)!}\int_{\mathbb{R}} e^{-\imath\theta}[d\sigma]\,e^{-\frac{1}{2}e^{-2\imath\theta}\sigma^2}\frac{\left(\imath e^{\imath\frac{\varphi-2\theta}{2}}\sqrt{\frac{|g|}{3}}\sigma\right)^{2q}}{\left(1-\imath e^{\imath\frac{\varphi-2\theta}{2}}\sqrt{\frac{|g|}{3}}\sigma u\right)^{2q}}\\ &\times \sum_{\substack{m_1,\dots m_q\\ \sum km_k=2q,\,\sum m_k\leq n}}\frac{(2q)!}{\prod_k m_k!k^{m_k}}\,\frac{(-1)^{\sum m_k}n!}{(n-\sum_k m_k)!}\left(\ln(1-\imath e^{\imath\frac{\varphi-2\theta}{2}}\sqrt{\frac{|g|}{3}}\sigma u)\right)^{n-\sum_k m_k}.\end{aligned} \tag{6.B.39}$$

[16] Namely, we evaluate the q-th term of the Taylor expansion using the following formula (at $u=0$)

$$\frac{d^q}{du^q}[\ln(1-ux)]^n = \sum_{\substack{m_1,\dots m_q\\ \sum km_k=q,\,\sum m_k\leq n}}\frac{q!}{\prod_k m_k!(k!)^{m_k}}\,\frac{n!}{(n-\sum_k m_k)!}\,[\ln(1-ux)]^{n-\sum_k m_k}\prod_k\left(\frac{-(k-1)!x^k}{(1-ux)^k}\right)^{m_k}.$$

[17] In the last step, we use: $\sum_{m_1,m_2,\dots\geq 0}\prod_{k\geq 1}\frac{1}{m_k!}\left(\frac{Nx^k}{2k}\right)^{m_k} = \exp\{\sum_{k\geq 1}\frac{Nx^k}{2k}\} = (1-x)^{-N/2} = \sum_{m=0}^{\infty}\frac{\Gamma(m+N/2)}{\Gamma(N/2)m!}x^m$.

Now $|1-\imath\sqrt{\frac{|g|}{3}}e^{\imath\frac{\varphi-2\theta}{2}}\sigma u|\geq\cos\frac{\varphi-2\theta}{2}$ and:

$$\frac{\left(\ln(1-\imath e^{\imath\frac{\varphi-2\theta}{2}}\sqrt{\frac{|g|}{3}}\sigma u)\right)^{n-\sum_k m_k}}{\left(1-\imath e^{\imath\frac{\varphi-2\theta}{2}}\sqrt{\frac{|g|}{3}}\sigma u\right)^{2q}}\leq\frac{\left|2^{1/2}(|\ln(\cos\frac{\varphi-2\theta}{2})|+1)\ln(e^{\pi}+|g||\sigma|)\right|^{n-\sum m_k}}{\left(\cos\frac{\varphi-2\theta}{2}\right)^{2q}}\,, \tag{6.B.40}$$

therefore:

$$\begin{aligned}
&|R^q_{n\theta}(g)|\\
&\leq\frac{n!2^{\frac{n}{2}}\left(|\ln(\cos\frac{\varphi-2\theta}{2})|+1\right)^n}{\left(\cos\frac{\varphi-2\theta}{2}\right)^{2q}}\left(\frac{|g|}{3}\right)^q\frac{\Gamma(2q+\frac{1}{2})}{(2q)!}\int[d\sigma]e^{-\frac{1}{2}\cos(2\theta)\sigma^2}\sigma^{2q}[\ln(e^{\pi}+|g||\sigma|)]^n\\
&\leq K\frac{\left(|\ln(\cos\frac{\varphi-2\theta}{2})|+1\right)^n}{\left(\cos\frac{\varphi-2\theta}{2}\right)^{2q}}\left(\frac{|g|}{3}\right)^q\left(\frac{(2q)!}{2^q q!\,(\cos(2\theta))^{q+1/2}}+2^q\frac{|g|^{\frac{n\varepsilon}{2}}\Gamma(q+\frac{n\varepsilon+1}{2})}{(\cos(2\theta))^{q+(n\varepsilon+1)/2}}\right)\,,
\end{aligned} \tag{6.B.41}$$

for any ε with (K depending on n and ε). Fixing for example $\varepsilon=1$ and $\theta=\frac{\varphi}{6}$ yields the desired result as in Property 3, Proposition 1.

Property 4. A slight variation on the bound in Property 1 yields:

$$|Z_{n\theta}(g)|\leq K^n\frac{\left(|\ln(\cos\frac{\varphi-2\theta}{2})|+1\right)^n}{\varepsilon^n}\left(1+\frac{|g|^{\frac{n\varepsilon}{2}}\Gamma(\frac{n\varepsilon+1}{2})}{(\cos(2\theta))^{(n\varepsilon+1)/2}}\right)\,. \tag{6.B.42}$$

Fixing for convenience $\theta=\frac{\varphi}{6}$, one observes that $\sum_{n\geq 0}\frac{1}{n!}(-N/2)^n Z_{n\theta}(g)$ has infinite radius of convergence in N for any $|\varphi|<3\pi/2$. Denoting, similarly to the notation we used for $Z(g,N)$, the analytic continuation of $Z_n(g)$ to the extended Riemann sheet $\mathbb{C}_{3\pi/2}$ by:

$$\theta>0\,,\qquad Z_{n+}(g)=Z_{n\theta}(g)\,,\qquad\qquad Z_{n-}(g)=Z_{n-\theta}(g)\,, \tag{6.B.43}$$

we note that the bound on the Taylor rest term in (6.B.41) is lost for $\varphi\to\pm 3\pi/2$, hence Borel summability is lost for $\varphi\to\pm\pi$. As in the case of $Z(g,N)$, after g crosses the cut at $\mathbb{R}_-$, say counterclockwise, in deforming the contour of integration $e^{-\imath\theta}\mathbb{R}$ back to the steepest-descent contour along the real line, we generate a clockwise-oriented Hankel contour around $\sigma_\star\times(1,+\infty)$:

$$\begin{aligned}
&Z_{n\pm}(g)\big|_{\substack{\varphi>\pi\\<-\pi}}=\int_{e^{\mp\imath\theta}\mathbb{R}}[d\sigma]\;e^{-\frac{1}{2}\sigma^2}\left(\ln(1-\imath\sqrt{\frac{g}{3}}\sigma)\right)^n=Z^{\mathbb{R}}_n(g)+Z^C_{n\pm}(g)\\
&Z^{\mathbb{R}}_n(g)=\int_{\mathbb{R}}[d\sigma]e^{-\frac{1}{2}\sigma^2}\left(\ln(1-\imath\sqrt{\frac{g}{3}}\sigma)\right)^n\,,\quad Z^C_{n\pm}(g)=\int_C[d\sigma]e^{-\frac{1}{2}\sigma^2}\left(\ln(1-\imath\sqrt{\frac{g}{3}}\sigma)\right)^n\,.
\end{aligned} \tag{6.B.44}$$

Property 5. We now compute $Z^C_{n\pm}(g)$. As in Proposition 1 this is given by integrating along the clockwise orientated Hankel contour $\mathcal{C}$. First we change variable to $\sigma=e^{-\imath\frac{\pi}{2}-\imath\frac{\varphi}{2}}\sqrt{3/|g|}\sigma'$ and the contour becomes C' clockwise oriented around $(1,\infty)$ and a shift $\sigma'=1+t$ brings C' to a clockwise

oriented contour around the positive real axis:

$$\begin{aligned} Z^C_{n\pm}(g) &= \left(\frac{3}{e^{\imath\pi}g}\right)^{1/2} \int_{C'} [d\sigma']\, e^{\frac{3}{2g}(\sigma')^2} [\ln(1-\sigma')]^n \\ &= \frac{1}{\sqrt{2\pi}} \left(\frac{3}{e^{\imath\pi}g}\right)^{1/2} \int_{C''} dt\, e^{\frac{3}{2g}(1+t)^2} [\ln(-t)]^n \,. \end{aligned} \tag{6.B.45}$$

A further change of variables $t = e^{\imath\tau\pi}\frac{g}{3}u$ with $\tau = -\mathrm{sgn}(\varphi)$ yields:[18]

$$\begin{aligned} Z^C_{n\pm}(g) =& \frac{e^{\imath\tau\pi}}{\imath} \frac{1}{\sqrt{2\pi}} \sqrt{\frac{g}{3}} e^{\frac{3}{2g}} \int_0^\infty du\, e^{-u+\frac{g}{6}u^2} \left[(\ln(\tfrac{e^{\imath\tau\pi}g}{3}u) - \imath\pi)^n - (\ln(\tfrac{e^{\imath\tau\pi}g}{3}u) + \imath\pi)^n \right] \\ =& \frac{e^{\imath\tau\pi}}{\imath} \frac{1}{\sqrt{2\pi}} \sqrt{\frac{g}{3}} e^{\frac{3}{2g}} \sum_{q\geq 0} \frac{1}{q!} \left(\frac{g}{6}\right)^q \sum_{p=0}^n \binom{n}{p} \\ & \times \int_0^\infty du\, e^{-u}\, u^{2q} (\ln u)^p \left[(\ln(\tfrac{e^{\imath\tau\pi}g}{3}) - \imath\pi)^{n-p} - (\ln(\tfrac{e^{\imath\tau\pi}g}{3}) + \imath\pi)^{n-p} \right] , \end{aligned} \tag{6.B.46}$$

and integrating over u we get

$$\begin{aligned} Z^C_{n\pm}(g) \simeq& \frac{e^{\imath\tau\pi}}{\imath} \frac{e^{\frac{3}{2g}}}{\sqrt{2\pi}} \sqrt{\frac{g}{3}} \sum_{q=0}^\infty \frac{1}{q!} \left(\frac{g}{6}\right)^q \sum_{p=0}^n \binom{n}{p} \frac{d^p\Gamma(z)}{dz^p}\Big|_{z=2q+1} \\ & \times \left[\left(\ln\left(\tfrac{e^{\imath\tau\pi}g}{3}\right) - \imath\pi\right)^{n-p} - \left(\ln\left(\tfrac{e^{\imath\tau\pi}g}{3}\right) + \imath\pi\right)^{n-p} \right] , \end{aligned} \tag{6.B.47}$$

which combined with Property 2 implies the full transseries expansion (6.1.26).

A good cross check of the results consist in summing over n:

$$\begin{aligned} \sum_{n\geq 0} \frac{1}{n!} \left(-\frac{N}{2}\right)^n Z^C_{n\pm}(g) =& \frac{e^{\imath\tau\pi}}{\imath} \frac{e^{\frac{3}{2g}}}{\sqrt{2\pi}} \sqrt{\frac{g}{3}} \sum_{q=0}^\infty \frac{1}{q!} \left(\frac{g}{6}\right)^q \sum_{p,k=0}^\infty \frac{1}{p!\,k!} \left(-\frac{N}{2}\right)^{p+k} \frac{d^p\Gamma(z)}{dz^p}\Big|_{z=2q+1} \\ & \times \left[\left(\ln\left(\tfrac{e^{\imath\tau\pi}g}{3}\right) - \imath\pi\right)^{k} - \left(\ln\left(\tfrac{e^{\imath\tau\pi}g}{3}\right) + \imath\pi\right)^{k} \right] \\ =& \frac{e^{\imath\tau\pi}}{\imath} \frac{e^{\frac{3}{2g}}}{\sqrt{2\pi}} \sqrt{\frac{g}{3}} \sum_{q=0}^\infty \frac{1}{q!} \left(\frac{g}{6}\right)^q \Gamma(2q+\frac{2-N}{2}) \left[e^{\imath\frac{N\pi}{2}} \left(\tfrac{e^{\imath\tau\pi}g}{3}\right)^{-\frac{N}{2}} - e^{-\imath\frac{N\pi}{2}} \left(\tfrac{e^{\imath\tau\pi}g}{3}\right)^{-\frac{N}{2}} \right] \\ =& \frac{e^{\imath\tau\pi(1-\frac{N}{2})}}{\imath} \frac{e^{\frac{3}{2g}}}{\sqrt{2\pi}} \left(\frac{g}{3}\right)^{\frac{1-N}{2}} \sum_{q\geq 0} \frac{\Gamma(2q+\frac{2-N}{2}) \frac{\sin\frac{N\pi}{2}}{\pi} 2\pi\imath}{2^{2q}q!} \left(\frac{2g}{3}\right)^q , \end{aligned} \tag{6.B.48}$$

Which coincides with the instanton part in (6.1.12).

Property 6. This follows from $\mathrm{disc}_\pi\big(Z_n(g)\big) = -Z^C_{n+}(e^{\imath\pi}|g|)$ combined with Properties 4 and 5.

Property 7. The derivation of (6.1.29) is straightforward. We substitute the small-N expansion (6.1.23), with the condition $Z(g,0) = 1$, in the partial differential equation for $Z(g,N)$, equation (6.1.16), and collect the terms with the same powers of N.

This concludes the proof of Proposition 2. □

[18] See comments below (6.B.16) for an explanation of the τ-dependence.

6.B.3 The LVE expansion, analyticity

Proof of Proposition 3. We review here briefly the proof the LVE formula for the free energy. For more details, see [22] and followup work. We use the notation of the Gaussian integral as a differential operator (see [214] for a detailed discussion of this notation), as a convenient bookkeeping device for the action of derivatives with respect to matrix elements of the covariance of a Gaussian measure and we denote $V(\sigma) = \ln(1 - \imath\sqrt{g/3}\,\sigma)$. Equation (6.1.23) becomes with this notation:

$$\begin{aligned} Z(g,N) &= \sum_{n\geq 0} \frac{1}{n!} \left(-\frac{N}{2}\right)^n Z_n \ , \\ Z_n(g) &= \int [d\sigma]\ e^{-\frac{1}{2}\sigma^2} [\ln(1 - \imath\sqrt{g/3}\,\sigma)]^n \equiv \left[e^{\frac{1}{2}\frac{\delta}{\delta\sigma}\frac{\delta}{\delta\sigma}} V(\sigma)^n \right]_{\sigma=0} \ , \end{aligned} \tag{6.B.49}$$

where $\delta/\delta\sigma$ denotes the derivative with respect to σ.

Let us take aside a term $Z_n(g)$. We introduce copies with degenerate covariance and we introduce fictitious interpolating link parameters $x_{kl} = x_{lk} = 1$:

$$Z_n(g) = \left[e^{\frac{1}{2}\sum_{k,l=1}^n \frac{\delta}{\delta\sigma_k}\frac{\delta}{\delta\sigma_l}} \prod_{i=1}^n V(\sigma_i) \right]_{\sigma_i=0} = \left[e^{\frac{1}{2}\sum_{k,l=1}^n x_{kl}\frac{\delta}{\delta\sigma_k}\frac{\delta}{\delta\sigma_l}} \prod_{i=1}^n V(\sigma_i) \right]_{\sigma_i=0, x_{ij}=1} . \tag{6.B.50}$$

We fix the diagonal elements $x_{ii} = 1$ and use symmetric interpolations $x_{ij} = x_{ji}$ where x_{ij} with $i < j$ are independent parameters. For all $i \neq j$:

$$\frac{\partial}{\partial x_{ij}} \left[e^{\frac{1}{2}\sum_{k,l=1}^n x_{kl}\frac{\delta}{\delta\sigma_k}\frac{\delta}{\delta\sigma_l}} \right] = e^{\frac{1}{2}\sum_{k,l=1}^n x_{kl}\frac{\delta}{\delta\sigma_k}\frac{\delta}{\delta\sigma_l}} \left(\frac{\delta}{\delta\sigma_i}\frac{\delta}{\delta\sigma_j} \right) , \tag{6.B.51}$$

and using Section 2.5.2, we get:

$$Z(g,N) = \sum_{n\geq 0} \frac{\left(-\frac{N}{2}\right)^n}{n!} \sum_{\mathcal{F}\in F_n} \int_0^1 \prod_{(i,j)\in\mathcal{F}} du_{ij} \left[e^{\frac{1}{2}\sum_{k,l} w^{\mathcal{F}}_{kl}\frac{\delta^2}{\delta\sigma_k\delta\sigma_l}} \left(\prod_{(i,j)\in\mathcal{F}} \frac{\delta^2}{\delta\sigma_i\sigma_j} \right) \prod_{i=1}^n V(\sigma_i) \right]_{\sigma_i=0} , \tag{6.B.52}$$

where F_n is the set of all the forests over n labeled vertices.

Observing that the contribution of a forest factors over the trees (connected components) in the forest, the logarithm is trivial: it comes to restricting the sum above to trees over n vertices (hence with $n-1$ edges):

$$W(g,N) = \sum_{n\geq 1} \frac{\left(-\frac{N}{2}\right)^n}{n!} \sum_{\mathcal{T}\in T_n} \int_0^1 \prod_{(i,j)\in\mathcal{T}} du_{ij} \left[e^{\frac{1}{2}\sum_{k,l} w^{\mathcal{T}}_{kl}\frac{\delta^2}{\delta\sigma_k\delta\sigma_l}} \left(\prod_{(i,j)\in\mathcal{T}} \frac{\delta^2}{\delta\sigma_i\delta\sigma_j} \right) \prod_{i=1}^n V(\sigma_i) \right]_{\sigma_i=0} . \tag{6.B.53}$$

Taking into account that the action of the derivatives on the interaction is:

$$\frac{\delta^d}{\delta\sigma^d} \ln\left(1 - \imath\sqrt{\tfrac{g}{3}}\sigma\right) = (-1)\, \frac{(d-1)! \left(\imath\sqrt{\frac{g}{3}}\right)^d}{\left(1 - \imath\sqrt{\frac{g}{3}}\sigma\right)^d} , \tag{6.B.54}$$

denoting d_i the degree of the vertex i in $\mathcal{T}$, recalling that $\sum_i d_i = 2(n-1)$ and observing that the terms $n = 1$ is special we get:

$$W(g,N) = -\frac{N}{2}\left[e^{\frac{1}{2}\frac{\delta}{\delta\sigma}\frac{\delta}{\delta\sigma}} \ln\left(1-\imath\sqrt{\tfrac{g}{3}}\sigma\right)\right]_{\sigma=0} - \sum_{n\geq 2}\frac{1}{n!}\left(-\frac{N}{2}\right)^n\left(\frac{g}{3}\right)^{n-1}\sum_{\mathcal{T}\in T_n}\int_0^1\prod_{(i,j)\in\mathcal{T}}du_{ij}\left[e^{\frac{1}{2}\sum_{i,j}w^{\mathcal{T}}_{ij}\frac{\delta}{\delta\sigma_i}\frac{\delta}{\delta\sigma_j}}\prod_i\frac{(d_i-1)!}{\left(1-\imath\sqrt{\frac{g}{3}}\sigma_i\right)^{d_i}}\right]_{\sigma_i=0}. \tag{6.B.55}$$

Reinstating the notation of the normalized Gaussian measure as a probability density, we obtain the series in (6.2.7), with coefficients (6.2.5).

Property 1 and 2. In order to determine the domain of convergence of (6.2.7), let us denote as usual $g = |g|e^{\imath\varphi}$, and take $-\pi < \varphi < \pi$. In this region, we can use the uniform bound $|1-\imath\sqrt{\frac{g}{3}}\sigma_i| \geq \cos\frac{\varphi}{2}$, remaining with Gaussian integrals over σ_i and integrals over u_{ij}, both bounded by 1. Therefore, for $n \geq 2$, a crude bound on $W_n(g)$ is:

$$|W_n(g)| \leq \left|\frac{g}{3}\right|^{n-1}\frac{(n-2)!}{(\cos\frac{\varphi}{2})^{2(n-1)}}\sum_{d_i\geq 1}^{\sum_{i=1}^n(d_i-1)=n-2} 1 = \frac{(2n-3)!}{(n-1)!}\left|\frac{g}{3(\cos\frac{\varphi}{2})^2}\right|^{n-1}, \tag{6.B.56}$$

where we used the fact that there are $(n-2)!/\prod_i(d_i-1)!$ trees over n labeled vertices with degree d_i at the vertex i, and that the sum over d_i is the coefficient of x^{n-2} in the expansion of $(1-x)^{-n} = \sum_{q\geq 0}\binom{n-1+q}{n-1}x^q$. Using Stirling's formula for the asymptotics of the factorials, it follows that $W(g,N)$ is convergent in a cardioid domain $|gN| < \frac{3}{2}(\cos\frac{\varphi}{2})^2$.

Property 3. The domain of convergence can be enlarged by turning $\sigma \to e^{-\imath\theta}\sigma$, which yields a convergent expansion in a subdomain of the extended Riemann sheet $\mathbb{C}_{3\pi/2}$. In order to make this precise, let us define:

$$W_\theta(g,N) = -\frac{N}{2}\int e^{-\imath\theta}[d\sigma]\, e^{-\frac{1}{2}e^{-2\imath\theta}\sigma^2}\ln\left(1-\imath\sqrt{\tfrac{g}{3}}e^{-\imath\theta}\sigma\right) - \sum_{n\geq 2}\frac{1}{n!}\left(-\frac{N}{2}\right)^n\left(\frac{g}{3}\right)^{n-1} \times \sum_{\mathcal{T}\in T_n}\int_0^1\prod_{(i,j)\in\mathcal{T}}du_{ij}\int_{\mathbb{R}}\frac{\prod_i e^{-\imath\theta}[d\sigma_i]}{\sqrt{\det w^{\mathcal{T}}}}\, e^{-\frac{1}{2}e^{-2\imath\theta}\sum_{i,j}\sigma_i(w^{\mathcal{T}})^{-1}_{ij}\sigma_j}\prod_i\frac{(d_i-1)!}{\left(1-\imath\sqrt{\frac{g}{3}}e^{-\imath\theta}\sigma_i\right)^{d_i}}, \tag{6.B.57}$$

and implicitly $W_{n\theta}(g)$. It is easy to check that, for g in the cut plane $\mathbb{C}_\pi$ both $W_\theta(g,N)$ and $W_{n\theta}(g)$ are independent of θ as long as they converge. As θ can be chosen such that the integrals converge for $|\varphi| > \pi$, $W_\theta(g,N)$ and $W_{n\theta}(g)$ analytically extend $W(g,N)$ and $W_n(g)$ to some maximal domain.

Property 4 and 5. We now have the bound $|1-\imath\sqrt{\frac{g}{3}}e^{-\imath\theta}\sigma_i| \geq \cos\frac{\varphi-2\theta}{2}$ and the Gaussian integral is bounded by:

$$\left|\int\frac{\prod_i e^{-\imath\theta}[d\sigma_i]}{\sqrt{\det w^{\mathcal{T}}}}\, e^{-\frac{1}{2}e^{-2\imath\theta}\sum_{i,j}\sigma_i(w^{\mathcal{T}})^{-1}_{ij}\sigma_j}\right| \leq \frac{1}{[\cos(2\theta)]^{\frac{n}{2}}}, \tag{6.B.58}$$

and the combinatorics runs as before leading to:

$$|W_{n\theta}(g)| \leq \frac{(2n-3)!}{(n-1)!} \frac{1}{\sqrt{\cos(2\theta)}} \left| \frac{g}{3\sqrt{\cos(2\theta)} \left(\cos\frac{\varphi-2\theta}{2}\right)^2} \right|^{n-1} . \tag{6.B.59}$$

Using again Stirling's formula, we find that $W(g,N)$ is convergent for $|g| < \frac{1}{|N|} \frac{3}{2} \sqrt{\cos(2\theta)} \left(\cos\frac{\varphi-2\theta}{2}\right)^2$. This concludes the proof of Proposition 3. □

6.B.4 Borel summability of $W_n(g)$ and $W(g,N)$ in $\mathbb{C}_\pi$

Proof of Proposition 4. We focus on $W(g,N)$: for $W_n(g)$ one follows the same steps without summing over n. Our starting point is the expression:

$$\begin{aligned} W_\theta(g,N) = &- \frac{N}{2} \left[e^{\frac{1}{2} e^{2\imath\theta} \frac{\delta}{\delta\sigma} \frac{\delta}{\delta\sigma}} \ln\left(1 - \imath\sqrt{\tfrac{g}{3}} e^{-\imath\theta}\sigma\right) \right]_{\sigma=0} - \sum_{n\geq 2} \frac{1}{n!} \left(-\frac{N}{2}\right)^n \left(\frac{g}{3}\right)^{n-1} \\ &\times \sum_{\mathcal{T}\in T_n} \int_0^1 \Big(\prod_{(i,j)\in\mathcal{T}} du_{ij} \Big) \left[e^{\frac{1}{2} e^{2\imath\theta} \sum_{i,j} w_{ij}^{\mathcal{T}} \frac{\delta}{\delta\sigma_i} \frac{\delta}{\delta\sigma_j}} \prod_i \frac{(d_i-1)!}{\left(1 - \imath\sqrt{\frac{g}{3}} e^{-\imath\theta}\sigma_i\right)^{d_i}} \right]_{\sigma_i=0} . \end{aligned} \tag{6.B.60}$$

for the analytical continuation $W_\theta(g,N)$ of the free energy.

We are interested in finding a good bound on the Taylor rest term of order q of the expansion of $W(g,N)$. This Taylor rest term consists in two pieces. We denote $Q_\theta^q(g)$ the sum over all the trees having at least q edges:

$$\begin{aligned} Q_\theta^q(g,N) = &- \sum_{n\geq q+1} \frac{1}{n!} \left(-\frac{N}{2}\right)^n \left(\frac{g}{3}\right)^{n-1} \\ &\times \sum_{\mathcal{T}\in T_n} \int_0^1 \Big(\prod_{(i,j)\in\mathcal{T}} du_{ij} \Big) \left[e^{\frac{1}{2} e^{2\imath\theta} \sum_{i,j} w_{ij}^{\mathcal{T}} \frac{\delta}{\delta\sigma_i} \frac{\delta}{\delta\sigma_j}} \prod_i \frac{(d_i-1)!}{\left(1 - \imath\sqrt{\frac{g}{3}} e^{-\imath\theta}\sigma_i\right)^{d_i}} \right]_{\sigma_i=0} . \end{aligned} \tag{6.B.61}$$

Due to the overall g^{n-1} factor, such trees contribute only to orders higher than q in the Taylor expansion of $W_\theta(g,N)$, hence are entirely contained in the Taylor rest term. The trees with less than q edges contribute both to the explicit terms of order lower than q in the Taylor expansion and to the rest term. In order to isolate their contribution to the rest term we perform for each of them a Taylor expansion with integral rest up to an appropriate order. We do this by Taylor expanding the Gaussian measure, which generates loop edges, each of which comes equipped with a g. For a tree with $n-1$ edges, $n-q$ explicit loop edges need to be expanded. The Taylor rest term coming from such trees writes then:

$$\begin{aligned} P_\theta^q(g,N) = &- \frac{N}{2} \int_0^1 \frac{(1-t)^{q-1}}{(q-1)!} \left(\frac{d}{dt}\right)^q \left[e^{\frac{t}{2} e^{2\imath\theta} \frac{\delta}{\delta\sigma} \frac{\delta}{\delta\sigma}} \ln\left(1 - \imath\sqrt{\tfrac{g}{3}} e^{-\imath\theta}\sigma\right) \right]_{\sigma=0} \\ &- \sum_{n=2}^{q} \frac{1}{n!} \left(-\frac{N}{2}\right)^n \left(\frac{g}{3}\right)^{n-1} \sum_{\mathcal{T}\in T_n} \int_0^1 \Big(\prod_{(i,j)\in\mathcal{T}} du_{ij} \Big) \int_0^1 dt \, \frac{(1-t)^{q-n}}{(q-n)!} \\ &\times \left(\frac{d}{dt}\right)^{q-n+1} \left[e^{\frac{t}{2} e^{2\imath\theta} \sum_{i,j} w_{ij}^{\mathcal{T}} \frac{\delta}{\delta\sigma_i} \frac{\delta}{\delta\sigma_j}} \prod_i \frac{(d_i-1)!}{\left(1 - \imath\sqrt{\frac{g}{3}} e^{-\imath\theta}\sigma_i\right)^{d_i}} \right]_{\sigma_i=0} . \end{aligned} \tag{6.B.62}$$

The total rest term of the Taylor expansion of $W_\theta(g,N)$ is the sum $R^q_\theta(g,N) = P^q_\theta(g,N) + Q^q_\theta(g,N)$.

The contribution of large trees $Q^q_\theta(g,N)$. Using (6.2.10), the contribution of large trees is immediately bounded by:

$$|Q^q_\theta(g,N)| \leq \frac{1}{\sqrt{\cos(2\theta)}} \sum_{n\geq q+1} \left|\frac{N}{2}\right|^n \left|\frac{g}{3}\right|^{n-1} \frac{1}{\left[\sqrt{\cos(2\theta)}(\cos\frac{\varphi-2\theta}{2})^2\right]^{n-1}} \frac{1}{n(n-1)}\binom{2n-3}{n-1}, \quad (6.B.63)$$

and using $\frac{1}{n(n-1)}\binom{2n-3}{n-1} \leq 2^{2n-3}$ we get:

$$\begin{aligned} |Q^q_\theta(g,N)| \leq & \frac{|N|}{4\sqrt{\cos(2\theta)}} \sum_{n\geq q+1} \left(\frac{1}{\frac{3}{2}\sqrt{\cos(2\theta)}(\cos\frac{\varphi-2\theta}{2})^2}\right)^{n-1} |Ng|^{n-1} \\ \leq & \frac{\frac{|N|}{4\sqrt{\cos(2\theta)}}}{1-\frac{|Ng|}{\frac{3}{2}\sqrt{\cos(2\theta)}(\cos\frac{\varphi-2\theta}{2})^2}} \left(\frac{1}{\frac{3}{2}\sqrt{\cos(2\theta)}(\cos\frac{\varphi-2\theta}{2})^2}\right)^q |Ng|^q . \end{aligned} \quad (6.B.64)$$

Observe that this bound *does not* have a $q!$ growth. This seems much better than expected. In fact this is not surprising: the factorial growth of the rest term comes from the divergent number of graphs in perturbation theory. As the large trees do not need to be further expanded in graphs, they do not generate a factorial growth. In fact it is the small trees that pose a problem.

The contribution of small trees $P^q_\theta(g,N)$. The contribution of small trees requires more work. We have:

$$\begin{aligned} P^q_\theta(g,N) = & -\frac{N}{2}\int_0^1 \frac{(1-t)^{q-1}}{(q-1)!} \left[e^{\frac{t}{2}e^{2\imath\theta}\frac{\delta}{\delta\sigma}\frac{\delta}{\delta\sigma}} \left(\frac{1}{2}e^{2\imath\theta}\right)^q \left(\frac{\delta}{\delta\sigma}\right)^{2q} \ln\left(1-\imath\sqrt{\tfrac{g}{3}}e^{-\imath\theta}\sigma\right)\right]_{\sigma=0} \\ & -\sum_{n=2}^{q} \frac{1}{n!}\left(-\frac{N}{2}\right)^n \left(\frac{g}{3}\right)^{n-1} \sum_{\mathcal{T}\in T_n} \int_0^1 \Big(\prod_{(i,j)\in\mathcal{T}} du_{ij}\Big) \int_0^1 dt\, \frac{(1-t)^{q-n}}{(q-n)!} \\ & \times \left[e^{\frac{t}{2}e^{2\imath\theta}\sum_{i,j} w^{\mathcal{T}}_{ij}\frac{\delta^2}{\delta\sigma_i\delta\sigma_j}} \left(\frac{1}{2}e^{2\imath\theta}\sum_{i,j} w^{\mathcal{T}}_{ij}\frac{\delta^2}{\delta\sigma_i\delta\sigma_j}\right)^{q-n+1} \prod_i \frac{(d_i-1)!}{\left(1-\imath\sqrt{\frac{g}{3}}e^{-\imath\theta}\sigma_i\right)^{d_i}}\right]_{\sigma_i=0} . \end{aligned} \quad (6.B.65)$$

The first term is bounded by:

$$\begin{aligned} & \frac{|N|}{2^{q+1}} \left|\int_0^1 \frac{(1-t)^{q-1}}{(q-1)!} \left[e^{\frac{t}{2}e^{2\imath\theta}\frac{\delta}{\delta\sigma}\frac{\delta}{\delta\sigma}} \frac{(2q-1)!\left(\imath\sqrt{\frac{g}{3}}\right)^{2q}}{\left(1-\imath\sqrt{\frac{g}{3}}e^{-\imath\theta}\sigma\right)^{2q}}\right]_{\sigma=0}\right| \\ & \leq \frac{|N|}{2\sqrt{\cos(2\theta)}} \left(\frac{|g|}{6}\right)^q \frac{(2q-1)!}{q!} \frac{1}{\left(\cos\frac{\varphi-2\theta}{2}\right)^{2q}} \\ & \leq \frac{|N|}{4\sqrt{\cos(2\theta)}} (q-1)! \left(\frac{1}{\frac{3}{2}(\cos\frac{\varphi-2\theta}{2})^2}\right)^q |g|^q . \end{aligned} \quad (6.B.66)$$

Observe that, due to the expansion of the q loop edges, this first term displays a $q!$ growth. Thus already the first term has a worse large-order behaviour than the sum over large trees.

We now analyze the contribution to the rest term of the trees with $2 \le n \le q$ vertices. Note that a term has initially $\sum d_i = 2(n-1)$ corners (factors $1/(1-\imath\sqrt{\frac{g}{3}}e^{-\imath\theta}\sigma_i)$) and $2(q-n+1)$ derivatives will act on it. The additional derivatives (corresponding to the loop edges) create each a new corner on which subsequent derivatives can act. In total, for each tree, the loop edges generate exactly:

$$[2(n-1)][2(n-1)+1]\dots[2(n-1)+2(q-n+1)-1] = \frac{(2q-1)!}{(2n-3)!}\,, \tag{6.B.67}$$

possible terms, each with $2(n-1)+2(q-n+1)$ corners (factors $1/(1-\imath\sqrt{\frac{g}{3}}e^{-\imath\theta}\sigma_i)$). The w's are bounded by 1 and the sum over trees is done as in (6.2.10) leading to the global bound:

$$\begin{aligned}&\sum_{n=2}^{q} \frac{|N|^n|g|^q}{2^{q+1}3^q}\,\frac{(2q-1)!}{(2n-3)!}\,\frac{1}{(q-n+1)!}\,\frac{(n-2)!}{n!}\binom{2n-3}{n-1}\left(\frac{1}{\cos\frac{\varphi-2\theta}{2}}\right)^{2q}\frac{1}{[\cos(2\theta)]^{n/2}}\\ &\le \frac{(2q-1)!\,|g|^q}{2^{q+1}3^q(\cos\frac{\varphi-2\theta}{2})^{2q}}\sum_{n=2}^{q}\frac{1}{(q-n+1)!n!(n-1)!}\,\frac{|N|^n}{[\cos(2\theta)]^{n/2}}\,.\end{aligned} \tag{6.B.68}$$

Now, using $(2q-1)! \le 2^{2q-1}q!(q-1)!$ we get and upper bound:

$$\begin{aligned}&\frac{1}{4}(q-1)!\left(\frac{1}{\frac{3}{2}(\cos\frac{\varphi-2\theta}{2})^2}\right)^q|g|^q\sum_{n=2}^{q}\frac{q!}{(q-n+1)!n!(n-1)!}\,\frac{|N|^n}{[\cos(2\theta)]^{n/2}}\\ &\le \frac{1}{4}(q-1)!\left(\frac{1}{\frac{3}{2}(\cos\frac{\varphi-2\theta}{2})^2}\right)^q|g|^q\,2^q e^{\frac{|N|}{\sqrt{\cos(2\theta)}}}\,.\end{aligned} \tag{6.B.69}$$

Adding up (6.B.64), (6.B.66) and (6.B.69) we get:

$$\begin{aligned}|R^q_\theta(g,N)| \le &\frac{\frac{|N|}{4\sqrt{\cos(2\theta)}}}{1-\frac{|Ng|}{\frac{3}{2}\sqrt{\cos(2\theta)}(\cos\frac{\varphi-2\theta}{2})^2}}\left(\frac{1}{\frac{3}{2}\sqrt{\cos(2\theta)}(\cos\frac{\varphi-2\theta}{2})^2}\right)^q|Ng|^q\\ &+\frac{1}{4}(q-1)!\left(\frac{1}{\frac{3}{2}(\cos\frac{\varphi-2\theta}{2})^2}\right)^q|g|^q\left(\frac{|N|}{\sqrt{\cos(2\theta)}}+2^q e^{\frac{|N|}{\sqrt{\cos(2\theta)}}}\right)\,.\end{aligned} \tag{6.B.70}$$

We opportunistically chose $\theta = \frac{\varphi}{6}$ and using some trivial bounds we get

$$|R^q_\theta(g,N)| \le \frac{\frac{|N|}{4\sqrt{\cos\frac{\varphi}{3}}}}{1-\frac{|Ng|}{\frac{3}{2}(\cos\frac{\varphi}{3})^{5/2}}}\left(\frac{1}{\frac{3}{2}(\cos\frac{\varphi}{3})^{5/2}}\right)^q|Ng|^q + (q-1)!\,|g|^q\left(\frac{1}{\frac{3}{2}(\cos\frac{\varphi}{3})^2}\right)^q 2^q e^{\frac{|N|}{\cos(\frac{\varphi}{3})^{1/2}}}\,. \tag{6.B.71}$$

We are now in the position to prove that $W(g,N)$ is Borel summable along all the directions in the cut plane $\mathbb{C}_\pi$ by verifying the conditions of Theorem 1, Appendix 2.A. This comes about as follows:

- let us fix some $\alpha \in (-\pi,\pi)$. As we are interested in analyticity and rest bound in some Sokal disk extending op to $\varphi = \alpha \pm \pi/2$, we denote $c = \min\{\cos\frac{\alpha+\pi/2}{3}); \cos\frac{\alpha-\pi/2}{3})\} > 0$ (because as $|\alpha| < \pi$).
- $W(g,N)$ can be analytically continued via $W_{\varphi/6}(g,N)$[19] to any g in a Sokal disk (with 0 on its boundary) tilted by α, that is $g \in \mathrm{Disk}^\alpha_R = \{z \mid \mathrm{Re}(e^{\imath\alpha}/z) > 1/R\}$ provided that $R =$

[19]Indeed, $W_{\varphi/6}(g,N) = Q^0_{\varphi/6}(g,N)$ and the series defining it converges absolutely in such a disk $|Q^0_{\varphi/6}(g,N)| \le 1/(4c^{1/2}\nu)$.

$\frac{3}{2|N|}c^{5/2}(1-\nu)$ for some fixed $\nu > 0$. In this disk the Taylor rest term obeys the uniform bound:

$$|R_\theta^q(g)| \leq \frac{|N|}{4c^{1/2}\nu}\left(\frac{1}{\frac{3}{2}c^{5/2}}\right)^q |g|^q + (q-1)!|g|^q\left(\frac{2}{\frac{3}{2}c^2}\right)^q e^{|N|/c^{1/2}} . \tag{6.B.72}$$

Fixing $K = \max\{|N|/(4c^{1/2}\nu), e^{|N|/c^{1/2}}\}$ and $\rho = \min\{3/2\, c^{5/2}; 3/4\, c^2)\}$, we finally obtain uniformly in the Sokal disk:

$$|R_\theta^q(g,N)| \leq K\; q!\; \rho^{-q}\; |g|^q , \tag{6.B.73}$$

hence the rest obeys the bound in (2.5.4) and from Theorem 1 we conclude that $W(g,N)$ is Borel summable along α.

Note that Borel summability is lost in the $N \to \infty$ limit.

This concludes the proof of Proposition 4. □

6.B.5 Transseries expansion of $W_n(g)$ and $W(g,N)$

Proof of Proposition 5. An explicit expression for $W_n(g)$ is obtained by combining the Möbis inversion formula in equation (6.2.3) with the transseries expansion of $Z_n(g)$ in (6.1.26). In order to prove Proposition 5, we have to use standard sum and product manipulation tricks and factor the powers of the transseries monomial $e^{\frac{3}{2g}}$ in front. Although the manipulations are not complicated, the expressions are very lengthy and we will introduce some bookkeeping notation to keep the formulas readable.

Property 1. Combining the Möbis inversion formula (6.2.3) with the transseries expansion of $Z_n(g)$ in (6.1.26) leads to:

$$W_n(g) \simeq \sum_{k=1}^{n}(-1)^{k-1}(k-1)! \sum_{\substack{n_1,\dots,n_{n-k+1}\geq 0 \\ \sum i n_i = n,\, \sum n_i = k}} \frac{n!}{\prod_i n_i!(i!)^{n_i}} \prod_{i=1}^{n-k+1}\left(Z_i^{\text{pert.}}(g) + \eta\, e^{\frac{3}{2g}} Z_i^{(\eta)}(g)\right)^{n_i} , \tag{6.B.74}$$

with:

$$Z_i^{\text{pert.}}(g) = \sum_{a=0}^{\infty}\left(-\frac{2g}{3}\right)^a G(a;i) , \qquad G(a;i) = \frac{(2a)!}{2^{2a}a!} \sum_{\substack{a_1,\dots,a_{2a-i+1}\geq 0 \\ \sum k a_k = 2a,\, \sum a_k = i}} \frac{(-1)^i i!}{\prod_k k^{a_k} a_k!} , \tag{6.B.75}$$

and:

$$\begin{aligned} Z_i^{(\eta)}(g) = \frac{\imath}{\sqrt{2\pi}}\sqrt{\frac{g}{3}} \sum_{a=0}^{\infty}\sum_{b=0}^{i}\frac{1}{a!}\left(\frac{g}{6}\right)^a \binom{i}{b} \frac{d^b\Gamma(z)}{dz^b}\Big|_{z=2a+1} \\ \tau\left[\left(\ln\left(\tfrac{g}{3}\right)\right)^{i-b} - \left(\ln\left(\tfrac{g}{3}\right) + \tau 2\pi\imath\right)^{i-b}\right] , \end{aligned} \tag{6.B.76}$$

where we used $\left[\left(\ln(e^{\imath\tau\pi}\tfrac{g}{3}) - \imath\pi\right)^{i-b} - \left(\ln(e^{\imath\tau\pi}\tfrac{g}{3}) + \imath\pi\right)^{i-b}\right] = \tau\left[\left(\ln\left(\tfrac{g}{3}\right)\right)^{i-b} - \left(\ln\left(\tfrac{g}{3}\right) + \tau 2\pi\imath\right)^{i-b}\right]$ as $\tau = \pm$. Using now $\tau\left[\left(\ln\left(\tfrac{g}{3}\right)\right)^{n} - \left(\ln\left(\tfrac{g}{3}\right) + \tau 2\pi\imath\right)^{n}\right] = -\tau\sum_{c=0}^{n-1}\binom{n}{c}\left(\ln\left(\tfrac{g}{3}\right)\right)^c (\tau 2\pi\imath)^{n-c}$, commuting

the sums over b and c, and combining the binomials, this can further be written as:

$$\begin{aligned} Z_i^{(\eta)}(g) &= \frac{\imath}{\sqrt{2\pi}}\sqrt{\frac{g}{3}}\sum_{a=0}^{\infty}\sum_{b=0}^{i-1}\frac{1}{a!}\left(\frac{g}{6}\right)^a\binom{i}{b} \\ &\qquad\qquad \times \frac{d^b\Gamma(z)}{dz^b}\Big|_{z=2a+1}(-\tau)\sum_{c=0}^{i-1-b}\binom{i-b}{c}\left(\ln\left(\tfrac{g}{3}\right)\right)^c(\tau 2\pi\imath)^{i-b-c} \\ &= \sqrt{2\pi}\sqrt{\frac{g}{3}}\sum_{a=0}^{\infty}\sum_{c=0}^{i-1}\left(\frac{g}{6}\right)^a\left(\ln\left(\tfrac{g}{3}\right)\right)^c G(a,c;i)\,, \end{aligned} \tag{6.B.77}$$

with:

$$G(a,c;i) = \sum_{b=0}^{i-1}(\imath\tau 2\pi)^{i-1-b-c}\frac{i!}{a!\,b!\,c!\,(i-b-c)!}\frac{d^b\Gamma(z)}{dz^b}\Big|_{z=2a+1}\,, \quad \text{and} \quad Z_0^{(\eta)} = 0\,. \tag{6.B.78}$$

First, we pull the transseries monomial to the front in (6.B.74):

$$\begin{aligned} W_n(g) &\simeq \sum_{k=1}^{n}(-1)^{k-1}(k-1)!\sum_{\substack{n_1,\dots,n_{n-k+1}\geq 0\\ \sum in_i=n,\,\sum n_i=k}}\frac{n!}{\prod_i n_i!(i!)^{n_i}}\prod_{i=1}^{n-k+1}\left(Z_i^{\text{pert.}}(g)+\eta e^{\frac{3}{2g}}Z_i^{(\eta)}(g)\right)^{n_i} \\ &= \sum_{p=0}^{n}e^{\frac{3}{2g}p}\sum_{\substack{k=p\\ k+p\geq 1}}^{n}(-1)^{k-1}(k-1)!\sum_{\substack{n_1,\dots,n_{n-k+1}\geq 0\\ \sum in_i=n,\,\sum n_i=k}} \\ &\qquad\qquad \times\sum_{\substack{\{0\leq p_i\leq n_i\}\\ i=1,\dots,n-k+1\\ \sum p_i=p}}\frac{n!\prod_{i=1}^{n-k+1}\left(Z_i^{\text{pert.}}(g)\right)^{n_i-p_i}\left(\eta Z_i^{(\eta)}(g)\right)^{p_i}}{\prod_i(n_i-p_i)!p_i!(i!)^{n_i}}\,. \end{aligned} \tag{6.B.79}$$

This is a transseries in g, with $Z_i^{(\eta)}(g)$ carrying also powers of $\sqrt{g}$ and $\ln(g)$. In a second step, we want to make this statement manifest and use the expressions for $Z_i^{\text{pert.}}$ and $Z_i^{(\eta)}$ to calculate:

$$\begin{aligned} \prod_{i\geq 1}\left(Z_i^{\text{pert.}}(g)\right)^{n_i-p_i}\left(\eta Z_i^{(\eta)}(g)\right)^{p_i} &= \prod_{i\geq 1}\left(\sum_{a_1^i,\dots a_{n_i-p_i}^i\geq 0}\prod_{j=1}^{n_i-p_i}\left(-\frac{2g}{3}\right)^{a_j^i}G(a_j^i;i)\right) \\ &\quad\cdot\left(\left(\eta\sqrt{2\pi}\sqrt{\frac{g}{3}}\right)^{p_i}\sum_{a_1^i,\dots a_{p_i}^i\geq 0}\sum_{c_1^i,\dots c_{p_i}^i=0}^{i-1}\prod_{j=1}^{p_i}\left(\frac{g}{6}\right)^{a_j^i}\left(\ln\left(\tfrac{g}{3}\right)\right)^{c_j^i}G(a_j^i,c_j^i;i)\right)\,, \\ &= \left(\eta\sqrt{2\pi}\sqrt{\frac{g}{3}}\right)^{\sum_{i\geq 1}p_i}\sum_{\substack{l\geq 0\\ \sum_i(i-1)p_i\geq l\geq 0}}g^l\left(\ln\left(\tfrac{g}{3}\right)\right)^{l'}\sum_{\substack{\{a_j^i\geq 0\}_{j=1,\dots,n_i}^{i=1,\dots,n-k+1}\\ \sum_i\sum_j a_j^i=l}}\sum_{\substack{\{i-1\geq c_j^i\geq 0\}_{j=1,\dots,p_i}^{i=1,\dots,n-k+1}\\ \sum_i\sum_j c_j^i=l'}} \\ &\quad\times\left(\frac{1}{6}\right)^{\sum_{i\geq 1}\sum_{j=1}^{p_i}a_j^i}\left(-\frac{2}{3}\right)^{\sum_{i\geq 1}\sum_{j=p_i+1}^{n_i}a_j^i}\prod_{i\geq 1}\left(\prod_{j=1}^{p_i}G(a_j^i,c_j^i;i)\right)\left(\prod_{j=p_i+1}^{n_i}G(a_j^i;i)\right)\,. \end{aligned} \tag{6.B.80}$$

Finally, inserting this into (6.B.79) we obtain the transseries expansion of $W_n(g)$, organized into instanton sectors:

$$W_n(g) \simeq \sum_{p=0}^{n} e^{\frac{3}{2g}p} \Big(\eta\sqrt{2\pi}\sqrt{\frac{g}{3}}\Big)^p \sum_{l\geq 0,\, n-p\geq l'\geq 0} g^l \left(\ln\left(\tfrac{g}{3}\right)\right)^{l'} W^{(p)}_{n;l,l'}\,, \tag{6.B.81}$$

with:

$$\begin{aligned} W^{(p)}_{n;l,l'} = \sum_{\substack{k=p\\ k+p\geq 1}}^{n} (-1)^{k-1}(k-1)! \sum_{\substack{n_1,\dots,n_{n-k+1}\geq 0\\ \sum i n_i = n,\, \sum n_i = k}} \sum_{\substack{\{0\leq p_i\leq n_i\}\\ i=1,\dots,n-k+1\\ \sum p_i = p}} \frac{n!}{\prod_i (n_i-p_i)!p_i!(i!)^{n_i}} \\ \sum_{\substack{\{a^i_j\geq 0\}^{i=1,\dots,n-k+1}_{j=1,\dots,n_i}\\ \sum_i\sum_j a^i_j = l}} \sum_{\substack{\{i-1\geq c^i_j\geq 0\}^{i=1,\dots,n-k+1}_{j=1,\dots,p_i}\\ \sum_i\sum_j c^i_j = l'}} \left(\frac{1}{6}\right)^{\sum_{i=1}^{n-k+1}\sum_{j=1}^{p_i} a^i_j} \left(-\frac{2}{3}\right)^{\sum_{i=1}^{n-k+1}\sum_{j=p_i+1}^{n_i} a^i_j} \\ \prod_{i=1}^{n-k+1} \left(\prod_{j=1}^{p_i} G(a^i_j, c^i_j; i)\right)\left(\prod_{j=p_i+1}^{n_i} G(a^i_j; i)\right), \end{aligned} \tag{6.B.82}$$

as advertised.

Property 2. It remains to transseries expansion for the full free energy $W(g,N)$. In this case, the expressions are simpler because the Z_i have been summed. Starting from the relation between $W(g,N)$ and the $W_n(g)$:

$$\begin{aligned} W(g,N) &= \sum_{n\geq 1} \frac{1}{n!}\left(-\frac{N}{2}\right)^n W_n(g) \\ &\simeq \sum_{n\geq 1} \frac{\left(-\frac{N}{2}\right)^n}{n!} \sum_{k=1}^{n} (-1)^{k-1}(k-1)! \sum_{\substack{n_1,\dots,n_{n-k+1}\geq 0\\ \sum i n_i = n,\, \sum n_i = k}} \frac{n!}{\prod_i n_i!(i!)^{n_i}} \prod_{i=1}^{n-k+1} \left(Z^{\text{pert.}}_i(g) + \eta e^{\frac{3}{2g}} Z^{(\eta)}_i(g)\right)^{n_i} \\ &= \sum_{k\geq 1} (-1)^{k-1}(k-1)! \sum_{\substack{n_1,n_2\dots\geq 0\\ \sum n_i = k}} \prod_{i\geq 1} \frac{1}{n_i!}\Big(\frac{1}{i!}\big(-\frac{N}{2}\big)^i \big(Z^{\text{pert.}}_i(g) + \eta e^{\frac{3}{2g}} Z^{(\eta)}_i(g)\big)\Big)^{n_i}, \end{aligned} \tag{6.B.83}$$

which becomes:

$$\begin{aligned} &\sum_{k\geq 1} (-1)^{k-1}(k-1)!\, \frac{1}{k!}\Big(\sum_{i\geq 1}\frac{1}{i!}\big(-\frac{N}{2}\big)^i \big(Z^{\text{pert.}}_i(g) + \eta e^{\frac{3}{2g}} Z^{(\eta)}_i(g)\big)\Big)^k \\ &= \sum_{k\geq 1} (-1)^{k-1}(k-1)!\, \frac{1}{k!}\big((Z^{\text{pert.}}(g,N) - 1 + \eta e^{\frac{3}{2g}} Z^{(\eta)}(g,N))\big)^k \\ &= \sum_{k\geq 1} \frac{(-1)^{k-1}}{k} (Z^{\text{pert.}}(g,N) - 1 + \eta e^{\frac{3}{2g}} Z^{(\eta)}(g,N))^k = \ln(Z^{\text{pert.}}(g,N) + \eta e^{\frac{3}{2g}} Z^{(\eta)}(g,N))\,, \end{aligned} \tag{6.B.84}$$

we unsurprisingly recover, that formally $W(g,N) = \ln(Z(g,N))$. Here, we used the notation (cf. equation (6.1.12)) $Z(g,N) = Z^{\text{pert.}}(g,N) + \eta e^{\frac{3}{2g}} Z^{(\eta)}(g,N)$, with:

$$\begin{aligned} Z^{\text{pert.}}(g,N) &= \sum_{n=0}^{\infty} \frac{\Gamma(2n+N/2)}{2^{2n} n!\,\Gamma(N/2)} \left(-\frac{2g}{3}\right)^n , \\ Z^{(\eta)}(g,N) &= e^{\imath\tau\pi(1-\frac{N}{2})}\, \sqrt{2\pi} \left(\frac{g}{3}\right)^{\frac{1-N}{2}} \sum_{q=0}^{\infty} \frac{1}{2^{2q} q!\,\Gamma(\frac{N}{2}-2q)} \left(\frac{2g}{3}\right)^q . \end{aligned} \tag{6.B.85}$$

As before, the expansion into instanton sectors can be made manifest, by pulling the transseries monomials to the front in $W(g,N)$. We start from the second to last line in (6.B.84)), that can also be written as:

$$\begin{aligned} W(g,N) &\simeq \sum_{k\geq 1} (-1)^{k-1}(k-1)! \sum_{\substack{p,q\geq 0 \\ p+q=k}} \frac{1}{p!q!} \big(Z^{\text{pert.}}(g)-1\big)^q \big(\eta e^{\frac{3}{2g}} Z^{(\eta)}(g)\big)^p \\ &= \sum_{p\geq 0} e^{\frac{3}{2g}p} \sum_{\substack{q\geq 0 \\ p+q\geq 1}} (-1)^{p+q-1} \frac{(p+q-1)!}{p!q!} \big(Z^{\text{pert.}}(g)-1\big)^q \big(\eta Z^{(\eta)}(g)\big)^p . \end{aligned} \tag{6.B.86}$$

Next, we use the expressions for $Z^{\text{pert.}}$ and $Z^{(\eta)}$ to calculate:

$$\begin{aligned} &\big(Z^{\text{pert.}}(g)-1\big)^q \big(\eta Z^{(\eta)}(g)\big)^p \\ &= \left(\sum_{n=1}^{\infty} \tfrac{\Gamma(2n+N/2)}{2^{2n} n!\,\Gamma(N/2)} \left(-\tfrac{2g}{3}\right)^n\right)^q \left(\eta\sqrt{2\pi} e^{\imath\tau\frac{\pi}{2}} \left(\tfrac{e^{\imath\tau\pi} g}{3}\right)^{\frac{1-N}{2}}\right)^p \\ &\qquad\qquad \times \left(\sum_{m\geq 0} \tfrac{1}{2^{2m} m!\,\Gamma(\frac{N}{2}-2m)} \left(\tfrac{2g}{3}\right)^m\right)^p \\ &= \left(\eta\sqrt{2\pi} e^{\imath\tau\frac{\pi}{2}} \left(\tfrac{e^{\imath\tau\pi} g}{3}\right)^{\frac{1-N}{2}}\right)^p \sum_{\substack{n_1,\ldots,n_q\geq 1 \\ m_1,\ldots,m_p\geq 0}} \left(\prod_{i=1}^{q} \tfrac{\Gamma(2n_i+\frac{N}{2})}{2^{2n_i} n_i!\,\Gamma(\frac{N}{2})} \left(-\tfrac{2g}{3}\right)^{n_i}\right) \\ &\qquad\qquad \times \left(\prod_{j=1}^{p} \tfrac{1}{2^{2m_j} m_j!\,\Gamma(\frac{N}{2}-2m_j)} \left(\tfrac{2g}{3}\right)^{m_j}\right) \\ &= \left(\eta\sqrt{2\pi} e^{\imath\tau\frac{\pi}{2}} \left(\tfrac{e^{\imath\tau\pi} g}{3}\right)^{\frac{1-N}{2}}\right)^p \sum_{l\geq 0} \left(-\tfrac{2g}{3}\right)^l \sum_{\substack{n_1,\ldots,n_q\geq 1 \\ m_1,\ldots,m_p\geq 0 \\ \sum n_i + \sum m_j = l}} \left(\prod_{i=1}^{q} \tfrac{\Gamma(2n_i+\frac{N}{2})}{2^{2n_i} n_i!\,\Gamma(\frac{N}{2})}\right) \\ &\qquad\qquad \times \left(\prod_{j=1}^{p} \tfrac{(-1)^{m_j}}{2^{2m_j} m_j!\,\Gamma(\frac{N}{2}-2m_j)}\right) . \end{aligned} \tag{6.B.87}$$

Finally, inserting this into (6.B.86) we obtain the transseries expansion of the free energy, organized into instanton sectors:

$$W(g,N) = \sum_{p\geq 0} e^{\frac{3}{2g}p} \left(\eta\sqrt{2\pi}e^{\imath\tau\frac{\pi}{2}}\left(\frac{e^{\imath\tau\pi}g}{3}\right)^{\frac{1-N}{2}}\right)^p \sum_{l\geq 0}\left(-\frac{2g}{3}\right)^l \times \left(\sum_{\substack{q\geq 0\\ p+q\geq 1}} (-1)^{p+q-1}\frac{(p+q-1)!}{p!q!} \sum_{\substack{n_1,\dots,n_q\geq 1\\ m_1,\dots,m_p\geq 0\\ \sum n_i+\sum m_j=l}} \left(\prod_{i=1}^{q}\frac{\Gamma(2n_i+N/2)}{2^{2n_i}n_i!\,\Gamma(N/2)}\right)\left(\prod_{j=1}^{p}\frac{(-1)^{m_j}}{2^{2m_j}m_j!\,\Gamma(N/2-2m_j)}\right)\right), \tag{6.B.88}$$

which has the desired form:

$$W(g) \simeq \sum_{p\geq 0} e^{\frac{3}{2g}p} \left(\eta\sqrt{2\pi}e^{\imath\tau\frac{\pi}{2}}\left(\frac{e^{\imath\tau\pi}g}{3}\right)^{\frac{1-N}{2}}\right)^p \sum_{l\geq 0}\left(-\frac{2g}{3}\right)^l W_l^{(p)}(N)\,, \tag{6.B.89}$$

and we can read up the coefficients $W_l^{(p)}$.

This concludes the proof of Proposition 5. □

6.C Feynman graphs and $W(g,N)$

Each term in the convergent series in (6.2.7) can be further expanded in a formal Taylor series in the coupling constant. The series thus obtained is asymptotic to $W(g,N)$ as long as (6.2.7) converges hence in a cardioid domain of the cut complex plane $\mathbb{C}_\pi$ (see Proposition 3) which sweeps all the directions in $\mathbb{C}_\pi$. In this range of g no singularity of the integrand crosses the real axis, which is the steepest-descent contour of the exponentials in (6.2.5).

The asymptotic series of $W(g,N)$ in the first Riemann sheet is well known to be the formal sum over connected Feynman graphs of amplitudes. However, due to the presence of the w parameters and the integrals over the us, it is not exactly transparent how this comes about starting from (6.2.7). The fact that (6.2.7) does indeed reproduce the Feynman graph expansion has been proven in [215]. We sketch below how this comes about.

Hepp sectors. To any graph G with vertices labeled $i, i = 1,\dots n$ one can associate a *characteristic* function depending on edge variables $f(x_{ij}) = \prod_{(i,j)\in G} x_{ij}$ where the product runs over the edges of G. The forest formula applied to this function yields:

$$1 = \sum_{\mathcal{F}\subset G} \underbrace{\int_0^1\cdots\int_0^1}_{|\mathcal{F}|\text{ times}} \left(\prod_{(i,j)\in\mathcal{F}} du_{ij}\right) \left[\prod_{(k,l)\notin\mathcal{F}} w_{kl}^{\mathcal{F}}(u_{\mathcal{F}})\right]. \tag{6.C.1}$$

Remark that the derivative of the characteristic function is nonzero only if the forest $\mathcal{F}$ is made of edges of G (which we signify by $\mathcal{F}\subset G$). Furthermore, if $\mathcal{F}$ has more than one block, then one of the ws in the product is set to zero. It follows that only trees contribute:

$$1 = \sum_{\mathcal{T}\subset G} \underbrace{\int_0^1\cdots\int_0^1}_{|\mathcal{T}|\text{ times}} \left(\prod_{(i,j)\in\mathcal{T}} du_{ij}\right) \left[\prod_{(k,l)\notin\mathcal{T}} w_{kl}^{\mathcal{T}}(u_{\mathcal{T}})\right]. \tag{6.C.2}$$

This formula defines normalized weights associated with the graph G and the spanning trees $\mathcal{T} \subset G$:

$$w(G,\mathcal{T}) = \underbrace{\int_0^1 \cdots \int_0^1}_{|\mathcal{T}| \text{ times}} \left(\prod_{(i,j)\in\mathcal{T}} du_{ij} \right) \left[\prod_{(k,l)\notin\mathcal{T}} w_{kl}^{\mathcal{T}}(u_{\mathcal{T}}) \right] , \qquad \sum_{\mathcal{T}\subset G} w(G,\mathcal{T}) = 1 , \tag{6.C.3}$$

which admit a striking combinatorial interpretation. We define a *Hepp sector* as a total ordering π of the edges of G, that is a bijection $\pi : E(G) \to \{1, \dots |E(G)|\}$, where $E(G)$ is the set of edges of G. For any π *the leading spanning tree* in π, denoted $\mathcal{T}(\pi)$, is the tree such that $\sum_{e\in\mathcal{T}(\pi)} \pi(e)$ is minimal. The tree $\mathcal{T}(\pi)$ is obtained by Kruskal's greedy algorithm: at each step one adds the edge $e \in G$ with minimal $\pi(e)$ that does not form a loop.

Lemma 1. *We have:*

$$w(G,\mathcal{T}) = \frac{N(G,\mathcal{T})}{|E(G)|!} , \tag{6.C.4}$$

where $N(G,\mathcal{T})$ is the number of sectors π such that $\mathcal{T}(\pi) = \mathcal{T}$, that is $w(G,\mathcal{T})$ is the percentage of Hepp sectors in which $\mathcal{T}$ is the leading spanning tree of G.

Proof. Let us define the function:

$$\chi(u_{E(G)\setminus\mathcal{T}} \le u_{\mathcal{T}}) \begin{cases} 1 , \text{ if } \forall (i,j) \in E(G)\setminus\mathcal{T} , \quad u_{ij} \le \inf_{(k,l)\in P_{i\to j}^{\mathcal{T}}} u_{kl} \\ 0 , \text{ otherwise} \end{cases} . \tag{6.C.5}$$

On the one hand we have:

$$w(G,\mathcal{T}) = \int_0^1 \left(\prod_{e\in E(G)} du_e \right) \chi(u_{G\setminus\mathcal{T}} \le u_{\mathcal{T}}) , \tag{6.C.6}$$

as, at any fixed $\{u_e, e \in \mathcal{T}\}$ the integral over the loop edge variable u_{kl} yields $w_{kl}^{\mathcal{T}}(u_{\mathcal{T}})$.

We now split the integration interval according to Hepp sectors. In the sector π corresponding to $u_{\pi^{-1}(1)} > u_{\pi^{-1}(2)} > \dots$ the characteristic function χ tests whether every loop edge (i,j) has smaller u_{ij} than $\inf\{u_{kl}\}$ in the tree path $P_{i\to j}^{\mathcal{T}}$ connecting i and j. This is true if and only if $\mathcal{T}$ is the leading spanning tree in π:

$$\begin{aligned} &\int_0^1 \left(\prod_{e\in\mathcal{E}(G)} du_e \right) \chi(u_{G\setminus\mathcal{T}} \le u_{\mathcal{T}}) \\ &= \sum_{\pi} \int_0^1 du_{\pi^{-1}(1)} \int_0^{u_{\pi^{-1}(1)}} du_{\pi^{-1}(2)} \cdots \int_0^{u_{\pi^{-1}(|E(G)|-1)}} du_{\pi^{-1}(|E(G)|)} \ \chi(u_{G\setminus\mathcal{T}} \le u_{\mathcal{T}}) \\ &= \sum_{\pi,\mathcal{T}(\pi)=\mathcal{T}} \int_0^1 du_{\pi^{-1}(1)} \int_0^{u_{\pi^{-1}(1)}} du_{\pi^{-1}(2)} \cdots \int_0^{u_{\pi^{-1}(|E(G)|-1)}} du_{\pi^{-1}(|E(G)|)} \\ &= \frac{1}{|E(G)|!} \sum_{\pi,\mathcal{T}(\pi)=\mathcal{T}} 1 . \end{aligned} \tag{6.C.7}$$

□

Lemma 2 (Asymptotic series [215].)**.** *The asymptotic expansion at zero of the free energy $W(g,N)$ in the cut plane $g \in \mathbb{C}_\pi$ is the formal sum over connected Feynman graphs of Feynman amplitudes.*

Proof. Taylor expanding the Gaussian integrals in (6.2.7) to infinity yields:

$$\begin{aligned} & W(g,N) \\ & \simeq -\tfrac{N}{2}\left[\sum_{l\geq 0}\tfrac{1}{l!}\left(\tfrac{1}{2}\tfrac{\delta}{\delta\sigma}\tfrac{\delta}{\delta\sigma}\right)^{l}\ln\left(1-\imath\sqrt{\tfrac{g}{3}}\sigma\right)\right]_{\sigma=0} - \sum_{n\geq 2}\frac{\left(-\frac{N}{2}\right)^{n}}{n!}\left(\tfrac{g}{3}\right)^{n-1}\sum_{\mathcal{T}\in T_n}\int_0^1\Big(\prod_{(i,j)\in\mathcal{T}}du_{ij}\Big) \\ & \quad\times\left[\sum_{\{l_i\geq 0\}}\tfrac{1}{l_i!}\left(\tfrac{1}{2}\tfrac{\delta}{\delta\sigma_i}\tfrac{\delta}{\delta\sigma_i}\right)^{l_i}\sum_{\{l_{ij}\geq 0\}_{i\leq j}}\tfrac{1}{l_{ij}!}\left(w_{ij}^{\mathcal{T}}\tfrac{\delta}{\delta\sigma_i}\tfrac{\delta}{\delta\sigma_j}\right)^{l_{ij}}\prod_i\frac{(d_i-1)!}{\left(1-\imath\sqrt{\frac{g}{3}}\sigma_i\right)^{d_i}}\right]_{\sigma_i=0} \\ & = \sum_{n\geq 1}\frac{1}{n!}\left(-\frac{N}{2}\right)^{n}\sum_{\mathcal{T}\in T_n}\sum_{\{l_i\geq 0\},\{l_{ij}\geq 0\}_{i<j}}\frac{\prod_i(d_i+l_i+\sum_j l_{ij}-1)!}{(\prod_i 2^{l_i}l_i!)(\prod_{i<j}l_{ij}!)} \\ & \qquad\left[\int_0^1\left(\prod_{(i,j)\in\mathcal{T}}du_{ij}\right)\left(\prod_{(i<j)}w_{ij}^{\mathcal{T}}\right)^{l_{ij}}\right]\left(-\frac{g}{3}\right)^{n-1+\sum_l l_i+\sum_{i<j}l_{ij}}. \end{aligned} \tag{6.C.8}$$

The additional derivatives with respect to σ generate loop edges decorating the tree $\mathcal{T}$: l_{ij} is the multiplicity of the loop edge between i and j and l_i the number of tadpole edges (or self loops) at the vertex i. We denote the graph consisting in $\mathcal{T}$ decorated by such extra loop edges by G. Of course, $\mathcal{T}$ is a spanning tree of G which we denote $G\supset\mathcal{T}$. From Lemma 1, the integral over u in (6.C.8) is:

$$w(G,\mathcal{T}) = \underbrace{\int_0^1\cdots\int_0^1}_{|\mathcal{T}|\text{ times}}\left(\prod_{(i,j)\in\mathcal{T}}du_{ij}\right)\left[\prod_{(k,l)\notin\mathcal{T}}w_{kl}^{\mathcal{T}}(u_{\mathcal{T}})\right] = \frac{N(G,\mathcal{T})}{|E(G)|!}\,, \tag{6.C.9}$$

yields the percentage of Hepp sectors in which $\mathcal{T}$ is the leading spanning tree of G. Collecting the coupling constants and the symmetry factor in the amplitude $A(G)$ of the graph G, we write:

$$W(g) = \sum_{n\geq 1}\frac{1}{n!}\sum_{\mathcal{T}\in\mathcal{T}_n}\sum_{G\supset\mathcal{T}}w(G,\mathcal{T})A(G)\,, \tag{6.C.10}$$

that is for each tree $\mathcal{T}$ we resum the amplitudes of the graphs in which $\mathcal{T}$ is a spanning tree with a weight given by the percentage of Hepp sectors of G in which $\mathcal{T}$ is the leading tree. Denoting G_n the set of connected graphs over n vertices, we commute the sums over trees $\mathcal{T}$ and graphs G and using $\sum_{T\subset G}w(G,\mathcal{T})=1$ we get:

$$W(g) = \sum_{n\geq 1}\frac{1}{n!}\sum_{G\in G_n}A(G)\,, \tag{6.C.11}$$

which is the familiar perturbative expansion of the free energy in connected graphs. □

Bibliography

[1] D. Benedetti et al. "The F-theorem in the melonic limit". In: *JHEP* 02 (2022), p. 147. DOI: 10.1007/JHEP02(2022)147. arXiv: 2111.11792 [hep-th].

[2] D. Benedetti et al. "The small-N series in the zero-dimensional $O(N)$ model: constructive expansions and transseries". In: *Annales Henri Poincare* (Apr. 2024). DOI: https://doi.org/10.1007/s00023-024-01437-y. arXiv: 2210.14776 [hep-th].

[3] D. Benedetti et al. "Finite-size versus finite-temperature effects in the critical long-range O(N) model". In: *JHEP* 02 (2024), p. 078. DOI: 10.1007/JHEP02(2024)078. arXiv: 2311.04607 [hep-th].

[4] D. Benedetti, R. Gurau, and D. Lettera. "Dynamic critical exponent in quantum long-range models". In: (Apr. 2024). arXiv: 2404.13963 [hep-th].

[5] N. Defenu et al. "Long-range interacting quantum systems". In: (Sept. 2021). arXiv: 2109.01063 [cond-mat.quant-gas].

[6] H. E. Stanley. "Spherical Model as the Limit of Infinite Spin Dimensionality". In: *Phys. Rev.* 176 (2 1968), pp. 718–722. DOI: 10.1103/PhysRev.176.718. URL: https://link.aps.org/doi/10.1103/PhysRev.176.718.

[7] K. G. Wilson. "Quantum field theory models in less than four-dimensions". In: *Phys.Rev.D* 7 (1973), pp. 2911–2926. DOI: 10.1103/PhysRevD.7.2911.

[8] G. 't Hooft. "A Planar Diagram Theory for Strong Interactions". In: *Nucl. Phys. B* 72 (1974). Ed. by J. C. Taylor, p. 461. DOI: 10.1016/0550-3213(74)90154-0.

[9] R. Gurau. "Colored Group Field Theory". In: *Commun. Math. Phys.* 304 (2011), pp. 69–93. DOI: 10.1007/s00220-011-1226-9. arXiv: 0907.2582 [hep-th].

[10] E. Witten. "An SYK-Like Model Without Disorder". In: *J. Phys. A* 52.47 (2019), p. 474002. DOI: 10.1088/1751-8121/ab3752. arXiv: 1610.09758 [hep-th].

[11] S. Carrozza and A. Tanasa. "$O(N)$ Random Tensor Models". In: *Lett. Math. Phys.* 106.11 (2016), pp. 1531–1559. DOI: 10.1007/s11005-016-0879-x. arXiv: 1512.06718 [math-ph].

[12] R. Gurau. "The complete $1/N$ expansion of a SYK–like tensor model". In: *Nucl. Phys.* B916 (2017), pp. 386–401. DOI: 10.1016/j.nuclphysb.2017.01.015. arXiv: 1611.04032 [hep-th].

[13] N. Sasakura. "Tensor model for gravity and orientability of manifold". In: *Mod. Phys. Lett.* A6 (1991), pp. 2613–2624. DOI: 10.1142/S0217732391003055.

[14] P. Di Francesco, P. H. Ginsparg, and J. Zinn-Justin. "2-D Gravity and random matrices". In: *Phys. Rept.* 254 (1995), pp. 1–133. DOI: 10.1016/0370-1573(94)00084-G. arXiv: hep-th/9306153.

[15] J. Maldacena and D. Stanford. "Remarks on the Sachdev-Ye-Kitaev model". In: *Phys. Rev.* D94.10 (2016), p. 106002. DOI: 10.1103/PhysRevD.94.106002. arXiv: 1604.07818 [hep-th].

[16] S. Giombi, I. R. Klebanov, and G. Tarnopolsky. "Bosonic tensor models at large N and small ϵ". In: *Phys. Rev. D* 96.10 (2017), p. 106014. DOI: 10.1103/PhysRevD.96.106014. arXiv: 1707.03866 [hep-th].

[17] D. Benedetti, R. Gurau, and S. Harribey. "Line of fixed points in a bosonic tensor model". In: *JHEP* 06 (2019), p. 053. DOI: 10.1007/JHEP06(2019)053. arXiv: 1903.03578 [hep-th].

[18] S. Prakash and R. Sinha. "A Complex Fermionic Tensor Model in d Dimensions". In: *JHEP* 02 (2018), p. 086. DOI: 10.1007/JHEP02(2018)086. arXiv: 1710.09357 [hep-th].

[19] D. Benedetti. "Melonic CFTs". In: *PoS* CORFU2019 (2020), p. 168. DOI: 10.22323/1.376.0168. arXiv: 2004.08616 [hep-th].

[20] K. G. Wilson. "The renormalization group and critical phenomena". In: *Rev. Mod. Phys.* 55 (1983), pp. 583–600. DOI: 10.1103/RevModPhys.55.583.

[21] J. Écalle. *Les fonctions résurgentes. Vol. I-III*. Orsay: Université de Paris-Sud, Département de Mathématique, 1981, p. 247.

[22] V. Rivasseau. "Constructive Matrix Theory". In: *JHEP* 09 (2007), p. 008. DOI: 10.1088/1126-6708/2007/09/008. arXiv: 0706.1224 [hep-th].

[23] D. C. Brydges and T. Kennedy. "Mayer expansions and the Hamilton-Jacobi equation". In: *Journal of Statistical Physics* 48 (July 1987), pp. 19–49. DOI: 10.1007/BF01010398.

[24] A. Abdesselam and V. Rivasseau. "Trees, forests and jungles: A Botanical garden for cluster expansions". In: *Lect. Notes Phys.* 446 (1995). Ed. by V. Rivasseau, p. 7. DOI: 10.1007/3-540-59190-7_20. arXiv: hep-th/9409094.

[25] J. Magnen and V. Rivasseau. "Constructive phi**4 field theory without tears". In: *Annales Henri Poincare* 9 (2008), pp. 403–424. DOI: 10.1007/s00023-008-0360-1. arXiv: 0706.2457 [math-ph].

[26] J. Zinn-Justin. *Quantum field theory and critical phenomena*. Vol. 77. International Series of Monographs on Physics. Oxford University Press, Apr. 2021. ISBN: 978-0-19-850923-3, 978-0-19-883462-5.

[27] M. E. Peskin and D. V. Schroeder. *An Introduction to quantum field theory*. Reading, USA: Addison-Wesley, 1995. ISBN: 978-0-201-50397-5.

[28] M. Maggiore. *A Modern introduction to quantum field theory*. Oxford Master Series in Physics. 2005. ISBN: 978-0-19-852074-0.

[29] S. Weinberg. *The Quantum theory of fields. Vol. 1: Foundations*. Cambridge University Press, June 2005. ISBN: 978-0-521-67053-1, 978-0-511-25204-4. DOI: 10.1017/CBO9781139644167.

[30] S. Weinberg. *The quantum theory of fields. Vol. 2: Modern applications*. Cambridge University Press, Aug. 2013. ISBN: 978-1-139-63247-8, 978-0-521-67054-8, 978-0-521-55002-4. DOI: 10.1017/CBO9781139644174.

[31] J.-P. Blaizot, J. M. Pawlowski, and U. Reinosa. "Functional renormalization group and 2PI effective action formalism". In: *Annals Phys.* 431 (2021), p. 168549. DOI: 10.1016/j.aop.2021.168549. arXiv: 2102.13628 [hep-th].

[32] S. Giombi and H. Khanchandani. "$O(N)$ Models with Boundary Interactions and their Long Range Generalizations". In: (Dec. 2019). arXiv: 1912.08169 [hep-th].

[33] L. P. Kadanoff. "Scaling laws for Ising models near T(c)". In: *Physics Physique Fizika* 2 (1966), pp. 263–272. DOI: 10.1103/PhysicsPhysiqueFizika.2.263.

[34] Y. Nakayama. "Scale invariance vs conformal invariance". In: *Physics Reports* 569 (2015). Scale invariance vs conformal invariance, pp. 1 –93. ISSN: 0370-1573. DOI: https://doi.org/10.1016/j.physrep.2014.12.003. eprint: 1302.0884. URL: http://www.sciencedirect.com/science/article/pii/S0370157314004499.

[35] P. Di Francesco, P. Mathieu, and D. Senechal. *Conformal Field Theory*. Graduate Texts in Contemporary Physics. New York: Springer-Verlag, 1997. ISBN: 978-0-387-94785-3, 978-1-4612-7475-9. DOI: 10.1007/978-1-4612-2256-9.

[36] S. Rychkov. *EPFL Lectures on Conformal Field Theory in D>= 3 Dimensions*. SpringerBriefs in Physics. Jan. 2016. ISBN: 978-3-319-43625-8, 978-3-319-43626-5. DOI: 10.1007/978-3-319-43626-5. arXiv: 1601.05000 [hep-th].

[37] D. Pappadopulo et al. "OPE Convergence in Conformal Field Theory". In: *Phys. Rev. D* 86 (2012), p. 105043. DOI: 10.1103/PhysRevD.86.105043. arXiv: 1208.6449 [hep-th].

[38] R. Rattazzi et al. "Bounding scalar operator dimensions in 4D CFT". In: *JHEP* 12 (2008), p. 031. DOI: 10.1088/1126-6708/2008/12/031. arXiv: 0807.0004 [hep-th].

[39] D. Poland, S. Rychkov, and A. Vichi. "The Conformal Bootstrap: Theory, Numerical Techniques, and Applications". In: *Rev. Mod. Phys.* 91 (2019), p. 015002. DOI: 10.1103/RevModPhys.91.015002. arXiv: 1805.04405 [hep-th].

[40] V. Dobrev et al. "Dynamical Derivation of Vacuum Operator Product Expansion in Euclidean Conformal Quantum Field Theory". In: *Phys. Rev. D* 13 (1976), p. 887. DOI: 10.1103/PhysRevD.13.887.

[41] V. Dobrev et al. "On the Clebsch-Gordan Expansion for the Lorentz Group in n Dimensions". In: *Rept. Math. Phys.* 9 (1976), pp. 219–246. DOI: 10.1016/0034-4877(76)90057-4.

[42] V. Dobrev et al. *Harmonic Analysis on the n-Dimensional Lorentz Group and Its Application to Conformal Quantum Field Theory*. Vol. 63. Springer, Berlin, Heidelberg, 1977. DOI: 10.1007/BFb0009678.

[43] M. Moshe and J. Zinn-Justin. "Quantum field theory in the large N limit: A Review". In: *Phys. Rept.* 385 (2003), pp. 69–228. DOI: 10.1016/S0370-1573(03)00263-1. arXiv: hep-th/0306133.

[44] D. Benedetti et al. "Hints of unitarity at large N in the $O(N)^3$ tensor field theory". In: *JHEP* 02 (2020). [Erratum: JHEP 08, 167 (2020)], p. 072. DOI: 10.1007/JHEP02(2020)072. arXiv: 1909.07767 [hep-th].

[45] I. R. Klebanov and G. Tarnopolsky. "Uncolored random tensors, melon diagrams, and the Sachdev-Ye-Kitaev models". In: *Phys. Rev. D* 95.4 (2017), p. 046004. DOI: 10.1103/PhysRevD.95.046004. arXiv: 1611.08915 [hep-th].

[46] V. Bonzom et al. "Critical behavior of colored tensor models in the large N limit". In: *Nucl. Phys. B* 853 (2011), pp. 174–195. DOI: 10.1016/j.nuclphysb.2011.07.022. arXiv: 1105.3122 [hep-th].

[47] D. Benedetti, R. Gurau, and K. Suzuki. "Conformal symmetry and composite operators in the $O(N)^3$ tensor field theory". In: *JHEP* 06 (2020), p. 113. DOI: 10.1007/JHEP06(2020)113. arXiv: 2002.07652 [hep-th].

[48] A. D. Sokal. "An improvement of Watson's theorem on Borel summability". In: *J. Math. Phys.* 21 (1980), pp. 261–263. DOI: 10.1063/1.524408.

[49] J. Magnen and V. Rivasseau. "Constructive ϕ^4 Field Theory without Tears". In: *Annales Henri Poincaré* 9.2 (Apr. 2008), 403–424. ISSN: 1424-0661. DOI: 10.1007/s00023-008-0360-1. URL: http://dx.doi.org/10.1007/s00023-008-0360-1.

[50] A. B. Zamolodchikov. "Irreversibility of the Flux of the Renormalization Group in a 2D Field Theory". In: *JETP Lett.* 43 (1986), pp. 730–732.

[51] Z. Komargodski and A. Schwimmer. "On Renormalization Group Flows in Four Dimensions". In: *JHEP* 12 (2011), p. 099. DOI: 10.1007/JHEP12(2011)099. arXiv: 1107.3987 [hep-th].

[52] D. L. Jafferis et al. "Towards the F-Theorem: N=2 Field Theories on the Three-Sphere". In: *JHEP* 06 (2011), p. 102. DOI: 10.1007/JHEP06(2011)102. arXiv: 1103.1181 [hep-th].

[53] I. R. Klebanov, S. S. Pufu, and B. R. Safdi. "F-Theorem without Supersymmetry". In: *JHEP* 10 (2011), p. 038. DOI: 10.1007/JHEP10(2011)038. arXiv: 1105.4598 [hep-th].

[54] J. L. Cardy. "Is There a c Theorem in Four-Dimensions?" In: *Phys. Lett. B* 215 (1988), pp. 749–752. DOI: 10.1016/0370-2693(88)90054-8.

[55] Z. Komargodski. "The Constraints of Conformal Symmetry on RG Flows". In: *JHEP* 07 (2012), p. 069. DOI: 10.1007/JHEP07(2012)069. arXiv: 1112.4538 [hep-th].

[56] D. L. Jafferis. "The Exact Superconformal R-Symmetry Extremizes Z". In: *JHEP* 05 (2012), p. 159. DOI: 10.1007/JHEP05(2012)159. arXiv: 1012.3210 [hep-th].

[57] S. S. Pufu. "The F-Theorem and F-Maximization". In: *J. Phys. A* 50.44 (2017), p. 443008. DOI: 10.1088/1751-8121/aa6765. arXiv: 1608.02960 [hep-th].

[58] H. Casini and M. Huerta. "On the RG running of the entanglement entropy of a circle". In: *Phys. Rev. D* 85 (2012), p. 125016. DOI: 10.1103/PhysRevD.85.125016. arXiv: 1202.5650 [hep-th].

[59] H. Casini, M. Huerta, and R. C. Myers. "Towards a derivation of holographic entanglement entropy". In: *JHEP* 05 (2011), p. 036. DOI: 10.1007/JHEP05(2011)036. arXiv: 1102.0440 [hep-th].

[60] H. Casini and M. Huerta. "A Finite entanglement entropy and the c-theorem". In: *Phys. Lett. B* 600 (2004), pp. 142–150. DOI: 10.1016/j.physletb.2004.08.072. arXiv: hep-th/0405111.

[61] H. Casini, E. Testé, and G. Torroba. "Markov Property of the Conformal Field Theory Vacuum and the a Theorem". In: *Phys. Rev. Lett.* 118.26 (2017), p. 261602. DOI: 10.1103/PhysRevLett.118.261602. arXiv: 1704.01870 [hep-th].

[62] S. Giombi and I. R. Klebanov. "Interpolating between a and F". In: *JHEP* 03 (2015), p. 117. DOI: 10.1007/JHEP03(2015)117. arXiv: 1409.1937 [hep-th].

[63] L. Fei et al. "Generalized F-Theorem and the ϵ Expansion". In: *JHEP* 12 (2015), p. 155. DOI: 10.1007/JHEP12(2015)155. arXiv: 1507.01960 [hep-th].

[64] S. Giombi, I. R. Klebanov, and G. Tarnopolsky. "Conformal QED$_d$, F-Theorem and the ϵ Expansion". In: *J. Phys. A* 49.13 (2016), p. 135403. DOI: 10.1088/1751-8113/49/13/135403. arXiv: 1508.06354 [hep-th].

[65] M. Hogervorst, S. Rychkov, and B. C. van Rees. "Unitarity violation at the Wilson-Fisher fixed point in 4-ϵ dimensions". In: *Phys. Rev. D* 93.12 (2016), p. 125025. DOI: 10.1103/PhysRevD.93.125025. arXiv: 1512.00013 [hep-th].

[66] M. F. Paulos et al. "Conformal Invariance in the Long-Range Ising Model". In: *Nucl.Phys.B* 902 (2016), pp. 246–291. DOI: 10.1016/j.nuclphysb.2015.10.018. arXiv: 1509.00008 [hep-th].

[67] D. Gaiotto. "Boundary F-maximization". In: (Mar. 2014). arXiv: 1403.8052 [hep-th].

[68] N. Kobayashi et al. "Towards a C-theorem in defect CFT". In: *JHEP* 01 (2019), p. 039. DOI: 10.1007/JHEP01(2019)039. arXiv: 1810.06995 [hep-th].

[69] J. Maldacena and A. Zhiboedov. "Constraining Conformal Field Theories with A Higher Spin Symmetry". In: *J. Phys. A* 46 (2013), p. 214011. DOI: 10.1088/1751-8113/46/21/214011. arXiv: 1112.1016 [hep-th].

[70] D. J. Binder and S. Rychkov. "Deligne Categories in Lattice Models and Quantum Field Theory, or Making Sense of $O(N)$ Symmetry with Non-integer N". In: *JHEP* 04 (2020), p. 117. DOI: 10.1007/JHEP04(2020)117. arXiv: 1911.07895 [hep-th].

[71] C. Behan et al. "A scaling theory for the long-range to short-range crossover and an infrared duality". In: *J.Phys.A* 50.35 (2017), p. 354002. DOI: 10.1088/1751-8121/aa8099. arXiv: 1703.05325 [hep-th].

[72] A. Campa, T. Dauxois, and S. Ruffo. "Statistical mechanics and dynamics of solvable models with long-range interactions". In: *Physics Reports* 480.3-6 (2009), pp. 57–159. ISSN: 0370-1573. DOI: 10.1016/j.physrep.2009.07.001. arXiv: 0907.0323. URL: http://dx.doi.org/10.1016/j.physrep.2009.07.001.

[73] D. E. Diaz and H. Dorn. "Partition functions and double-trace deformations in AdS/CFT". In: *JHEP* 05 (2007), p. 046. DOI: 10.1088/1126-6708/2007/05/046. arXiv: hep-th/0702163.

[74] D. Benedetti and R. Gurau. "2PI effective action for the SYK model and tensor field theories". In: *JHEP* 05 (2018), p. 156. DOI: 10.1007/JHEP05(2018)156. arXiv: 1802.05500 [hep-th].

[75] J. Berges. "Introduction to nonequilibrium quantum field theory". In: *AIP Conf. Proc.* 739 (2005), pp. 3–62. DOI: 10.1063/1.1843591. arXiv: hep-ph/0409233 [hep-ph].

[76] V. Bonzom, V. Nador, and A. Tanasa. "Diagrammatics of the quartic $O(N)^3$-invariant Sachdev-Ye-Kitaev-like tensor model". In: *J. Math. Phys.* 60.7 (2019), p. 072302. DOI: 10.1063/1.5095248. arXiv: 1903.01723 [hep-th].

[77] D. Grabner et al. "Strongly γ-Deformed $\mathcal{N} = 4$ Supersymmetric Yang-Mills Theory as an Integrable Conformal Field Theory". In: *Phys.Rev.Lett.* 120.11 (2018), p. 111601. DOI: 10.1103/PhysRevLett.120.111601. arXiv: 1711.04786 [hep-th].

[78] V. Kazakov and E. Olivucci. "Biscalar Integrable Conformal Field Theories in Any Dimension". In: *Phys.Rev.Lett.* 121.13 (2018), p. 131601. DOI: 10.1103/PhysRevLett.121.131601. arXiv: 1801.09844 [hep-th].

[79] D. Karateev, P. Kravchuk, and D. Simmons-Duffin. "Harmonic Analysis and Mean Field Theory". In: *JHEP* 10 (2019), p. 217. DOI: 10.1007/JHEP10(2019)217. arXiv: 1809.05111 [hep-th].

[80] D. Benedetti, R. Gurau, and S. Harribey. "The tri-fundamental quartic model". In: *Phys. Rev. D* 103.4 (2021), p. 046018. DOI: 10.1103/PhysRevD.103.046018. arXiv: 2011.11276 [hep-th].

[81] S. S. Gubser and I. R. Klebanov. "A Universal result on central charges in the presence of double trace deformations". In: *Nucl. Phys. B* 656 (2003), pp. 23–36. DOI: 10.1016/S0550-3213(03)00056-7. arXiv: hep-th/0212138.

[82] S. Sachdev and J. Ye. "Gapless spin fluid ground state in a random, quantum Heisenberg magnet". In: *Phys. Rev. Lett.* 70 (1993), p. 3339. DOI: 10.1103/PhysRevLett.70.3339. arXiv: cond-mat/9212030 [cond-mat].

[83] A. Kitaev. "A simple model of quantum holography". In: *KITP strings seminar and Entanglement 2015* (Feb. 12, April 7, and May 27, 2015). URL: http://online.kitp.ucsb.edu/online/entangled15/.

[84] D. J. Gross and V. Rosenhaus. "A line of CFTs: from generalized free fields to SYK". In: *JHEP* 07 (2017), p. 086. DOI: 10.1007/JHEP07(2017)086. arXiv: 1706.07015 [hep-th].

[85] M. A. Rubin and C. R. Ordonez. "Eigenvalues and degeneracies for n-dimensional tensor spherical harmonics". In: *Journal of Mathematical Physics* 25.10 (1984), pp. 2888–2894. DOI: 10.1063/1.526034. URL: https://doi.org/10.1063/1.526034.

[86] S. Samko. *Hypersingular Integrals and Their Applications*. 1st ed. An optional note. London: CRC Press, 2002. ISBN: 0415272688. DOI: 10.1201/9781482264968.

[87] K. Farnsworth, M. A. Luty, and V. Prilepina. "Weyl versus Conformal Invariance in Quantum Field Theory". In: *JHEP* 10 (2017), p. 170. DOI: 10.1007/JHEP10(2017)170. arXiv: 1702.07079 [hep-th].

[88] B. Allen and T. Jacobson. "Vector Two Point Functions in Maximally Symmetric Spaces". In: *Commun. Math. Phys.* 103 (1986), p. 669. DOI: 10.1007/BF01211169.

[89] J. S. Dowker and R. Critchley. "Effective Lagrangian and Energy Momentum Tensor in de Sitter Space". In: *Phys. Rev. D* 13 (1976), p. 3224. DOI: 10.1103/PhysRevD.13.3224.

[90] M. Kwasnicki. "Ten equivalent definitions of the fractional Laplace operator". In: *Fractional Calculus and Applied Analysis* 20 (2017), pp. 51 –7. arXiv: 1507.07356 [math.AP].

[91] P. Stinga and J. Torrea. "Extension Problem and Harnack's Inequality for Some Fractional Operators". In: *Communications in Partial Differential Equations* 35 (2009), pp. 2092 –2122. arXiv: 0910.2569 [math.AP].

[92] S. Ferrara et al. "The shadow operator formalism for conformal algebra. Vacuum expectation values and operator products". In: *Lett. Nuovo Cim.* 4S2 (1972), pp. 115–120. DOI: 10.1007/BF02907130.

[93] S. Samko. "On Inversion of Fractional Spherical Potentials by Spherical Hypersingular Operators". In: *Singular Integral Operators, Factorization and Applications*. Ed. by A. Böttcher et al. Basel: Birkhäuser Basel, 2003, pp. 357–368. ISBN: 978-3-0348-8007-7. DOI: 10.1007/978-3-0348-8007-7_19.

[94] T. Branson. "Spectral theory of invariant operators, sharp inequalities, and representation theory". In: *Proceedings of the 16th Winter School "Geometry and Physics"*. Palermo: Circolo Matematico di Palermo, 1997, [29]–54. URL: http://eudml.org/doc/220067.

[95] M. del Mar Gonzalez. "Recent progress on the fractional Laplacian in conformal geometry". In: (2016). arXiv: 1609.08988 [math.AP].

[96] T. P. Branson. "Sharp Inequalities, the Functional Determinant, and the Complementary Series". In: *Transactions of the American Mathematical Society* 347.10 (1995), pp. 3671–3742. ISSN: 00029947. URL: http://www.jstor.org/stable/2155203.

[97] P. M. Pavlov and S. G. Samko. "Description of spaces $L_p^\alpha(S_{n-1})$ in terms of spherical hypersingular integrals". In: *Dokl. Akad. Nauk SSSR* 276 (3 1984), pp. 546–550. URL: http://mi.mathnet.ru/dan9633.

[98] S. Caron-Huot. "Analyticity in Spin in Conformal Theories". In: *JHEP* 09 (2017), p. 078. DOI: 10.1007/JHEP09(2017)078. arXiv: 1703.00278 [hep-th].

[99] D. Simmons-Duffin, D. Stanford, and E. Witten. "A spacetime derivation of the Lorentzian OPE inversion formula". In: *JHEP* 07 (2018), p. 085. DOI: 10.1007/JHEP07(2018)085. arXiv: 1711.03816 [hep-th].

[100] J. Liu et al. "d-dimensional SYK, AdS Loops, and $6j$ Symbols". In: *JHEP* 03 (2019), p. 052. DOI: 10.1007/JHEP03(2019)052. arXiv: 1808.00612 [hep-th].

[101] G. Mack. "D-independent representation of Conformal Field Theories in D dimensions via transformation to auxiliary Dual Resonance Models. Scalar amplitudes". In: (July 2009). arXiv: 0907.2407 [hep-th].

[102] M. S. Costa, V. Goncalves, and J. Penedones. "Conformal Regge theory". In: *JHEP* 12 (2012), p. 091. DOI: 10.1007/JHEP12(2012)091. arXiv: 1209.4355 [hep-th].

[103] J. Murugan, D. Stanford, and E. Witten. "More on Supersymmetric and 2d Analogs of the SYK Model". In: *JHEP* 08 (2017), p. 146. DOI: 10.1007/JHEP08(2017)146. arXiv: 1706.05362 [hep-th].

[104] A. Gadde. "In search of conformal theories". In: (Feb. 2017). arXiv: 1702.07362 [hep-th].

[105] M. Hogervorst and B. C. van Rees. "Crossing symmetry in alpha space". In: *JHEP* 11 (2017), p. 193. DOI: 10.1007/JHEP11(2017)193. arXiv: 1702.08471 [hep-th].

[106] C. Sleight and M. Taronna. "Anomalous Dimensions from Crossing Kernels". In: *JHEP* 11 (2018), p. 089. DOI: 10.1007/JHEP11(2018)089. arXiv: 1807.05941 [hep-th].

[107] C. Sleight and M. Taronna. "Spinning Mellin Bootstrap: Conformal Partial Waves, Crossing Kernels and Applications". In: *Fortsch. Phys.* 66.8-9 (2018), p. 1800038. DOI: 10.1002/prop.201800038. arXiv: 1804.09334 [hep-th].

[108] R. de Mello Koch et al. "AdS Maps and Diagrams of Bi-local Holography". In: *JHEP* 03 (2019), p. 133. DOI: 10.1007/JHEP03(2019)133. arXiv: 1810.02332 [hep-th].

[109] O. Aharony, S. M. Chester, and E. Y. Urbach. "A Derivation of AdS/CFT for Vector Models". In: *JHEP* 03 (2021), p. 208. DOI: 10.1007/JHEP03(2021)208. arXiv: 2011.06328 [hep-th].

[110] D. Benedetti. "Instability of complex CFTs with operators in the principal series". In: *JHEP* 05 (2021), p. 004. DOI: 10.1007/JHEP05(2021)004. arXiv: 2103.01813 [hep-th].

[111] F. A. Dolan and H. Osborn. "Conformal Partial Waves: Further Mathematical Results". In: (Aug. 2011). arXiv: 1108.6194 [hep-th].

[112] K. Hepp. "Proof of the Bogolyubov-Parasiuk theorem on renormalization". In: *Commun. Math. Phys.* 2 (1966), pp. 301–326. DOI: 10.1007/BF01773358.

[113] W. Zimmermann. "Convergence of Bogolyubov's method of renormalization in momentum space". In: *Commun. Math. Phys.* 15 (1969), pp. 208–234. DOI: 10.1007/BF01645676.

[114] V. Rivasseau. *From perturbative to constructive renormalization*. Princeton University Press, 2014.

[115] M. C. Bergere and J. B. Zuber. "Renormalization of feynman amplitudes and parametric integral representation". In: *Commun. Math. Phys.* 35 (1974), pp. 113–140. DOI: 10.1007/BF01646611.

[116] M. C. Bergere and F. David. "Integral Representation for the Dimensionally Renormalized Feynman Amplitude". In: *Commun. Math. Phys.* 81 (1981), p. 1. DOI: 10.1007/BF01941797.

[117] M. S. Costa et al. "Projectors and seed conformal blocks for traceless mixed-symmetry tensors". In: *JHEP* 07 (2016), p. 018. DOI: 10.1007/JHEP07(2016)018. arXiv: 1603.05551 [hep-th].

[118] D. Benedetti et al. "Long-range multi-scalar models at three loops". In: *J. Phys. A* 53.44 (2020), p. 445008. DOI: 10.1088/1751-8121/abb6ae. arXiv: 2007.04603 [hep-th].

[119] F. J. Dyson. "Existence of a phase transition in a one-dimensional Ising ferromagnet". In: *Commun. Math. Phys.* 12 (1969), pp. 91–107. DOI: 10.1007/BF01645907.

[120] M. E. Fisher, S.-k. Ma, and B. Nickel. "Critical Exponents for Long-Range Interactions". In: *Phys.Rev.Lett.* 29 (1972), pp. 917–920. DOI: 10.1103/PhysRevLett.29.917.

[121] Y. Yamazaki and M. Suzuki. "Critical Behavior of Isotropic Systems with Long Range Interactions". In: *Prog. Theor. Phys.* 57 (1977), pp. 1886–1899. DOI: 10.1143/PTP.57.1886.

[122] C. Behan et al. "Analytic and numerical bootstrap for the long-range Ising model". In: (Nov. 2023). arXiv: 2311.02742 [hep-th].

[123] J. Sak. "Recursion Relations and Fixed Points for Ferromagnets with Long-Range Interactions". In: *Phys. Rev. B* 8 (1 1973), pp. 281–285. DOI: 10.1103/PhysRevB.8.281. URL: https://link.aps.org/doi/10.1103/PhysRevB.8.281.

[124] E. Brezin, G. Parisi, and F. Ricci-Tersenghi. "The Crossover Region Between Long-Range and Short-Range Interactions for the Critical Exponents". In: *J. Stat. Phys.* 157.4-5 (2014), p. 855. ISSN: 1572-9613. DOI: 10.1007/s10955-014-1081-0. arXiv: 1407.3358 [cond-mat.stat-mech]. URL: http://dx.doi.org/10.1007/s10955-014-1081-0.

[125] C. Behan et al. "Long-range critical exponents near the short-range crossover". In: *Phys. Rev. Lett.* 118.24 (2017), p. 241601. DOI: 10.1103/PhysRevLett.118.241601. arXiv: 1703.03430 [cond-mat.stat-mech].

[126] D. C. Brydges, P. K. Mitter, and B. Scoppola. "Critical (Phi**4)(3, epsilon)". In: *Commun. Math. Phys.* 240 (2003), pp. 281–327. DOI: 10.1007/s00220-003-0895-4. arXiv: hep-th/0206040 [hep-th].

[127] A. Abdesselam. "A Complete Renormalization Group Trajectory Between Two Fixed Points". In: *Commun.Math.Phys.* 276 (2007), pp. 727–772. DOI: 10.1007/s00220-007-0352-x. arXiv: math-ph/0610018.

[128] G. Slade. "Critical Exponents for Long-Range $O(n)$ Models Below the Upper Critical Dimension". In: *Communications in Mathematical Physics* 358.1 (2017), 343?436. ISSN: 1432-0916. DOI: 10.1007/s00220-017-3024-5. arXiv: 1611.06169 [math-ph]. URL: http://dx.doi.org/10.1007/s00220-017-3024-5.

[129] M. Lohmann, G. Slade, and B. C. Wallace. "Critical Two-Point Function for Long-Range O(n) Models Below the Upper Critical Dimension". In: *Journal of Statistical Physics* 169.6 (2017), pp. 1132–1161. ISSN: 1572-9613. DOI: 10.1007/s10955-017-1904-x. arXiv: 1705.08540 [math-ph]. URL: http://dx.doi.org/10.1007/s10955-017-1904-x.

[130] A. Giuliani, V. Mastropietro, and S. Rychkov. "Gentle introduction to rigorous Renormalization Group: a worked fermionic example". In: (Aug. 2020). arXiv: 2008.04361 [hep-th].

[131] J. Cardy, ed. *Finite-size Scaling*. Current physics. North-Holland, 1988. ISBN: 9780444871107. URL: https://books.google.fr/books?id=lqPvAAAAMAAJ.

[132] C. Linhares, A. Malbouisson, and I. Roditi. "Ginzburg–Landau Theory of Phase Transitions in Compactified Spaces". In: *Advances in Quantum Field Theory, Prof. Sergey Ketov (Ed.), InTech* (2012). DOI: 10.5772/37560. URL: https://doi.org/10.5772/37560.

[133] M. Le Bellac. *Thermal Field Theory*. Cambridge Monographs on Mathematical Physics. Cambridge University Press, 2011. ISBN: 978-0-511-88506-8, 978-0-521-65477-7. DOI: 10.1017/CBO9780511721700.

[134] A. Dutta and J. K. Bhattacharjee. "Phase transitions in the quantum Ising and rotor models with a long-range interaction". In: *Phys. Rev. B* 64 (18 2001), p. 184106. DOI: 10.1103/PhysRevB.64.184106. URL: https://link.aps.org/doi/10.1103/PhysRevB.64.184106.

[135] N. Defenu, A. Trombettoni, and S. Ruffo. "Criticality and phase diagram of quantum long-range O(N) models". In: *Physical Review B* 96.10 (2017). DOI: 10.1103/physrevb.96.104432. arXiv: 1704.00528. URL: https://doi.org/10.1103%2Fphysrevb.96.104432.

[136] E. Gonzalez-Lazo et al. "Finite-temperature critical behavior of long-range quantum Ising models". In: *SciPost Phys.* 11 (2021), p. 076. DOI: 10.21468/SciPostPhys.11.4.076. arXiv: 2104.15070. URL: https://scipost.org/10.21468/SciPostPhys.11.4.076.

[137] J. Zhao et al. "Finite-temperature critical behaviors in 2D long-range quantum Heisenberg model". In: (2023). arXiv: 2306.01044 [cond-mat.str-el].

[138] M. Suzuki. "Relationship between d-Dimensional Quantal Spin Systems and (d+1)-Dimensional Ising Systems: Equivalence, Critical Exponents and Systematic Approximants of the Partition Function and Spin Correlations". In: *Progress of Theoretical Physics* 56.5 (Nov. 1976), pp. 1454–1469. ISSN: 0033-068X. DOI: 10.1143/PTP.56.1454. eprint: https://academic.oup.com/ptp/article-pdf/56/5/1454/5264429/56-5-1454.pdf. URL: https://doi.org/10.1143/PTP.56.1454.

[139] S. Sachdev. *Quantum Phase Transitions*. Cambridge University Press, Apr. 2011. DOI: 10.1017/cbo9780511973765.

[140] K. Osterwalder and R. Schrader. "AXIOMS FOR EUCLIDEAN GREEN'S FUNCTIONS". In: *Commun. Math. Phys.* 31 (1973), pp. 83–112. DOI: 10.1007/BF01645738.

[141] A. Winter et al. "Quantum Phase Transition in the Sub-Ohmic Spin-Boson Model: Quantum Monte-Carlo Study with a Continuous Imaginary Time Cluster Algorithm". In: *Physical Review Letters* 102.3 (2009). ISSN: 1079-7114. DOI: 10.1103/physrevlett.102.030601. arXiv: 0807.4716 [cond-mat.stat-mech]. URL: http://dx.doi.org/10.1103/PhysRevLett.102.030601.

[142] M. Henkel and M. Pleimling. *Non-equilibrium phase transitions. Vol. 2: ageing and dynamical scaling far from equilibrium*. Theoretical and Mathematical Physics. Springer Dordrecht, 2010. ISBN: 978-90-481-2868-6. DOI: 10.1007/978-90-481-2869-3.

[143] A. C. Petkou and N. D. Vlachos. "Finite size effects and operator product expansions in a CFT for d > 2". In: *Phys. Lett. B* 446 (1999), pp. 306–313. DOI: 10.1016/S0370-2693(98)01530-5. arXiv: hep-th/9803149.

[144] A. C. Petkou and N. D. Vlachos. "Finite size and finite temperature effects in the conformally invariant O(N) vector model for 2 less than d less than 4". In: *5th International Workshop on Thermal Field Theories and Their Applications*. Sept. 1998. arXiv: hep-th/9809096.

[145] L. Iliesiu et al. "The Conformal Bootstrap at Finite Temperature". In: *JHEP* 10 (2018), p. 070. DOI: 10.1007/JHEP10(2018)070. arXiv: 1802.10266 [hep-th].

[146] A. C. Petkou and A. Stergiou. "Dynamics of Finite-Temperature Conformal Field Theories from Operator Product Expansion Inversion Formulas". In: *Phys. Rev. Lett.* 121.7 (2018), p. 071602. DOI: 10.1103/PhysRevLett.121.071602. arXiv: 1806.02340 [hep-th].

[147] J. R. David and S. Kumar. "Thermal one-point functions: CFT's with fermions, large d and large spin". In: *JHEP* 10 (2023), p. 143. DOI: 10.1007/JHEP10(2023)143. arXiv: 2307.14847 [hep-th].

[148] O. Diatlyk, F. K. Popov, and Y. Wang. "Beyond $N = \infty$ in Large N Conformal Vector Models at Finite Temperature". In: (Sept. 2023). arXiv: 2309.02347 [hep-th].

[149] P. Chaikin and T. Lubensky. *Principles of Condensed Matter Physics*. Cambridge University Press, 2000. ISBN: 9780521794503.

[150] P. C. Hohenberg and B. I. Halperin. "Theory of Dynamic Critical Phenomena". In: *Rev. Mod. Phys.* 49 (1977), pp. 435–479. DOI: 10.1103/RevModPhys.49.435.

[151] E. Ardonne, P. Fendley, and E. Fradkin. "Topological order and conformal quantum critical points". In: *Annals Phys.* 310 (2004), pp. 493–551. DOI: 10.1016/j.aop.2004.01.004. arXiv: cond-mat/0311466.

[152] D. Anselmi and M. Halat. "Renormalization of Lorentz violating theories". In: *Phys. Rev. D* 76 (2007), p. 125011. DOI: 10.1103/PhysRevD.76.125011. arXiv: 0707.2480 [hep-th].

[153] A. Lodhia et al. "Fractional Gaussian fields: A survey". In: *Probability Surveys* 13 (2016), pp. 1 –56. DOI: 10.1214/14-PS243. arXiv: 1407.5598 [math.PR].

[154] Z. Komargodski and A. Zhiboedov. "Convexity and Liberation at Large Spin". In: *JHEP* 11 (2013), p. 140. DOI: 10.1007/JHEP11(2013)140. arXiv: 1212.4103 [hep-th].

[155] D. Simmons-Duffin, D. Stanford, and E. Witten. "A spacetime derivation of the Lorentzian OPE inversion formula". In: *Journal of High Energy Physics* 2018.7 (2018). DOI: 10.1007/jhep07(2018)085. URL: https://doi.org/10.1007%2Fjhep07%282018%29085.

[156] R. Gurau. "Notes on Tensor Models and Tensor Field Theories". In: (July 2019). arXiv: 1907.03531 [hep-th].

[157] N. S. Craigie, V. K. Dobrev, and I. T. Todorov. "Conformally Covariant Composite Operators in Quantum Chromodynamics". In: *Annals Phys.* 159 (1985), pp. 411–444. DOI: 10.1016/0003-4916(85)90118-6.

[158] E. D. Skvortsov. "On (Un)Broken Higher-Spin Symmetry in Vector Models". In: *International Workshop on Higher Spin Gauge Theories*. 2017, pp. 103–137. DOI: 10.1142/9789813144101_0008. arXiv: 1512.05994 [hep-th].

[159] A. L. Fitzpatrick and J. Kaplan. "Unitarity and the Holographic S-Matrix". In: *JHEP* 10 (2012), p. 032. DOI: 10.1007/JHEP10(2012)032. arXiv: 1112.4845 [hep-th].

[160] S. Sachdev. "Polylogarithm identities in a conformal field theory in three-dimensions". In: *Phys. Lett. B* 309 (1993), pp. 285–288. DOI: 10.1016/0370-2693(93)90935-B. arXiv: hep-th/9305131.

[161] N. Defenu, A. Trombettoni, and S. Ruffo. "Anisotropic Long-Range Spin Systems". In: *Phys. Rev. B* 94.22 (2016), p. 224411. DOI: 10.1103/PhysRevB.94.224411. arXiv: 1606.07756 [cond-mat.stat-mech].

[162] M. Henkel. "Schrodinger invariance in strongly anisotropic critical systems". In: *J. Statist. Phys.* 75 (1994), pp. 1023–1061. DOI: 10.1007/BF02186756. arXiv: hep-th/9310081.

[163] M. Henkel. "Local Scale Invariance and Strongly Anisotropic Equilibrium Critical Systems". In: *Phys. Rev. Lett.* 78 (1997), pp. 1940–1943. DOI: 10.1103/PhysRevLett.78.1940. arXiv: cond-mat/9610174.

[164] H. Shimada and H. Shimada. "Exact four-point function and OPE for an interacting quantum field theory with space/time anisotropic scale invariance". In: *JHEP* 10 (2021), p. 030. DOI: 10.1007/JHEP10(2021)030. arXiv: 2107.07770 [hep-th].

[165] S. Giombi. "Higher Spin — CFT Duality". In: *Theoretical Advanced Study Institute in Elementary Particle Physics: New Frontiers in Fields and Strings*. 2017, pp. 137–214. DOI: 10.1142/9789813149441_0003. arXiv: 1607.02967 [hep-th].

[166] M. Salmhofer. *Renormalization: An Introduction*. Theoretical and Mathematical Physics. Springer-Verlag Berlin Heidelberg, 1999. ISBN: 9783540646662. DOI: 10.1007/978-3-662-03873-4.

[167] M. Aizenman and R. Fernández. "Critical exponents for long-range interactions". In: *Letters in Mathematical Physics* 16.1 (1988), pp. 39–49.

[168] S. Zeng and F. Zhong. "Theory of critical phenomena with long-range temporal interaction". In: *Physica Scripta* 98.7 (2023), p. 075017. DOI: 10.1088/1402-4896/acdcc0. arXiv: 2212.11076.

[169] R. M. Hornreich, M. Luban, and S. Shtrikman. "Critical Behavior at the Onset of $\vec{k}$-Space Instability on the λ Line". In: *Phys. Rev. Lett.* 35 (1975), pp. 1678–1681. DOI: 10.1103/PhysRevLett.35.1678.

[170] H. W. Diehl and M. Shpot. "Critical behavior at m axial Lifshitz points: Field theory analysis and epsilon expansion results". In: *Phys. Rev. B* 62 (2000), p. 12338. DOI: 10.1103/PhysRevB.62.12338. arXiv: cond-mat/0006007.

[171] M. Shpot and H. Diehl. "Two-loop renormalization-group analysis of critical behavior at m-axial Lifshitz points". In: *Nuclear Physics B* 612.3 (2001), pp. 340–372. ISSN: 0550-3213. DOI: https://doi.org/10.1016/S0550-3213(01)00309-1. arXiv: cond-mat/0106105 [cond-mat.stat-mech]. URL: https://www.sciencedirect.com/science/article/pii/S0550321301003091.

[172] H. W. Diehl. "Critical behavior at M-axial Lifshitz points". In: *Acta Phys. Slov.* 52.4 (2002), pp. 271–283. arXiv: cond-mat/0205284 [cond-mat.stat-mech].

[173] K. Essafi, J. P. Kownacki, and D. Mouhanna. "Nonperturbative renormalization group approach to Lifshitz critical behaviour". In: *EPL* 98.5 (2012), p. 51002. DOI: 10.1209/0295-5075/98/51002. arXiv: 1202.5946 [cond-mat.stat-mech].

[174] M. A. Shpot, Y. M. Pis'mak, and H. W. Diehl. "Large-n expansion for m-axial Lifshitz points". In: *J. Phys. Condens. Matter* 17 (2005), S1947–S1972. DOI: 10.1088/0953-8984/17/20/020. arXiv: cond-mat/0412405.

[175] M. A. Shpot, H. W. Diehl, and Y. M. Pis'mak. "Compatibility of 1/n and ϵ expansions for critical exponents at m-axial Lifshitz points". In: *J. Phys. A* 41.13 (2008), p. 135003. DOI: 10.1088/1751-8113/41/13/135003. arXiv: 0802.2434 [cond-mat.stat-mech].

[176] M. A. Shpot and Y. M. Pis'mak. "Lifshitz-point correlation length exponents from the large-n expansion". In: *Nucl. Phys. B* 862 (2012), pp. 75–106. DOI: 10.1016/j.nuclphysb.2012.04.011. arXiv: 1202.2464 [hep-th].

[177] P. Horava. "Quantum Gravity at a Lifshitz Point". In: *Phys. Rev. D* 79 (2009), p. 084008. DOI: 10.1103/PhysRevD.79.084008. arXiv: 0901.3775 [hep-th].

[178] D. Zappala. "Ultraviolet properties of Lifshitz-type scalar field theories". In: *Eur. Phys. J. C* 82.4 (2022), p. 341. DOI: 10.1140/epjc/s10052-022-10309-w. arXiv: 2111.08385 [hep-th].

[179] M. E. Fisher. "Yang-Lee Edge Singularity and phi**3 Field Theory". In: *Phys. Rev. Lett.* 40 (1978), pp. 1610–1613. DOI: 10.1103/PhysRevLett.40.1610.

[180] J. Cardy. "The Yang-Lee Edge Singularity and Related Problems". In: *50 Years of the Renormalization Group*. Ed. by A. Aharony et al. World Scientific, 2024. DOI: 10.1142/13571. arXiv: 2305.13288 [cond-mat.stat-mech].

[181] H. Kleinert and V. Schulte-Frohlinde. *Critical properties of ϕ^4-theories*. River Edge, USA: World Scientific, 2001.

[182] J. Zinn-Justin. *Quantum Field Theory and Critical Phenomena (4th ed.)* Vol. 113. Internat. Ser. Mono. Phys. Oxford: Clarendon Press, 2002. DOI: 10.1093/acprof:oso/9780198509233.001.0001. URL: https://cds.cern.ch/record/572813.

[183] D. Sauzin. "Resurgent functions and splitting problems". In: (2007). arXiv: 0706.0137 [math.DS].

[184] M. Mariño. "Lectures on non-perturbative effects in large N gauge theories, matrix models and strings". In: *Fortsch. Phys.* 62 (2014), pp. 455–540. DOI: 10.1002/prop.201400005. arXiv: 1206.6272 [hep-th].

[185] D. Dorigoni. "An Introduction to Resurgence, Trans-Series and Alien Calculus". In: *Annals Phys.* 409 (2019), p. 167914. DOI: 10.1016/j.aop.2019.167914. arXiv: 1411.3585 [hep-th].

[186] G. V. Dunne and M. Ünsal. "What is QFT? Resurgent trans-series, Lefschetz thimbles, and new exact saddles". In: *PoS* LATTICE2015 (2016), p. 010. DOI: 10.22323/1.251.0010. arXiv: 1511.05977 [hep-lat].

[187] I. Aniceto, G. Basar, and R. Schiappa. "A Primer on Resurgent Transseries and Their Asymptotics". In: *Phys. Rept.* 809 (2019), pp. 1–135. DOI: 10.1016/j.physrep.2019.02.003. arXiv: 1802.10441 [hep-th].

[188] P. Di Vecchia, M. Kato, and N. Ohta. "Double scaling limit in O(N) vector models". In: *Nucl. Phys. B* 357 (1991), pp. 495–520. DOI: 10.1016/0550-3213(91)90478-G.

[189] R. Gurau. *Random Tensors*. Oxford: Oxford University Press, 2016. ISBN: 9780198787938. URL: https://books.google.ca/books?id=6RjGDQAAQBAJ.

[190] F. Fauvet, F. Menous, and J. Quéva. "Resurgence and holonomy of the ϕ^{2k} model in zero dimension". In: *J. Math. Phys.* 61.9 (2020), p. 092301. DOI: 10.1063/5.0009292. arXiv: 1910.01606 [math-ph].

[191] A. Jaffe. "Constructive quantum field theory". In: *Mathematical physics* 2000 (2000), pp. 111–127.

[192] V. Rivasseau. "Constructive Field Theory in Zero Dimension". In: *Advances in Mathematical Physics* 2009 (2009), p. 180159. DOI: 10.1155/2009/180159. eprint: 0906.3524. URL: https://doi.org/10.1155%2F2009%2F180159.

[193] J. Bersini, A. Maiezza, and J. C. Vasquez. "Resurgence of the renormalization group equation". In: *Annals of Physics* 415 (2020). ISSN: 0003-4916. DOI: https://doi.org/10.1016/j.aop.2020.168126. arXiv: 1910.14507 [hep-th]. URL: https://www.sciencedirect.com/science/article/pii/S0003491620300592.

[194] Y. Tanizaki. "Lefschetz-thimble techniques for path integral of zero-dimensional $O(n)$ sigma models". In: *Phys. Rev. D* 91.3 (2015), p. 036002. DOI: 10.1103/PhysRevD.91.036002. arXiv: 1412.1891 [hep-th].

[195] C. M. Bender and S. A. Orszag. *Advanced Mathematical Methods for Scientists and Engineers I. Asymptotic methods and perturbation theory*. 1st ed. New York: Springer, 1999, pp. XIV, 593. ISBN: 978-0-387-98931-0. DOI: 10.1007/978-1-4757-3069-2.

[196] E. Witten. "Analytic Continuation Of Chern-Simons Theory". In: *AMS/IP Stud. Adv. Math.* 50 (2011). Ed. by J. E. Andersen et al., pp. 347–446. arXiv: 1001.2933 [hep-th].

[197] P. de Gennes. "Exponents for the excluded volume problem as derived by the Wilson method". In: *Physics Letters A* 38.5 (1972), pp. 339–340. ISSN: 0375-9601. DOI: https://doi.org/10.1016/0375-9601(72)90149-1. URL: https://www.sciencedirect.com/science/article/pii/0375960172901491.

[198] G. Slade. "Self-avoiding walk, spin systems, and renormalization". In: *Proc. Roy. Soc. Lond. A* 475.2221 (2019), p. 20180549. DOI: 10.1098/rspa.2018.0549. arXiv: 1808.04476 [math-ph].

[199] S. Baldino et al. "Resurgent Stokes Data for Painleve Equations and Two-Dimensional Quantum (Super) Gravity". In: (Mar. 2022). arXiv: 2203.13726 [hep-th].

[200] S. Hikami and E. Brezin. "Large-order behaviour of the 1/N expansion in zero and one dimensions". In: *Journal of Physics A: Mathematical and General* 12.6 (June 1979), p. 759. DOI: 10.1088/0305-4470/12/6/006.

[201] L. Di Pietro et al. "Resurgence and 1/N Expansion in Integrable Field Theories". In: *Journal of High Energy Physics* 2021.10, 166 (Oct. 2021), p. 166. DOI: 10.1007/JHEP10(2021)166. arXiv: 2108.02647 [hep-th].

[202] L. Ferdinand et al. "Borel summability of the 1/N expansion in quartic O(N)-vector models". In: (Sept. 2022). arXiv: 2209.09045 [math-ph].

[203] R. Gurau, V. Rivasseau, and A. Sfondrini. "Renormalization: an advanced overview". In: (Jan. 2014). arXiv: 1401.5003 [hep-th].

[204] *NIST Digital Library of Mathematical Functions*. https://dlmf.nist.gov/, Release 1.1.9 of 2023-03-15. F. W. J. Olver, A. B. Olde Daalhuis, D. W. Lozier, B. I. Schneider, R. F. Boisvert, C. W. Clark, B. R. Miller, B. V. Saunders, H. S. Cohl, and M. A. McClain, eds. URL: https://dlmf.nist.gov/.

[205] J. Hubbard. "Calculation of Partition Functions". In: *Phys. Rev. Lett.* 3 (2 July 1959), pp. 77–78. DOI: 10.1103/PhysRevLett.3.77. URL: https://link.aps.org/doi/10.1103/PhysRevLett.3.77.

[206] R. L. Stratonovich. "On a Method of Calculating Quantum Distribution Functions". In: *Soviet Physics Doklady* 2 (July 1957), p. 416.

[207] G. N. Watson. *A Treatise on the Theory of Bessel Functions*. Cambridge, England: Cambridge University Press, 1944.

[208] B. Y. Sternin and V. E. Shatalov. "Saddle-point method and resurgent analysis". In: *Math. Notes* 61 (Feb. 1997), pp. 227–241. DOI: 10.1007/BF02355733.

[209] E. Witten. "A New Look At The Path Integral Of Quantum Mechanics". In: (Sept. 2010). arXiv: 1009.6032 [hep-th].

[210] H. Fujii et al. "Hybrid Monte Carlo on Lefschetz thimbles - A study of the residual sign problem". In: *JHEP* 10 (2013), p. 147. DOI: 10.1007/JHEP10(2013)147. arXiv: 1309.4371 [hep-lat].

[211] G. Aarts et al. "Some remarks on Lefschetz thimbles and complex Langevin dynamics". In: *JHEP* 10 (2014), p. 159. DOI: 10.1007/JHEP10(2014)159. arXiv: 1407.2090 [hep-lat].

[212] S. Bluecher et al. "Reweighting Lefschetz Thimbles". In: *SciPost Phys.* 5.5 (2018), p. 044. DOI: 10.21468/SciPostPhys.5.5.044. arXiv: 1803.08418 [hep-lat].

[213] Y. Tanizaki, H. Nishimura, and J. J. M. Verbaarschot. "Gradient flows without blow-up for Lefschetz thimbles". In: *JHEP* 10 (2017), p. 100. DOI: 10.1007/JHEP10(2017)100. arXiv: 1706.03822 [hep-lat].

[214] R. Bauerschmidt, D. C. Brydges, and G. Slade. *Introduction to a renormalisation group method*. Vol. 2242. Springer Nature, 2019.

[215] V. Rivasseau and Z. Wang. "How to Resum Feynman Graphs". In: *Annales Henri Poincare* 15.11 (2014), pp. 2069–2083. DOI: 10.1007/s00023-013-0299-8. arXiv: 1304.5913 [math-ph].